Euclidean and Affine Symmetry Sets and Medial Axes

Thesis submitted in accordance
with the requirements of the
University of Liverpool
for the degree of
Doctor in Philosophy

by

Anthony James Pollitt

September 2004

Abstract

Symmetry sets and medial axes of curves in the plane or of surfaces in three-space have been extensively investigated and used in a wide variety of applications. There are different types of symmetry set and medial axis; this thesis examines two of these. Firstly, planar affine-invariant symmetry sets and medial axes are considered, in particular in relation to a query posed by W. Thurston: do the existing affine-invariant symmetry sets preserve their 'essential structures' under projective transformations? This question is answered negatively in the case of two types of affine-invariant symmetry sets and medial axes. Secondly, we consider the Euclidean medial axis in three-space. The major part of the investigation is the derivation of conditions on the medial axis, imposed by the requirement of a smooth boundary, for the various local forms of the medial axis. Used in this derivation was Damon's work on the radial shape operator. Finally, we study transitions on a one-parameter family of symmetry sets in three-space using methods of Bruce and Giblin and using and verifying the work of Bogaevsky. We obtain conditions for realizing certain of the expected transitions on the symmetry set and on the medial axis. This is the beginning of a larger study of the conditions for realization of all the possible transitions on one-parameter families of symmetry sets and of medial axes in three-space and includes a procedure for deciding which abstract forms occur in the considered geometrical setting.

Acknowledgements

My thanks go to my supervisor Professor Peter Giblin for introducing the subject of symmetry sets and for his patience, willingness to help and good humour.

I am grateful to the Department of Mathematical Sciences at the University of Liverpool for a friendly working atmosphere, and EPSRC for funding my research. The hospitality of Brown University was much appreciated during my two visits there; in particular conversations with Professor Benjamin Kimia which greatly advanced the work on the consistency conditions. My thanks also go to Professor Ilya Bogaevsky for his work on transitions on families of symmetry sets.

Finally, I thank my parents and the rest of my family for their love and encouragement.

Contents

Chapter 1

Introduction

The *medial axis* of a curve in the plane or surface in 3-space has been the subject of extensive investigation since it was introduced by Blum (see [Blu02]) to describe the symmetry of a plane curve. The medial axis is contained in another set, the *symmetry set* of the curve or surface. Other types of symmetry set have also been studied, such as the various *affine-invariant* ones. These symmetry sets are used in a wide variety of applications, all coming under the umbrella term of computer vision. For example, object recognition, stochastic shape [M03], industrial design [CP89] and medical imaging [GreMil98], among many others.

Now follows an introduction to the subject of symmetry sets.

1.1 Euclidean Symmetry Sets

Definition 1.1.1 ([BGG85]) *The Euclidean symmetry set (SS) of a smooth, simple, closed plane curve is the closure of the locus of centres of circles bitangent to the curve.*

Bitangent circles are circles tangent to a curve in at least two distinct points. Alternatively, we have the following, which is equivalent to Definition 1.1.1.

Definition 1.1.2 *The Euclidean symmetry set (SS) of a smooth, simple, closed plane curve is the closure of the locus of points on at least two Euclidean normals and equidistant from the corresponding points on the curve.*

The Euclidean symmetry set can be interpreted as follows. Consider two smooth segments of curve, γ_1, γ_2. Let there be a circle tangent to these curve segments respectively at $\gamma_1(t_1)$, $\gamma_1(t_2)$. Let m be the midpoint of the chord joining $\gamma_1(t_1)$, $\gamma_1(t_2)$ and let p be the intersection of the tangent lines to γ_1, γ_2 at $\gamma_1(t_1)$, $\gamma_1(t_2)$. Then the line L through m and p is tangent to the Euclidean symmetry set at the corresponding point. There exists a reflexion in L taking $\gamma_1(t_1)$ and its tangent line to $\gamma_2(t_2)$ and its tangent line. Hence the Euclidean symmetry set is a measurement of the local reflexional symmetry of a plane curve. See Figure 1.1.

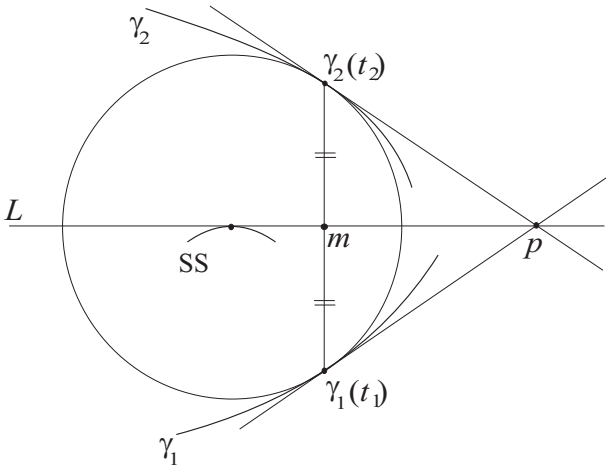

Figure 1.1: The line L, tangent to the SS, passes through the midpoint m of the line which passes through the two points of contact $\gamma_1(t_1)$, $\gamma_2(t_2)$ with the circle. Hence the line L is an infinitesimal axis of symmetry for $\gamma_1 \cup \gamma_2$.

The Euclidean symmetry set is invariant under the Euclidean group of transformations of $\mathbb{R}^2$, which preserve contact between curves and take centres of circles to centres of circles.

Definition 1.1.3 *The Euclidean medial axis of a simple, smooth, closed plane curve is the points of the corresponding Euclidean symmetry set for which the radii of the bitangent circles are maximal. (A maximal circle is a circle whose radius is equal to the least distance from its centre to the curve.)*

Now we consider the analogous definitions of the Euclidean symmetry set and Euclidean medial axis in $\mathbb{R}^3$.

Definition 1.1.4 *The Euclidean symmetry set (SS) of a smooth, simple, closed surface in $\mathbb{R}^3$ is the closure of the locus of centres of spheres bitangent to the surface.*

As in $\mathbb{R}^2$ there is an alternative definition for the Euclidean symmetry set in $\mathbb{R}^3$, which is equivalent to Definition 1.1.4.

Definition 1.1.5 *The Euclidean symmetry set (SS) of a smooth, simple, closed surface in $\mathbb{R}^3$ is the closure of the locus of points on at least two Euclidean normals and equidistant from the corresponding points on the surface.*

Definition 1.1.6 *The Euclidean medial axis of a simple, smooth, closed surface in $\mathbb{R}^3$ is the points of the corresponding Euclidean symmetry set for which the radii of the bitangent spheres are maximal. (A maximal sphere is a sphere whose radius is equal to the least distance from its centre to the surface.)*

Note. In Chapter 2, we respectively refer to the Euclidean symmetry set, Euclidean medial axis as SS, MA. This is because we also consider some other types of symmetry sets which have long names which require the use of abbreviations. In Chapters 3, 4 we refer to the symmetry set and medial axis.

1.2 Overview of Thesis

In Chapter 1 there is an introduction to symmetry sets (above) and then we introduce some definitions and results about planar affine differential geometry to be used in Chapter 2.

Chapter 2 is concerned with affine-invariant symmetry sets and medial axes in the plane, namely the *affine distance symmetry set* (ADSS), *affine distance medial axis* (ADMA) and *affine envelope symmetry set* (AESS), which are defined here. The question posed by W. Thurston is investigated: do any of the affine-invariant symmetry sets preserve their 'essential structures' under projective transformations? We answer Thurston's question negatively for the ADSS and ADMA by example and also show that the ADMA cannot have cusps. In order to answer Thurston's question for the AESS we examine how cusps and swallowtail points can occur on the AESS and the connection with another affine-invariant set, the MPTL, at some of these cusps and swallowtail points. Again the question is answered negatively, by showing that swallowtail points can be created or destroyed on the AESS and on the MPTL by a family of projective transformations.

Chapter 3 deals with the Euclidean medial axis in three-space and lists the local forms it can take. We introduce some quantities defined on the medial axis involving the associated radius function and also introduce Damon's *radial shape operator* [D03, D04, D05] and some results which connect the differential geometry of a boundary surface and its medial axis. These results are then used to obtain consistency conditions on the medial axis, imposed by the requirement of a smooth boundary, in the major case of the local form of the medial axis as three sheets meeting along a curve, called a triple junction. The limiting forms of these conditions are then obtained in the two degenerate cases of a triple junction. Also studied is the remaining local form, where two points of tangency between a sphere and a surface coincide; we obtain conditions for smoothness and connections between the geometry of the surface and of its medial axis.

In Chapter 4 we examine transitions on a one-parameter family of symmetry sets in three-space. Using the methods of [BG86] and using and verifying some of the work by Bogaevsky [Bog02b] about the possible singularities on the symmetry set, we obtain conditions for realizing certain of the expected transitions on the symmetry set and on the medial axis. This is a beginning of

a larger study of the conditions for realization of all the possible transitions on one-parameter families of symmetry sets and of medial axes in three-space and includes a procedure for deciding which abstract forms occur in our geometrical setting.

1.3 Affine Transformations and Planar Affine Differential Geometry

For the following, see Chapter 1 of [Su83]. For $\mathbf{x} = (x_1, x_2)^\top$ a point in a two-dimensional affine space, a non-singular affine transformation is

$$\mathbf{x} \mapsto A\mathbf{x} + \mathbf{b} \ ,$$

where A is a non-singular (2×2) matrix and $\mathbf{b}$ is a (2×1) matrix. Non-singular affine transformations with $\det(A) = 1$ are area-preserving, and so are called *equi-affine transformations*, and those with $\det(A) = d$ multiply areas by d. Non-singular affine transformations preserve the degree of a curve, parallelness, contact between curves and ratios of Euclidean distance. In general these transformations do not preserve Euclidean lengths, distances or angles and do not map circles to circles. For example, an ellipse is the same as a circle under an affine transformation. Contrast this with Euclidean transformations – these are given by letting $\mathbf{x} \in \mathbb{R}^2$ and only allowing A to be an *orthogonal* (2×2) matrix. These transformations preserve all of the properties that an affine transformation does, but also preserve Euclidean lengths, distances and angles and also map circles to circles. Considering these differences and similarities, the analogue of Euclidean distance in an affine space will be based on area, since Euclidean transformations preserve Euclidean distance, whereas equi-affine transformations preserve areas (or multiply areas by a constant for non-equi-affine transformations). Hence we introduce the ideas of *affine arclength* and the *affine distance from a fixed point to a point of a curve*, which are both based on area.

Now we introduce some definitions and results from Chapter 1 of [Su83]

and [GS98, pp.241-244] about affine differential geometry in $\mathbb{R}^2$, to be used in Chapter 2 of this thesis. For $\gamma : [0,1] \to \mathbb{R}^2$ a smooth planar curve parametrized by t, and considering equi-affine transformations only, a simple affine-invariant parametrization s is given by requiring that

$$[\gamma'(s), \gamma''(s)] = 1 \tag{1.1}$$

holds for every point $\gamma(s)$, where $[\mathbf{a}, \mathbf{b}]$ is the determinant of the 2×2 matrix with $\mathbf{a}, \mathbf{b}$ as its columns.

Convention. When considering the affine-invariant parametrization in this section (§1.3) and in Chapter 2, we will denote differentiation with respect to the affine-invariant parameter s by $'$ (prime), and $\dot{}$ (dot) will denote differentiation with respect to t.

Since (1.1) cannot hold at points of inflexion of γ, affine differential geometry is not defined at inflexions. One can get round this problem by dividing γ into segments, each of which has no inflexions (which are affinely invariant). However, Chapter 2 will only deal with curves without inflexions, so we do not need to carry out this segmentation of curves. From (1.1), it follows that for an arbitrary parametrization t,

$$ds = [\dot{\gamma}, \ddot{\gamma}]^{1/3} dt \ . \tag{1.2}$$

Differentiating (1.1) with respect to s gives $[\gamma', \gamma'''] = 0$ for all s. Hence

$$\gamma''' + \mu\gamma' = 0 \tag{1.3}$$

for some $\mu(s) \in \mathbb{R}$. This function μ is the *affine curvature*, and it is easy to see that

$$\mu = [\gamma'', \gamma'''] \ . \tag{1.4}$$

Definition 1.3.1 *The vector $\gamma'(s)$ is called the affine tangent to γ at $\gamma(s)$ and the vector $\gamma''(s)$ is called the affine normal to γ at $\gamma(s)$. It can be shown that*

$$\begin{aligned} \gamma' &= k^{-1/3}\dot{\gamma} \\ \textit{and} \quad \gamma'' &= k^{-2/3}\ddot{\gamma} - \frac{1}{3}\dot{k}k^{-5/3}\dot{\gamma} \ , \end{aligned}$$

where $k \equiv [\dot{\gamma}, \ddot{\gamma}]$.

Now we consider the idea of affine distance, from [IS98] and [GS98].

Definition 1.3.2 *The affine distance function* $d(\mathbf{x}, s)$ *is*

$$d(\mathbf{x}, s) \equiv [\mathbf{x} - \gamma(s), \gamma'(s)] \ , \tag{1.5}$$

which is the affine distance between a point $\mathbf{x} \in \mathbb{R}^2$ *and a non-inflexional point* $\gamma(s)$ *of the strictly convex curve* γ*.*

Note. In [GS98] it is noted that in order to be consistent with the Euclidean case and the geometric interpretation of affine arclength, $d(\mathbf{x}, s)$ should be defined as the $1/3$ power of $[\mathbf{x} - \gamma(s), \gamma'(s)]$. This is resisted in order to avoid introducing further notation. In [IS98] the function $d(\mathbf{x}, s)$ is called the *affine distance-cubed function.*

Lemma 1.3.3 ([GS98, from Proposition 1])

The curve γ *is a conic and* $\mathbf{x}$ *its centre if and only if* $d(\mathbf{x}, s)$ *is constant.*

Consider the case of γ as an ellipse:

$$\gamma(t) = (a\cos t, b\sin t) \ ,$$

where a, b are constants and so the centre $\mathbf{x}$ is the origin. Then using Definition 1.3.1 and (1.5) it is easy to show that $d(\mathbf{0}, s) = -(ab)^{2/3}$, which is a constant.

Chapter 2

Affine-Invariant Symmetry Sets and Projective Transformations

2.1 Introduction

As mentioned at the start of Chapter 1, one of the applications of symmetry sets is in computer vision and there has been interest in symmetry sets or medial axes which give affine-invariant information, for example the detection of affine symmetry. However, the transformations actually occurring in computer vision are projective, but a projective-invariant symmetry set would depend on very high derivatives and so would be too sensitive for curves given by data sets. Thus it would be useful to have an affine-invariant symmetry set, or better an affine-invariant medial axis, which under projective transformations preserved its 'essential structure'. W. Thurston posed the question: do the existing affine-invariant symmetry sets have this property?

2.1.1 Digression on Linear Fractional Transformations

An analogy with the question of whether the affine-invariant symmetry sets preserve their structures under projective transformations is the Euclidean symmetry set (SS) and the Euclidean medial axis (MA) under linear fractional transformations. The SS and MA were introduced in §1.1. The MA of a generic

curve has two features: its endpoints and 'Y-junctions', or triple points.

Definition 2.1.1.1 *A linear fractional transformation is given by*

$$z \mapsto \frac{nz+p}{qz+r}, \quad \textit{where} \quad nr-pq \neq 0, \quad \textit{for} \quad z,n,p,q,r \in \mathbb{C}\ . \tag{2.1}$$

Its inverse is given by

$$w \mapsto \frac{rw-p}{-qw+n}, \quad \textit{where} \quad nr-pq \neq 0, \quad \textit{for} \quad w,n,p,q,r \in \mathbb{C}\ . \tag{2.2}$$

So, for a point on a curve given by $(\Re(x+iy), \Im(x+iy))$, the transformed point of the curve is given by

$$\begin{array}{rcl} M & : & \mathbb{R}^2 \to \mathbb{R}^2 \\ (x,y) & \mapsto & \left(\Re\left(\dfrac{n(x+iy)+p}{q(x+iy)+r}\right), \Im\left(\dfrac{n(x+iy)+p}{q(x+iy)+r}\right)\right). \end{array} \tag{2.3}$$

The map M takes circles and lines to circles or lines and preserves contact between curves. However, the centres of circles are not preserved by linear fractional transformations.

Consider the part of the MA corresponding to maximal bitangent circles which are completely inside the curve. Suppose this 'interior' MA is finite. Can we guarantee that the interior MA of the image of the curve under a linear fractional transformation is also finite? In other words, can any of the points on the inner bitangent circles to the original curve be taken to infinity by a linear fractional transformation? Consider the point $z = \alpha + \beta e^{i\theta}$ lying on the circle centre α, radius β. This point is taken to infinity if and only if

$$\begin{array}{rcl} q(\alpha+\beta e^{i\theta})+r & = & 0 \\ \iff \dfrac{1}{\beta}\left(\dfrac{-r}{q}-\alpha\right) & = & e^{i\theta} \\ \iff \left|\dfrac{-r-\alpha q}{\beta q}\right| & = & 1 \\ \iff \left|\dfrac{-r}{q}-\alpha\right| & = & \beta\ , \end{array}$$

that is if and only if $z = -r/q$ lies on the circle centre α, radius β. A bitangent circle might pass through $z = -r/q$ if $z = -r/q$ were inside the curve. Then this

circle would pass through the point at infinity and so there would be a crossing on the MA at infinity. If we ensure $z = -r/q$ is outside the curve then $z = -r/q$ will not lie on any of the interior bitangent circles contributing to the MA. Therefore the MA will not gain a self-crossing at infinity. Another possibility is a point of the MA at infinity becoming finite. However, we assumed that the MA of the original curve is finite so this cannot happen. Hence we have the following.

Lemma 2.1.1.2 *For a simple, smooth, closed curve γ with a finite MA, the structure of the interior MA of the curve given by a linear fractional transformation of γ is unchanged if $z = -r/q$ is outside the original curve.*

Now follows the SS condition.

Lemma 2.1.1.3 *For $\gamma(t) : [0, 1] \to \mathbb{R}^2$ a smooth planar curve parametrized by t, the necessary and sufficient condition for there to be a circle tangent to γ at $\gamma(t_1)$ and at $\gamma(t_2)$ (for t_1, t_2 distinct) is*

$$(\gamma(t_1) - \gamma(t_2)).(T(t_1) - T(t_2)) = 0 \ , \tag{2.4}$$

where $T(t_1)$, $T(t_2)$ are respectively the unit tangents to γ at $\gamma(t_1)$, $\gamma(t_2)$.

(See [GB85, p.693].) So two distinct parameter values correspond to one point of the SS.

Definition 2.1.1.4 *The pre-SS is the set of parameter pairs (t_1, t_2) (t_1, t_2 distinct) which satisfy the SS condition* (2.4) *and the limit of such points. The pre-MA is the set of parameter pairs (t_1, t_2) in the pre-SS which correspond to maximal circles.*

2.1.2 Example

Consider the curve given by

$$\left.\begin{array}{c}(x(t), y(t)) = ((e + a\sin t + b\cos 2t)\cos t, (f + c\sin t + d\cos t)\sin t) \\ \text{where } a = -0.34,\ b = -0.15,\ c = -0.17,\ d = 0.2,\ e = 1.7,\ f = 1.\end{array}\right\} \tag{2.5}$$

Figure 2.1 has pictures of this curve and its SS and MA. The picture at the top of the figure contains the pre-SS, the pre-MA, and the original curve and its SS and MA. The pre-SS is the box on the far left of the picture at the top and the pre-MA is the box to the right of the pre-SS box. The pre-SS is represented as a curve on the torus, which means that the left and right edges of the pre-SS box are identified, as are the edges at the top and the bottom.

Figure 2.2 is of the curve after a linear fractional transformation as in (2.1) where $n = 1$, $p = 1$, $q = 0.3$, $r = 1$ (so $nr - pq \neq 0$). The criterion for the MA of the transformed curve to be finite given that the original MA is finite was for $z = -r/q$ to be outside the original curve (see Lemma 2.1.1.2). For the transformation in this example $-r/q = -1 \div 0.3 = -3\frac{1}{3}$, so the requirement is that the point $(-3\frac{1}{3}, 0)$ is outside the curve. It is easy to check that the x-values of the curve are between -1.55 and 1.55, so the condition is satisfied. By (2.3) a point $(x(t), y(t))$ on the curve is sent to $(X(t), Y(t))$, where

$$\begin{aligned} X(t) &= \frac{(x(t))^2 + (y(t))^2 + 1.3x(t) + 1}{0.9((x(t))^2 + (y(t))^2) + 0.6x(t) + 1} \ , \\ Y(t) &= \frac{0.7y(t)}{0.9((x(t))^2 + (y(t))^2) + 0.6x(t) + 1} \ . \end{aligned}$$

As before, the picture at the top has the pre-SS and pre-MA of the transformed curve and its SS and MA. The figures were drawn using the graphics package LSMP (see [LSMP]).

As can be seen from Figures 2.1 and 2.2, the structure of the SS and of the MA has remained the same. The pre-SS is the same in both figures, which means the number of endpoints and branches of the SS is the same for both curves. Also, the number of cusps of the SS is the same in both cases. The pre-MA also is unaltered, so the number of endpoints and branches of the MA is the same for both curves. There is only one triple point in the MA of each figure. Triple points can be recognized on the pre-SS by there being four points on the pre-SS which are corners of a rectangle, one of the points being on the diagonal and the other three points being on the same side of the diagonal (see Figure 2.3). Since the pre-SS and the pre-MA are unchanged by linear fractional transformations, the rectangle of points on the original pre-SS will

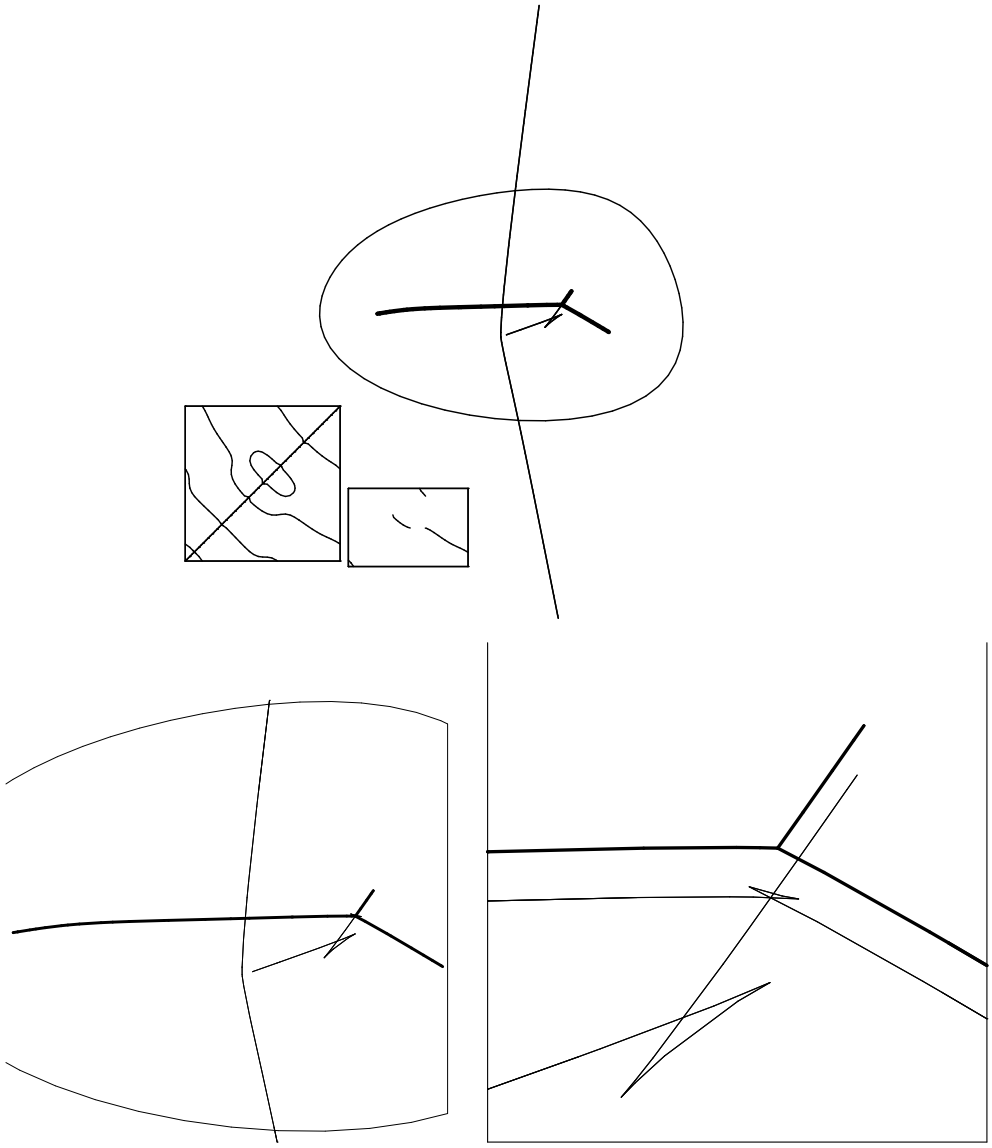

Figure 2.1: This figure and the following are concerned with linear fractional transformations of plane curves and how this type of transformation preserves the SS and the MA of the curve. This figure is of the curve given by (2.5) and its SS and MA. Top: the curve, its pre-SS, its pre-MA, its SS and its MA are shown (see Definition 2.1.1.4) Bottom left: zoom on the picture at the top. Bottom right: zoomed further and the MA has been shifted up so that the structure of the SS can be seen.

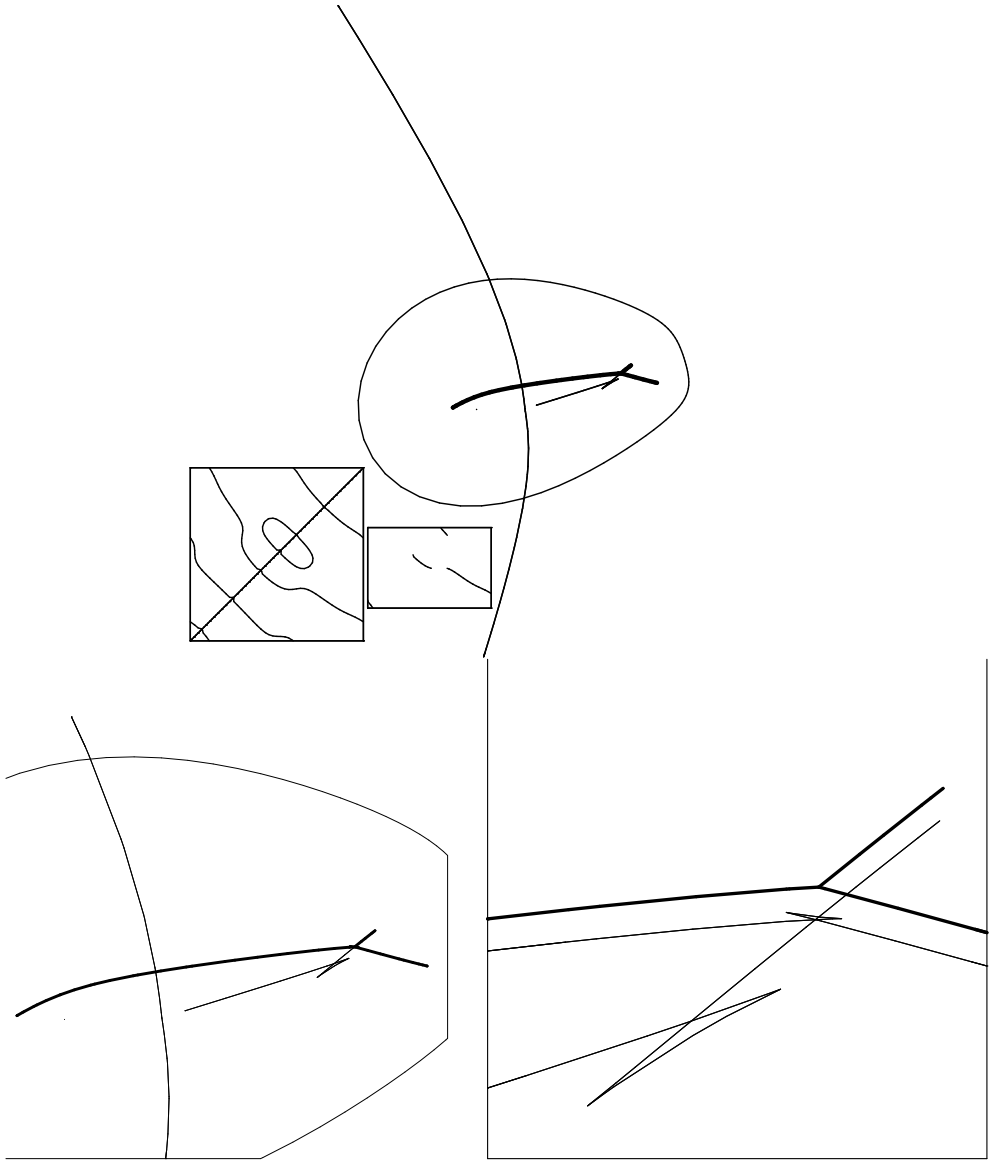

Figure 2.2: This figure is of the curve resulting from a linear fractional transformation acting on (2.5) and the SS and MA of the new curve. Top: the new curve, its pre-SS, its pre-MA, its SS and its MA are shown. Note the pre-SS and pre-MA are unaltered by the transformation. Bottom left: zoom on the picture at the top. Bottom right: zoomed further and the MA has been shifted up so that the structure of the SS can be seen.

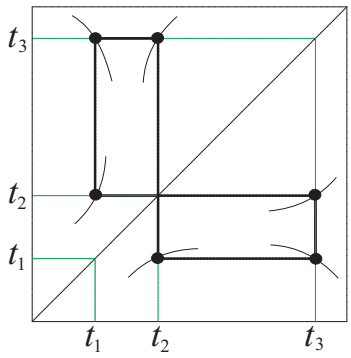

Figure 2.3: The pre-SS in the case of a triple point on the SS, where three branches of the SS intersect. (The pre-SS is represented as a curve on the torus, which means that the left and right edges of the pre-SS box are identified, as are the edges at the top and the bottom.) Hence there is a branch of the SS corresponding to parameter values t_1 and t_2, and similarly for t_1 and t_3, and for t_2 and t_3. So we get two rectangles of points on the pre-SS. The corners of the rectangles which lie on the diagonal correspond to an endpoint of the SS. Given a rectangle of points on the pre-SS it is not certain that it corresponds to a triple point on the SS, but searching for such rectangles yields all of the triple points.

also be there on the pre-SS of the transformed curve.

2.1.3 The Affine-Invariant Symmetry Sets

The affine-invariant symmetry sets which we consider in this chapter are the affine distance symmetry set (ADSS), affine distance medial axis (ADMA) and affine envelope symmetry set (AESS). These will be defined in §2.2. In order to answer Thurston's question at the start of §2.1 for these affine-invariant symmetry sets, we need to state what we mean by 'essential structure' in each case. The essential structure for the ADSS is the number of cusps, smooth branches, endpoints of branches, triple crossings and the pre-ADSS. For the ADMA it refers to the number of smooth branches, endpoints of branches, triple crossings and the pre-ADMA. For the AESS it means the number of cusps, branches, endpoints of branches and the pre-AESS. Also, for each of

these, the essential structure includes the graph defined by cusps, endpoints, triple crossings as its vertices and smooth branches as its edges. The pre-ADSS, pre-ADMA, pre-AESS contain respectively the parameter pairs which contribute to the ADSS, ADMA, AESS – compare with Definition 2.1.1.4, the definition of the pre-SS.

The aim of this chapter is to decide whether or not these affine-invariant symmetry sets do have the property of preserving their structures under projective transformations. In order to decide whether or not the structure of an affine-invariant symmetry set of a curve has changed, it has to be compared with the corresponding affine-invariant symmetry set of the curve given after a projective transformation has acted on the original curve.

Note: in this chapter the abbreviations SS and MA are used respectively for the Euclidean symmetry set and medial axis. We do this because the affine-invariant symmetry sets have very long names and so we refer to the ADSS, ADMA and AESS. In Chapters 3 and 4, the abbreviations SS and MA are *not* used respectively for the Euclidean symmetry set and medial axis; they are written in full as 'symmetry set' and 'medial axis'.

Here is a summary of what follows in this chapter.

§2.2: **Preliminary Definitions and Results.** This includes definitions of the ADSS, ADMA, AESS; conditions for points to be in the ADSS, ADMA, AESS; and a definition of a projective transformation.

§2.3: **Affine Distance Symmetry Set and Affine Distance Medial Axis.** We show by an example that the structure of the ADSS and of the ADMA can be altered by projective transformations. Also it is shown that cusps of the ADSS cannot lie on the ADMA.

§2.4: **Affine Envelope Symmetry Set.** Proceeding by arbitrary example as in §2.3 does not work in this case. Hence, using results about how cusps arise in the AESS, we obtain a family of projective transformations which can make cusps arising in certain situations appear or disappear. This approach involves another affine-invariant set, the MPTL

(the *mid-parallel-tangents locus*, also called the *anti-symmetry set*), and the conditions for cusps to appear in the MPTL. The obtained family of projective transformations is illustrated by an example in which cusps are destroyed in pairs in the AESS – a so-called swallowtail transition. The method used is checked to ensure it yields the standard pictures of the swallowtail transition.

§2.5: **Further Research.** This section considers the possibility of an affine envelope medial axis.

2.2 Preliminary Definitions and Results

In this section we use the definitions about affine geometry from §1.3 to introduce some affine-invariant symmetry sets (see [GS98, pp.241-244]). Note that a natural definition of an affine-invariant symmetry set has not yet been proposed, but rather there are a number of different ones. This is an area for further research (see §2.5).

Definition 2.2.1 *The affine distance symmetry set (ADSS) of a simple, smooth plane curve is the closure of the locus of points* $\mathbf{x} \in \mathbb{R}^2$ *on two affine normals and affine-equidistant from the corresponding points on the curve.*

As mentioned in §1.3, in this chapter we only consider curves without inflexions in the above definition. Compare this definition of the ADSS with the definition of the SS in Definition 1.1.2.

Lemma 2.2.2 *Given a simple, smooth curve* $\gamma(s)$*, the necessary and sufficient condition for distinct* s_1, s_2 *to give a point of the ADSS is*

$$[\gamma(s_1) - \gamma(s_2), \gamma''(s_1) - \gamma''(s_2)] = 0 \ . \tag{2.6}$$

Therefore, the pre-ADSS is the parameter pairs (s_1, s_2) *which are solutions of* (2.6) *and the limit of such points. (Note : affine arclength parametrization is assumed, so condition* (1.1) *holds).*

An alternative form of the ADSS condition involves the affine distance function, which was defined in Definition 1.3.2:

Lemma 2.2.3 *A point* $\mathbf{x} \in \mathbb{R}^2$ *is on the ADSS if and only if there are two distinct points* $\gamma(s_1), \gamma(s_2)$ *such that*

$$d(\mathbf{x}, s_1) = d(\mathbf{x}, s_2) \quad \textit{and} \quad d'(\mathbf{x}, s_1) = d'(\mathbf{x}, s_2) = 0$$

or if $\mathbf{x}$ *is the limit of such points.*

Then, given a pair of points $\gamma(s_1), \gamma(s_2)$ *which satisfy the ADSS condition* (2.6) *(so* s_1, s_2 *are in the pre-ADSS), the corresponding ADSS point is given by*

$$\gamma(s_1) + \frac{[\gamma(s_1) - \gamma(s_2), \gamma''(s_1)]}{[\gamma''(s_2), \gamma''(s_1)]}\gamma''(s_1) \ . \tag{2.7}$$

Geometrically, $\mathbf{x}$ being on the ADSS is equivalent to $\mathbf{x}$ *being at the common centre of two distinct conics having 4-point contact with the curve and sharing the same affine radius (defined to be* $1/\mu$*, where* μ *is given by* (1.4)*).* Contrast this with the Euclidean SS: a point of the SS is the centre of a *single* circle which is tangent to the curve in two places. Then

Lemma 2.2.4 *A point* $\mathbf{x}$ *on the ADSS is an ordinary cusp when one of the conics has 5-point contact with* γ*. This is equivalent to there being a horizontal or vertical tangent to the pre-ADSS at some* s_1*,* s_2 *pair.*

Definition 2.2.5 *The affine distance medial axis (ADMA) of a simple, smooth plane curve is*

$$\begin{aligned}
&\{\mathbf{x} \in \mathbb{R}^2 : \exists \ \ \textit{distinct} \ \ s_1, s_2 : \\
&\quad d(\mathbf{x}, s_1) = d(\mathbf{x}, s_2) \quad \textit{and} \quad d'(\mathbf{x}, s_1) = d'(\mathbf{x}, s_2) = 0 \\
&\quad \textit{where } d(\mathbf{x}, s) \textit{ has an absolute minimum at } s_1 \textit{ (or } s_2)\} \ .
\end{aligned}$$

In Definition 2.2.5, *minimum* could be replaced by *maximum*, since there is no convincing argument yet for having *minimum* rather than *maximum*. The ADMA is part of the ADSS, which is analogous to the MA being part of the SS.

For the following definitions and results about the AESS see [GS00, pp.174, 180].

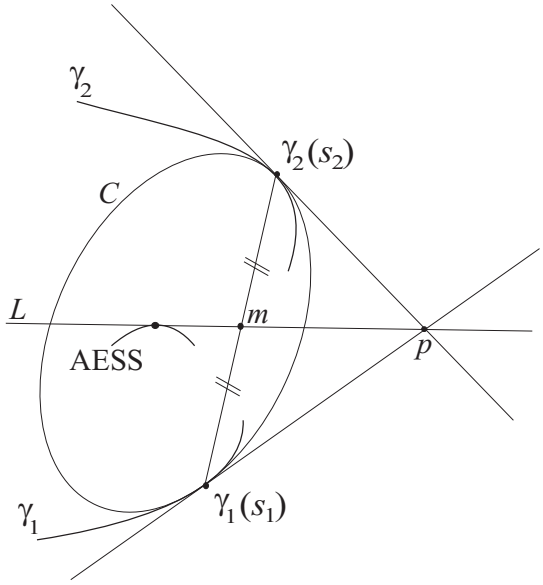

Figure 2.4: The line L, tangent to the AESS, passes through the midpoint m of the line which passes through the two points of contact $\gamma_1(s_1)$, $\gamma_2(s_2)$ with the conic C. Hence an alternative to Definition 2.2.6 is that the AESS is *the envelope of lines halfway between points of a curve with at least 3-point contact with a conic.* See [GS00]. Compare this with Figure 1.1.

Definition 2.2.6 *The affine envelope symmetry set (AESS) of a simple, closed, smooth plane curve is the closure of the locus of centres of conics with (at least) 3-point contact with the curve in at least two distinct points.*

Alternatively, the AESS can be interpreted as the *envelope of infinitesimal axes of affine reflexional symmetry of a curve.* This is what will be used later when finding examining swallowtail transitions on the AESS (see §2.4.7). The AESS will be calculated as an envelope of 'midlines' since an infinitesimal axis of affine reflexional symmetry of a curve is a line tangent to the AESS and which passes through the midpoint of the chord which passes through the points of contact between the curve and the corresponding conic (see Figure 2.4 and compare with Figure 1.1).

Lemma 2.2.7 *There is a non-degenerate conic with (at least) 3-point contact with γ at two distinct points $\gamma(s_1), \gamma(s_2)$, neither of which is an inflexion, if and only if*

$$[\gamma(s_1) - \gamma(s_2), \gamma'(s_1) + \gamma'(s_2)] = 0 \ . \tag{2.8}$$

There is an alternative condition for when γ is not an oval, but since this chapter does not deal with such curves, it has been omitted. Then, given a pair of points $\gamma(s_1), \gamma(s_2)$ which satisfy the AESS condition (2.8) *(so s_1, s_2 are in the pre-AESS), the corresponding AESS point is given by*

$$\frac{1}{2}\left(\gamma_1 + \gamma_2 + \frac{[\gamma_1 - \gamma_2, \gamma_1'][\gamma_1', \gamma_2']}{2[\gamma_1 - \gamma_2, \gamma_1'] - [\gamma_1', \gamma_2']^2}(\gamma_2' - \gamma_1')\right), \tag{2.9}$$

writing γ_1, γ_2, γ_1', γ_2' for $\gamma(s_1)$, $\gamma(s_2)$, $\gamma'(s_1)$, $\gamma'(s_2)$.

Definition 2.2.8 *A non-singular projective transformation is a map ϕ from the projective plane to the projective plane, such that*

$$\begin{aligned} (x : y : z) &\mapsto \phi(x : y : z) \\ &= (Ax + By + Cz : Dx + Ey + Fz : Gx + Hy + Kz) \ , \\ &\quad \textit{where} \begin{vmatrix} A & B & C \\ D & E & F \\ G & H & K \end{vmatrix} \neq 0 \ . \end{aligned}$$

(See [Gibs98].) In our case we are dealing with the affine plane, so after taking a projective transformation we specialize to the affine plane by letting $X = x/z$, $Y = y/z$ and then setting $z = 1$, so in the affine plane

$$(X, Y) \mapsto \left(\frac{AX + BY + C}{GX + HY + K}, \frac{DX + EY + F}{GX + HY + K}\right), \tag{2.10}$$

and $GX + HY + K = 0$ is taken to the line at infinity.

2.3 Affine Distance Symmetry Set and Affine Distance Medial Axis

2.3.1 Altering the Structure of the ADSS and of the ADMA by Projective Transformations

The ADSS differs from the SS in that a point $\mathbf{x}$ being on the ADSS is equivalent to $\mathbf{x}$ being at the common centre of two distinct conics having 4-point contact with the curve and sharing the same affine radius (see immediately after Lemma 2.2.3), whereas a point of the SS is the centre of a *single* circle which is tangent to the curve in two places.

An experimental approach was enough to decide whether the structure of the ADSS and of the ADMA remained the same after a projective transformation. In the following example the graphics package LSMP was used to draw the curve given by

$$\left.\begin{array}{c}(X,Y) = ((e + a\sin t + b\cos 2t)\cos t, (f + c\sin t + d\cos t)\sin t) \\ \text{for } a = -0.34,\ b = -0.15,\ c = -0.17,\ d = 0.2,\ e = 1.7,\ f = 1,\end{array}\right\} \quad (2.11)$$

and also its pre-ADSS, pre-ADMA, its ADSS and its ADMA. Then LSMP was used to draw the curve given by (2.10), that is after a projective transformation, for chosen values of constants $A, \ldots, K$ with its pre-ADSS, its pre-ADMA, ADSS and ADMA. Then the method was to compare the original ADSS with the new ADSS to see whether or not the structure had changed. Taking $A = 1$, $B = 0$, $C = 0$, $D = 0$, $E = 1$, $F = 0$, $G = 0$, $K = 1$, H close to 0 and then increasing H in each example was enough to decide this. These values give a non-singular projective transformation. Hence a point of the transformed curve for a chosen value of H is

$$\left(\frac{X}{HY+1}\ ,\ \frac{Y}{HY+1}\right),\ \text{where } (X,Y) \text{ is given by (2.11).} \quad (2.12)$$

Figures 2.5 to 2.11 show how the ADSS and the ADMA of the transformed curve change as we take various values for H, corresponding to taking a family of projective transformations. As in the case of the pre-SS, the pre-ADSS is

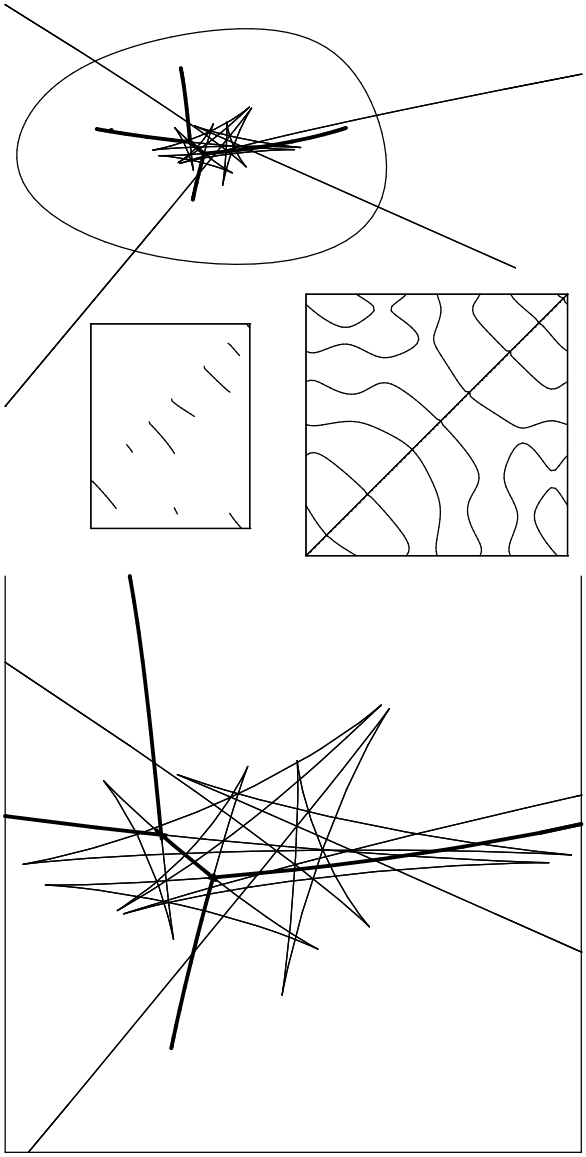

Figure 2.5: Figures 2.5 to 2.11 show the altering of the combinatorial structure of the ADSS and of the ADMA by a family of projective transformations. In each of these figures, the curve is drawn with its ADSS and ADMA. The pre-ADSS and pre-ADMA are in boxes below the curve. Top: the curve given by (2.11), its ADSS and ADMA are shown. Bottom: a closer look at its ADSS and ADMA.

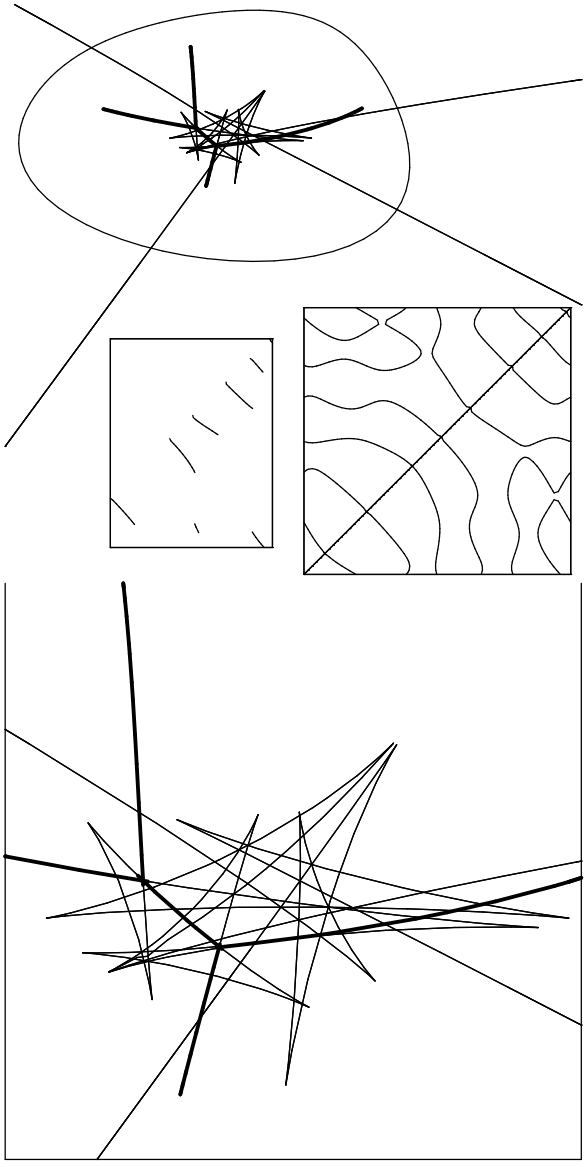

Figure 2.6: The curve given by (2.11) has now undergone a projective transformation to give (2.12). This figure, and Figures 2.7 to 2.11, are of the transformed curve for various values of H. This one is for $H = 0.11$. In this picture the structure of the pre-ADSS is about to change in the top left corner of the pre-ADSS box; there is going to be a crossing as H increases.

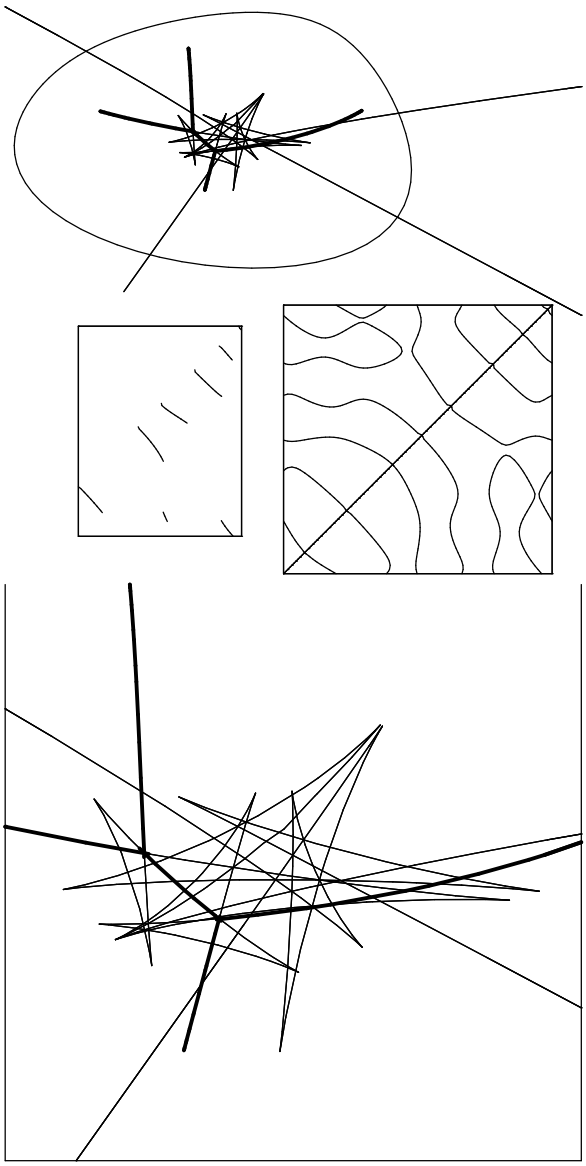

Figure 2.7: Here $H = 0.12$. The crossing has now occurred in the pre-ADSS, so a 'nib' transition has happened on the ADSS (see Figure 2.12 for an explanation of a nib transition). In this picture it is clear that one of the branches of the ADMA is shorter than before.

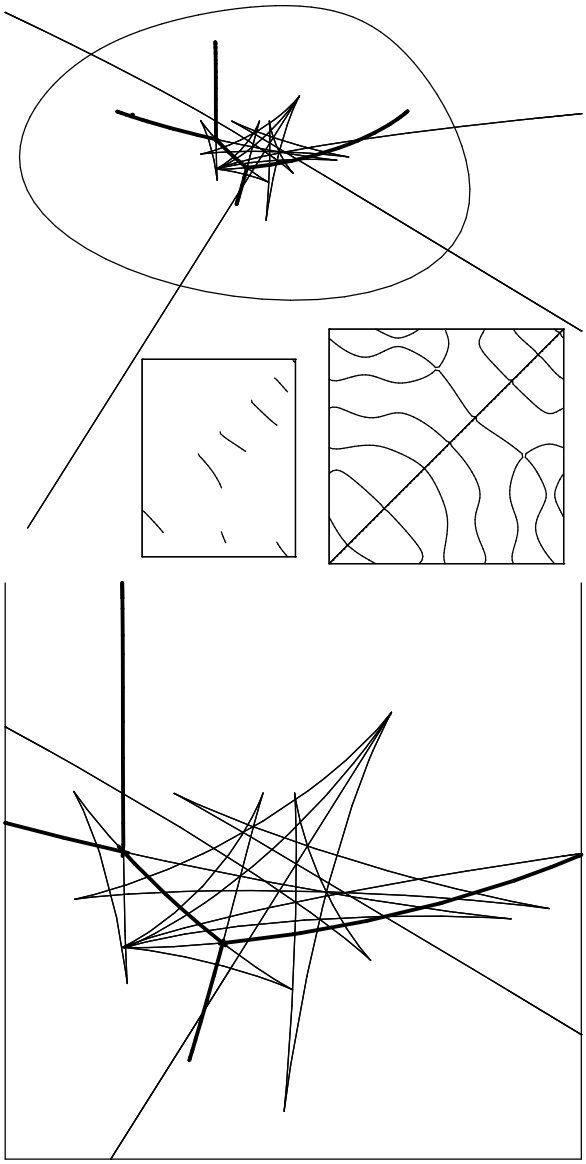

Figure 2.8: Now $H = 0.2$. There has been another crossing in the pre-ADSS, so there has been another nib transition in the ADSS. The same branch of the ADMA is shrinking and near to this branch there is a swallowtail of the ADSS which is also shrinking. On the pre-ADMA this corresponds to the gap between two pieces becoming smaller – see the second piece from the left which intersects with the diagonal. (The diagonal is not drawn in the pre-ADMA.)

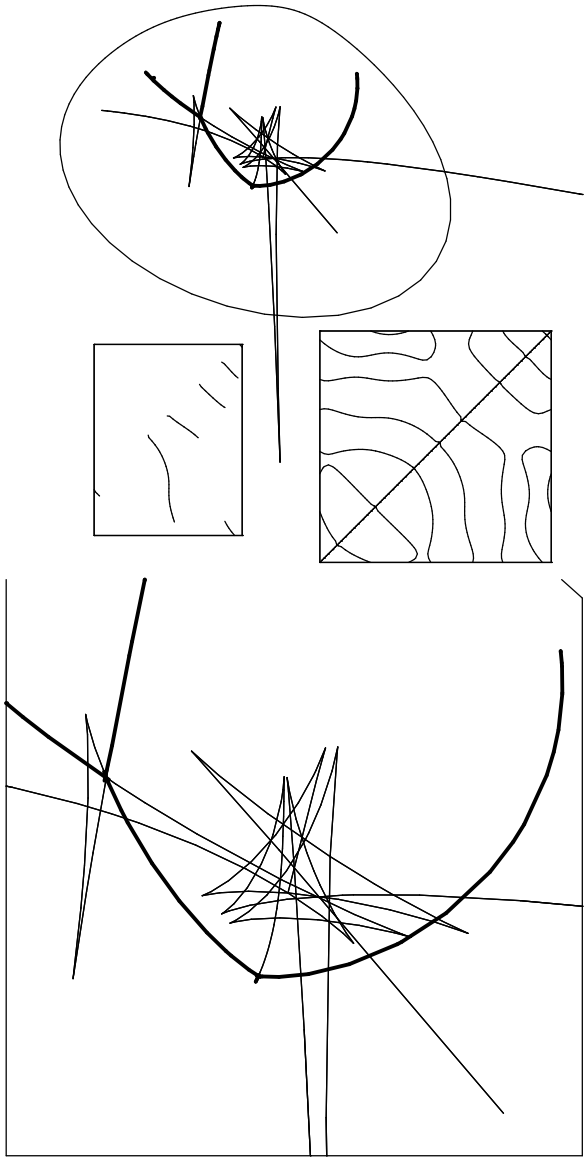

Figure 2.9: This figure is for $H = 0.54$. The structure of the ADMA is about to change, as the branch that is shrinking will disappear, as will the swallowtail of the ADSS. Also, the third piece along the bottom side of the pre-ADSS box starting from the right is about to have a vertical inflexion – this corresponds to the swallowtail collapsing to a swallowtail point. Also it corresponds to two branches of the pre-ADMA being joined up (the picture shows the two branches joined up, but this is just a numerical error; there should be a tiny gap).

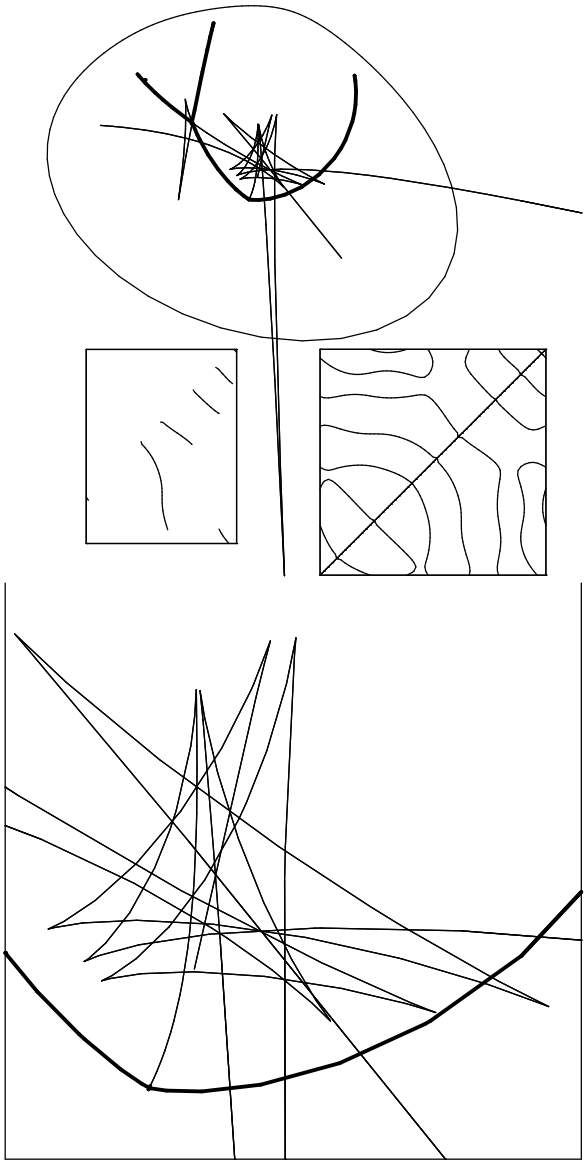

Figure 2.10: Here $H = 0.56$. This is the moment of transition; the branch of the ADMA is disappearing. The ADMA is changing from five branches, two triple crossings to three branches, one triple crossing. Also the ADSS has a swallowtail point and the pre-ADSS has a vertical inflexion at the corresponding (t_1, t_2) pair.

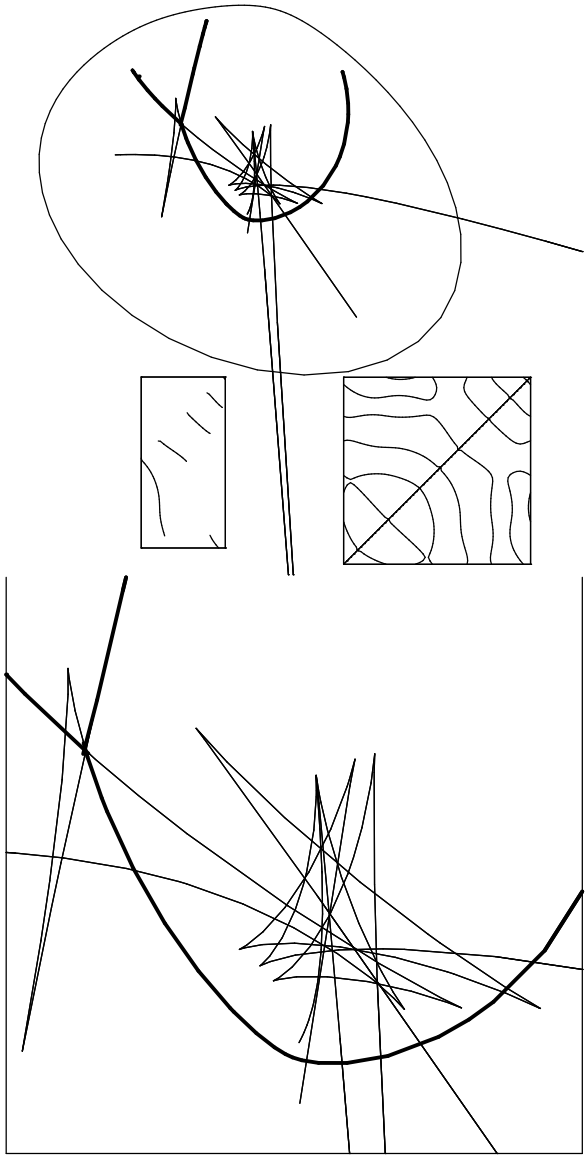

Figure 2.11: Now $H = 0.61$: there is no longer an inflexion on the pre-ADSS. Now there is a gap between an endpoint of the ADSS and a branch of the ADMA, and two cusps of the ADSS in the swallowtail have disappeared. In the first figure there were 16 cusps, now there are 14 cusps (one is off the bottom of the picture – see previous figures to follow its progress).

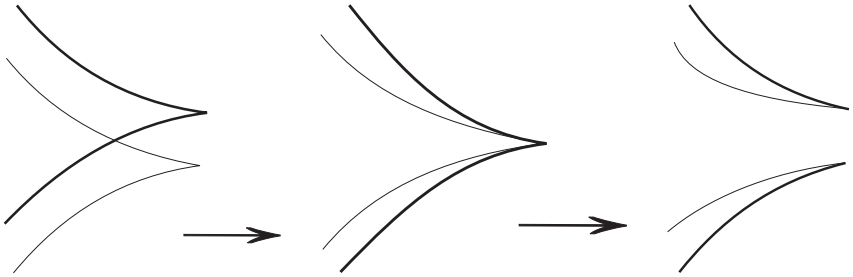

Figure 2.12: A nib transition: the cusps come into coincidence and then the branches pair off differently from before.

represented as a curve in the torus, so the left and right edges of the pre-ADSS boxes in the figures are identified, as are the top and bottom edges. The figures do not show all of the ADSS; it is truncated to show the interesting features, so not all of the endpoints of the ADSS are displayed in the pictures.

In this example it was possible to alter the pre-ADSS and the pre-ADMA and so make nib transitions occur on the ADSS. This also meant that the structure of the ADMA changed, as the ADMA of the original curve had five smooth branches and two triple points (a triple point is a point at which three smooth branches meet) and the final curve's ADMA (when $H = 0.61$) had three smooth branches and one triple point. Thus one branch of the ADMA was destroyed and two branches joined to become one smooth branch.

When this transition occurred on the ADMA, a swallowtail transition happened on the ADSS – a swallowtail collapsed to a swallowtail point and after this the ADSS became a smooth curve at this point. See Figure 2.13. When there is a swallowtail point on the ADSS, there is an inflexion at the corresponding point (t_1, t_2) on the pre-ADSS. Figures 2.9 to 2.11 show this transition: in Figure 2.9 there are two vertical tangents to the pre-ADSS nearby, in Figure 2.10 at the inflexion there is one vertical tangent to the pre-ADSS, and in Figure 2.11 there are no vertical tangents to the pre-ADSS. As this happened, two branches of the pre-ADMA joined up at the exact moment of the inflexion on the pre-ADSS. The affect on the ADMA was that two branches became smoothly joined after another branch of the ADMA had disappeared.

The result of all of this is that two cusps were destroyed, as there were sixteen cusps in the ADSS of the original curve, but there were only fourteen cusps in the ADSS of the final curve. Hence we have the following.

Proposition 2.3.1.1 *A projective transformation can make self-crossings occur on the pre-ADSS. Also, the number of cusps of the ADSS and the number of branches and triple points of the ADMA can be altered by a projective transformation.*

Remark 2.3.1.2 Projective transformations preserve contact between curves, but they do not send centres of conics to centres. Since a point $\mathbf{x}$ being on the ADSS is equivalent to $\mathbf{x}$ being at the common centre of two distinct conics having 4-point contact with the curve and sharing the same affine radius (see just after Lemma 2.2.3), it was not likely that the structure of the ADSS and ADMA would remain the same after projective transformations. Triple points of the MA can be detected on the pre-MA (see Figure 2.3), but a similar way of detecting triple points of the pre-ADMA is not known.

The moment of transition of the ADMA when one branch disappears and two others become one smooth branch corresponds to an A_1A_3 transition. The A_3 singularity means that the corresponding point of the curve is a sextactic point, so the centre of affine curvature at a sextactic point in this case is also the centre of an A_1 conic with the same affine radius. It is interesting that this can happen under a projective transformation.

2.3.2 Cusps and the ADMA

From Lemma 2.2.4 it is known how cusps arise on the ADSS, but can there be cusps on the ADMA? For a cusp of the ADSS to be a cusp of the ADMA, it would need to satisfy the conditions for it to be in the ADMA. In other words, from Definition 2.2.5, the affine distance function from the ADSS point to one of the corresponding points of the curve would need to have an absolute minimum. In order to prove that this cannot happen, it will be necessary to prove another result from which this automatically follows.

Consider two curves γ and δ given by $\gamma(t) = (t, f(t))$ and $\delta(t) = (t, g(t)))$ which are tangent to each other at $t = 0$, so $f(0) = g(0) = 0$ and $\dot{f}(0) = \dot{g}(0) = 0$, and a point $\mathbf{x} = (a, b)$. Assume $b \neq 0$ so that $\mathbf{x}$ is not on the tangent to γ at $\gamma(0) = (0, 0)$, which is also the tangent to δ at $\delta(0) = (0, 0)$. Then, by taking affine transformations, it can be assumed that $\mathbf{x} = (0, 1)$. We require $(0, 0)$ not to be an inflexion (so the affine tangent and affine normal exist), so we need $\ddot{f}(0) \neq 0$, $\ddot{g}(0) \neq 0$. We shall establish a relationship between the number of points of contact between γ and δ at $(0, 0)$ and the vanishing of derivatives of the affine distance function with respect to an arbitrary parameter (not necessarily the affine arclength parameter).

The curves γ and δ have at least k-point contact at $(0, 0)$ $\iff$ the $(k-1)$-jets of f and g are equal at $t = 0$. Using (1.5), the affine distance from $\mathbf{x}$ to $(0, 0)$ on γ is

$$\begin{aligned} d_\gamma(\mathbf{x}, t) &= [\mathbf{x} - \gamma(t), \gamma'(t)] \\ &= [\mathbf{x} - \gamma(t), (k_\gamma(t))^{-1/3}\dot{\gamma}(t)] \ . \end{aligned}$$

Here, $k_\gamma(t)$ is given by

$$k_\gamma(t) = [\dot{\gamma}(t), \ddot{\gamma}(t)] = \dddot{f}(t) \ .$$

So

$$d_\gamma = (-t\dot{f} + f - 1)(\ddot{f})^{-1/3} \ ,$$

dropping the dependence on t. For the affine distance from $\mathbf{x}$ to $(0, 0)$ on δ, replace f by g in the above:

$$d_\delta = (-t\dot{g} + g - 1)(\ddot{g})^{-1/3} \ .$$

Then

$$\begin{aligned} d_\gamma(\mathbf{x}, 0) &= d_\delta(\mathbf{x}, 0) \iff \\ (-(0)\dot{f}(0) + f(0) - 1)(\ddot{f}(0))^{-1/3} &= (-(0)\dot{g}(0) + g(0) - 1)(\ddot{g}(0))^{-1/3} \\ \iff \quad (-1)(\ddot{f}(0))^{-1/3} &= (-1)(\ddot{g}(0))^{-1/3} \\ \iff \quad \ddot{f}(0) &= \ddot{g}(0) \ . \end{aligned}$$

Now d_γ and d_δ can be regarded as functions of t and so for the purposes of this section it will not be necessary to differentiate with respect to the affine arclength parameter. Hence all the following derivatives are with respect to t. So

$$\begin{aligned} \dot{d}_\gamma &= -t(\ddot{f})^{2/3} - \dddot{f}\left(\frac{1}{3}\right)(\ddot{f})^{-4/3}(f - t\dot{f} - 1) \ , \\ \dot{d}_\delta &= -t(\ddot{g})^{2/3} - \dddot{g}\left(\frac{1}{3}\right)(\ddot{g})^{-4/3}(g - t\dot{g} - 1) \ . \end{aligned}$$

Then

$$\begin{aligned} \dot{d}_\gamma(\mathbf{x},0) &= \dot{d}_\delta(\mathbf{x},0) \\ \iff \quad 0 - \dddot{f}(0)\left(\frac{1}{3}\right)(\ddot{f}(0))^{-4/3}(-1) &= 0 - \dddot{g}(0)\left(\frac{1}{3}\right)(\ddot{g}(0))^{-4/3}(-1) \ , \end{aligned}$$

and if $d_\gamma(\mathbf{x},0) = d_\delta(\mathbf{x},0)$ is assumed, so $\ddot{f}(0) = \ddot{g}(0)$, then

$$\begin{aligned} \dot{d}_\gamma(\mathbf{x},0) &= \dot{d}_\delta(\mathbf{x},0) \\ \iff \quad \dddot{f}(0)\left(\frac{1}{3}\right)(\ddot{f}(0))^{-4/3}(-1) &= \dddot{g}(0)\left(\frac{1}{3}\right)(\ddot{f}(0))^{-4/3}(-1) \\ \iff \quad \dddot{f}(0) &= \dddot{g}(0) \ , \\ \text{since} \quad \ddot{f}(0) &\neq 0 \ . \end{aligned}$$

These calculations point towards the following.

Lemma 2.3.2.1 *Consider two curves γ and δ given respectively by $\gamma(t) = (t, f(t))$ and $\delta(t) = (t, g(t))$, where $f(0) = g(0) = 0$ and $\dot{f}(0) = \dot{g}(0) = 0$. Then the affine distance functions d_γ, d_δ of γ, δ satisfy*

$$\begin{aligned} & \left\{ {d_\gamma}^{(i)}(\mathbf{x},0) = {d_\delta}^{(i)}(\mathbf{x},0) \quad \textit{for } i = 0,\ldots,n \right\} \\ \iff \quad & \left\{ f^{(i+2)}(0) = g^{(i+2)}(0) \quad \textit{for } i = 0,\ldots,n \right\} . \end{aligned}$$

Proof. This can be proved by induction. This relies on the fact that $d_\gamma^{(i)} = A_i + Bf^{(i+2)}$, where A_i is in terms of t, f, $\dot{f}, \ldots, f^{(i+1)}$, and

$$B = \left(\frac{1}{3}\right)(\ddot{f})^{-4/3}(t\dot{f} + 1 - f) \ .$$

Also, $B(0) \neq 0$ since $B(0) = (1/3)(\ddot{f}(0))^{-4/3}(1)$, and $\ddot{f}(0) \neq 0$ since $(0,0)$ is not an inflexion (see the second paragraph of §2.3.2). Also $d_\delta^{(i)} = \tilde{A}_i + \tilde{B}g^{(i+2)}$, where $\tilde{A}_i$ is A_i with $f,\ \dot{f}, \ldots, f^{(i+1)}$ replaced respectively by $g,\ \dot{g}, \ldots, g^{(i+1)}$, and $\tilde{B}$ is B with $f,\ \dot{f},\ \ddot{f}$ replaced respectively by $g,\ \dot{g},\ \ddot{g}$. This means that $\tilde{A}_i(0) = A_i(0)$ and $\tilde{B}(0) = B(0)$. These can also be proved by induction. Then at each step of the induction

$$
\begin{aligned}
& & {d_\gamma}^{(i)}(\mathbf{x},0) &= {d_\delta}^{(i)}(\mathbf{x},0) \\
& \iff & A_i(0) + B(0)f^{(i+2)}(0) &= \tilde{A}_i(0) + \tilde{B}(0)g^{(i+2)}(0) \\
& \iff & B(0)f^{(i+2)} &= \tilde{B}(0)g^{(i+2)}\ , \\
\text{since} & & \tilde{A}_i(0) &= A_i(0) \\
& \iff & f^{(i+2)}(0) &= g^{(i+2)}(0)\ , \\
\text{since} & & \tilde{B}(0) &= B(0) \neq 0\ .
\end{aligned}
$$

Hence the result. □

Lemma 2.3.2.1 leads to the following.

Proposition 2.3.2.2 *Given two curves γ and δ given by $(t, f(t))$ and $(t, g(t))$ which have at least 2-point contact with each other at $\gamma(0) = \delta(0) = (0,0)$, which is not an inflexion of γ or of δ, and a point $\mathbf{x}$ which does not lie on the tangent to γ at $(0,0)$ (so $\mathbf{x}$ can be taken to be $(0,1)$ by affine transformations), then γ and δ have k-point contact at $(0,0)$ if and only if*

$$
\begin{aligned}
{d_\gamma}^{(i)}(\mathbf{x},0) &= {d_\delta}^{(i)}(\mathbf{x},0) \quad \textit{for } i = 0, \ldots, k-3 \\
\textit{and}\ \ {d_\gamma}^{(k-2)}(\mathbf{x},0) &\neq {d_\delta}^{(k-2)}(\mathbf{x},0)\ .
\end{aligned}
$$

What relevance does this result have for deciding whether or not it is possible for cusps of the ADSS to be in the ADMA? By Lemma 2.2.4 a point of the ADSS of a curve is an ordinary cusp when one of the corresponding conics has exactly 5-point contact with the curve (recall that a point of the ADSS is the centre of two conics having 4-point contact with the curve and sharing the

same affine radius). Take δ to be a conic which has exactly 5-point contact with a curve γ at $(0,0)$ and let $\mathbf{x}$ be its centre. Then, by Lemma 1.3.3, $d_\delta(\mathbf{x},t) = c$ (a constant) for all t and all derivatives of $d_\delta(\mathbf{x},t)$ are zero. Then Proposition 2.3.2.2 implies that

$$\begin{aligned} d_\gamma(\mathbf{x},0) &= d_\delta(\mathbf{x},0) = c \ , \\ \dot{d}_\gamma(\mathbf{x},0) &= \dot{d}_\delta(\mathbf{x},0) = 0 \ , \\ \ddot{d}_\gamma(\mathbf{x},0) &= \ddot{d}_\delta(\mathbf{x},0) = 0 \ , \\ \text{and} \quad \dddot{d}_\gamma(\mathbf{x},0) &\neq \dddot{d}_\delta(\mathbf{x},0) = 0 \ . \end{aligned}$$

This means that the affine distance from the centre of the conic δ to the point of contact of the curve γ *cannot* be an absolute minimum; in fact it cannot even be a maximum or a minimum. Therefore we have the following.

Proposition 2.3.2.3 *Cusps of the ADSS are not in the ADMA.*

Remark 2.3.2.4 A singularity of the ADSS worse than a cusp can lie on the ADMA, for example when two cusps disappear at an A_1A_3 transition – see Figures 2.5 to 2.11.

2.4 Affine Envelope Symmetry Set

2.4.1 Discussion of Features of the AESS

As shown in §2.3.1, the pre-ADSS and the pre-ADMA can be altered by projective transformations, since the number of horizontal or vertical tangents can be changed and self-crossings can be caused. This is not true of the pre-AESS; it will be unchanged by a projective transformation, since projective transformations preserve contact between curves. The reason for this is that the AESS is obtained by finding points where the curve has (at least) 3-point contact with a *single* conic. Contrast this with Remark 2.3.1.2. The AESS also differs from the ADSS in that there does not appear to be a sensible definition of an affine envelope medial axis (AEMA). This is because the AESS is not defined

in terms of a distance function which can be maximized (or minimized). This is an area of further research: is there such a definition of the AESS? (see §2.5).

Since the pre-AESS is unchanged by projective transformations, the number of branches and the number of endpoints will be unaltered by projective transformations. Because of this, it seems less likely than for the ADSS that the structure of the AESS of a given curve would be altered by arbitrary projective transformations. Consider cusps on the AESS. These occur in two different ways, one type arising when tangents to the curve are parallel at two points contributing to the AESS, the other because of horizontal or vertical tangents to the pre-AESS (see [GS00]). Since the pre-AESS is unaltered by projective transformations, the latter type of cusp of the AESS cannot be destroyed or created by projective transformations. The remaining possibility is whether the former type of cusp can be destroyed or created by a projective transformation.

Here is a result about the existence of such cusps, which comes from [GS00, pp.181, 182].

Lemma 2.4.1.1 *As for the pre-ADSS, the pre-AESS is represented as a curve in the torus and a component which is* (m,n) *winds* m *times round one way and* n *times round the other. For a generic oval curve (that is one for which the pre-AESS is non-singular) the pre-AESS has the following global properties:*

(i) For any (1,1) *component of the pre-AESS there is always at least one point corresponding to a pair of parallel tangents of the curve. Hence there is always at least one cusp along this branch belonging to the AESS.*

(ii) There are no (1,-1) *components and there is an odd number of* (1,1) *components; hence at least one. (The only other possibility is a* (0,0) *component).*

So we know that there is at least one cusp in the AESS corresponding to parallel tangents. These cusps connect the AESS and another affine-invariant set called the MPTL, which is defined below:

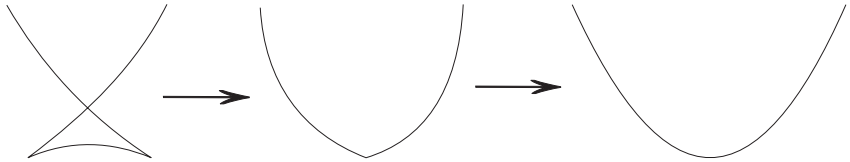

Figure 2.13: The standard swallowtail transition: a swallowtail (left) shrinks to a swallowtail point (centre) and then the curve becomes smooth (right).

Definition 2.4.1.2 *The MPTL (mid-parallel-tangents locus) of a smooth plane curve γ is the locus of midpoints of chords joining points of contact of parallel tangents to γ.*

The MPTL is sometimes called the *anti-symmetry set* and can also be defined as the *envelope of lines halfway between points of γ with parallel tangents.*

Cusps of the AESS corresponding to parallel tangents to the curve are also part of the MPTL, in fact they are also cusps of the MPTL. And it is also known that if a point of the AESS corresponding to a (t_1, t_2) pair coincides with a point of the MPTL corresponding to the same (t_1, t_2) pair then they meet in a dual beaks singularity at the cusps. Because of this it is necessary to treat the AESS and the MPTL together.

Consider a point of the AESS which is a cusp corresponding to a pair of parallel tangents and so is also a cusp of the MPTL. Is it possible to make this a swallowtail point, which is a higher singularity, by a projective transformation? If so, we could take 'nearby' projective transformations, ones for which $A, \ldots, K$ (as in Definition 2.2.8) differ slightly, to get a swallowtail transition. A swallowtail transition is when a swallowtail gets smaller and smaller until it becomes a swallowtail point and then becomes a smooth point, as in Figure 2.13. If it were possible to make this transition happen, the cusps of the AESS and of the MPTL would be destroyed and the AESS and MPTL would both be smooth.

This section shows that it is possible to make a swallowtail transition occur simultaneously on the AESS and on the MPTL. Hence we must first obtain the conditions for a swallowtail point to occur on the AESS and on the MPTL.

2.4.2 Conditions for Cusps and for Swallowtail Points on the AESS

The AESS is affine-invariant, so we can set up a local coordinate system as follows, without loss of generality. We take two arcs γ_1, γ_2 of a curve respectively near the points $t_1 = 0$, $t_2 = 0$:

$$\left.\begin{aligned} \gamma_1(t_1) &= (t_1, f(t_1)) = (t_1, c_2t_1^2 + c_3t_1^3 + c_4t_1^4 + \cdots) \ , \\ \gamma_2(t_2) &= (t_2, a + g(t_2)) = (t_2, a + b_1t_2 + b_2t_2^2 + b_3t_2^3 + b_4t_2^4 + \cdots) \ . \end{aligned}\right\} \tag{2.13}$$

The pre-AESS, that is the set of parameter pairs (t_1, t_2) which contribute points to the AESS, is given by the AESS condition (2.8) from Lemma 2.2.7. These are then mapped to the AESS using (2.9). For the coordinate system given by (2.13), the AESS condition becomes

$$\begin{aligned} & & [\gamma(t_1) - \gamma(t_2), \gamma'(t_1) + \gamma'(t_2)] &= 0 \\ \iff & \left| \begin{array}{cc} t_1 - t_2 & (\ddot{f}(t_1))^{1/3} + (\ddot{g}(t_2))^{1/3} \\ f(t_1) - g(t_2) & (\ddot{f}(t_1))^{1/3}\dot{f}(t_1) + (\ddot{g}(t_2))^{1/3}\dot{g}(t_2) \end{array} \right| &= 0 \ . \end{aligned} \tag{2.14}$$

Hence t_1 and t_2 are in the pre-AESS if and only if this condition holds. It is easy to show that $(t_1, t_2) = (0, 0)$ is in the pre-AESS if and only if

$$\begin{aligned} a(b_2 + c_2) = 0 \iff b_2 + c_2 = 0 \\ \text{(since } a = 0 \text{ means the curve would be non-simple)} \\ \iff \kappa_1(0) + \kappa_2(0) = 0 \ , \end{aligned}$$

where $\kappa_i(t_i)$ is the Euclidean curvature of the arc γ_i at t_i. We consider ovals, so there are no inflexions on the two arcs, so $b_2 \neq 0$, $c_2 \neq 0$. Now let $b_2 + c_2 = 0$, so that $(t_1, t_2) = (0, 0)$ is in the pre-AESS.

In order to obtain the pre-AESS, we express one of t_1, t_2 as a function of the other and solve (2.14) for this function. Firstly, we need to examine which is an appropriate parameter for the pre-AESS. By differentiating the left-hand side of (2.14) with respect to t_1 and to t_2, we find the following.

- When $(b_1b_2 + ab_3) \neq 0$ then t_1 is a parameter.

- When $(b_1c_2 + ac_3) \neq 0$ then t_2 is a parameter.
- When $(b_1b_2 + ab_3) = (b_1c_2 + ac_3) = 0$ then the pre-AESS is singular.

We are interested in cusps of the AESS, so we ignore the case of the pre-AESS being singular. In each of the cases $(b_1b_2 + ab_3) \neq 0$, $(b_1b_2 + ab_3) \neq 0$ we can map the pre-AESS to the AESS using (2.9). Then we get the following.

Proposition 2.4.2.1 *There is an ordinary cusp on the AESS of a smooth plane curve γ corresponding to $\gamma(t_1)$ and $\gamma(t_2)$, neither of which is an inflexion, if and only if one of the following occurs.*

1. *The tangents to γ at $\gamma(t_1)$ and $\gamma(t_2)$ are parallel; the affine normals at $\gamma(t_1)$ and $\gamma(t_2)$ are not parallel; and the tangent to the pre-AESS at (t_1, t_2) is not parallel to the diagonal ($t_1 = t_2$), not horizontal and not vertical.*
2. *The tangent to the pre-AESS at (t_1, t_2) is horizontal, at which the pre-AESS is not an inflexion, and the tangents to γ at $\gamma(t_1)$ and $\gamma(t_2)$ are not parallel.*
3. *The tangent to the pre-AESS at (t_1, t_2) is vertical, at which the pre-AESS is not an inflexion, and the tangents to γ at $\gamma(t_1)$ and $\gamma(t_2)$ are not parallel.*

There is a swallowtail point on the AESS of a smooth plane curve γ corresponding to $\gamma(t_1)$ and $\gamma(t_2)$, neither of which is an inflexion, if and only if one of the following occurs.

1. *The tangents to γ at $\gamma(t_1)$ and $\gamma(t_2)$ are parallel, the affine normals at $\gamma(t_1)$ and $\gamma(t_2)$ are parallel and the affine curvatures of γ at $\gamma(t_1)$ and $\gamma(t_2)$ are not equal.*
2. *The tangents to γ at $\gamma(t_1)$ and $\gamma(t_2)$ are parallel and the tangent to the pre-AESS is horizontal at (t_1, t_2), at which the pre-AESS does not have an inflexion.*

3. *The tangents to γ at $\gamma(t_1)$ and $\gamma(t_2)$ are parallel and the tangent to the pre-AESS is vertical at (t_1, t_2), at which the pre-AESS does not have an inflexion.*

4. *The tangent to the pre-AESS is horizontal at (t_1, t_2), at which the pre-AESS has an inflexion, but not a vertex, and the tangents to γ at $\gamma(t_1)$ and $\gamma(t_2)$ are not parallel.*

5. *The tangent to the pre-AESS is vertical at (t_1, t_2), at which the pre-AESS has an inflexion, but not a vertex, and the tangents to γ at $\gamma(t_1)$ and $\gamma(t_2)$ are not parallel.*

Proof. For the AESS at $t_1 = t_2 = 0$ to be an ordinary cusp, we need that the first derivative of the parametrization of the AESS is the zero vector at $t_1 = t_2 = 0$ and that the second and third derivatives are independent. Recall that $b_2 + c_2 = 0$, which means that $(t_1, t_2) = (0, 0)$ is on the pre-AESS and that $b_2 \neq 0$, $c_2 \neq 0$, so $\gamma_1(0)$, $\gamma_2(0)$ are not inflexions.

Consider firstly the case when t_1 is a parameter, that is when $(b_1 b_2 + a b_3) \neq 0$. Then the pre-AESS is given by

$$t_2 = -\frac{(b_1 c_2 + a c_3)}{(b_1 b_2 + a b_3)} t_1 + \cdots$$

and so the pre-AESS does not have a vertical tangent at $t_1 = t_2 = 0$. Then, the AESS is non-regular at $t_1 = t_2 = 0$ if and only if

$$a b_1 (b_1 c_2 + a c_3) = 0 \ .$$

We ignore the case of $a = 0$, since the two arcs γ_1, γ_2 would cross if $a = 0$. Hence there are two cases that could possibly mean there were cusps on the AESS. The condition $b_1 = 0$ is the same as the two arcs γ_1, γ_2 having parallel tangents at $t_1 = t_2 = 0$ and the condition $(b_1 c_2 + a c_3) = 0$ is the same as the pre-AESS having a horizontal tangent at $t_1 = t_2 = 0$.

When $b_1 = 0$ the second and third derivatives of the parametrization of the

AESS at $t_1 = t_2 = 0$ are independent if and only if $c_3(b_3 - c_3)(b_3 + c_3) \neq 0$.

$$\text{When } b_1 = 0, \qquad c_3 \neq 0 \iff \frac{dt_2}{dt_1}(0) \neq 0 \ ,$$
$$(b_3 + c_3) \neq 0 \iff \frac{dt_2}{dt_1}(0) \neq 1 \ .$$

Hence, when $b_1 = (b_2 - c_2) = 0$, then $c_3(b_3 + c_3) \neq 0$ if and only if the tangent to the pre-AESS is not horizontal and not parallel to the diagonal $t_1 = t_2$. When $b_1 = 0$ the affine normals $\gamma_1''(0)$, $\gamma_2''(0)$ are as follows, using Definition 1.3.1:

$$\gamma_1''(0) = \left(-2c_3(2c_2)^{-5/3}, (2c_2)^{1/3}\right) \ , \ \gamma_2''(0) = \left(-2b_3(2b_2)^{-5/3}, (2b_2)^{1/3}\right).$$

Hence, when $b_1 = (b_2 - c_2) = 0$ then $(b_3 - c_3) \neq 0$ if and only if the affine normals at $t_1 = t_2 = 0$ are not parallel.

When $(b_1c_2 + ac_3) = 0$, the second and third derivatives of the parametrization of the AESS at $t_1 = t_2 = 0$ are independent if and only if $b_1(ac_2^2 + b_1^2 - a^2c_4) \neq 0$. When $(b_1c_2 + ac_3) = 0$ the pre-AESS has a horizontal tangent at $t_1 = t_2 = 0$ and becomes

$$t_2 = -\frac{2(a^2c_4 - ac_2^2 - b_1^2c_2)}{a(b_1b_2 + ab_3)}t_1^2 + \cdots \ .$$

Hence, when $(b_1c_2 + ac_3) = (b_2 - c_2) = 0$, then $b_1(ac_2^2 + b_1^2 - a^2c_4) \neq 0$ if and only if the tangents to the two arcs γ_1, γ_2 at $t_1 = t_2 = 0$ are not parallel and the pre-AESS does not have a horizontal inflexion.

In summary, when a point of the pre-AESS does not have a vertical tangent, the corresponding point of the AESS is a cusp if and only if

- the two arcs γ_1, γ_2 have parallel tangents and the tangent to the pre-AESS is not horizontal and not parallel to the diagonal $t_1 = t_2$

or

- the point of the pre-AESS has a horizontal tangent, but is not an inflexion, and the two arcs γ_1, γ_2 do not have parallel tangents.

Similarly, in the case when t_2 is a parameter, that is when a point of the pre-AESS does not have a horizontal tangent, the corresponding point of the AESS is a cusp if and only if

- the two arcs γ_1, γ_2 have parallel tangents and the tangent to the pre-AESS is not vertical and not parallel to the diagonal $t_1 = t_2$

or

- the point of the pre-AESS has a vertical tangent, but is not an inflexion, and the two arcs γ_1, γ_2 do not have parallel tangents.

We assumed that the pre-AESS does not have both a horizontal and a vertical tangent at the same point, since otherwise it would be singular. Hence there are only three ways in which there is a cusp on the AESS, as described in the result.

Now we consider the condition for the AESS at $t_1 = t_2 = 0$ to be a swallowtail point. The canonical form for an ordinary cusp is (t^2, t^3) and from this are obtained the criteria for a curve to have an ordinary cusp. Similarly, the canonical form for a swallowtail point is (t^3, t^4) and so the criteria for a swallowtail point are that the first two derivatives of a curve are the zero vector and that the third and fourth derivatives are independent.

Again we consider firstly the case when t_1 is a parameter ($b_1 b_2 + a b_3 \neq 0$), so that the pre-AESS does not have a horizontal tangent. Again ignoring the case $a = 0$, the first two derivatives of the parametrization of the AESS are the zero vector at $t_1 = t_2 = 0$ if and only if one of the following cases occurs:

$$\begin{aligned} & b_1 = c_3 = 0 \ , \\ \text{or} \quad & b_1 = b_3 - c_3 = 0 \ , \\ \text{or} \quad & a c_3 + b_1 c_2 = a^2 c_4 - a c_2^2 - b_1^2 c_2 = 0 \ . \end{aligned}$$

When $b_1 = c_3 = 0$, the third and fourth derivatives of the parametrization of the AESS are independent if and only if $(ac_4 - c_2^2) \neq 0$. When $b_1 = c_3 = 0$ the pre-AESS has a horizontal tangent at $t_1 = t_2 = 0$ and becomes

$$t_2 = -\frac{2(ac_4 - c_2^2)}{ab_3} t_1^2 + \cdots \ .$$

Hence, when $b_1 = c_3 = 0$, then $(ac_4 - c_2^2) \neq 0$ if and only if the pre-AESS does not have a horizontal inflexion. When $b_1 = b_3 - c_3 = 0$, the third and fourth

derivatives of the parametrization of the AESS are independent if and only if $(b_4 + c_4) \neq 0$. Using Definition 1.3.1 and (1.4), we get formulae for the affine curvatures μ_1, μ_2 of the arcs γ_1, γ_2 at $t_1 = 0$, $t_2 = 0$:

$$\mu_1(0) = (2c_2)^{1/3}\left(\frac{2c_4}{c_2^2} - \frac{5c_3^2}{2c_2^3}\right) \ , \quad \mu_2(0) = (2b_2)^{1/3}\left(\frac{2b_4}{b_2^2} - \frac{5b_3^2}{2b_2^3}\right).$$

Hence, when $b_2 = -c_2$, $b_1 = b_3 - c_3 = 0$, then the affine curvatures at $t_1 = t_2 = 0$ are not equal if and only if $(b_4 + c_4) \neq 0$. When $(ac_3 + b_1c_2) = (a^2c_4 - ac_2^2 - b_1^2c_2) = 0$, the third and fourth derivatives of the parametrization of the AESS are independent if and only if $b_1(a^3c_5 + 3ab_1c_2^2 + b_1^3c_2) \neq 0$. When $(ac_3 + b_1c_2) = (a^2c_4 - ac_2^2 - b_1^2c_2) = 0$, the pre-AESS is given by

$$t_2 = -\frac{10(a^3c_5 + 3ab_1c_2^2 + b_1c_2)}{3a^2(ab_3 - b_1c_2)}t_1^3 + \cdots \ .$$

Hence, when $(ac_3 + b_1c_2) = (a^2c_4 - ac_2^2 - b_1^2c_2) = 0$, then $b_1(a^3c_5 + 3ab_1c_2^2 + b_1^3c_2) \neq 0$ if and only if the tangents to the two arcs γ_1, γ_2 at $t_1 = t_2 = 0$ are not parallel and the pre-AESS does not have a horizontal vertex.

In summary, we have shown the possibilities **1.**, **2.** and **4.** for a swallowtail point on the AESS when the pre-AESS does not have a vertical tangent. When the pre-AESS does not have a horizontal tangent we get the remaining cases **3.** and **5.** Hence the result. □

This result gives us a candidate for a type of swallowtail point which could be created or destroyed on the AESS by a family of projective transformations, namely case **1.** An interesting question is what happens on the MPTL when there is a swallowtail point on the AESS? The next section deals with this matter.

2.4.3 Conditions for Cusps and for Swallowtail Points on the MPTL

The MPTL is affine-invariant, so we can use the coordinate system (2.13), but with $b_1 = 0$ so that the two arcs γ_1 and γ_2 are parallel at $t_1 = t_2 = 0$. The

pre-MPTL is the parameter pairs (t_1, t_2) such that $df/dt_1 = dg/dt_2$ for all t_1, t_2 near $t_1 = t_2 = 0$. As for the pre-AESS, we obtain the pre-MPTL by expressing one of t_1, t_2 as a function of the other and solving $df/dt_1 = dg/dt_2$ for this function. Differentiating $(df/dt_1 - dg/dt_2)$ with respect to t_1 and to t_2, we find the following.

- When $b_2 \neq 0$ then t_1 is a parameter.
- When $c_2 \neq 0$ then t_2 is a parameter.
- When $b_2 = c_2 = 0$ then the pre-MPTL is singular.

We are interested in cusps of the MPTL, so we ignore the case of the pre-MPTL being singular. By Definition 2.4.1.2 the parametrization of the MPTL is

$$\frac{1}{2}\left(t_1 + t_2, a + f(t_1) + g(t_2)\right).$$

We have the following.

Proposition 2.4.3.1 *A point of the MPTL of a smooth plane curve γ corresponding to $\gamma(t_1)$ and $\gamma(t_2)$, neither of which is an inflexion, is an ordinary cusp if and only if it is also on the AESS and the affine normals of γ at $\gamma(t_1)$ and at $\gamma(t_2)$ are not parallel. The point of the MPTL is a swallowtail point if and only if it is also on the AESS, the affine normals at $\gamma(t_1)$ and at $\gamma(t_2)$ are parallel, and the affine curvatures of γ at $\gamma(t_1)$ and $\gamma(t_2)$ are not equal.*

Proof. Solving $df/dt_1 = dg/dt_2$ for t_2 in terms of t_1 gives the following parametrization $M(t_1)$ of the MPTL near $t_1 = 0$:

$$M(t_1) = \left(\left(\frac{b_2 + c_2}{2b_2}\right)t_1 + \cdots, \frac{a}{2} + \frac{c_2(b_2 + c_2)}{2b_2}t_1^2 \cdots\right).$$

Note that this assumes $b_2 \neq 0$. Hence the MPTL is non-regular at $t_1 = 0$ if and only if $b_2 + c_2 = 0$, and so we require that $b_2 = -c_2 \neq 0$. (We ignore the case $b_2 = c_2 = 0$, since in this case the pre-MPTL is singular.) When $b_2 = -c_2$,

it can be shown that

$$\begin{aligned}\frac{d^2M}{dt_1^2}(0) &= \left(\frac{3(c_3-b_3)}{2b_2},0\right),\\ \frac{d^3M}{dt_1^3}(0) &= \left(\frac{3(9b_3(c_3-b_3)+4b_2(b_4+c_4)}{2b_2^2},6(b_3-c_3)\right).\end{aligned}$$

These are linearly independent if and only if $b_3 \neq c_3$. Hence, there is an ordinary cusp on the MPTL at $t_1 = t_2 = 0$ if and only if $b_2 = -c_2 \neq 0$ and $b_3 \neq c_3$. Now consider when the first two derivatives of $M(t_1)$ are zero. This is happens if and only if $(b_2 + c_2) = (b_3 - c_3) = 0$. Then

$$\begin{aligned}\frac{d^3M}{dt_1^3}(0) &= \left(\frac{6(b_4+c_4)}{b_2},0\right),\\ \frac{d^4M}{dt_1^4}(0) &= \left(\frac{6(12(b_4+c_4)+5b_2(c_5-b_5)}{b_2^2},-36(b_4+c_4)\right).\end{aligned}$$

These are linearly independent if and only if $b_4 + c_4 \neq 0$. Hence, there is a swallowtail point on the MPTL at $t_1 = t_2 = 0$ if and only if $b_2 = -c_2 \neq 0$, $b_3 = c_3$ and $b_4 \neq c_4$. The proof of Proposition 2.4.2.1 gives the interpretations of these conditions, and so we get the required result. □

2.4.4 A Projective Transformation which Creates a Swallowtail Point on the AESS

From Propositions 2.4.2.1, 2.4.3.1 we know that a swallowtail point occurs on the AESS and on the MPTL when the tangents to the curves at the contributing points are parallel, the affine normals are parallel and the affine curvatures are not equal. The question is, can such a swallowtail point be created on the AESS and on the MPTL by a family of projective transformations? This section gives an example of such a transition. We start with a cusp of the AESS given by parallel tangents to the two arcs and then take a projective transformation on the two arcs so the corresponding point of the AESS becomes a swallowtail point given by parallel tangents and parallel affine normals at the corresponding

points of the transformed arcs. Hence, the local coordinate system of such a situation is given by (2.13), but with $b_2 = -c_2$:

$$\left.\begin{array}{rcl} \gamma_1(t_1) = (t_1, f(t_1)) & = & (t_1, c_2t_1^2 + c_3t_1^3 + c_4t_1^4 + \cdots) \ , \\ \gamma_2(t_2) = (t_2, a + g(t_2)) & = & (t_2, a - c_2t_2^2 + b_3t_2^3 + b_4t_2^4 + \cdots) \ . \end{array}\right\} \tag{2.15}$$

So the tangents are parallel at the points $\gamma_1(0)$ and $\gamma_2(0)$, which, because $b_2 = -c_2$, contribute to the AESS (see the start of §2.4.2). Then, by Propositions 2.4.2.1, 2.4.3.1, the point $(0, a/2)$ is a cusp of the AESS and of the MPTL. We assume that $b_3 \neq c_3$, since this means that the affine normals $\gamma_1''(0)$, $\gamma_2''(0)$ are not parallel, and so, again by Propositions 2.4.2.1, 2.4.3.1, the point $(0, a/2)$ is neither a swallowtail point of the AESS nor of the MPTL.

It can be shown that an example of a projective transformation which keeps the tangents parallel at the points to which $\gamma_1(0)$ and $\gamma_2(0)$ are taken, while making parallel the affine normals at these transformed points is

$$\begin{array}{l} (x : y : z) \mapsto (Ax + By + Cz : Dx + Ey + Fz : Gx + Hy + Kz) \ , \\ \text{where} \ \ G = 0, \quad H = \dfrac{K(c_3 - b_3)}{ab_3} \ . \end{array}$$

So there is some freedom of choice for the other constants in the projective transformation. If one chooses $A = 1$, $B = C = D = 0$, $E \neq 0$, $F = 0$, $K = 1$ then the result is a non-singular projective transformation. It can be shown that this transformation keeps the tangents to the curve parallel at $\gamma_1(0)$ and at $\gamma_2(0)$, so the swallowtail point can be easily identified in pictures of the example to follow in §2.4.5. A point of the transformed curve is given by

$$(x, y) \mapsto \left(\frac{x}{Hy + 1} \ , \frac{Ey}{Hy + 1} \right), \quad \text{where} \ \ H = \frac{c_3 - b_3}{ab_3} \ .$$

If we also want the point $(0, a)$ to be sent to $(0, a)$ then

$$(0, a) \mapsto \left(0, \frac{Ea}{Ha + 1} \right) = (0, a) \iff E = Ha + 1 \ ,$$

and so a point of the transformed curve is given by

$$\left(\frac{x}{Hy + 1} \ , \frac{(Ha + 1)y}{Hy + 1} \right), \quad \text{where} \ \ H = \frac{c_3 - b_3}{ab_3} \ . \tag{2.16}$$

Hence, the points of the transformed arcs are given by

$$\gamma_1(t_1) \mapsto \left(\frac{ab_3t_1}{(c_3-b_3)(c_2t_1^2+\cdots)+ab_3}, \frac{ac_3(c_2t_1^2+\cdots)}{(c_3-b_3)(c_2t_1^2+\cdots)+ab_3} \right),$$
$$\gamma_2(t_2) \mapsto \left(\frac{ab_3t_2}{(c_3-b_3)(a-c_2t_2^2+\cdots)+ab_3}, \frac{ac_3(a-c_2t_2^2+\cdots)}{(c_3-b_3)(a-c_2t_2^2+\cdots)+ab_3} \right).$$

From Propositions 2.4.2.1, 2.4.3.1, the condition to ensure that no worse than a swallowtail point occurs on the AESS and on the MPTL of the transformed curve is that the affine curvatures of the transformed arcs at $t_1 = t_2 = 0$ are not equal. Calculation shows that this is true for the projectively transformed curve given by (2.16) if and only if

$$c_2^2(c_3^2 - b_3^2) + a(b_4c_3^2 + c_4b_3^2) \neq 0 \ . \tag{2.17}$$

2.4.5 Example of Creating a Swallowtail Transition on the AESS and on the MPTL

Taking projective transformations near to the one which creates a swallowtail point on the MPTL and on the AESS at the point corresponding to $t_1 = t_2 = 0$, a swallowtail transition can be created on the MPTL and on the AESS. The following example shows this. The standard swallowtail transition is as in Figure 2.13, which we want to happen on the MPTL and on the AESS for the following choice of arcs. The local coordinate system of the original two arcs is as in (2.15), with

$$a = 4, \quad b_2 = -0.2, \quad b_3 = 0.2, \quad b_4 = -0.25, \quad c_2 = 0.2, \quad c_3 = 0.3, \quad c_4 = 0.35$$

and all of the higher order coefficients zero, so that the arcs of (2.15) become the following:

$$\left.\begin{array}{rcl} \gamma_1(t_1) = (t_1, f(t_1)) & = & (t_1, 0.2t_1^2 + 0.3t_1^3 + 0.35t_1^4) \ , \\ \gamma_2(t_2) = (t_2, a + g(t_2)) & = & (t_2, 4 - 0.2t_2^2 + 0.2t_2^3 - 0.25t_2^4) \ . \end{array}\right\} \tag{2.18}$$

Note that $b_3 - c_3 = -0.1 \neq 0$, which ensures there is not a swallowtail point on the AESS and on the MPTL of the two arcs γ_1, γ_2 near to $t_1 = t_2 = 0$.

Finally we need the condition (2.17) to be satisfied for there to be a swallowtail point and no worse created on the AESS and on the MPTL. This condition is satisfied, since

$$c_2^2(c_3^2 - b_3^2) + a(b_4c_3^2 + c_4b_3^2) = -0.032 \neq 0 \ .$$

Then the projective transformation as in Definition 2.2.8 making the point of the AESS and the point of the MPTL corresponding to $t_1 = t_2 = 0$ a swallowtail point of the AESS and of the MPTL has

$$\begin{aligned} &A = 1, \quad B = C = D = 0, \quad F = 0, \quad G = 0, \quad K = 1, \\ &H = \frac{K(c_3 - b_3)}{(ab_3)} = 0.125, \quad \text{so} \quad E = Ha + 1 = 1.5. \end{aligned}$$

If we take these values for $A, \ldots, K$, but treat H as a parameter, we get a family of transformed arcs:

$$\left(\frac{t_1}{H(0.2t_1^2 + 0.3t_1^3 + 0.35t_1^4) + 1}, \frac{1.5(0.2t_1^2 + 0.3t_1^3 + 0.35t_1^4)}{H(0.2t_1^2 + 0.3t_1^3 + 0.35t_1^4) + 1} \right), \quad (2.19)$$

$$\left(\frac{t_2}{H(4 - 0.2t_2^2 + 0.2t_2^3 - 0.25t_2^4) + 1}, \frac{1.5(4 - 0.2t_2^2 + 0.2t_2^3 - 0.25t_2^4)}{H(4 - 0.2t_2^2 + 0.2t_2^3 - 0.25t_2^4) + 1} \right). \quad (2.20)$$

Figures 2.14 and 2.15 are of the original arcs before any projective transformation, that is γ_1 and γ_2 as in (2.18). Figures 2.16 to 2.19 are of arcs given by taking projective transformations on the arcs (2.18), which result in the arcs given by (2.19), (2.20), for different values of H. In this way we observe a swallowtail transition on the AESS and on the MPTL. It is hard to see what is happening in the pictures, as what we are interested in takes place in a very small neighbourhood of a point of the MPTL and AESS. The transition is clearer in Figure 2.20, which is a 'cartoon' of the transition, showing the main features of Figures 2.16 to 2.19. This example shows that the combinatorial structure of the AESS (and of the MPTL) can be altered by a family of projective transformations, since two swallowtails (the piece of curve with two cusps as in Figure 2.13, right) are created and then made smooth, one on the AESS and one on the MPTL.

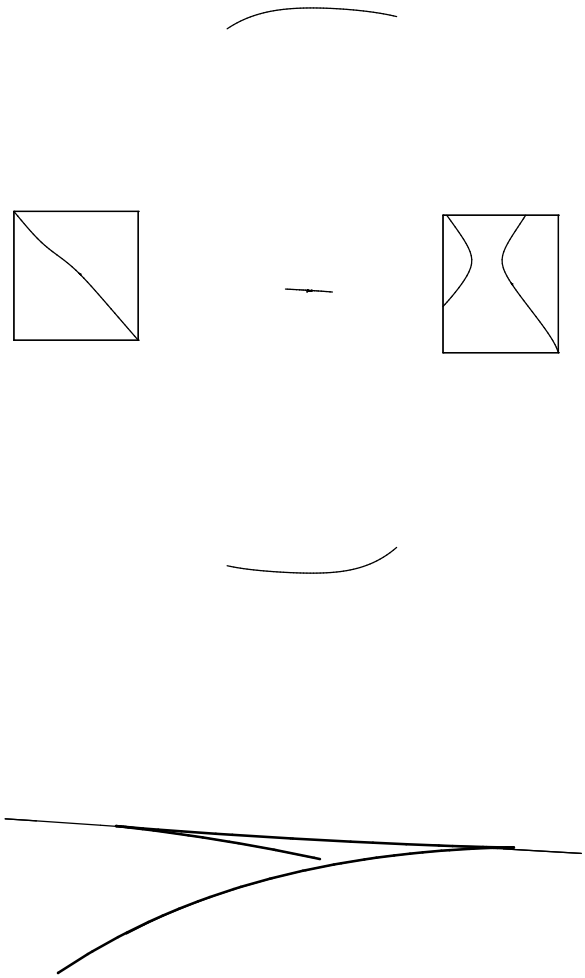

Figure 2.14: Top: the two arcs given by (2.18) are drawn with the MPTL (thick curve) and AESS (thin curve) corresponding to points of contact between a conic and a point on each of the two arcs. The pre-MPTL is in a box on the left of the picture, with the pre-AESS in a box on the right of the picture. Bottom: a closer look at the AESS and MPTL.

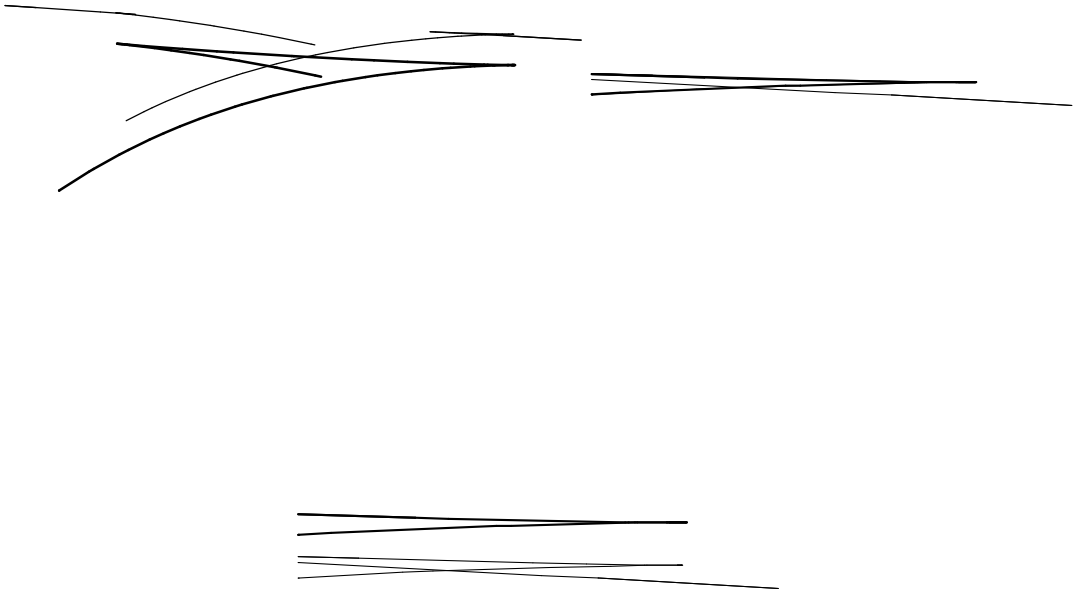

Figure 2.15: Top: the same view as for Figure 2.14, but with the MPTL shifted down. There are two swallowtails on the AESS, but two of the cusps result from vertical tangents to the pre-AESS (see Figure 2.14). Bottom left: zoom on the right-hand cusp of the MPTL. We are only interested in what happens near here since the MPTL has a horizontal tangent at the cusp. Bottom right: same view as for bottom left but with the MPTL shifted up.

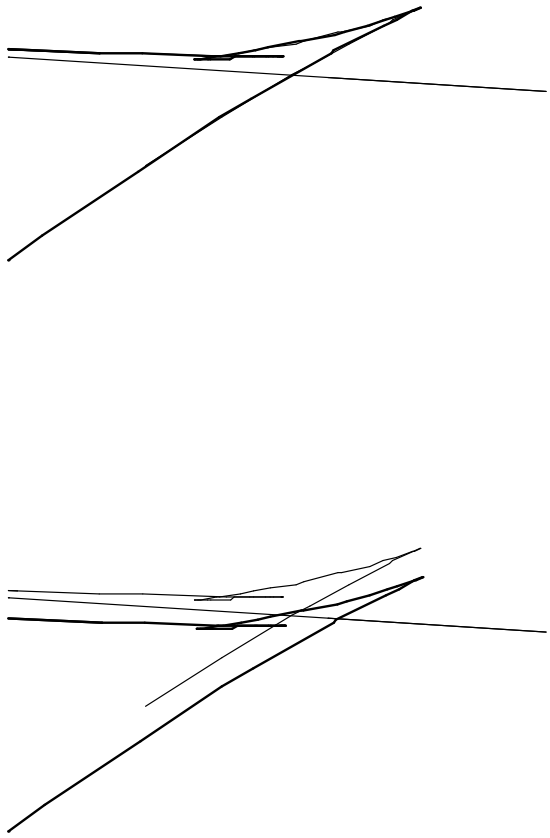

Figure 2.16: The sequence of Figures 2.16 to 2.19 are of arcs given by taking projective transformations on those of Figure 2.14, which result in the arcs given by (2.19), (2.20), for different values of H. This figure is for $H = 0.093$. We concentrate on the neighbourhood of the points of the AESS and MPTL with horizontal tangents, since it has been shown in §§2.4.4, 2.4.5 that when $H = 0.125$ a swallowtail point will be created here on the AESS and on the MPTL. Bottom: the MPTL is shifted down in the same view as in the picture at the top. Each of the MPTL and the AESS has acquired a swallowtail.

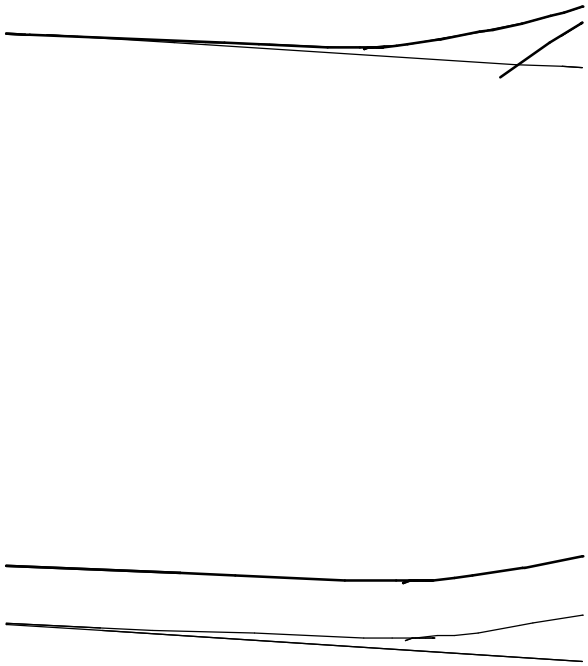

Figure 2.17: This figure is for $H = 0.1$. Again the picture at the bottom is of the same view as in the picture at the top, but with the MPTL shifted up. The two swallowtails have got smaller and they will continue to shrink until they become swallowtail points.

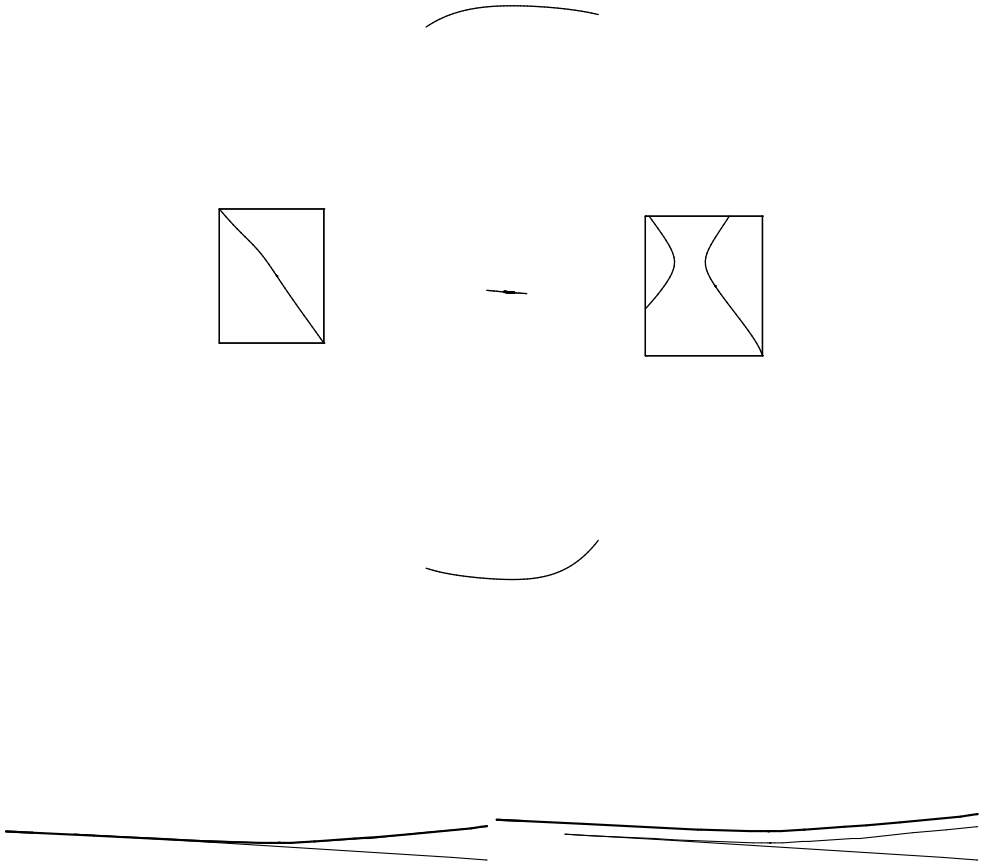

Figure 2.18: Here $H = 0.125$, so the MPTL and the AESS have a swallowtail point. Top: the transformed arcs, MPTL, AESS, pre-MPTL, and pre-AESS. Note the pre-AESS has not changed, as expected. Bottom left: a closer look at the area near the swallowtail point (recognized by the MPTL having a horizontal tangent), bottom right: same view as for bottom left, but with the MPTL shifted up.

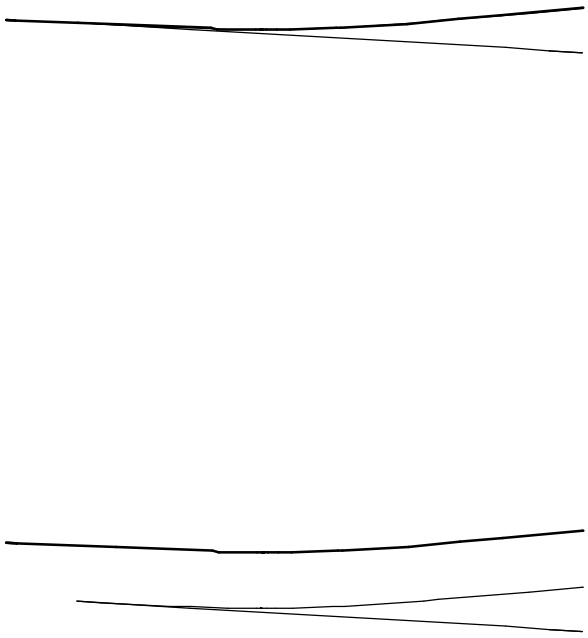

Figure 2.19: Now $H = 0.14$, and the picture at the bottom has the MPTL shifted up in the same view as in the picture at the top. This figure shows the area near where the swallowtail point *was* – now the AESS and the MPTL are smooth curves at the point where the tangent to the MPTL and to the AESS is horizontal.

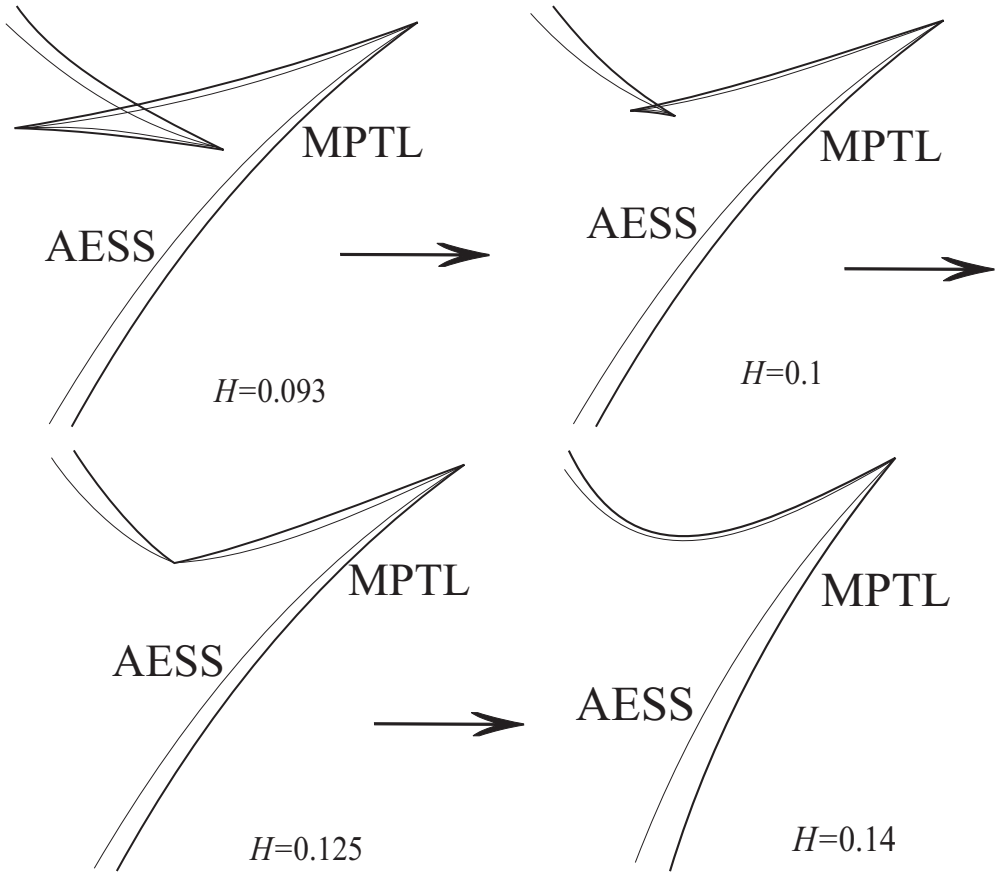

Figure 2.20: Cartoon of the example of creating a swallowtail transition by a family of projective transformations, as in Figures 2.16 to 2.19. The two swallowtails shrink until they become coincident swallowtail points and then these points become smooth points of the MPTL and AESS.

2.4.6 Examining the Direction in which Cusps Face on the MPTL and AESS

Figures 2.16 to 2.19 show a swallowtail transition in which a cusp of the swallowtail on the AESS faced in the same direction as a cusp of the swallowtail on the MPTL. In other examples cusps of the MPTL have been observed to face the coincident cusps of the AESS. Hence an interesting question is whether or not coincident cusps of the AESS and of the MPTL face in the same direction or the opposite direction 'near' to a swallowtail point arising because of tangents being parallel and affine normals being parallel at two points of the curve contributing to the AESS? If so, a swallowtail transition such as that of Figure 2.21 might be possible on the AESS and one the MPTL. 'Near' means curves which can be perturbed slightly to give a swallowtail point on the MPTL and on the AESS. One would suspect that the cusps do face the same way near to such a swallowtail point, since the MPTL and the AESS both have swallowtails in which each cusp of the MPTL coincides with a cusp of the AESS. The following shows this is true.

If we go back to the local coordinate system with two arcs parallel to the x-axis and a cusp on the MPTL at the point corresponding to $t_1 = t_2 = 0$, so this point is a cusp of the AESS, then the two arcs γ_1, γ_2 are given by (2.15). The corresponding parametrization of the MPTL as used in the proof of Proposition 2.4.3.1 is given by:

$$\left(\frac{3}{4}\frac{(b_3 - c_3)}{c_2}t_1^2 + \cdots, \frac{a}{2} + (b_3 - c_3)t_1^3 + \cdots\right).$$

The sign of $\epsilon_1 = \frac{(b_3 - c_3)}{c_2}$ determines which side of the y-axis the MPTL lies on:

$$\text{if } \epsilon_1 = \frac{(b_3 - c_3)}{c_2} > 0 \quad , \quad \text{the cusp is to the right of the } y\text{-axis},$$

$$\epsilon_1 = \frac{(b_3 - c_3)}{c_2} < 0 \quad , \quad \text{the cusp is to the left of the } y\text{-axis}.$$

The proof of Proposition 2.4.2.1 also used a parametrization of the AESS of the arcs γ_1, γ_2 given by (2.15):

$$\left(\frac{3}{4}\frac{c_3}{b_3}\frac{(b_3 - c_3)}{c_2}t_1^2 + \cdots, \frac{a}{2} + \frac{1}{2}\frac{c_3(b_3 - c_3)(b_3 + c_3)}{b_3^2}t_1^3 + \cdots\right).$$

The sign of $\epsilon_2 = \frac{c_3}{b_3}\frac{(b_3-c_3)}{c_2}$ determines which side of the y-axis the AESS lies on:

$$\text{if } \epsilon_2 = \frac{c_3}{b_3}\frac{(b_3-c_3)}{c_2} > 0 \quad , \quad \text{the cusp is to the right of the } y\text{-axis,}$$
$$\epsilon_2 = \frac{c_3}{b_3}\frac{(b_3-c_3)}{c_2} < 0 \quad , \quad \text{the cusp is to the left of the } y\text{-axis.}$$

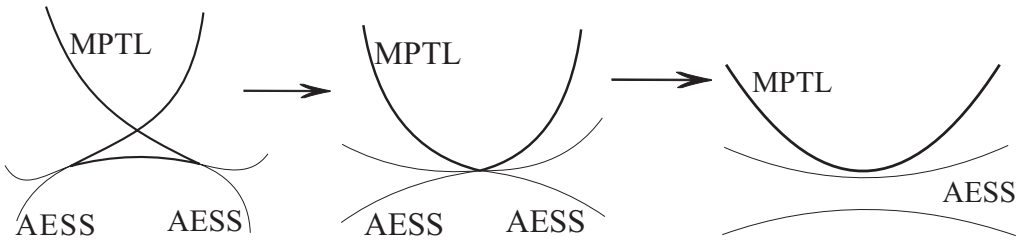

Figure 2.21: From Proposition 2.4.6.1 for curves close to a swallowtail point given by parallel affine tangents and parallel affine normals, coincident cusps on the AESS and on the MPTL face in the same direction. Hence, in this case, the swallowtail transition as pictured cannot happen.

For the two cusps to face each other then ϵ_1 and ϵ_2 must have opposite signs, but $\epsilon_2 = \epsilon_1 c_3/b_3$, so we need c_3/b_3 to be negative. However,we are interested in cusps that are part of a swallowtail of the AESS of curves 'near to' a curve with a swallowtail point given by parallel affine tangents and parallel affine normals at points which contribute to the AESS, and this means that b_3 is close to c_3. So c_3/b_3 cannot be negative for curves near to one with such a swallowtail point. Hence

Proposition 2.4.6.1 *For curves close to a curve with a swallowtail point arising because of parallel tangents and parallel affine normals at points contributing to the AESS, a cusp that is part of the swallowtail of the MPTL faces in the same direction as the corresponding cusp of the AESS.*

This means that the swallowtail transition as in Figure 2.21 cannot occur for a swallowtail point arising in this way. The swallowtail transition which does happen is as in the last three pictures of Figure 2.20.

2.4.7 Conditions for the Standard Swallowtail Transition

Figures 2.14 to 2.19 show swallowtail transitions on the AESS and on the MPTL, but it would be good to check that these are the standard pictures of a swallowtail transition. We shall do this by regarding each as an envelope of lines: from Definition 2.4.1.2 it can be shown that the MPTL can also be defined as the envelope of lines halfway between points of γ with parallel tangents, and it can also be shown that the AESS is the envelope of lines halfway between points of γ with at least 3-point contact with a conic (see [GS00]).

Consider a family of lines in the plane given by

$$F(t,x,y) \equiv y + m(t)x + c(t) = 0 \ . \tag{2.21}$$

The envelope is obtained by solving (2.21) with

$$\frac{\partial F}{\partial t} = \dot{m}(t)x + \dot{c}(t) = 0 \ ,$$

where $\dot{}$ (dot) denotes differentiation with respect to t. Now consider a family of these envelopes:

$$\left.\begin{array}{r} G(t,u,x,y) \equiv y + m(t,u)x + c(t,u) = 0, \\ \text{where} \ \ G_0(t) = G(t,u_0,x_0,y_0) \ \ \text{for } u_0,\ x_0,\ y_0 \text{ constants.} \end{array}\right\} \tag{2.22}$$

For $u = u_0$ the situation is the same as in (2.21). Consider the set

$$E = \left\{ (u,x,y) \in \mathbb{R}^3 : G = \frac{\partial G}{\partial t} = 0 \ \ \text{at} \ \ (t,u,x,y) \ \ \text{for some} \ \ t \right\}. \tag{2.23}$$

For $u = u_0$ this is an envelope of lines and as u_0 varies the envelopes of various families of lines are obtained. The envelopes form a surface E in (u,x,y)-space. The conditions for the sections as u_0 is changed to give the standard swallowtail transition as in Figure 2.13 are:

- (i) we need G_0 to have a singularity of type A_3 at $t = 0$,
- (ii) we need G to be a versal unfolding of the A_3 singularity,
- (iii) we require a generic family of sections of the surface E.

Compare this with [BG86, pp.179-187].

(i)

From [BG92, p.51], the condition for G_0 to have an A_3 singularity at $t = 0$ is that

$$\frac{dG_0}{dt}(0) = \frac{d^2G_0}{dt^2}(0) = \frac{d^3G_0}{dt^3}(0) = 0 \quad \text{and} \quad \frac{d^4G_0}{dt^4}(0) \neq 0 \ .$$

We also need $G_0(0) = 0$ from (2.22). Hence we require

$$\left.\begin{aligned} y_0 + m(0,u_0)x_0 + c(0,u_0) &= 0 \ , \\ m_t(0,u_0)x_0 + c_t(0,u_0) &= 0 \ , \\ m_{tt}(0,u_0)x_0 + c_{tt}(0,u_0) &= 0 \ , \\ m_{ttt}(0,u_0)x_0 + c_{ttt}(0,u_0) &= 0 \ , \\ \text{and} \quad m_{tttt}(0,u_0)x_0 + c_{tttt}(0,u_0) &\neq 0 \ , \end{aligned}\right\} \tag{2.24}$$

where suffices denote differentiation.

If $m_t(0,u_0) = 0$ then t does not give a unique point of the envelope when $u = u_0$. As an example, consider the tangents to $y = x^3$. The tangent through the point (t, t^3) is given by

$$\begin{aligned} (y - t^3) &= \frac{3t^2}{1}(x - t) \\ \text{so} \quad y &= x(3t^2) - 2t^3 \ . \end{aligned}$$

The envelope of tangents is then given by $F = \partial F/\partial t = 0$, where $F = y - x(3t^2) + 2t^3$. So the envelope is given by

$$\begin{aligned} y - x(3t^2) + 2t^3 &= 0 \\ \text{and} \quad -x(6t) + 6t^2 &= 0 \ . \end{aligned}$$

For $t = 0$ this gives the whole of the x-axis, $y = 0$, so $t = 0$ does not give a unique point of the envelope. Hence, going back to our case of a swallowtail transition, we also require that $m_t \neq 0$ at $(0, u_0)$ and therefore nearby.

We can solve the first two equations of (2.24) for x_0 and y_0 and so, for G_0

to have type A_3 at $t = 0$, we require

$$\left.\begin{array}{rcl} x_0 &=& -\frac{c_t(0,u_0)}{m_t(0,u_0)}\ , \\ y_0 &=& m(0,u_0)\frac{c_t(0,u_0)}{m_t(0,u_0)} - c(0,u_0)\ , \\ -m_{tt}(0,u_0)\frac{c_t(0,u_0)}{m_t(0,u_0)} + c_{tt}(0,u_0) &=& 0\ , \\ -m_{ttt}(0,u_0)\frac{c_t(0,u_0)}{m_t(0,u_0)} + c_{ttt}(0,u_0) &=& 0\ , \\ -m_{tttt}(0,u_0)\frac{c_t(0,u_0)}{m_t(0,u_0)} + c_{tttt}(0,u_0) &\neq& 0\ . \end{array}\right\} \quad (2.25)$$

(ii)

The second condition is that G must be a versal unfolding of the A_3 singularity. From [BG92, pp.134-140], we consider the 2-jets with constant at $t = 0$ of $\partial G/\partial u$, $\partial G/\partial x$, $\partial G/\partial y$, all evaluated at (t, u_0, x_0, y_0):

$$\begin{array}{rcl} \dfrac{\partial G}{\partial u}(t,u_0,x_0,y_0) &=& (m_u(0,u_0)x_0 + c_u(0,u_0)) \\ && + (m_{tu}(0,u_0)x_0 + c_{tu}(0,u_0))\, t \\ && + \dfrac{1}{2!}\left(m_{ttu}(0,u_0)x_0 + c_{ttu}(0,u_0)\right) t^2 + \cdots\ , \\ \dfrac{\partial G}{\partial x}(t,u_0,x_0,y_0) &=& (m(0,u_0)) + (m_t(0,u_0))t + \dfrac{1}{2!}(m_{tt}(0,u_0))t^2 + \cdots\ , \\ \dfrac{\partial G}{\partial x}(t,u_0,x_0,y_0) &=& 1\ . \end{array}$$

Then, we have versality if and only if the rank of the matrix of coefficients is 3

$$\begin{array}{rcl} & & \left|\begin{array}{ccc} m_u(0,u_0)x_0 + c_u(0,u_0) & m(0,u_0) & 1 \\ m_{tu}(0,u_0)x_0 + c_{tu}(0,u_0) & m_t(0,u_0) & 0 \\ m_{ttu}(0,u_0)x_0 + c_{ttu}(0,u_0) & m_{tt}(0,u_0) & 0 \end{array}\right| \neq 0 \\ \iff & & \left.\begin{array}{c} m_t(0,u_0)(m_{ttu}(0,u_0)x_0 + c_{ttu}(0,u_0)) \\ \neq m_{tt}(0,u_0)(m_{tu}(0,u_0)x_0 + c_{tu}(0,u_0))\ . \end{array}\right\} \quad (2.26) \end{array}$$

(iii)

To ensure that the family of sections $u = u_0$ of the surface E from (2.23) gives the standard pictures, we require that the plane $u = u_0$ does not contain the limit of any tangents to any of the strata passing through the (A_3) swallowtail

point. For the standard swallowtail surface, the limiting tangents to the A_2 and A_1A_1 strata are the same line, and this line is contained in the limiting tangent planes to the A_1 strata at points tending to the A_3 point. So in our case, we need only check that the limiting tangent to the A_2 stratum does not lie in the plane $u = u_0$. Hence for our surface E we need to verify that the limiting tangent to the cuspidal edge (A_2 stratum) does not lie in the plane $u = u_0$.

The cuspidal edge of E is the set (a curve in (u, x, y)-space)

$$\Sigma = \left\{ (u, x, y) \in \mathbb{R}^3 : G = \frac{\partial G}{\partial t} = \frac{\partial^2 G}{\partial t^2} = 0 \ \text{ at } \ (t, u, x, y) \ \text{ for some } \ t \right\}.$$

A tangent vector to this is obtained in the usual way:

$$\begin{array}{ccc} \mathbb{R}^4 & \xrightarrow{\tilde{G}} & \mathbb{R}^3 \\ (t, u, x, y) & \longmapsto & \left(G, \frac{\partial G}{\partial t}, \frac{\partial^2 G}{\partial t^2}\right) \\ \pi \big\downarrow & & \\ \mathbb{R}^3 & & \\ (u, x, y) & & \end{array}$$

The cuspidal edge is given by $\pi(\tilde{G}(0, 0, 0))$, and a tangent vector to the A_2 stratum is (θ, ξ, η), where $(\tau, \theta, \xi, \eta)$ is a non-zero kernel vector of the Jacobian matrix of $\tilde{G}$. So, what is required is that the limit of these tangent vectors at smooth points (u, x, y) tending to the swallowtail point does *not* lie in the plane $u = u_0$, that is the limit of u-coordinates of these vectors (θ above) is *not* zero.

The Jacobian matrix of $\tilde{G}$ is

$$\begin{pmatrix} G_t & G_u & G_x & G_y \\ G_{tt} & G_{tu} & G_{tx} & G_{ty} \\ G_{ttt} & G_{ttu} & G_{ttx} & G_{tty} \end{pmatrix}.$$

At a point of the cuspidal edge which is not the swallowtail point, $G = G_t = G_{tt} = 0$ and $G_{ttt} \neq 0$, so kernel vectors of the Jacobian matrix evaluated at this

point of the cuspidal edge are given by

$$\begin{pmatrix} 0 & m_u x + c_u & m & 1 \\ 0 & m_{tu} x + c_{tu} & m_t & 0 \\ G_{ttt} & m_{ttu} x + c_{ttu} & m_{tt} & 0 \end{pmatrix} \begin{pmatrix} \tau \\ \theta \\ \xi \\ \eta \end{pmatrix} = \begin{pmatrix} 0 \\ 0 \\ 0 \end{pmatrix}.$$

This gives an equation to determine η:

$$(m_u x + c_u)\theta + m\xi + \eta = 0 \ , \tag{2.27}$$

an equation to determine τ:

$$G_{ttt}\tau + (m_{ttu} x + c_{ttu})\theta + m_{tt}\xi = 0 \ , \tag{2.28}$$

and another equation to get ξ in terms of θ:

$$(m_{tu} x + c_{tu})\theta + m_t \xi = 0 \ . \tag{2.29}$$

We start with a non-zero tangent vector (θ, ξ, η) to the A_2 stratum in (u, x, y)-space where $(\tau, \theta, \xi, \eta)$ is a non-zero kernel vector of the Jacobian of G. Then we let this tangent vector tend towards a non-zero tangent vector at the A_3 point. Now consider when $\theta = 0$, then by (2.29) ξ must also be zero as $m_t(0, u_0) \neq 0$ is assumed. Then, by (2.27) η must also be zero, which gives $(\tau, \theta, \xi, \eta) = \mathbf{0}$. Hence no non-zero tangent vector to the cuspidal edge in (u, x, y)-space exists with the first component $\theta = 0$. Therefore the limiting tangent to the cuspidal edge cannot lie in the plane $u = u_0$.

In summary, *the sections of $u = u_0$ and E as u_0 varies form the standard swallowtail transition if and only if the point $(t, u, x, y) = (0, u_0, x_0, y_0)$ is an A_3 singularity (and so satisfies (2.25)), and u, x, y are versal unfolding parameters (so (2.26) is satisfied at $(0, u_0, x_0, y_0)$).*

2.4.8 Verification of Conditions for the Swallowtail Transitions on the AESS and on the MPTL

The conditions (2.25) and (2.26) for a family of envelopes of lines to give the standard swallowtail transition need to be checked for the swallowtail transitions of the AESS and MPTL from §2.4.4 and §2.4.5. The two arcs γ_1, γ_2 as

in (2.15) that were projectively transformed so that a swallowtail point was created on the AESS and on the MPTL were given by (2.16):

$$\gamma_1(t_1) \mapsto \left(\frac{ab_3t_1}{(c_3-b_3)(c_2t_1^2+\cdots)+ab_3}, \frac{ac_3(c_2t_1^2+\cdots)}{(c_3-b_3)(c_2t_1^2+\cdots)+ab_3} \right),$$
$$\gamma_2(t_2) \mapsto \left(\frac{ab_3t_2}{(c_3-b_3)(a-c_2t_2^2+\cdots)+ab_3}, \frac{ac_3(a-c_2t_2^2+\cdots)}{(c_3-b_3)(a-c_2t_2^2+\cdots)+ab_3} \right).$$

Using the same method as in the proof of Proposition 2.4.2.1, we can express t_2 in terms of t_1 such that the points of the transformed curve corresponding to t_1, t_2 contribute to the AESS. Then the family of midlines (that is infinitesimal axes of affine reflexional symmetry of a curve) whose envelope is the AESS is given by

$$G_1(t_1, x, y) \equiv M_1(t_1, t_2(t_1))x + y + C_1(t_1, t_2(t_1)) \ ,$$

where M_1, and C_1 are known functions of t_1. If we now assume H is a function of u, so $H = q_0+q_1u+q_2u^2+q_3u^3+\cdots$, then $M_1 = M_1(t_1, u)$ and $C_1 = C_1(t_1, u)$ so we have the same situation as in (2.22). Hence, increasing u from positive to negative values gives a transition. We want $u = 0$ to correspond to the A_3 point, so we let $q_0 = (c_3 - b_3)/ab_3$.

The conditions for $t_1 = 0$ to give an A_3 singularity are given by replacing m, c by M_1, C_1 in (2.25) and (2.26). The first two conditions of (2.25) give x_0 and y_0 in terms of the original arcs and it can be shown that the third and fourth conditions of (2.25) are automatically satisfied. Also, from (2.25) we require

$$\frac{\partial M_1}{\partial t_1}(0,0) \neq 0 \iff c_2c_3 \neq 0 \ .$$

Then, the last condition of (2.25) is satisfied if and only if

$$c_3\left(ac_4b_3^2 + ab_4c_3^2 + c_2^2(c_3^2 - b_3^2)\right) \neq 0 \ . \tag{2.30}$$

Given that the A_3 conditions are satisfied, the versality condition (2.26) is satisfied if and only if $c_3c_2aq_1 \neq 0$, so let $q_1 = 1$, so that $H(u) = (c_3 - b_3)/(ab_3) + u + \cdots$. Then the versality condition is that

$$ac_2c_3 \neq 0 \ . \tag{2.31}$$

The condition (2.30) is the same as (2.17), which is the condition to ensure that no worse than a swallowtail point occurs on the AESS and on the MPTL of the transformed curve, given at least an A_3 singularity. This is the same as the affine curvatures of the transformed arcs at $t_1 = t_2 = 0$ being not equal.

The same method can be carried out for the MPTL, which is the envelope of the family of lines halfway between points of a curve with parallel tangents. This gives rise to the same conditions (2.30) and (2.31) for the transition on the MPTL to be a swallowtail transition. Hence we can check (2.30) and (2.31) for both the AESS and the MPTL.

In the example of §2.4.5, the values taken for the arcs of (2.15) were

$$a = 4, \quad b_2 = -0.2, \quad b_3 = 0.2, \quad b_4 = -0.25, \quad c_2 = 0.2, \quad c_3 = 0.3, \quad c_4 = 0.35$$

and all coefficients of higher order terms zero (that is $b_i = c_j = 0$ for $i \geq 5$, $j \geq 5$). Since the conditions (2.30), (2.31) do not involve the coefficients of $H(u) = (c_3 - b_3)/(ab_3) + u + q_2u^2 + q_3u^3 + \cdots$, we can let $H = (c_3 - b_3)/ab_3 + u$, so $H(0) = q_0 = 0.125$. The values of H giving the transition were $H = 0.1$, $H = 0.125$, and $H = 0.14$. Then the values of u corresponding to these values of H are $u = -0.025$, $u = 0$, and $u = 0.15$. These values of the parameter values satisfy both (2.30) and (2.31). Therefore the transition in the example of §2.4.5 is the standard swallowtail transition on the AESS and on the MPTL.

2.4.9 Altering the Structure of the AESS and of the MPTL by Projective Transformations

In §2.4.4 we showed that a projective transformation can simultaneously create a swallowtail point on the AESS and on the MPTL. Then §2.4.5 gave an example of a family of projective transformations which seemed to cause a swallowtail transition on the AESS and on the MPTL. In §§2.4.7, 2.4.8 we obtained and verified the conditions for the transition observed to be a genuine swallowtail transition. Hence we have the following.

Proposition 2.4.9.1 *A family of projective transformations can destroy or create cusps in pairs on the AESS and on the MPTL by causing a swallowtail*

transition to occur on the AESS and on the MPTL. Hence the combinatorial structure of the AESS can be altered by a projective transformation.

2.5 Further Research

There is a natural restriction of the ADSS by requiring that the affine distance function $d(\mathbf{x}, s)$ has an absolute minimum at one of s_1, s_2 in the pre-ADSS. By doing this the ADMA is obtained. This is because the ADSS is part of the bifurcation set of the family of affine distance functions on γ. An analogous definition of the AESS is not known, since the AESS is defined in terms of contact between curves and conics or by an envelope of lines, and so the AESS is not part of a bifurcation set. Can the AESS be defined using a distance function? If this could be done then an AEMA could be found by minimizing this distance function. Then the question is whether or not the combinatorial structure of this medial axis is unchanged by projective transformations. This topic is still to be investigated.

Also, as noted in §2.2, as yet there is no natural definition for one affine-invariant symmetry set. Hence this is a problem to be decided.

Chapter 3

The Euclidean Medial Axis in Three Dimensions

3.1 Introduction

The Euclidean symmetry set and medial axis were introduced in §1.1. In $\mathbb{R}^2$, the medial axis of a generic curve consists of smooth branches with endpoints, the branches meeting in threes at special points (see for example [GK99]). Given a smooth branch γ and a radius function r of arclength s satisfying $|dr/ds| < 1$ we can reconstruct, at any rate locally, the two corresponding parts γ^+ and γ^- of the outer boundary as an envelope of circles, centred on the smooth branch and of radius r. (See for example [GK03]; there will be other conditions which are needed for the circles to be maximal.)

However, given a connected set of smooth branches with endpoints and triple junctions it is far from obvious that this can be the medial axis of a shape with a smooth boundary. Even considering the local situation, it is not clear that from an arbitrary triple junction furnished with three radius functions (agreeing at the junction point) we can expect to recover a smooth shape. Nor is it clear that an arbitrary smooth curve with an endpoint, furnished with a radius function satisfying $r' = \pm 1$ at the endpoint, can be the medial axis of a smooth curve with a curvature extremum. In fact these two questions were

examined in detail in [GK03], where it was shown that at the triple junction there are constraints on the geometry of the three branches and on the 'dynamics', that is the derivatives of the three radius functions. Two of the simplest of these constraints are

$$\left.\begin{array}{l} \cos(\phi_2+\phi_3) = -\cos\phi_1 = \frac{dr_1}{ds_1} \ , \\ \frac{\kappa_1}{\sin\phi_1} + \frac{\kappa_2}{\sin\phi_2} + \frac{\kappa_3}{\sin\phi_3} = 0 \ , \end{array}\right\} \tag{3.1}$$

where ϕ_i is the angle between the tangent to the medial curve γ_i and the line joining the point of contact and the centre of the tritangent circle. The first of these is a constraint on the velocities of the medial curves near to an A_1^3 point. It comes from the fact that the ϕ_i add to π. Also, κ_i is the curvature of the medial curve γ_i. (See also [S99, SSG99] for work on the relationship between the curvatures of the medial axis and the boundary.)

Constraints such as those above have an important application in the study of stochastic shape. For work on this by D. Mumford, see [M03]. The constraints arise because close to a triple junction there are two ways to use the medial axis to construct each piece of the shape boundary. Given two smooth medial axis branches γ_1, γ_2, close to a triple junction, and choosing orientations suitably, we reconstruct $\gamma_1^{\pm}$ and $\gamma_2^{\pm}$. Then γ_1^+ must agree with γ_2^- at the point where they meet. (See Figure 3.1.)

On the other hand in [GK03] it is shown that there is no constraint on the medial axis and radius function at an endpoint, beyond the fact that r'' should be non-zero at the endpoint – in fact if arclength is measured towards the endpoint then r'' should be > 0 to ensure a minimum of radius. An explicit formula is given for the curvature κ of the medial axis at its endpoint, in terms of the curvature k say of the boundary curve of the shape at the corresponding point, an extremum of curvature:

$$\kappa = -\frac{3}{5}\frac{k^3 k'''}{(k'')^2} \ , \tag{3.2}$$

where $'$ ('prime') means differentiation with respect to arclength on the boundary of the shape. Notice that this formula does not make any reference to the radius function.

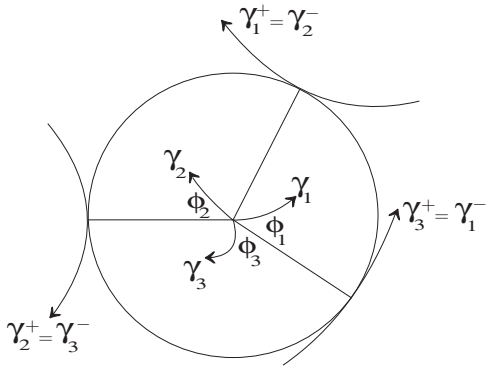

Figure 3.1: The A_1^3 case in 2D, where three smooth medial branches meet at an A_1^3 point. At this point the medial axis must satisfy certain conditions, such as (3.1), in order for the boundary to be smoothly reconstructed by an envelope of circles centred on the medial axis.

In this chapter we take the step from $\mathbb{R}^2$ into $\mathbb{R}^3$. In $\mathbb{R}^3$, the medial axis M of a generic surface S, referred to as the boundary surface, has one of the local forms given in Figure 3.2. We shall refer to these by their standard names from singularity theory, where A_k means that the contact between S and a sphere has this singularity type. Thus A_1 means that the centre c of the sphere lies on the normal line to S at a point p, making 'ordinary tangency' between the sphere and S at p; A_2 means that c is a centre of principal curvature of S at p; and A_3 that in addition p is a 'ridge point' (see for example [HGYGM99]). Juxtaposition indicates more than one contact point; thus $A_1A_1 = A_1^2$ indicates a sphere ordinarily tangent at two points.

This chapter examines in greater detail research that has already appeared [PGK04] and in a form [PGK05] intended for submission to in a journal. It examines connections between the geometry of the medial axis and dynamics of the associated radius functions at points of these local forms of the medial axis. The following cases are examined.

- The A_1^3 case: when three smooth sheets of the medial axis intersect in a curve, called the A_1^3 curve. Points of this curve are called A_1^3 points. Alternatively they are referred to as 'Y-junction curves, points'.

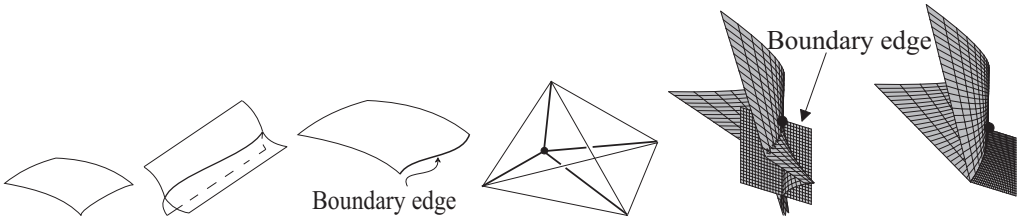

A_1^2 A_1^3 A_3 A_1^4 A_1A_3 SS A_1A_3 MA

Figure 3.2: The local forms of the medial axis in $\mathbb{R}^3$ in the generic case. Thus A_1^2 is a smooth sheet, A_1^3 is a Y-junction curve, A_3 is a boundary edge of a smooth sheet, A_1^4 is a point where four A_1^3 curves lying on six sheets meet. Finally the 'A_1A_3 SS' picture shows the 'symmetry set', consisting of a swallowtail surface and a smooth sheet with boundary; this is truncated as shown in the A_1A_3 medial axis picture. The point where the boundary (A_3) edge and the Y-junction (A_1^3) curve end is the A_1A_3 point, also called a 'fin point'.

- The A_3 case: where the two points of contact on the boundary surface of a single medial axis sheet come into coincidence. This corresponds to the medial axis being locally a surface with boundary – this boundary is the A_3 curve, referred to as the 'edge' of the medial axis, whose points are A_3 points.

- The A_1^4 case: the point at which six smooth sheets of the medial axis intersect, called an A_1^4 point, or '6-junction point'. At this point, four A_1^3 curves intersect, corresponding to a sphere tangent to the boundary in four points.

- The A_1A_3 case: where an A_1^3 curve and an A_3 curve meet and end, also called a 'fin point', since the medial axis looks locally like a fin emerging from another surface.

Here is a brief summary of the sections of this chapter.

§3.2: **A Coordinate System for the Medial Axis in Three Dimensions.** This introduces the geometry and dynamics of the medial axis and gives formulae to be used in the rest of the chapter.

§3.3: **Radial Shape Operator.** We review the definitions of Damon's radial shape operator [D03, D04, D05] and formulae connecting the differential shape operator of the boundary and radial shape operator. We choose a basis for our case of a two-dimensional medial axis and obtain a connection between the trace, determinant of the corresponding radial shape operator matrix. Also we obtain an expression for the principal directions on the boundary to be used in the A_1^3 case in §3.4.

§3.4: **The A_1^3 Case.** We obtain constraints on the geometry and dynamics of the three medial sheets analogous to those discovered in the case of the medial axis in two dimensions. We equate normals of the corresponding boundary surfaces to discover first order information about the medial axis. Then we use §3.3 to equate principal curvatures and principal directions on the boundaries to discover second order information about the medial axis.

§3.5: **First Example of the A_1^3 Case.** We take three general cylinders as the medial axis near to an A_1^3 curve, where the radius functions r_1, r_2, r_3 are unknown. Then we see what information we can obtain from the A_1^3 constraints of §3.4 about the radius functions.

§3.6: **Second Example of the A_1^3 Case.** We take a parabolic gutter and a plane as the boundary near to an A_1^3 curve, so all of the terms in the A_1^3 constraints of §3.4 can be calculated. Hence we can check that these constraints are satisfied in this example.

§3.7: **The A_1^4 Case.** Consistency conditions on the medial axis are obtained at A_1^4 points, using the constraints of §3.4.

§3.8: **The A_3 Case.** We discover a restriction on the radius function at an A_3 point similar to that in two dimensions. Also we find a limiting value for the Gauss curvature of the medial axis in terms of the geometry of the boundary at an A_3 point.

§3.9: **The A_1A_3 Case.** We obtain the limiting form of the constraints in the A_1^3 case as two of the points of contact come into coincidence. We revisit the second A_1^3 example from §3.6 to illustrate the A_1A_3 case.

3.2 A Coordinate System for the Medial Axis in Three Dimensions

In order to obtain results analogous to (3.1) in $\mathbb{R}^3$ we shall need to describe carefully the construction of the boundary surface S from its medial axis M and the radius function r. We begin with some definitions and formulae concerning the geometry of the medial axis in $\mathbb{R}^3$, quoted from [GK04]. Consider Figure 3.3, where there is a smooth (A_1^2) medial axis sheet γ and its corresponding local boundary surfaces γ^+ and γ^-. Thus spheres of radius r and centred on γ are tangent to the $\gamma^\pm$. We have

$$\gamma^\pm = \gamma - rN^\pm \ , \tag{3.3}$$

where $N^\pm$ is the unit normal to the boundary surface $\gamma^\pm$, oriented towards the centre of the bitangent sphere. We shall assume that near a point of interest on γ the gradient of r is non-zero and use the coordinate system given by the lines r = constant, parametrized by t, say and referred to as 't-curves', and the gradient lines of r, parametrized by r and referred to as 'r-curves'. We can fix the (r,t) coordinate system close to $(r_0,0)$ say, by taking t to be arclength along the t-curve $r = r_0$. Arclength along the r-curves will be denoted by s. Partial derivatives will be denoted by suffices in what follows.

The unit vector T is defined to be parallel to γ_r, with N a unit normal vector to the medial axis and taking $U = N \times T$ makes an orthonormal triad T, U, N. The velocity v is defined by

$$\gamma_r = vT \ , \qquad \gamma_t = wU \ , \tag{3.4}$$

for w a function which satisfies $w(r_0,t) = 1$ for all t. The velocity v is ds/dr along the r-curves and when the medial axis is a locally a smooth (A_1^2) sheet we

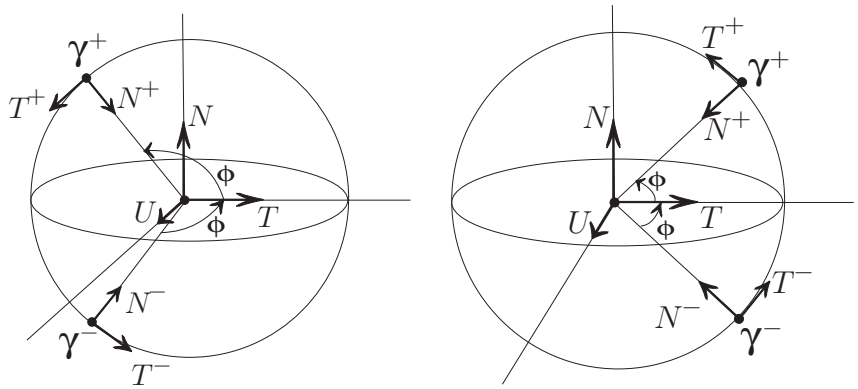

Figure 3.3: The A_1^2 case in $\mathbb{R}^3$: there is a sphere of contact between the boundary at $\gamma^{\pm}$. At the centre of the sphere of contact the unit vectors T and U lie in the tangent plane to γ and the vector N is the unit normal to γ. Also, N^+ is the unit normal to the boundary surface at γ^+ and T^+ is in the tangent plane to the boundary surface at γ^+. Similarly for N^- and T^- at γ^-. The angle ϕ is the angle between the line joining one of the contact points and the centre of the bitangent sphere. On the left ϕ is obtuse, on the right ϕ is acute. The cases where $\phi = 0, \pi/2, \pi$ are limiting cases.

can choose $v > 0$, that is T to be in the direction of ∇r (that is grad(r)), and so $T = \nabla r / \|\nabla r\|$. This corresponds to the picture on the left of Figure 3.3. In the (A_1^3) case of the medial axis being locally three intersecting sheets there are three such velocities v_i, for i =1, 2, 3, but it is not possible to choose each v_i to be positive (see §3.4.1). Even so, in this case each v_i is taken to be non-zero.

The convention of taking the boundary point γ^+ to be on the '$+N$' side of T and denoting ϕ to be the angle $(0 < \phi < \pi)$ turned anti-clockwise from T to $-N^+$, in the plane oriented by T, N, means that

$$\left.\begin{aligned} N^{\pm} &= -\cos\phi T \mp \sin\phi N \ , \\ T^{\pm} &= \mp\sin\phi T + \cos\phi N \ . \end{aligned}\right\} \tag{3.5}$$

Here the unit vector $T^{\pm}$ is tangent to $\gamma^{\pm}$ and parallel to $U \times N^{\pm}$. We have the important equation

$$\cos\phi = -\frac{1}{v} \ , \tag{3.6}$$

so that $T^{\pm}$ and $N^{\pm}$ can also be expressed in terms of v as follows:

$$\begin{aligned} N^{\pm} &= \frac{1}{v}T \mp \sqrt{1-\frac{1}{v^2}}N \ , \\ T^{\pm} &= \mp\sqrt{1-\frac{1}{v^2}}T - \frac{1}{v}N \ . \end{aligned}$$

These formulae for $N^{\pm}$, $T^{\pm}$ hold for all points of γ.

Three 'accelerations' are important and are defined by:

$$\text{radial}: \quad a = v_r \ ; \quad \text{transverse}: \quad a^t = v_t \ ; \quad \text{mixed}: \quad a^* = w_r \ .$$

Then, at $\gamma(r_0, 0)$, we have

$$\left.\begin{aligned} &\gamma_{rr} = aT + v^2 g^r U + v^2 \kappa^r N \ , \\ &\gamma_{rt} = -v g^r T + v g^t U + f N \ , \quad (\text{where} \quad f = v\tau^r = -v\tau^t) \ , \\ &\gamma_{tt} = -g^t T + \kappa^t N \ . \end{aligned}\right\} \tag{3.7}$$

Here g^r, κ^r, τ^r are the *geodesic curvature*, *normal curvature*, *geodesic torsion* of the r-curve at $(r_0, 0)$. Similarly, g^t, κ^t, τ^t are the *geodesic curvature*, *normal curvature*, *geodesic torsion* of the t-curve at $(r_0, 0)$. Some of the terms in the above can be expressed in terms of the above accelerations. We have

$$-v g^r = a^t \ \text{ and } \ v g^t = a^* \ . \tag{3.8}$$

Now consider the medial axis as an arbitrary local parametrization $\gamma(x, y)$ with an associated radius function $r(x, y)$. Then the envelope of spheres centred on γ is

$$\begin{aligned} &\left\{ \mathbf{x} : \quad \text{there exist } x, \, y \text{ with } \ F_d = \frac{\partial F_d}{\partial x} = \frac{\partial F_d}{\partial y} = 0 \right\} \ , \\ &\text{where} \ \ F_d = (\mathbf{x} - \gamma(x,y)) \cdot (\mathbf{x} - \gamma(x,y)) - (r(x,y))^2 \ . \end{aligned}$$

(This function is labelled F_d since it is similar to the distance-squared function.) Let us calculate the envelope. Let $(\mathbf{x} - \gamma(x, y)) = \lambda\gamma_x + \mu\gamma_y + \eta N$ for some λ, μ, η, where suffices denote differentiation and N is the unit normal to γ at

(x, y). So

$$\begin{aligned} F_d &= \|\mathbf{x}-\gamma\|^2 - r^2 = \lambda^2 E + 2\lambda\mu F + \mu^2 G + \eta^2 = 0 \ , \\ \frac{\partial F_d}{\partial x} &= -2\gamma_x \cdot (\mathbf{x}-\gamma) - 2rr_x = -2(\lambda E + \mu F) - 2rr_x = 0 \ , \\ \frac{\partial F_d}{\partial y} &= -2\gamma_y \cdot (\mathbf{x}-\gamma) - 2rr_y = -2(\lambda F + \mu GF) - 2rr_y = 0 \ , \end{aligned}$$

where $E = \gamma_x \cdot \gamma_x$, $F = \gamma_x \cdot \gamma_y$, $G = \gamma_y \cdot \gamma_y$. Solving the these equations for λ, μ, η gives

$$\lambda = \frac{r(Fr_y - Gr_x)}{EG - F^2} \ , \ \mu = \frac{r(Fr_x - Er_y)}{EG - F^2} \ , \ \eta = r\sqrt{1 - \frac{Er_y^2 - 2Fr_xr_y + Gr_x^2}{EG - F^2}} \ .$$

Hence, relabelling $\mathbf{x}$ as $\gamma^{\pm}$ and using (3.3), we have

$$\begin{aligned} \gamma^{\pm} &= \gamma + \frac{r\left(\gamma_x(Fr_y - Gr_x) + \gamma_y(Fr_x - Er_y)\right)}{EG - F^2} \\ &\quad \pm r\sqrt{1 - \left(\frac{Er_y^2 - 2Fr_xr_y + Gr_x^2}{EG - F^2}\right)} N \ . \end{aligned} \tag{3.9}$$

Comparison with (3.4), (3.3), (3.5) gives

$$\sin\phi = \sqrt{1 - \left(\frac{Er_y^2 - 2Fr_xr_y + Gr_x^2}{EG - F^2}\right)} \ , \tag{3.10}$$

$$\cos^2\phi = \frac{1}{v^2} = \frac{Er_y^2 - 2Fr_xr_y + Gr_x^2}{EG - F^2} \ , \tag{3.11}$$

$$\gamma_r = \frac{\gamma_x(Gr_x - Fr_y) + \gamma_y(Er_y - Fr_x)}{Er_y^2 - 2Fr_xr_y + Gr_x^2} \ . \tag{3.12}$$

3.3 Radial Shape Operator

This section contains results connecting the geometry and dynamics of a medial axis sheet with the two corresponding boundary surfaces in three-space. These are Lemmas 3.3.1.4, 3.3.2.1, 3.3.2.2 and 3.3.3.2, and will enable us to obtain expressions for the principal curvatures and principal directions on the boundary in terms of information about the medial axis and radius function. This has most importance in the A_1^3 case, in §3.4. In order to obtain these lemmas we consider the *radial shape operator* from [D03, D04, D05], introduced below.

3.3.1 Introducing the Radial Shape Operator

We consider from [D04, D05] a smooth n-dimensional boundary $B \subset \mathbb{R}^{n+1}$ with its n-dimensional medial axis $M \subset \mathbb{R}^{n+1}$ and the multivalued vector field R on M such that $B = \{x + R(x) : x \in M, \text{ all values of } R\}$. The pair (M, R) is referred to as the *skeletal structure*. (In [D03] Damon considers a more general M, that is an n-dimensional *skeletal set*, a special type of Whitney stratified set, of which a medial axis is a special case.) We have $R = rR_1$, where R_1 is a unit vector field and r is the radius function. Defined below is the *radial shape operator* S_{rad} of the skeletal structure (M, R). (In [D03, D04, D05] U is used for our R, but for us U is already in use.)

Definition 3.3.1.1 ([D04, §1]) *In a neighbourhood of a point $x_0 \in M$ with a single smooth choice of value for R, let $\psi_t(x) = x + tR(x)$ be a local representation of the radial flow from M to B, and let the radial map be given by $\psi_1(x) = x + R(x)$. (The radial map is the time one map of the radial flow.)*

See Figure 3.4, left for a picture of the radial flow.

Definition 3.3.1.2 ([D04, §1]) *At a non-edge point x_0 of M with a smooth value of R, let*

$$S_{\text{rad}}(v) = -\text{proj}_R \left(\frac{\partial R_1}{\partial v} \right),$$

for $v \in T_{x_0}M$. Here proj_R denotes projection onto $T_{x_0}M$ along R. Also, $\partial R_1/\partial v$ is the covariant derivative of R_1 in the direction of v. The principal radial curvatures κ_{ri} are the eigenvalues of S_{rad}. The corresponding eigenvectors are the principal radial directions.

In the above, the boundary points of M are called *edge points* so as not to be confused with points of B. See Figure 3.4, right for a picture of the radial shape operator.

We choose a basis $\mathbf{v} = \{v_1, \ldots, v_n\}$ for $T_{x_0}M$ and let $S_{\mathbf{v}}$ denote the matrix representation of S_{rad} with respect to this basis. Then $\partial R_1/\partial v_i$ is represented

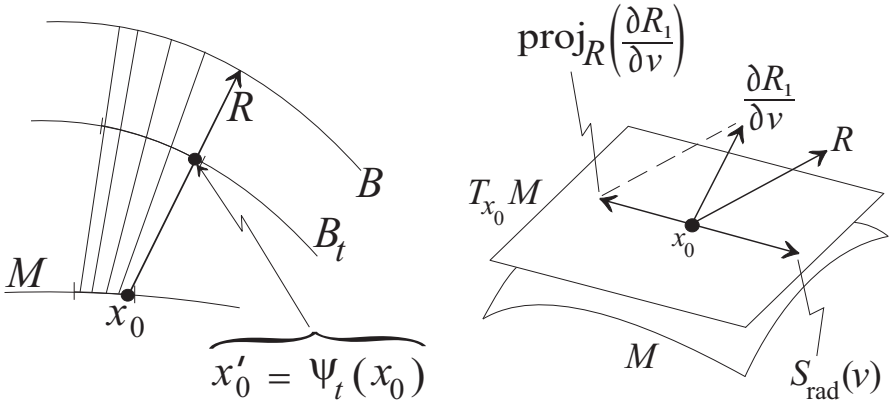

Figure 3.4: Left: the local representation of the radial flow from the medial axis M to the associated boundary B in $\mathbb{R}^2$, where R is a multivalued vector field from points of M to B. Right: the projection for defining the radial shape operator S_{rad}; this picture is in $\mathbb{R}^3$.

for each i by

$$\frac{\partial R_1}{\partial v_i} = a_i \cdot R_1 - \sum_{j=1}^{n} s_{ji} v_j \ . \tag{3.13}$$

Using this, we can write

$$\frac{\partial R_1}{\partial \mathbf{v}} = A_{\mathbf{v}} \cdot R_1 - S_{\mathbf{v}}^{\mathrm{T}} \cdot \mathbf{v} \ ,$$

where $\partial R_1/\partial \mathbf{v}$ is a column vector with vector entries $\partial R_1/\partial v_i$, and $A_{\mathbf{v}} R_1$ is the column vector with entries $a_i R_1$. Also, $\mathbf{v}$ denotes the column vector with i-th entry v_i (allowing an abuse of notation). The derivative of the radial flow can be written as

$$\frac{\partial \psi_t}{\partial v_i} = v_i + t\left(\frac{\partial r}{\partial v_i} \cdot R_1 + r \cdot \frac{\partial R_1}{\partial v_i}\right). \tag{3.14}$$

Let $d\psi_t(v_i) = \partial \psi_t / \partial v_i$ and $dr(v_i) = \partial r / \partial v_i$.

In [D04] Damon proves the following.

Lemma 3.3.1.3 ([D04, Lemma 3.1]) *Suppose (M, R) is a skeletal structure and that $x_0 \in M$ is a non-edge point. Let R be a smooth value (on a non-edge local manifold component M_B of x_0) for which $1/r$ is not an eigenvalue*

of S_{rad} at x_0. Then, the corresponding 'compatibility 1-form' η_R, given by $\eta_R(v) = v.R_1 + dr(v)$, vanishes at x_0 if and only if $R(x_0)$ is orthogonal to the associated boundary at $\psi_1(x_0)$.

Lemma 3.3.1.4 ([D04, Theorem 3.2]) *Suppose (M, R) is a skeletal structure such that, for a choice of smooth value of R, the associated compatibility 1-form η_R vanishes identically on a neighbourhood of a smooth point x_0 of M, and $1/r$ is not an eigenvalue of S_{rad} at x_0. Let $x_0' = \psi_1(x_0)$, and $\mathbf{v}'$ be the image of $\mathbf{v}$ for a basis $\{v_1, \ldots, v_n\}$.*

1. *The differential geometric shape operator S_B of B at x_0' has a matrix representation with respect to $\mathbf{v}'$ given by*

$$S_{B\mathbf{v}'} = (I - r \cdot S_{\mathbf{v}})^{-1} S_{\mathbf{v}} \ . \tag{3.15}$$

2. *Hence, there is a bijection between the principal curvatures κ_i of B at x_0' and the principal radial curvatures κ_{ri} of M at x_0 (counted with multiplicities) given by*

$$\kappa_i = \frac{\kappa_{ri}}{1 - r\kappa_{ri}} \quad \textit{or equivalently} \quad \kappa_{ri} = \frac{\kappa_i}{1 + r\kappa_i} \ . \tag{3.16}$$

3. *Also, the principal radial directions corresponding to κ_{ri} are mapped by $d\psi_1$ to the principal directions corresponding to κ_i.*

The above definitions and results about the radial shape operator are for a medial axis $M \subset \mathbb{R}^{n+1}$. Now we will specialize to consider a smooth two-dimensional medial axis M of a smooth boundary B and a radius function $r > 0$ in three-space. We will choose a basis $\mathbf{v} = \{v_1, v_2\}$ for $T_{x_0}M$ and obtain the matrix representation of the radial shape operator with respect to this basis. The matrix $S_{\mathbf{v}}$ will be expressed in terms of the geometry and dynamics of the medial axis and, using Lemma 3.3.1.4, we will obtain an expression for the principal curvatures and principal directions on the boundary.

Before Lemma 3.3.1.4 can be used, we need to check that its conditions are satisfied in our situation of a medial axis in three dimensions. Firstly, we

require that for a choice of smooth value of R, the associated compatibility 1-form η_R vanishes identically on a neighbourhood of a smooth point x_0 of M. In our situation of smooth medial axis with smooth boundary we only consider R_1 orthogonal to the boundary B. By Lemma 3.3.1.3 this means the compatibility 1-form η_R vanishes for all points of the medial axis. Hence

$$\begin{aligned} \eta_R(v) &= v \cdot R_1 + dr(v) = 0 \\ \Rightarrow \quad dr(v) &= -v \cdot R_1 \ , \end{aligned}$$

for all $v \in T_{x_0}M$, taking $-N^+$ or $-N^-$ as R_1 (see (3.5)). Secondly, we need $1/r$ not to be an eigenvalue of S_{rad} at x_0. Since the boundary B is assumed to be smooth, by Lemma 4.1 of [D05] we have that

$$r \ < \ \min\left\{\frac{1}{\kappa_{ri}}\right\} \text{ for all positive principal radial curvatures } \kappa_{ri}$$

and for $\kappa_{ri} < 0$ we have $1 - r\kappa_{ri} > 0$. Therefore $1/r$ cannot be an eigenvalue of S_{rad} at any point of M. Hence the conditions of Lemma 3.3.1.4 are satisfied, so we can apply its results.

3.3.2 A Matrix Representation of S_{rad} in Three Dimensions

Now we shall calculate the radial shape operator of γ with respect to a chosen basis $\{T, U\}$, where T, U are the vectors as defined in §3.2 at the point $\gamma(r = r_0, t = 0)$. Also, as in §3.2, the medial axis will be labelled γ, and the two boundary sheets are $\gamma^{\pm}$. The derivatives $\partial R_1/\partial v_i$, for $i = 1, 2$, are needed for the radial shape operator. Note that R is assumed to be pointing from points of the medial axis to points of the boundary, whereas $N^{\pm}$ points in the opposite direction, from points of the boundary to points of the medial axis. Therefore we shall take R_1 as $-N^{\pm}$ in what follows. Let $S^{\pm}_{\mathbf{v}}$ denote the matrix representation of the radial shape operator of γ corresponding to boundary $\gamma^{\pm}$ with respect to the basis $\mathbf{v} = \{T, U\}$ at $\gamma(r_0, 0)$. Then we can write

$$S^{\pm}_{\mathbf{v}} = \begin{pmatrix} s^{\pm}_{11} & s^{\pm}_{12} \\ s^{\pm}_{21} & s^{\pm}_{22} \end{pmatrix}.$$

By (3.13), we need $\partial N^{\pm}/\partial T$, $\partial N^{\pm}/\partial U$ in order to calculate the $s_{ij}^{\pm}$ at $\gamma(r_0, 0)$. At a point of the medial axis T is tangent to the curve $t =$ constant, that is the 'r-curve' parametrized by r. So the covariant derivative $\partial N^{\pm}/\partial T$ is the same as $\partial N^{\pm}/\partial s$, where s is arclength along the r-curve. Similarly, U is tangent to the curve $r =$ constant, that is the 't-curve' parametrized by t, which is arclength along this t-curve. Hence $\partial N^{\pm}/\partial U$ is the same as $\partial N^{\pm}/\partial t$. Since the following calculations will be used for the A_1^3 case, we do not assume that $v = ds/dr$ is positive along the r-curves, which can be done when the medial axis is locally a smooth A_1^2 sheet (see §§3.2, 3.4.1). Then, using suffices to denote differentiation, (3.13) for the chosen basis becomes

$$\left.\begin{aligned} N_s^{\pm} &= a_1^{\pm} N^{\pm} + s_{11}^{\pm} T + s_{21}^{\pm} U \ , \\ N_t^{\pm} &= a_2^{\pm} N^{\pm} + s_{12}^{\pm} T + s_{22}^{\pm} U \ . \end{aligned}\right\} \tag{3.17}$$

Now consider $N_s^{\pm}$ and $N_t^{\pm}$. By (3.5) we have

$$\begin{aligned} N_s^{\pm} &= \phi_s \left(\sin\phi T \mp \cos\phi N\right) - \cos\phi T_s \mp \sin\phi N_s \ , \\ N_t^{\pm} &= \phi_t \left(\sin\phi T \mp \cos\phi N\right) - \cos\phi T_t \mp \sin\phi N_t \ . \end{aligned}$$

By definition, at $\gamma(r_0, 0)$ we can write the derivatives of T, U, N in the schematic form

$$\frac{\partial}{\partial s}\begin{pmatrix} T \\ U \\ N \end{pmatrix} = \begin{pmatrix} 0 & g^r & \kappa^r \\ -g^r & 0 & \tau^r \\ -\kappa^r & -\tau^r & 0 \end{pmatrix}\begin{pmatrix} T \\ U \\ N \end{pmatrix},$$

$$\text{and} \quad \frac{\partial}{\partial t}\begin{pmatrix} U \\ -T \\ N \end{pmatrix} = \begin{pmatrix} 0 & g^t & \kappa^t \\ -g^t & 0 & \tau^t \\ -\kappa^t & -\tau^t & 0 \end{pmatrix}\begin{pmatrix} U \\ -T \\ N \end{pmatrix}.$$

Hence $N_s^{\pm}$, $N_t^{\pm}$ become

$$\begin{aligned} N_s^{\pm} &= (\phi_s \pm \kappa^r)\sin\phi T + (-g^r\cos\phi \pm \tau^r \sin\phi)U + (\mp\phi_s - \kappa^r)\cos\phi N \ , \\ N_t^{\pm} &= (\phi_t \mp \tau^t)\sin\phi T + (-g^t\cos\phi \pm \kappa^t \sin\phi)U + (\mp\phi_t + \tau^t)\cos\phi N \ . \end{aligned}$$

We can simplify these expressions further by differentiating (3.6) with respect to arclength along the t-curve, that is set $r = r_0$ and differentiate with respect

to t. (This is allowed since (3.6) holds for all points of γ.) Then we can set $t = 0$ to evaluate the derivative with respect to t at the point $\gamma(r_0, 0)$. This gives

$$\phi_t = -v_t \frac{1}{v^2 \sin\phi} = -\frac{a^t}{v^2 \sin\phi} \ ,$$

since $a^t = v_t$ by definition. Then differentiate (3.6) with respect to arclength along the r-curve, that is set $t = 0$ and differentiate with respect to s. Then we can set $r = r_0$ to evaluate the derivative with respect to s at the point $\gamma(r_0, 0)$. This gives

$$\phi_s = -\frac{1}{v^2 \sin\phi} \left(v_r \frac{dr}{ds} \right) = -\frac{a}{v^3 \sin\phi} \ ,$$

since we know ds/dr is v along the r-curve. Also, from (3.7) and (3.8) we have $\tau^r = -\tau^t$, $g^r = -a^t/v$, and $g^t = a^*/v$. Then, using (3.5), we get the following:

$$N_s^{\pm} = \left(\pm \frac{a}{v^3 \sin\phi} - \kappa^r \right) T^{\pm} + \left(\frac{a^t \cos\phi}{v} \mp \tau^t \sin\phi \right) U \ , \qquad (3.18)$$

$$N_t^{\pm} = \left(\pm \frac{a^t}{v^2 \sin\phi} + \tau^t \right) T^{\pm} + \left(-\frac{a^* \cos\phi}{v} \pm \kappa^t \sin\phi \right) U \ . \qquad (3.19)$$

In order to calculate the radial shape operator, we must deduce $a_1^{\pm}$, $a_2^{\pm}$, $s_{11}^{\pm}$, $s_{12}^{\pm}$, $s_{21}^{\pm}$, $s_{22}^{\pm}$ from (3.17), using (3.18) and (3.19). This gives two vector equations to be solved, the first of which (from (3.17) and (3.18)) is as follows:

$$\begin{aligned} & a_1^{\pm}(-\cos\phi T \mp \sin\phi N) + s_{11}^{\pm} T + s_{21}^{\pm} U \\ = \ & \left(-\frac{a}{v^3 \sin\phi} \pm \kappa^r \right) (\sin\phi T \mp \cos\phi N) + \left(\frac{a^t \cos\phi}{v} \mp \tau^t \sin\phi \right) U \end{aligned}$$

$$\begin{aligned} \iff \mathbf{0} = \ & \left(-a_1^{\pm} \cos\phi + s_{11}^{\pm} + \frac{a}{v^3} \mp \kappa^r \sin\phi \right) T \\ & + \left(s_{21}^{\pm} - \frac{a^t \cos\phi}{v} \pm \tau^t \sin\phi \right) U \\ & + \left(\mp a_1^{\pm} \sin\phi \mp \frac{a \cos\phi}{v^3 \sin\phi} + \kappa^r \cos\phi \right) N \ . \end{aligned}$$

By definition, T, U, N form an orthonormal triad, so the above holds if and only if the coefficients of T, U, N are zero. Solving the coefficients of T, U,

N equal to zero and using the fact that $\cos\phi = -1/v$ from (3.6) gives the following:

$$\begin{aligned} a_1^{\pm} &= \left(\frac{-a}{v^3\sin^2\phi} \pm \frac{\kappa^r}{\sin\phi}\right)\cos\phi \ , \\ s_{11}^{\pm} &= \frac{-a}{v^3\sin^2\phi} \pm \frac{\kappa^r}{\sin\phi} \ , \\ s_{21}^{\pm} &= -\frac{a^t}{v^2} \mp \tau^t \sin\phi \ . \end{aligned}$$

The second vector equation to be solved (from (3.17) and (3.19)) is as follows:

$$\begin{aligned} & a_2^{\pm}(-\cos\phi T \mp \sin\phi N) + s_{12}^{\pm}T + s_{22}^{\pm}U \\ = \ & \left(-\frac{a^t}{v^2\sin\phi} \mp \tau^t\right)(\sin\phi T \mp \cos\phi N) + \left(-\frac{a^*\cos\phi}{v} \pm \kappa^t \sin\phi\right)U \\ \iff \mathbf{0} &= \left(-a_2^{\pm}\cos\phi + s_{12}^{\pm} + \frac{a^t}{v^2} \pm \tau^t\sin\phi\right)T \\ &\quad + \left(s_{22}^{\pm} + \frac{a^*\cos\phi}{v} \mp \kappa^t\sin\phi\right)U \\ &\quad + \left(\mp a_2^{\pm}\sin\phi \mp \frac{a^t\cos\phi}{v^3\sin\phi} - \tau^t\cos\phi\right)N \ . \end{aligned}$$

Again, this holds if and only if the coefficients of T, U, N are zero in the above. Solving the coefficients of T, U, N equal to zero and using the fact that $\cos\phi = -1/v$ from (3.6) gives the following:

$$\begin{aligned} a_2^{\pm} &= \left(\frac{-a^t}{v^2\sin^2\phi} \mp \frac{\tau^r}{\sin\phi}\right)\cos\phi \ , \\ s_{12}^{\pm} &= \frac{-a^t}{v^2\sin^2\phi} \mp \frac{\tau^r}{\sin\phi} \ , \\ s_{22}^{\pm} &= \frac{a^*}{v^2} \pm \kappa^t\sin\phi \ . \end{aligned}$$

Hence we have the following.

Lemma 3.3.2.1 *The radial shape operator $S_{\mathbf{v}}^{\pm}$ with respect to $-N^{\pm}$ and the basis $\{T, U\}$ at $\gamma(r_0, 0)$ is as below:*

$$S_{\mathbf{v}}^{\pm} = \begin{pmatrix} s_{11}^{\pm} & s_{12}^{\pm} \\ s_{21}^{\pm} & s_{22}^{\pm} \end{pmatrix} = \begin{pmatrix} -\frac{a}{v^3\sin^2\phi} \pm \frac{\kappa^r}{\sin\phi} & \left(-\frac{a^t}{v^2} \mp \tau^t\sin\phi\right)\frac{1}{\sin^2\phi} \\ -\frac{a^t}{v^2} \mp \tau^t\sin\phi & \frac{a^*}{v^2} \pm \kappa^t\sin\phi \end{pmatrix} . \quad (3.20)$$

Let $\text{trace}^{\pm}$, $\det^{\pm}$ denote $\text{trace}(S^{\pm}_{\mathbf{v}})$, $\text{determinant}(S^{\pm}_{\mathbf{v}})$. Then

$$\begin{aligned}
\text{trace}^{\pm} &= -\frac{a}{v^3 \sin^2\phi} + \frac{a^*}{v^2} \pm \left(\frac{\kappa^r}{\sin\phi} + \kappa^t \sin\phi \right), \\
\det^{\pm} &= -\frac{a^* a}{v^5 \sin^2\phi} + \kappa^r \kappa^t - \frac{(a^t)^2}{v^4 \sin^2\phi} - (\tau^t)^2 \\
&\quad \pm \left(\frac{a^* \kappa^r v - a\kappa^t - 2a^t \tau^t v}{v^3 \sin\phi} \right).
\end{aligned}$$

So we have the following.

Lemma 3.3.2.2 *The trace and determinant of $S^{\pm}_{\mathbf{v}}$ satisfy*

$$\frac{1}{2}(\text{trace}^+ - \text{trace}^-) = \frac{\kappa^r}{\sin\phi} + \kappa^t \sin\phi \ , \tag{3.21}$$

$$\frac{1}{2}(\det^+ - \det^-) = \frac{a^* \kappa^r v - a\kappa^t - 2a^t \tau^t v}{v^3 \sin\phi} \ . \tag{3.22}$$

3.3.3 Principal Directions on the Boundary

The principal directions on the boundary can be expressed in terms of the geometry of the medial axis by using (3.14) and Lemma 3.3.1.4. Let $\kappa^{\pm}_{ri}$ be one of the principal radial curvatures, that is an eigenvalue of $S^{\pm}_{\mathbf{v}}$ given by (3.20). The corresponding principal radial direction is given by

$$V_1^{\pm} = s_{12}^{\pm} T + (\kappa_{ri}^{\pm} - s_{11}^{\pm}) U \ , \tag{3.23}$$

or, alternatively,

$$V_2^{\pm} = (\kappa_{ri}^{\pm} - s_{22}^{\pm}) T + s_{21}^{\pm} U \ .$$

The expression for the principal direction on the boundary using (3.23) is

$$\begin{aligned}
d\psi_1^{\pm}(V_1^{\pm}) &= s_{12}^{\pm}T + (\kappa_{ri}^{\pm} - s_{11}^{\pm})U + \frac{\partial r}{\partial V_1}(-N^{\pm}) + r\left(\frac{-\partial N^{\pm}}{\partial V_1}\right) \\
&= s_{12}^{\pm}T + (\kappa_{ri}^{\pm} - s_{11}^{\pm})U - (V_1^{\pm}\cdot(-N^{\pm}))(-N^{\pm}) \\
&\quad + r\left(-s_{12}^{\pm}\frac{\partial N^{\pm}}{\partial s} - (\kappa_{ri}^{\pm} - s_{11}^{\pm})\frac{\partial N^{\pm}}{\partial t}\right) \\
&= s_{12}^{\pm}T + (\kappa_{ri}^{\pm} - s_{11}^{\pm})U + s_{12}^{\pm}\cos\phi N^{\pm} \\
&\quad + r s_{12}^{\pm}\left(-a_1^{\pm}N^{\pm} - s_{11}^{\pm}T - s_{21}^{\pm}U\right) \\
&\quad + r(\kappa_{ri}^{\pm} - s_{11}^{\pm})\left(-a_2^{\pm}N^{\pm} - s_{12}^{\pm}T - s_{22}^{\pm}U\right) \\
&= s_{12}^{\pm}T + (\kappa_{ri}^{\pm} - s_{11}^{\pm})U + s_{12}^{\pm}\cos\phi(-\cos\phi T \mp \sin\phi N) \\
&\quad + r s_{12}^{\pm}\left(-a_1^{\pm}(-\cos\phi T \mp \sin\phi N) - s_{11}^{\pm}T - s_{21}^{\pm}U\right) \\
&\quad + r(\kappa_{ri}^{\pm} - s_{11}^{\pm})\left(-a_2^{\pm}(-\cos\phi T \mp \sin\phi N) - s_{12}^{\pm}T - s_{22}^{\pm}U\right).
\end{aligned}$$

After substitution for $s_{ij}^{\pm}$ and $a_{1,2}^{\pm}$ we get

$$\begin{aligned}
d\psi_1^{\pm}(V_1^{\pm}) &= \left(-\frac{a^t}{v^2} \mp \tau^t \sin\phi\right)(1 - r\kappa_{ri}^{\pm})T \\
&\quad + (\kappa_{ri}^{\pm} - s_{11}^{\pm} + r(\det^{\pm} - s_{22}^{\pm}\kappa_{ri}^{\pm}))U \\
&\quad \mp \left(-\frac{a^t}{v^2} \mp \tau^t \sin\phi\right)\frac{\cos\phi}{\sin\phi}(1 - r\kappa_{ri}^{\pm})N\ ,
\end{aligned}$$

which is the same as

$$\begin{aligned}
d\psi_1^{\pm}(V_1^{\pm}) = {} & s_{12}^{\pm}\sin^2\phi(1 - r\kappa_{ri}^{\pm})T + (\kappa_{ri}^{\pm} - s_{11}^{\pm} + r(\det^{\pm} - s_{22}^{\pm}\kappa_{ri}^{\pm}))U \\
& \mp s_{12}^{\pm}\cos\phi\sin\phi(1 - r\kappa_{ri}^{\pm})N\ .
\end{aligned} \tag{3.24}$$

This is not the end, since by the following lemma we can further simplify the right-hand side of (3.24).

Lemma 3.3.3.1 *The principal radial curvatures $\kappa_{ri}^{\pm}$ and the principal curvatures $\kappa_j^{\pm}$ on the boundary $\gamma^{\pm}$ at $\gamma^{\pm}(r_0, 0)$ satisfy*

$$\kappa_j^{\pm}(1 - r\mathrm{trace}^{\pm} + r^2\det^{\pm}) = \kappa_{ri}^{\pm} - r\det^{\pm}, \tag{3.25}$$

for $i = 1, 2$, $j = 1, 2$.

Proof. Since the boundary sheet $\gamma^{\pm}$ is smooth, we know that $1/r$ is not an eigenvalue of $S^{\pm}_{\mathbf{v}}$ and, using (3.15) from Lemma 3.3.1.4, we have a matrix representation $S_{\gamma^{\pm}\mathbf{v}'}$ of $S_{\gamma^{\pm}}$, the differential geometric shape operator of $\gamma^{\pm}$ at $\psi_1^{\pm}(\gamma(r_0,0))$ with respect to $\mathbf{v}'$, as follows:

$$S_{\gamma^{\pm}\mathbf{v}'} = (I - r \cdot S^{\pm}_{\mathbf{v}})^{-1} S^{\pm}_{\mathbf{v}} \ .$$

It is easy to show from this that

$$\begin{aligned}
\mathrm{trace}(S_{\gamma^{\pm}\mathbf{v}'}) &= \frac{\mathrm{trace}^{\pm} - 2r\mathrm{det}^{\pm}}{1 - r\mathrm{trace}^{\pm} + r^2\mathrm{det}^{\pm}} \ , \\
\det(S_{\gamma^{\pm}\mathbf{v}'}) &= \frac{\mathrm{det}^{\pm}}{1 - r\mathrm{trace}^{\pm} + r^2\mathrm{det}^{\pm}} \ , \\
\text{and} \quad (\mathrm{trace}(S_{\gamma^{\pm}\mathbf{v}'}))^2 - 4\det(S_{\gamma^{\pm}\mathbf{v}'}) &= \frac{(\mathrm{trace}^{\pm})^2 - 4\mathrm{det}^{\pm}}{(1 - r\mathrm{trace}^{\pm} + r^2\mathrm{det}^{\pm})^2} \ ,
\end{aligned}$$

so the eigenvalues $\kappa_j^{\pm}$ of $S_{\gamma^{\pm}\mathbf{v}'}$ are

$$\frac{\mathrm{trace}^{\pm} - 2r\mathrm{det}^{\pm} \pm \eta\sqrt{(\mathrm{trace}^{\pm})^2 - 4\mathrm{det}^{\pm}}}{2(1 - r\mathrm{trace}^{\pm} + r^2\mathrm{det}^{\pm})} \ ,$$

where $\eta = \mathrm{sign}(1 - r\mathrm{trace}^{\pm} + r^2\mathrm{det}^{\pm})$. So

$$\begin{aligned}
\kappa_j^{\pm}(1 - r\mathrm{trace}^{\pm} + r^2\mathrm{det}^{\pm}) &= \frac{\mathrm{trace}^{\pm} \pm \eta\sqrt{(\mathrm{trace}^{\pm})^2 - 4\mathrm{det}^{\pm}}}{2} - r\mathrm{det}^{\pm} \\
&= \kappa_{ri}^{\pm} - r\mathrm{det}^{\pm},
\end{aligned}$$

where $i = 1, 2$, $j = 1, 2$, as required. □

We can use Lemma 3.3.3.1 to simplify the expression for a principal direction on the boundary from (3.24) as follows. Since we have a smooth boundary we know that $1 - r\kappa_{ri}^{\pm} \neq 0$ and so

$$\begin{aligned}
\frac{d\psi_1^{\pm}(V_1^{\pm})}{1 - r\kappa_{ri}^{\pm}} &= s_{12}^{\pm}\sin^2\phi T + \frac{(\kappa_{ri}^{\pm} - s_{11}^{\pm} + r(\mathrm{det}^{\pm} - s_{22}^{\pm}\kappa_{ri}^{\pm}))}{1 - r\kappa_{ri}^{\pm}} U \\
&\quad \mp s_{12}^{\pm}\cos\phi\sin\phi N \ .
\end{aligned}$$

Using (3.16) from Lemma 3.3.1.4, the coefficient of U in the above becomes

$$\begin{aligned}
& \frac{\kappa_{ri}^{\pm}}{1-r\kappa_{ri}^{\pm}}(1-rs_{22}^{\pm}) + \frac{r\det^{\pm} - s_{11}^{\pm}}{1-r\kappa_{ri}^{\pm}} \\
= \;& \kappa_i^{\pm}(1-rs_{22}^{\pm}) + (1+r\kappa_i^{\pm})(r\det^{\pm} - s_{11}^{\pm}) \ , \\
& \text{since } \frac{1}{1-r\kappa_{ri}^{\pm}} = 1 + r\kappa_i^{\pm} \\
= \;& \kappa_i^{\pm}(1 - r\mathrm{trace}^{\pm} + r^2\det^{\pm}) + r\det^{\pm} - s_{11}^{\pm} \\
= \;& \kappa_{rj}^{\pm} - s_{11}^{\pm}, \quad \text{using Lemma 3.3.3.1.}
\end{aligned}$$

Hence we have the following.

Lemma 3.3.3.2 *The principal directions on $\gamma^{\pm}$ at $\gamma^{\pm}(r_0, 0)$ are given by*

$$s_{12}^{\pm}\sin^2\phi T + (\kappa_{ri}^{\pm} - s_{11}^{\pm})U \mp s_{12}^{\pm}\cos\phi\sin\phi N \ , \tag{3.26}$$

for $i = 1, 2$ and where $s_{11}^{\pm}$, $s_{12}^{\pm}$, $s_{21}^{\pm}$, $s_{22}^{\pm}$ are given in (3.20).

The results connecting $\mathrm{trace}^+, \mathrm{trace}^-$ and $\det^+, \det^-$, and the expressions for the principal directions on the boundary will be used in the following section in the A_1^3 case.

3.4 The A_1^3 Case

The A_1^3 case of the medial axis in $\mathbb{R}^3$ is that of points which are the centres of spheres tangent to a surface in three points. In this case the medial axis is locally three sheets intersecting transversally along a curve, called the A_1^3 curve or Y-junction curve. Points of this curve are called A_1^3 points or Y-junction points and are centres of *tritangent* spheres, that is the spheres tangent to the boundary in three points. The A_1^4 case corresponds to the centre of a sphere with tangency with a surface in four points; it is a point where four A_1^3 curves meet. An A_1A_3 point is an A_1^3 point where two of the points of contact have come into coincidence. Hence the A_1^3 case is the major case to consider, since A_1^4 and A_1A_3 points are limits of A_1^3 points.

Let the medial sheets intersecting along an A_1^3 curve be labelled γ_1, γ_2, γ_3. Associated to each γ_i are two boundary surfaces $\gamma_i^{\pm}$ and so there are six associated boundary surfaces, but each coincides with one, and only one, of the others, so there are three distinct surfaces. Let the identifications be $\gamma_i^+ = \gamma_{i+1}^-$, where we evaluate $(i+1)$ modulo 3 when $(i+1) > 3$. Hence we have $\gamma_1^+ = \gamma_2^-$, $\gamma_2^+ = \gamma_3^-$, $\gamma_3^+ = \gamma_1^-$. This is analogous to the A_1^3 case in $\mathbb{R}^2$ – see Figure 3.1. In $\mathbb{R}^2$ the identifications $\gamma_i^+ = \gamma_{i+1}^-$ had consequences for the geometry and dynamics of the medial curves in the form of constraints such as (3.1). Similarly, in $\mathbb{R}^3$ the identifications $\gamma_i^+ = \gamma_{i+1}^-$ give rise to conditions which must be satisfied by the medial axis. These conditions are obtained in this section.

Here is a brief summary of what is to come in this section. The coordinate systems used in the A_1^3 case are described and summarized in Table 3.1. Using this the consequences of making the identifications $\gamma_i^+ = \gamma_{i+1}^-$ at first order derivatives are examined, which result in Theorem 3.4.2.1. Then, using the first coordinate system, we go to the next order of derivatives and obtain Theorem 3.4.3.2, which contains consistency conditions on the medial axis. However, this does not obtain all of the information given by making the identifications $\gamma_i^+ = \gamma_{i+1}^-$ up to second order derivatives and so, to extract all of this information, the second coordinate system is used. This means that we can reduce the number of variables involved in the conditions and so we obtain Theorem 3.4.5.2. Alternative forms of the consistency conditions from Theorem 3.4.5.2 are contained in Theorems 3.4.5.3, 3.4.5.4.

3.4.1 Coordinate Systems for the A_1^3 Case

The consistency conditions of this section are expressed in terms of two coordinate systems, the first of which is based on the '(r,t)' coordinate system defined in §3.2 for a single A_1^2 sheet. For the A_1^3 case we define the same quantities on each medial sheet γ_i meeting along the A_1^3 curve at an A_1^3 point $\gamma_i(r_i = r_0, t_i = 0)$ for r_0 constant. See Table 3.1 for a summary of the notation used in this system.

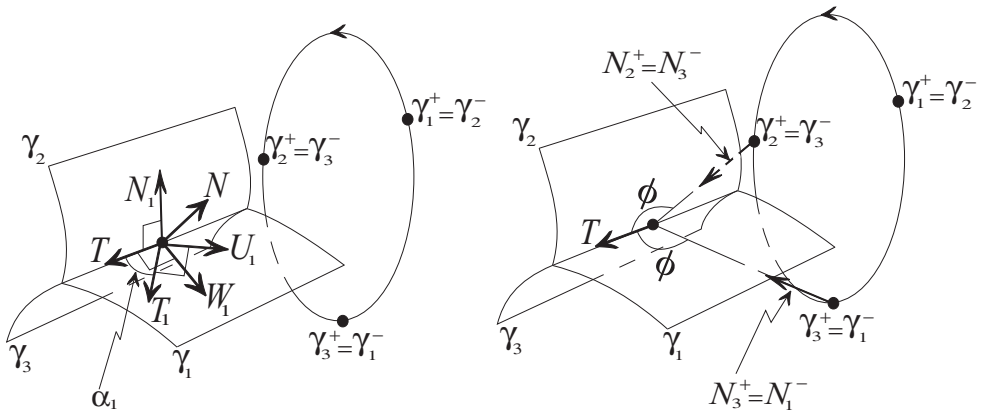

Figure 3.5: The medial sheets γ_1, γ_2, and γ_3 intersecting along an A_1^3 curve in $\mathbb{R}^3$ and the corresponding points of contact on the boundaries. Left: the vectors T, T_1, W_1, U_1 are all in the tangent plane to γ_1; N_1 is the unit normal to γ_1 and N is the principal normal to the A_1^3 curve. Each T_i points into γ_i, but depending on whether α_i is obtuse or not U_i might point out of the medial axis. Right: the angle ϕ between T and $-N_i^{\pm}$, where ϕ is chosen to be obtuse and so T is in the direction of r increasing (r is the radius of the tritangent sphere).

The other coordinate system used is specially suited to the A_1^3 case. We consider the generic case of the medial axis, which means that the curvature of the A_1^3 curve is never zero. In this case we can set up a local Frenet frame $[T, N, B]$ at a point of the A_1^3 curve, so T is the unit tangent to the A_1^3 curve. Then α_i is defined as the angle between T_i and T (see Figure 3.5, left), and ψ_i is defined as the angle between N and N_i. Let the ψ_i be such that $0 \leq \psi_1 < \psi_2 < \psi_3 < 2\pi$ (see Figure 3.6). The angle between N_{i+1} and N_{i+2} is important when obtaining the consistency conditions, so let $\theta_i = \psi_{i+2} - \psi_{i+1}$ and $\epsilon_i = \text{sign}(\cos\theta_i)$. Let r be the radius of tritangent spheres centred on the A_1^3 curve. Then ϕ is defined to be the angle between T and the line joining one of the points of contact with the centre of a tritangent sphere (see Figure 3.5, right). Take r to be increasing along the A_1^3-curve so T is in the direction of r increasing, and so ϕ is obtuse. Let the tangents T_i for $i = 1, 2, 3$ point into γ_i. Now consider the circle passing through the points of contact, looking along

the direction of $-T$. The normal N_i to the medial axis sheet γ_i is given by rotating by $\pi/2$ coherently with this circle the projection of T_i into the plane of contact points perpendicular to T, as in Figure 3.7. This gives the required identifications $\gamma_i^+ = \gamma_{i+1}^-$. Then T_i is determined by the relation

$$\text{proj}(T_i) = N_i \times T \ ,$$

since we know that T_i is parallel to the direction of ∇r_i.

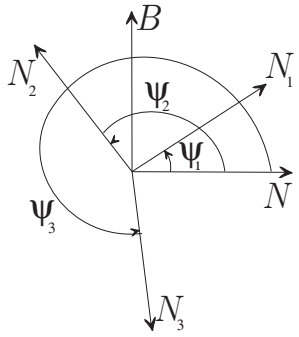

Figure 3.6: This is in the plane of N and B, which are respectively the principal normal and the binormal to the A_1^3 curve. The unit normals N_i to the medial sheets γ_i and the angles ψ_i between N and N_i are shown. The ψ_i are chosen so that $0 \leq \psi_1 < \psi_2 < \psi_3 < 2\pi$.

These conventions mean we cannot assume each T_i is in the direction of ∇r_i. In the case of the medial axis being locally one A_1^2 sheet we could choose the velocity v to be positive (see §3.2). For example, from Figure 3.7, left we have $T_2 = -\nabla r_2/\|\nabla r_2\|$ and in Figure 3.7, right we have $T_2 = +\nabla r_2/\|\nabla r_2\|$. Hence, for s_i arclength on the r_i-curve, we let $v_i = ds_i/dr_i$ be non-zero along the r_i-curves and so $T_i = \pm\nabla r_i/\|\nabla r_i\|$. Then ϕ_i might be acute or obtuse and so we allow v_i to be positive or negative, but not zero.

The vectors T_i, U_i, and N_i can be expressed in terms of ψ_i and α_i for all

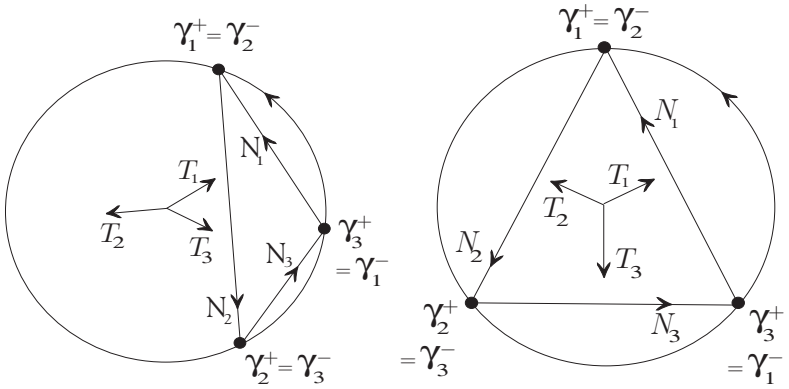

Figure 3.7: The two possibilities for the points of contact in the A_1^3 case. The view of the points of contact looking along the direction of $-T$: on the left the points of contact are in a semicircle, on the right they are not.

points of the A_1^3 curve, as follows:

$$\begin{aligned} N_i &= \cos\psi_i N + \sin\psi_i B \ , \\ T_i &= \cos\alpha_i T + pN + qB \ , \\ U_i &= N_i \times T_i \\ &= (q\cos\psi_i - p\sin\psi_i)T + \sin\psi_i\cos\alpha_i N - \cos\psi_i\cos\alpha_i B \ , \end{aligned}$$

where p, q are to be determined. From Figure 3.5 we have that

$$\begin{aligned} T\cdot U_i = \cos\left(\frac{\pi}{2}+\alpha_i\right) &= -\sin\alpha_i \\ &= (q\cos\psi_i - p\sin\psi_i) \ , \end{aligned}$$

from the above expression for U_i. We also have $T_i \cdot N_i = 0$ by definition, and so $p\cos\psi_i + q\sin\psi_i = 0$. Hence we can solve for p and q and we get

$$p = \sin\alpha_i \sin\psi_i \ , \quad q = -\sin\alpha_i\cos\psi_i \ .$$

Hence we get the following formulae, which are valid at all points of the A_1^3 curve:

$$\left.\begin{aligned} T_i &= \cos\alpha_i T + \sin\alpha_i\sin\psi_i N - \sin\alpha_i\cos\psi_i B \ , \\ U_i &= -\sin\alpha_i T + \cos\alpha_i\sin\psi_i N - \cos\alpha_i\cos\psi_i B \ , \\ N_i &= \cos\psi_i N + \sin\psi_i B \ . \end{aligned}\right\} \tag{3.27}$$

Alternatively, we can obtain T, N, B in terms of T_i, U_i, N_i:

$$\left.\begin{aligned} T &= \cos\alpha_i T_i - \sin\alpha_i U_i \ , \\ N &= \sin\alpha_i \sin\psi_i T_i + \cos\alpha_i \sin\psi_i U_i + \cos\psi_i N_i \ , \\ B &= -\sin\alpha_i \cos\psi_i T_i - \cos\alpha_i \cos\psi_i U_i + \sin\psi_i N_i \ . \end{aligned}\right\} \tag{3.28}$$

An important direction is the one perpendicular to T in the tangent plane to γ_i, which will be called $W_i = N_i \times T$. Using (3.27) we get the following formula for W_i, valid at points of the A_1^3 curve:

$$W_i = \sin\psi_i N - \cos\psi_i B \ . \tag{3.29}$$

The first order notation for the coordinate system based on the A_1^3 curve has been covered, so now for the second order information. Let κ, τ be respectively the curvature, torsion of the A_1^3 curve, where, as before, κ is assumed to be non-zero for all points of the A_1^3 curve. Also, let κ_i^W be the normal curvature of γ_i in the direction of W_i. Differentiation with respect to arclength along the A_1^3 curve is denoted by $'$ ('prime') and differentiation with respect to arclength along a curve lying on γ_i passing through the point $\gamma_i(r_0, 0)$ on the A_1^3 curve with tangent W_i is denoted by $\dot{}$ ('dot'). Table 3.1 contains all of the new symbols and their meanings.

3.4.2 Equating Normals of the Boundaries at A_1^3 Points

A point of the A_1^3 curve is a point of each γ_i, so the identifications $\gamma_i^+ = \gamma_{i+1}^-$ and (3.3) mean that, for $r = r(s)$ the radius of a tritangent sphere centred at a point $\gamma_1(s) = \gamma_2(s) = \gamma_3(s)$ of the A_1^3 curve, where s is arclength along the A_1^3 curve, we have

$$\begin{aligned} \gamma_i - rN_i^+ &= \gamma_{i+1} - rN_{i+1}^- \\ \iff \quad N_i^+ &= N_{i+1}^- \\ \iff \quad -\cos\phi_i T_i - \sin\phi_i N_i &= -\cos\phi_{i+1} T_{i+1} + \sin\phi_{i+1} N_{i+1} \ , \end{aligned}$$

using (3.5). Adding the three equations given by $N_i^+ = N_{i+1}^-$ gives

$$\sin\phi_1 N_1 + \sin\phi_2 N_2 + \sin\phi_3 N_3 = \mathbf{0} \ . \tag{3.30}$$

The '(r_i, t_i)' Coordinate System	
Symbol	Explanation of Notation
γ_i, r_i	A sheet of the medial axis near to an A_1^3 curve ($i = 1, 2, 3$) with associated radius function r_i
r_i-curves	Gradient lines of r_i, parametrized by r_i
t_i-curves	Lines r_i = constant, parametrized by t_i
$\gamma_i(r_0, 0)$	Point on the A_1^3 curve, where $r_i = r_0$ (constant) and $t_i = 0$
T_i, N_i, U_i	Unit tangent to the r_i-curve, unit normal to γ_i, $U_i = N_i \times T_i$
$\gamma_i^{\pm}$	The two boundary surfaces corresponding to γ_i
$N_i^{\pm}$	Unit normal to $\gamma_i^{\pm}$
ϕ_i, v_i	Angle from T_i to $-N_i^{\pm}$, velocity $v_i = -1/\cos\phi_i$
a_i, a_i^t, a_i^*	Accelerations on γ_i (see (3.7) for a single medial sheet γ)
κ_i^r	Normal curvature of γ_i in the direction of the r_i-curve
κ_i^t	Normal curvature of γ_i in the direction of the t_i-curve
τ_i^t	Geodesic torsion of γ_i in the direction of the t_i-curve
The 'A_1^3 Curve' Coordinate System	
Symbol	Explanation of Notation
T, N, B	Unit tangent, principal normal, binormal of the A_1^3 curve
κ, τ	Curvature, torsion of the A_1^3 curve
α_i	Angle from T to T_i
ψ_i	Angle from N to N_i, chosen so that $0 \le \psi_1 < \psi_2 < \psi_3 < 2\pi$
θ_i	$\theta_i = (\psi_{i+2} - \psi_{i+1})$, the angle between N_{i+1} and N_{i+2}
ϵ_i	The sign of $\cos\theta_i$
ϕ	Angle between T and $-N_i^{\pm}$, chosen to be obtuse
κ_i^W	Normal curvature of γ_i in the direction of $W_i = N_i \times T$
$'$ (prime)	Differentiation with respect to arclength along the A_1^3 curve
$\dot{}$ (dot)	Differentiation with respect to arclength along a curve tangent to W_i

Table 3.1: Table of notation for the A_1^3 case.

Using (3.5), (3.27) we have the following formula for $N_i^{\pm}$ in terms of ϕ_i, α_i, and ψ_i:

$$\begin{aligned} N_i^{\pm} = &- \cos\phi_i \left(\cos\alpha_i T + \sin\alpha_i \sin\psi_i N - \sin\alpha_i \cos\psi_i B\right) \\ &\mp \sin\phi_i \left(\cos\psi_i N + \sin\psi_i B\right) \ . \end{aligned} \tag{3.31}$$

We want to set $N_i^+ = N_{i+1}^-$ at points of the A_1^3 curve. From the formula above for $N_i^{\pm}$, the T components of N_i^+ and of N_{i+1}^- are equal. This gives $\cos\phi_1 \cos\alpha_1 = \cos\phi_2 \cos\alpha_2 = \cos\phi_3 \cos\alpha_3$. Then we have

$$\cos\phi = \cos\phi_i \cos\alpha_i \ , \tag{3.32}$$

since $\cos\phi = -N_i^{\pm} \cdot T$ by the definition of ϕ. Let $\hat{N}_i^{\pm}$ be the normalized component of $N_i^{\pm}$ in the N, B plane. Then we have the following:

$$\begin{aligned} \hat{N}_i^{\pm} &= \frac{\cos\phi_i \sin\alpha_i}{\sin\phi} \left(\sin\psi_i N - \cos\psi_i B\right) \\ &\quad \pm \frac{\sin\phi_i}{\sin\phi} \left(\cos\psi_i N + \sin\psi_i B\right) \ , \\ \text{so} \quad N_i^{\pm} &= -\cos\phi T - \sin\phi \hat{N}_i^{\pm} \ . \end{aligned} \tag{3.33}$$

Using (3.33) we have

$$N_i^+ - N_i^- = -\sin\phi(\hat{N}_i^+ - \hat{N}_i^-) = -\sin\phi(\hat{N}_{i+1}^- - \hat{N}_i^-) \ .$$

From (3.5) we have

$$N_i^+ - N_i^- = -\cos\phi_i T_i - \sin\phi N_i - (-\cos\phi_i T_i + \sin\phi N_i) = -2\sin\phi_i N_i \ .$$

Hence $N_i^+ = N_{i+1}^-$ implies the following vector equation:

$$\sin\phi(\hat{N}_{i+1}^- - \hat{N}_i^-) = 2\sin\phi_i N_i \ . \tag{3.34}$$

Let us introduce auxiliary variables in order to solve (3.34). Set

$$\hat{N}_i^+ = \hat{N}_{i+1}^- = \cos\beta_{i,i+1} N + \sin\beta_{i,i+1} B \tag{3.35}$$

for $i = 1, 2, 3$ at points of the A_1^3 curve, and where $(i+1)$, $(i+2)$ are evaluated modulo 3 when $(i+1)$, $(i+2)$ are respectively greater than 3. And so

$$\begin{aligned} & \hat{N}^-_{i+1} - \hat{N}^-_i = (\cos\beta_{i,i+1}N + \sin\beta_{i,i+1}B) - (\cos\beta_{i-1,i}N + \sin\beta_{i-1,i}B) \\ = \;& 2\sin\left(\frac{\beta_{i,i+1}+\beta_{i-1,i}}{2}\right)\sin\left(\frac{\beta_{i-1,i}-\beta_{i,i+1}}{2}\right)N \\ & +2\sin\left(\frac{\beta_{i,i+1}-\beta_{i-1,i}}{2}\right)\cos\left(\frac{\beta_{i,i+1}+\beta_{i-1,i}}{2}\right)B\ . \end{aligned}$$

Hence

$$\begin{aligned} & \frac{\hat{N}^-_{i+1} - \hat{N}^-_i}{2} = \\ & \sin\left(\frac{\beta_{i-1,i}-\beta_{i,i+1}}{2}\right)\left(\sin\left(\frac{\beta_{i,i+1}+\beta_{i-1,i}}{2}\right)N - \cos\left(\frac{\beta_{i,i+1}+\beta_{i-1,i}}{2}\right)B\right). \end{aligned}$$

Using this, (3.34) becomes the following:

$$\sin\phi_i(\cos\psi_i N + \sin\psi_i B) =$$

$$\sin\phi\sin\left(\frac{\beta_{i-1,i}-\beta_{i,i+1}}{2}\right)\left(\sin\left(\frac{\beta_{i,i+1}+\beta_{i-1,i}}{2}\right)N - \cos\left(\frac{\beta_{i,i+1}+\beta_{i-1,i}}{2}\right)B\right).$$

This equation is of the form $\mu P_1 = \lambda Q_1$ where P_1, Q_1 are unit vectors, and so gives the following two cases:

1. $\sin\phi_i = \sin\phi\sin\left(\dfrac{\beta_{i-1,i}-\beta_{i,i+1}}{2}\right)$,
   $(\cos\psi_i, \sin\psi_i) = \left(\sin\left(\dfrac{\beta_{i,i+1}+\beta_{i-1,i}}{2}\right), -\cos\left(\dfrac{\beta_{i,i+1}+\beta_{i-1,i}}{2}\right)\right)$;
2. $\sin\phi_i = -\sin\phi\sin\left(\dfrac{\beta_{i-1,i}-\beta_{i,i+1}}{2}\right)$,
   $(\cos\psi_i, \sin\psi_i) = -\left(\sin\left(\dfrac{\beta_{i,i+1}+\beta_{i-1,i}}{2}\right), -\cos\left(\dfrac{\beta_{i,i+1}+\beta_{i-1,i}}{2}\right)\right)$.

We can rule out case 2 given the conventions taken earlier, as follows. We

have

$$
\begin{aligned}
(\cos\psi_i, \sin\psi_i) &= \left(-\sin\left(\frac{\beta_{i,i+1}+\beta_{i-1,i}}{2}\right), \cos\left(\frac{\beta_{i,i+1}+\beta_{i-1,i}}{2}\right)\right) \\
&= \left(\cos\left(\frac{-\beta_{i,i+1}-\beta_{i-1,i}}{2}-\frac{\pi}{2}\right), -\sin\left(\frac{\beta_{i,i+1}+\beta_{i-1,i}}{2}-\frac{\pi}{2}\right)\right) \\
&= \left(\cos\left(\frac{\beta_{i,i+1}+\beta_{i-1,i}+\pi}{2}\right), -\sin\left(\frac{\beta_{i,i+1}+\beta_{i-1,i}+\pi}{2}-\pi\right)\right) \\
&= \left(\cos\left(\frac{\beta_{i,i+1}+\beta_{i-1,i}+\pi}{2}\right), \sin\left(\frac{\beta_{i,i+1}+\beta_{i-1,i}+\pi}{2}\right)\right).
\end{aligned}
$$

Therefore we have

$$
\begin{aligned}
\psi_i &= \frac{\beta_{i,i+1}+\beta_{i-1,i}+\pi}{2}\ , \quad \text{which gives} \\
\beta_{i,i+1} &= \psi_i + \psi_{i+1} - \psi_{i+2} - \frac{\pi}{2}\ , \\
\text{so}\quad \beta_{i-1,i} &= \beta_{i+2,i} \quad \text{since } i-1 \equiv i+2 \bmod 3 \\
&= \psi_{i+2} + \psi_i - \psi_{i+1} - \frac{\pi}{2}\ , \\
\text{hence}\quad \sin\phi_i &= -\sin\phi\sin\left(\frac{\beta_{i-1,i}-\beta_{i,i+1}}{2}\right) \\
&= \sin\phi\sin(\psi_{i+1}-\psi_{i+2})\ , \\
\text{so}\quad \sin\phi_1 &= \sin\phi\sin(\psi_2-\psi_3)\ , \\
\sin\phi_2 &= \sin\phi\sin(\psi_3-\psi_1)\ , \\
\sin\phi_3 &= \sin\phi\sin(\psi_1-\psi_2)\ .
\end{aligned}
$$

We know that N_1, N_2, and N_3 cannot lie in an angle of π for γ_1, γ_2, and γ_3 to be the medial axis near to an A_1^3 curve. This means that, since

$$
\begin{aligned}
& 0 \le \psi_1 < \psi_2 < \psi_3 < 2\pi\ , \text{ we must have} \\
& 0 < \psi_2 - \psi_1 < \pi\ ,\ 0 < \psi_3 - \psi_2 < \pi\ ,\ \pi < \psi_3 - \psi_1 < 2\pi \\
\Rightarrow\quad & \sin(\psi_1-\psi_2) < 0\ ,\ \sin(\psi_2-\psi_3) < 0\ ,\ \sin(\psi_3-\psi_1) < 0\ .
\end{aligned}
$$

Since $\sin\phi > 0$ and $\sin\phi_i > 0$ this means that $\sin\phi_i = \sin\phi\sin(\psi_{i+1}-\psi_{i+2})$ cannot be true. Therefore, we get a contradiction and so case 2 cannot be true.

The remaining possibility is case 1. We have

$$(\cos\psi_i, \sin\psi_i) = \left(\sin\left(\frac{\beta_{i,i+1}+\beta_{i-1,i}}{2}\right), -\cos\left(\frac{\beta_{i,i+1}+\beta_{i-1,i}}{2}\right)\right)$$
$$= \left(\cos\left(\frac{\beta_{i,i+1}+\beta_{i-1,i}}{2}-\frac{\pi}{2}\right), \sin\left(\frac{\beta_{i,i+1}+\beta_{i-1,i}}{2}-\frac{\pi}{2}\right)\right).$$

Hence we have

$$\begin{aligned}
\psi_i &= \frac{\beta_{i,i+1}+\beta_{i-1,i}}{2}-\frac{\pi}{2}\ , \\
\text{which gives}\quad \beta_{i,i+1} &= \psi_i+\psi_{i+1}-\psi_{i+2}+\frac{\pi}{2}\ , \\
\text{so}\quad \beta_{i-1,i} &= \beta_{i+2,i}\ \text{ since } i-1\equiv i+2 \bmod 3 \\
&= \psi_{i+2}+\psi_i-\psi_{i+1}+\frac{\pi}{2}\ , \\
\text{hence}\quad \sin\phi_i &= \sin\phi\sin\left(\frac{\beta_{i-1,i}-\beta_{i,i+1}}{2}\right) \\
&= \sin\phi\sin(\psi_{i+2}-\psi_{i+1})\ , \\
\text{and so}\quad \sin\phi_1 &= \sin\phi\sin(\psi_3-\psi_2)\ , \\
\sin\phi_2 &= \sin\phi\sin(\psi_1-\psi_3)\ , \\
\sin\phi_3 &= \sin\phi\sin(\psi_2-\psi_1)\ .
\end{aligned}$$

These solutions for $\sin\phi_i$ are consistent with the conventions, since $\sin(\psi_2-\psi_1)$, $\sin(\psi_3-\psi_2)$, $\sin(\psi_1-\psi_3)$, $\sin\phi$, and $\sin\phi_i$ are all greater than zero.

Lemma 3.4.1 *Setting* $N_i^+ = N_{i+1}^-$ *implies* $\sin\phi_i = \sin\phi\sin(\psi_{i+2}-\psi_{i+1})$.

We can substitute for $\beta_{i,i+1}$ in (3.35) to get more information about ϕ_i, α_i. We get

$$\begin{aligned}
&\hat{N}_i^+ (= \hat{N}_{i+1}^-) = \cos\beta_{i,i+1}N + \sin\beta_{i,i+1}B \iff \\
&\frac{\cos\phi_i\sin\alpha_i}{\sin\phi}(\sin\psi_i N - \cos\psi_i B) + \frac{\sin\phi_i}{\sin\phi}(\cos\psi_i N + \sin\psi_i B) \\
&= \cos\left(\psi_i+\psi_{i+1}-\psi_{i+2}+\frac{\pi}{2}\right)N + \sin\left(\psi_i+\psi_{i+1}-\psi_{i+2}+\frac{\pi}{2}\right)B \\
&= -\sin(\psi_i+\psi_{i+1}-\psi_{i+2})N + \cos(\psi_i+\psi_{i+1}-\psi_{i+2})B\ .
\end{aligned}$$

Equating the components of N and the components of B of the above vector equation gives the following:

$$\begin{aligned}\cos\phi_i \sin\alpha_i \sin\psi_i + \sin\phi_i \cos\psi_i &= -\sin\phi \sin(\psi_i + \psi_{i+1} - \psi_{i+2}) \ , \\ -\cos\phi_i \sin\alpha_i \cos\psi_i + \sin\phi_i \sin\psi_i &= \sin\phi \cos(\psi_i + \psi_{i+1} - \psi_{i+2}) \ .\end{aligned}$$

Then, $\sin\psi_i \times$ first $-\cos\psi_i \times$ second gives the following:

$$\begin{aligned} & \cos\phi_i \sin\alpha_i \\ = \quad & -\sin\phi(\cos(\psi_i + \psi_{i+1} - \psi_{i+2})\cos\psi_i + \sin(\psi_i + \psi_{i+1} - \psi_{i+2})\sin\psi_i) \\ \iff \quad & \cos\phi_i \sin\alpha_i = -\sin\phi\cos(\psi_{i+2} - \psi_{i+1}) \\ \iff \quad & \cos\phi_i = -\frac{\sin\phi\cos(\psi_{i+2} - \psi_{i+1})}{\sin\alpha_i} \ . \end{aligned} \tag{3.36}$$

Assume $\cos\phi \neq 0$ which, by (3.32), means $\cos\phi_i \neq 0$ and $\cos\alpha_i \neq 0$. Then we have

$$\cos\alpha_i = \frac{\cos\phi}{\cos\phi_i} = -\frac{\cos\phi\sin\alpha_i}{\sin\phi\cos(\psi_{i+2} - \psi_{i+1})} \ . \tag{3.37}$$

We can now solve for $\sin\alpha_i$ in terms of ϕ, ψ_i by using $\cos^2\alpha_i + \sin^2\alpha_i = 1$:

$$\begin{aligned} & \cos^2\alpha_i + \sin^2\alpha_i = 1 \iff \\ & \sin^2\alpha_i \left(\frac{\cos^2\phi}{\sin^2\phi\cos^2(\psi_{i+2} - \psi_{i+1})} + 1 \right) = 1 \\ \text{and so} \quad \sin\alpha_i &= \sqrt{\frac{\tan^2\phi\cos^2(\psi_{i+2} - \psi_{i+1})}{1 + \tan^2\phi\cos^2(\psi_{i+2} - \psi_{i+1})}} \ , \quad \text{since } \sin\alpha_i > 0 \\ &= \frac{-\tan\phi|\cos(\psi_{i+2} - \psi_{i+1})|}{\sqrt{1 + \tan^2\phi\cos^2(\psi_{i+2} - \psi_{i+1})}} \ , \end{aligned}$$

since we took ϕ to be obtuse. Then from (3.37) we have

$$\cos\alpha_i = \frac{-\cos\phi\sin\alpha_i}{\sin\phi\cos(\psi_{i+2} - \psi_{i+1})} = \frac{\text{sign}(\cos(\psi_{i+2} - \psi_{i+1}))}{\sqrt{1 + \tan^2\phi\cos^2(\psi_{i+2} - \psi_{i+1})}} \ .$$

Also from (3.36) we have

$$\begin{aligned}\cos\phi_i &= -\frac{\sin\phi\cos(\psi_{i+2} - \psi_{i+1})}{\sin\alpha_i} \\ &= \text{sign}(\cos(\psi_{i+2} - \psi_{i+1}))\cos\phi\sqrt{1 + \tan^2\phi\cos^2(\psi_{i+2} - \psi_{i+1})} \ .\end{aligned}$$

Now let us substitute the solutions for ϕ_i, α_i into the expression (3.31) for $N_i^{\pm}$. We get

$$\begin{aligned} N_i^{\pm} &= -\cos\phi_i\,(\cos\alpha_i T + \sin\alpha_i \sin\psi_i N - \sin\alpha_i\cos\psi_i B) \\ &\quad \mp \sin\phi_i\,(\cos\psi_i N + \sin\psi_i B) \\ &= -\cos\phi T \\ &\quad + \sin\phi\,(\sin\psi_i\cos(\psi_{i+2}-\psi_{i+1}) \mp \cos\psi_i\sin(\psi_{i+2}-\psi_{i+1}))\,N \\ &\quad + \sin\phi\,(-\cos\psi_i\cos(\psi_{i+2}-\psi_{i+1}) \mp \sin\psi_i\sin(\psi_{i+2}-\psi_{i+1}))\,B \\ &= -\cos\phi T + \sin\phi\sin(\psi_i \mp (\psi_{i+2}-\psi_{i+1}))N \\ &\quad - \sin\phi\cos(\psi_i \mp (\psi_{i+2}-\psi_{i+1}))B\ . \end{aligned}$$

Hence we have

$$\begin{aligned} N_{i+1}^{-} &= -\cos\phi T + \sin\phi\sin(\psi_{i+1}+\psi_i-\psi_{i+2})N \\ &\quad - \sin\phi\cos(\psi_{i+1}+\psi_i-\psi_{i+2})B \\ &= N_i^{+}\ . \end{aligned}$$

Hence the solutions for $\cos\phi_i$, $\sin\phi_i$, $\cos\alpha_i$, $\sin\alpha_i$ imply $N_i^+ = N_{i+1}^-$ and so at all points of the A_1^3 curve, $N_i^+ = N_{i+1}^-$ for $i = 1, 2, 3$ if and only if the solutions for $\cos\phi_i$, $\sin\phi_i$, $\cos\alpha_i$, $\sin\alpha_i$ hold. Hence we have the following.

Theorem 3.4.2.1 *The angles ϕ_i, α_i are uniquely determined at all points of the A_1^3 curve by the following:*

$$\cos\phi_i = -\epsilon_i\sqrt{\cos^2\phi + \sin^2\phi\cos^2\theta_i}\ , \tag{3.38}$$

$$\sin\phi_i = \sin\phi\sin\theta_i\ , \tag{3.39}$$

$$\cos\alpha_i = \frac{-\epsilon_i\cos\phi}{\sqrt{\cos^2\phi + \sin^2\phi\cos^2\theta_i}}\ , \tag{3.40}$$

$$\sin\alpha_i = \frac{\sin\phi|\cos\theta_i|}{\sqrt{\cos^2\phi + \sin^2\phi\cos^2\theta_i}}\ , \tag{3.41}$$

where $\theta_i = \psi_{i+2} - \psi_{i+1}$ and $\epsilon_i = \mathrm{sign}(\cos(\psi_{i+2}-\psi_{i+1}))$. There are no other conditions on the medial axis along the A_1^3 curve at the level of first order derivatives. (See Table 3.1 for a summary of the notation used.)

Remark 3.4.2.2 The equations (3.38), (3.39), (3.40), and (3.41) uniquely determine α_i, ϕ_i, in terms of ϕ, ψ_i, and so the normals $N_i^{\pm}$ to the boundaries are uniquely determined by ϕ, ψ_i. Hence Theorem 3.4.2.1 gives the complete first order information about the boundaries $\gamma_i^{\pm}$ at points corresponding to the A_1^3 curve. Now $\theta_3 = \psi_2 - \psi_1 = -\theta_1 - \theta_2$, and so $\cos\phi_i$, $\sin\phi_i$, $\cos\alpha_i$, $\sin\alpha_i$ can be expressed in terms of three variables ϕ, θ_1, and θ_2. In the case when $\cos\theta_i = 0$ for some i the formulae of Theorem 3.4.2.1 are still valid, but we must interpret $-\epsilon_i$ as the sign of $\cos\phi_i$. Note that for any ϕ, ψ_1, ψ_2, ψ_3 we have $\text{sign}(\cos\phi_i) = -\epsilon_i$, since ϕ is obtuse. Then, from (3.6), we have that $\text{sign}(v_i) = \epsilon_i$.

3.4.3 Equating Principal Curvatures, Directions of the Boundaries at A_1^3 Points

The normal to a surface determines the surface up to first order; it determines the tangent plane to the surface. Then, in addition, the principal curvatures and principal directions determine the surface up to second order. Setting $N_i^+ = N_{i+1}^-$ gave first order information about the three medial sheets. Now we want to gain second order information about the three medial sheets, so we need to equate the principal curvatures and principal directions of γ_i^+ and γ_{i+1}^- at a point $\gamma_i(r_i = r_0, t_i = 0)$ of the A_1^3 curve. Let $S_{\mathbf{v}_i}^{\pm}$ denote the matrix representation of the radial shape operator of γ_i corresponding to boundary $\gamma_i^{\pm}$ with respect to the basis $\mathbf{v}_i = \{T_i, U_i\}$ at $\gamma_i(r_0, 0)$. Then let $\text{trace}_i^{\pm}$, $\det_i^{\pm}$ be the trace, determinant of $S_{\mathbf{v}_i}^{\pm}$. From (3.20) and using the notation of Table 3.1 we have

$$\left.\begin{aligned} S_{\mathbf{v}_i}^{\pm} &= \begin{pmatrix} (s_{11}^{\pm})_i & (s_{12}^{\pm})_i \\ (s_{21}^{\pm})_i & (s_{22}^{\pm})_i \end{pmatrix} \\ &= \begin{pmatrix} -\frac{a_i}{v_i^3 \sin^2\phi_i} \pm \frac{\kappa_i^r}{\sin\phi_i} & \left(-\frac{a_i^t}{v_i^2} \mp \tau_i^t \sin\phi_i\right) \frac{1}{\sin^2\phi_i} \\ -\frac{a_i^t}{v_i^2} \mp \tau_i^t \sin\phi_i & \frac{a_i^*}{v_i^2} \pm \kappa_i^t \sin\phi_i \end{pmatrix}. \end{aligned}\right\} \tag{3.42}$$

We have the following.

Lemma 3.4.3.1 *Equating principal curvatures on* γ_i^+, γ_{i+1}^- *at* $(r_0, 0)$ *is the same as setting* $\text{trace}_i^+ = \text{trace}_{i+1}^-$ *and* $\det_i^+ = \det_{i+1}^-$.

Proof. Let η be a principal radial curvature of γ_i corresponding to boundary γ_i^+. Similarly, let ν be a principal radial curvature of γ_{i+1} corresponding to boundary γ_{i+1}^-. Then, using (3.16) from Lemma 3.3.1.4, equating principal curvatures on γ_i^+, γ_{i+1}^- is the same as setting

$$\begin{aligned} \frac{\eta}{1 - r_i\eta} &= \frac{\nu}{1 - r_{i+1}\nu} \\ \iff \eta(1 - r_i\nu) &= \nu(1 - r_i\eta) \text{ , since } r_{i+1} = r_i \text{ at points of the } A_1^3 \text{ curve} \\ \iff \eta &= \nu \text{ .} \end{aligned}$$

So equating principal curvatures on γ_i^+, γ_{i+1}^- is the same as setting the principal radial curvatures of γ_i corresponding to boundary γ_i^+ equal to the principal radial curvatures of γ_{i+1} corresponding to boundary γ_{i+1}^-. Then, equating eigenvalues of two matrices is the same as equating the traces of the two matrices and equating the determinants of the two matrices. Hence the result. □

Equating principal curvatures on γ_i^+, γ_{i+1}^- gives the following.

Theorem 3.4.3.2 (Consistency Conditions at A_1^3 Points) *The following is satisfied at* $\gamma_i(r_0, 0)$ *on the* A_1^3 *curve lying on* γ_i *for i =1, 2, 3:*

$$\sum_{i=1}^{3} \left(\kappa_i^t \sin\phi_i + \frac{\kappa_i^r}{\sin\phi_i} \right) = 0 \text{ ,} \tag{3.43}$$

$$\text{and} \quad \sum_{i=1}^{3} \left(\frac{a_i^* \kappa_i^r v_i - a_i \kappa_i^t - 2a_i^t \tau_i^t v_i}{v_i^3 \sin\phi_i} \right) = 0 \text{ .} \tag{3.44}$$

(See Table 3.1 for a summary of the notation used.)

Proof. By Lemma 3.4.3.1 we need to set $\text{trace}_i^+ = \text{trace}_{i+1}^-$ and $\det_i^+ = \det_{i+1}^-$ for $i = 1, 2, 3$ in order to equate the principal curvatures on γ_i^+, γ_{i+1}^-. Then, by

equation (3.21) from Lemma 3.3.2.2, we have

$$\begin{aligned} \frac{1}{2}(\text{trace}_i^+ - \text{trace}_i^-) &= \frac{\kappa_i^r}{\sin\phi_i} + \kappa_i^t \sin\phi_i \ , \\ \text{so } \frac{1}{2}\sum_{i=1}^{3}(\text{trace}_i^+ - \text{trace}_i^-) &= \sum_{i=1}^{3}\left(\kappa_i^t \sin\phi_i + \frac{\kappa_i^r}{\sin\phi_i}\right). \end{aligned}$$

But the left-hand side is zero, since $\text{trace}_i^+ = \text{trace}_{i+1}^-$. Hence equation (3.43). Similarly, equation (3.22) from Lemma 3.3.2.2 gives

$$\begin{aligned} \frac{1}{2}(\det_i^+ - \det_i^-) &= \frac{a_i^*\kappa_i^r v_i - a_i\kappa_i^t - 2a_i^t\tau_i^t v_i}{v_i^3 \sin\phi_i} \ , \\ \text{so } \frac{1}{2}\sum_{i=1}^{3}(\det_i^+ - \det_i^-) &= \sum_{i=1}^{3}\left(\frac{a_i^*\kappa_i^r v_i - a_i\kappa_i^t - 2a_i^t\tau_i^t v_i}{v_i^3 \sin\phi_i}\right). \end{aligned}$$

Again the left-hand side is zero, hence equation (3.44). □

Now to equate principal directions on γ_i^+, γ_{i+1}^- at the A_1^3 point $\gamma_i(r_0, 0)$ using (3.26) from Lemma 3.3.3.2. The method for this is as follows. Consider principal directions $\{P_1, P_2\}$ on γ_i^+ and principal directions $\{Q_1, Q_2\}$ on γ_{i+1}^-, all evaluated at $(r_0, 0)$. If we say P_1 is in the same direction as Q_1 and P_2 is in the same direction as Q_2 on $\gamma_i^+ = \gamma_{i+1}^-$, this is the same as saying $P_1 \cdot Q_2 = 0$. This is because, given that the principal curvatures on γ_i^+ are equal to those on γ_{i+1}^- at $(r_0, 0)$, it is only one extra condition to say the principal directions are equal. Therefore, for another constraint, we want to identify the non-corresponding principal directions on γ_i^+ and on γ_{i+1}^- and set their dot product equal to zero.

We assume $\gamma_i^+(r_0, 0) = \gamma_{i+1}^-(r_0, 0)$ is not an umbilic. Let $(\kappa_{r1}^{\pm})_i$, $(\kappa_{r2}^{\pm})_i$ be the two principal radial curvatures of γ_i corresponding to $\gamma_i^{\pm}$. Given that the principal curvatures on γ_i^+, γ_{i+1}^- are equal at $\gamma_i^+(r_0, 0) = \gamma_{i+1}^-(r_0, 0)$, from Lemma 3.4.3.1 we have that $\{(\kappa_{r1}^+)_i, (\kappa_{r2}^+)_i\}$ is the same as $\{(\kappa_{r1}^-)_{i+1}, (\kappa_{r2}^-)_{i+1}\}$. Let

$$\begin{aligned} (\kappa_{r1}^{\pm})_i &= \frac{1}{2}\left(\text{trace}_i^{\pm} + \sqrt{(\text{trace}_i^{\pm})^2 - 4\text{det}_i^{\pm}}\right), \\ (\kappa_{r2}^{\pm})_i &= \frac{1}{2}\left(\text{trace}_i^{\pm} - \sqrt{(\text{trace}_i^{\pm})^2 - 4\text{det}_i^{\pm}}\right). \end{aligned}$$

Then we must have $(\kappa_{r1}^+)_i = (\kappa_{r1}^-)_{i+1}$, $(\kappa_{r2}^+)_i = (\kappa_{r2}^-)_{i+1}$ when $\gamma_i^+(r_0,0) = \gamma_{i+1}^-(r_0,0)$ is a non-umbilic, since $\text{trace}_i^+ = \text{trace}_{i+1}^-$, $\det_i^+ = \det_{i+1}^-$ at $(r_0,0)$. We introduce a shortened notation:

$$\begin{aligned}
(\kappa_{r1}^+)_i &= (\kappa_{r1}^-)_{i+1} = \frac{(\text{tr})_{i,i+1} + \text{D}_{i,i+1}}{2} \ , \\
(\kappa_{r2}^+)_i &= (\kappa_{r2}^-)_{i+1} = \frac{(\text{tr})_{i,i+1} - \text{D}_{i,i+1}}{2} \ , \\
\text{where} \quad (\text{tr})_{i,i+1} &= \text{trace}_i^+ = \text{trace}_{i+1}^- \ , \\
\text{and} \quad \text{D}_{i,i+1} &= \sqrt{(\text{trace}_i^+)^2 - 4\det_i^+} = \sqrt{(\text{trace}_{i+1}^-)^2 - 4\det_{i+1}^-} \ .
\end{aligned}$$

Using (3.26) from Lemma 3.3.3.2, the principal directions on $\gamma_i^\pm$ are

$$\begin{aligned}
& \left((s_{12}^\pm)_i T_i + ((\kappa_{r1}^\pm)_i - (s_{11}^\pm)_i) U_i + (s_{12}^\pm)_i \cos\phi_i N_i^\pm\right) \\
\text{and} \qquad & \left((s_{12}^\pm)_i T_i + ((\kappa_{r2}^\pm)_i - (s_{11}^\pm)_i) U_i + (s_{12}^\pm)_i \cos\phi_i N_i^\pm\right) .
\end{aligned}$$

The dot product of perpendicular principal directions on $\gamma_i^+ = \gamma_{i+1}^-$ at $\gamma_i^+(r_0,0) = \gamma_{i+1}^-(r_0,0)$ on the A_1^3 curve is zero, so

$$\begin{aligned}
&\left((s_{12}^-)_{i+1} T_{i+1} + ((\kappa_{r2}^-)_{i+1} - (s_{11}^-)_{i+1}) U_{i+1} + (s_{12}^-)_{i+1} \cos\phi_{i+1} N_{i+1}^-\right) \\
&\qquad \cdot \left((s_{12}^+)_i T_i + ((\kappa_{r1}^+)_i - (s_{11}^+)_i) U_i + (s_{12}^+)_i \cos\phi_i N_i^+\right) = 0 \ .
\end{aligned} \tag{3.45}$$

Since $N_i^+(r_0,0) = N_{i+1}^-(r_0,0)$, we have

$$\begin{aligned}
& U_i \perp N_{i+1}^-, U_{i+1} \perp N_i^+ \ , \\
& T_i \cdot N_{i+1}^- = T_i \cdot N_i^+ = -\cos\phi_i \ , \\
\text{and} \qquad & T_{i+1} \cdot N_i^+ = T_{i+1} \cdot N_{i+1}^- = -\cos\phi_{i+1} \ .
\end{aligned}$$

So (3.45) becomes

$$\begin{aligned}
& \left((s_{12}^+)_i (s_{12}^-)_{i+1}\right) T_i \cdot T_{i+1} \\
& + \left(\left(\tfrac{(\text{tr})_{i,i+1} + \text{D}_{i,i+1}}{2} - (s_{11}^+)_i\right)(s_{12}^-)_{i+1}\right) U_i \cdot T_{i+1} \\
& + \left(\left(\tfrac{(\text{tr})_{i,i+1} - \text{D}_{i,i+1}}{2} - (s_{11}^-)_{i+1}\right)(s_{12}^+)_i\right) T_i \cdot U_{i+1} \\
& + \left(\left(\tfrac{(\text{tr})_{i,i+1} + \text{D}_{i,i+1}}{2} - (s_{11}^+)_i\right)\left(\tfrac{(\text{tr})_{i,i+1} - \text{D}_{i,i+1}}{2} - (s_{11}^-)_{i+1}\right)\right) U_i \cdot U_{i+1} \\
& = (s_{12}^+)_i (s_{12}^-)_{i+1} \cos\phi_i \cos\phi_{i+1} \ .
\end{aligned} \tag{3.46}$$

Similarly, the two principal directions corresponding to $(\kappa_{r2}^+)_i$ and $(\kappa_{r1}^-)_{i+1}$ are perpendicular, so

$$\begin{aligned}&\left((s_{12}^-)_{i+1}T_{i+1}+((\kappa_{r1}^-)_{i+1}-(s_{11}^-)_{i+1})U_{i+1}+(s_{12}^-)_{i+1}\cos\phi_{i+1}N_{i+1}^-\right)\\&\qquad\cdot\left((s_{12}^+)_iT_i+((\kappa_{r2}^+)_i-(s_{11}^+)_i)U_i+(s_{12}^+)_i\cos\phi_iN_i^+\right)=0\ .\end{aligned}$$

Similarly, this simplifies to become

$$\begin{aligned}&\left((s_{12}^+)_i(s_{12}^-)_{i+1}\right)T_i\cdot T_{i+1}\\&+\left(\left(\tfrac{(\mathrm{tr})_{i,i+1}-\mathrm{D}_{i,i+1}}{2}-(s_{11}^+)_i\right)(s_{12}^-)_{i+1}\right)U_i\cdot T_{i+1}\\&+\left(\left(\tfrac{(\mathrm{tr})_{i,i+1}+\mathrm{D}_{i,i+1}}{2}-(s_{11}^-)_{i+1}\right)(s_{12}^+)_i\right)T_i\cdot U_{i+1}\\&+\left(\left(\tfrac{(\mathrm{tr})_{i,i+1}-\mathrm{D}_{i,i+1}}{2}-(s_{11}^+)_i\right)\left(\tfrac{(\mathrm{tr})_{i,i+1}+\mathrm{D}_{i,i+1}}{2}-(s_{11}^-)_{i+1}\right)\right)U_i\cdot U_{i+1}\\&=(s_{12}^+)_i(s_{12}^-)_{i+1}\cos\phi_i\cos\phi_{i+1}\ .\end{aligned}\tag{3.47}$$

Then (3.46) − (3.47) is the same as

$$\begin{aligned}0=\mathrm{D}_{i,i+1}&\left((s_{12}^-)_{i+1}T_{i+1}\cdot U_i-(s_{12}^+)_iT_i\cdot U_{i+1}\right.\\&\left.+((s_{11}^+)_i-(s_{11}^-)_{i+1})U_i\cdot U_{i+1}\right).\end{aligned}\tag{3.48}$$

and (3.46) + (3.47) is the same as

$$\begin{aligned}&2(s_{12}^+)_i(s_{12}^-)_{i+1}T_i\cdot T_{i+1}+(s_{12}^-)_{i+1}((\mathrm{tr})_{i,i+1}-2(s_{11}^+)_i)T_{i+1}\cdot U_i\\&+(s_{12}^+)_i((\mathrm{tr})_{i,i+1}-2(s_{11}^-)_{i+1})T_i\cdot U_{i+1}\\&\left(\frac{1}{2}\left(((\mathrm{tr})_{i,i+1})^2-(\mathrm{D}_{i,i+1})^2\right)\right.\\&\quad\left.-(\mathrm{tr})_{i,i+1}((s_{11}^+)_i)+(s_{11}^-)_{i+1})+2(s_{11}^+)_i(s_{11}^-)_{i+1}\right)U_i\cdot U_{i+1}\\&=(s_{12}^+)_i(s_{12}^-)_{i+1}\cos\phi_i\cos\phi_{i+1}\ .\end{aligned}$$

This simplifies (using the definitions of $(\mathrm{tr})_{i,i+1}$, $\mathrm{D}_{i,i+1}$, $\mathrm{trace}_i^{\pm}$, and $\det_i^{\pm}$) to become

$$\begin{aligned}&2(s_{12}^+)_i(s_{12}^-)_{i+1}(T_i\cdot T_{i+1}-\cos\phi_i\cos\phi_{i+1})\\&+(s_{12}^-)_{i+1}\left((s_{22}^+)_i-(s_{11}^+)_i\right)T_{i+1}\cdot U_i\\&+(s_{12}^+)_i\left((s_{22}^-)_{i+1}-(s_{11}^-)_{i+1}\right)T_i\cdot U_{i+1}\\&+\left(\left((s_{11}^+)_i-(s_{11}^-)_{i+1}\right)\left((s_{22}^+)_i-(s_{22}^-)_{i+1}\right)\right.\\&\quad\left.-(s_{12}^+)_i(s_{21}^+)_i-(s_{12}^-)_{i+1}(s_{21}^-)_{i+1}\right)U_i\cdot U_{i+1}=0\ .\end{aligned}\tag{3.49}$$

Hence we have shown that $\{(3.46), (3.47)\}$ is the same as $\{(3.48), (3.49)\}$ and so equating principal directions on γ_i^+, γ_{i+1}^- is the same as $\{(3.48), (3.49)\}$ being true at $\gamma_i(r_0, 0)$. But we know that $\mathrm{D}_{i,i+1} \neq 0$ since we assumed that the principal radial curvatures are distinct. Therefore we can cancel $\mathrm{D}_{i,i+1}$ from (3.48). We can also use (3.27) to substitute for $T_i \cdot T_{i+1}$, $T_{i+1} \cdot U_i$, $T_i \cdot U_{i+1}$, and $U_i \cdot U_{i+1}$. We get

$$\begin{aligned}
T_i \cdot T_{i+1} &= \cos\alpha_i \cos\alpha_{i+1} + \sin\alpha_i \sin\alpha_{i+1} \cos\theta_{i+2} \ , \\
T_i \cdot U_{i+1} &= -\cos\alpha_i \sin\alpha_{i+1} + \sin\alpha_i \cos\alpha_{i+1} \cos\theta_{i+2} \ , \\
T_{i+1} \cdot U_i &= -\sin\alpha_i \cos\alpha_{i+1} + \cos\alpha_i \sin\alpha_{i+1} \cos\theta_{i+2} \ , \\
U_i \cdot U_{i+1} &= \sin\alpha_i \sin\alpha_{i+1} + \cos\alpha_i \cos\alpha_{i+1} \cos\theta_{i+2} \ .
\end{aligned}$$

Then, using Theorem 3.4.2.1, we get

$$\begin{aligned}
& T_i \cdot T_{i+1} \epsilon_i \epsilon_{i+1} \sqrt{1 + \tan^2\phi \cos^2\theta_i} \sqrt{1 + \tan^2\phi \cos^2\theta_{i+1}} \\
= \ & 1 + \frac{\sin^2\phi}{\cos^2\phi} \cos\theta_i \cos\theta_{i+1} \cos\theta_{i+2} \ , \\
& T_i \cdot U_{i+1} \epsilon_i \epsilon_{i+1} \sqrt{1 + \tan^2\phi \cos^2\theta_i} \sqrt{1 + \tan^2\phi \cos^2\theta_{i+1}} \\
= \ & \frac{\sin\phi}{\cos\phi} \left(\cos\theta_{i+1} - \cos\theta_i \cos\theta_{i+2}\right) \ , \\
& T_{i+1} \cdot U_i \epsilon_i \epsilon_{i+1} \sqrt{1 + \tan^2\phi \cos^2\theta_i} \sqrt{1 + \tan^2\phi \cos^2\theta_{i+1}} \\
= \ & \frac{\sin\phi}{\cos\phi} \left(\cos\theta_i - \cos\theta_{i+1} \cos\theta_{i+2}\right) \ , \\
& U_i \cdot U_{i+1} \epsilon_i \epsilon_{i+1} \sqrt{1 + \tan^2\phi \cos^2\theta_i} \sqrt{1 + \tan^2\phi \cos^2\theta_{i+1}} \\
= \ & \frac{\sin^2\phi}{\cos^2\phi} \cos\theta_i \cos\theta_{i+1} + \cos\theta_{i+2} \ .
\end{aligned}$$

Using these, and substituting for $(s_{12}^+)_i$, $(s_{12}^-)_{i+1}$, $(s_{11}^+)_i$, and $(s_{11}^-)_{i+1}$ into (3.48) and (3.49), we get the following.

Proposition 3.4.3.3 (Constraint on Curvatures) *Given that the principal curvatures on γ_i^+, γ_{i+1}^- are equal, the principal directions on γ_i^+, γ_{i+1}^- are equal at a non-umbilic point $\gamma_i^+(r_0, 0) = \gamma_{i+1}^-(r_0, 0)$ corresponding to $\gamma_i(r_0, 0)$*

on the A_1^3 curve if and only if the following equations hold:

$$\begin{aligned} 0 \;=\; & \left(\frac{a_i^t}{v_i^2}+\tau_i^t\sin\phi_i\right)\frac{(\cos\theta_{i+1}-\cos\theta_i\cos\theta_{i+2})}{\cos\phi\sin\phi\sin^2\theta_i} \\ & +\left(-\frac{a_{i+1}^t}{v_{i+1}^2}+\tau_{i+1}^t\sin\phi_{i+1}\right)\frac{(\cos\theta_i-\cos\theta_{i+1}\cos\theta_{i+2})}{\cos\phi\sin\phi\sin^2\theta_{i+1}} \\ & +\left(-\frac{a_i}{v_i^3\sin^2\phi_i}+\frac{\kappa_i^r}{\sin\phi_i}\right)\left(\frac{\sin^2\phi}{\cos^2\phi}\cos\theta_i\cos\theta_{i+1}+\cos\theta_{i+2}\right) \\ & +\left(\frac{a_{i+1}}{v_{i+1}^3\sin^2\phi_{i+1}}+\frac{\kappa_{i+1}^r}{\sin\phi_{i+1}}\right)\left(\frac{\sin^2\phi}{\cos^2\phi}\cos\theta_i\cos\theta_{i+1}+\cos\theta_{i+2}\right) \end{aligned} \tag{3.50}$$

and

$$\begin{aligned} 0 = {} & (s_{12}^-)_{i+1}\left((s_{22}^+)_i-(s_{11}^+)_i\right)\tfrac{\sin\phi}{\cos\phi}\left(\cos\theta_i-\cos\theta_{i+1}\cos\theta_{i+2}\right) \\ & +(s_{12}^+)_i\left((s_{22}^-)_{i+1}-(s_{11}^-)_{i+1}\right)\tfrac{\sin\phi}{\cos\phi}\left(\cos\theta_{i+1}-\cos\theta_i\cos\theta_{i+2}\right) \\ & +2(s_{12}^+)_i(s_{12}^-)_{i+1}\left(1+\tfrac{\sin^2\phi}{\cos^2\phi}\cos\theta_i\cos\theta_{i+1}\cos\theta_{i+2}-\tfrac{\cos^2\phi_i\cos^2\phi_{i+1}}{\cos^2\phi}\right) \\ & +\left[\left((s_{11}^+)_i-(s_{11}^-)_{i+1}\right)\left((s_{22}^+)_i-(s_{22}^-)_{i+1}\right)\right. \\ & \left.-(s_{12}^+)_i(s_{21}^+)_i-(s_{12}^-)_{i+1}(s_{21}^-)_{i+1}\right]\left(\tfrac{\sin^2\phi}{\cos^2\phi}\cos\theta_i\cos\theta_{i+1}+\cos\theta_{i+2}\right) \end{aligned} \tag{3.51}$$

where $(s_{11}^\pm)_i$, $(s_{12}^\pm)_i$, $(s_{21}^\pm)_i$, $(s_{22}^\pm)_i$ are given by (3.42) *and* $\cos\phi_i=-1/v_i$, $\sin\phi_i$ *are given by Theorem 3.4.2.1. (See Table 3.1 for a summary of the notation used.)*

3.4.4 Reducing the Number of Variables

Setting equal the principal curvatures on $\gamma_i^+=\gamma_{i+1}^-$ at $(r_0,0)$ *implies* (3.43) and (3.44) from Theorem 3.4.3.2, but we want all of the information about the medial axis given by equating principal curvatures and principal directions. We want to reduce the number of variables involved in the principal curvatures and principal directions, which can be done by involving the geometry of the A_1^3 curve. Consider the following lemma.

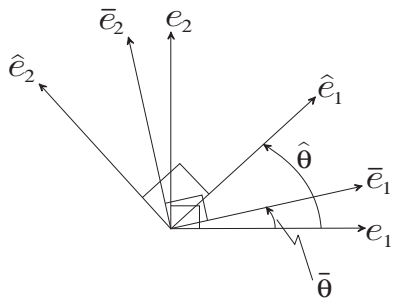

Figure 3.8: Two sets $\{\overline{e}_1, \overline{e}_2\}$, $\{\hat{e}_1, \hat{e}_2\}$ of perpendicular tangent directions in relation to the principal directions e_1, e_2 on the surface S. These directions are used to obtain formulae (3.56), (3.57), (3.58) for the normal curvatures and geodesic torsions of S in the directions $\hat{e}_1$, $\hat{e}_2$ in terms of the normal curvatures of and geodesic torsions of S in the directions $\{\overline{e}_1, \overline{e}_2\}$ and the angle $(\hat{\theta} - \overline{\theta})$.

Lemma 3.4.4.1 (Euler Formula) *Let the principal curvatures on a surface S at a point p be k_1, k_2 with corresponding principal directions e_1, e_2. Then the normal curvature k_n of S in the direction of $V = e_1 \cos\theta + e_2 \sin\theta$ (where θ is the angle from e_1 to V) is*

$$k_n = k_1 \cos^2\theta + k_2 \sin^2\theta \ .$$

This equation is called the Euler formula. Also, the geodesic torsion t_g of S in the direction V is

$$t_g = (k_2 - k_1) \cos\theta \sin\theta \ .$$

Assume we are given k_1, k_2 and e_1, e_2. Then assume we are given the normal curvatures $\overline{\kappa}_{n1}$, $\overline{\kappa}_{n2}$ respectively in two perpendicular directions $\overline{e}_1$, $\overline{e}_2$, where the angle from e_1 to $\overline{e}_1$ is $\overline{\theta}$, and the geodesic torsion $\overline{\tau}_{g1}$ in the direction of $\overline{e}_1$. Now consider an unknown set of 'geometries' $\hat{\kappa}_{n1}$, $\hat{\kappa}_{n2}$, $\hat{\tau}_{g1}$, which are defined similarly as follows. We define $\hat{\kappa}_{n1}$, $\hat{\kappa}_{n2}$ as the normal curvatures of S at p in the corresponding perpendicular directions $\hat{e}_1$, $\hat{e}_2$ where the angle from e_1 to $\hat{e}_1$ is $\hat{\theta}$. Also, let $\hat{\tau}_{g1}$ be the geodesic torsion of S at p in the direction of $\hat{e}_1$. We want to obtain formulae for $\{\hat{\kappa}_{n1}, \hat{\kappa}_{n2}, \hat{\tau}_{g1}\}$ in terms of $\{\overline{\kappa}_{n1}, \overline{\kappa}_{n2}, \overline{\tau}_{g1}\}$. See Figure 3.8.

By Lemma 3.4.4.1 we have

$$\begin{aligned}\overline{\kappa}_{n1} &= k_1\cos^2\overline{\theta} + k_2\sin^2\overline{\theta}\ , \quad \overline{\kappa}_{n2} = k_1\sin^2\overline{\theta} + k_2\cos^2\overline{\theta}\ , \\ \overline{\tau}_{g1} &= (k_2-k_1)\cos\overline{\theta}\sin\overline{\theta}\ .\end{aligned}$$

Solving these for k_1, k_2 in terms of $\overline{\kappa}_{n1}$, $\overline{\kappa}_{n2}$ gives the following:

$$k_1 = \frac{\overline{\kappa}_{n1}\cos^2\overline{\theta} - \overline{\kappa}_{n2}\sin^2\overline{\theta}}{\cos(2\overline{\theta})}, \quad k_2 = \frac{-\overline{\kappa}_{n1}\sin^2\overline{\theta} + \overline{\kappa}_{n2}\cos^2\overline{\theta}}{\cos(2\overline{\theta})} \tag{3.52}$$

$$\Rightarrow k_2 - k_1 = \frac{(\overline{\kappa}_{n2}-\overline{\kappa}_{n1})}{\cos(2\overline{\theta})} \ \Rightarrow\ \overline{\tau}_{g1} = \frac{(\overline{\kappa}_{n2}-\overline{\kappa}_{n1})\sin 2\overline{\theta}}{2\cos(2\overline{\theta})}\ . \tag{3.53}$$

Also by Lemma 3.4.4.1 we have

$$\hat{\kappa}_{n1} = k_1\cos^2\hat{\theta} + k_2\sin^2\hat{\theta}\ , \quad \hat{\kappa}_{n2} = k_1\sin^2\hat{\theta} + k_2\cos^2\hat{\theta}\ , \tag{3.54}$$

$$\hat{\tau}_{g1} = (k_2-k_1)\cos\hat{\theta}\sin\hat{\theta}\ . \tag{3.55}$$

Hence, using (3.52), (3.54),

$$\begin{aligned}\hat{\kappa}_{n1}\cos 2\overline{\theta} &= \overline{\kappa}_{n1}\left(\cos^2\hat{\theta}\cos^2\overline{\theta} - \sin^2\hat{\theta}\sin^2\overline{\theta}\right) \\ &\quad +\overline{\kappa}_{n2}\left(\sin^2\hat{\theta}\cos^2\overline{\theta} - \cos^2\hat{\theta}\sin^2\overline{\theta}\right) \\ &= \overline{\kappa}_{n1}\cos(\hat{\theta}-\overline{\theta})\cos(\hat{\theta}+\overline{\theta}) + \overline{\kappa}_{n2}\sin(\hat{\theta}-\overline{\theta})\sin(\hat{\theta}+\overline{\theta}) \\ &= \overline{\kappa}_{n1}\cos(\hat{\theta}-\overline{\theta})\left(\cos(\hat{\theta}-\overline{\theta})\cos(2\overline{\theta}) - \sin(\hat{\theta}-\overline{\theta})\sin(2\overline{\theta})\right) \\ &\quad +\overline{\kappa}_{n2}\sin(\hat{\theta}-\overline{\theta})\left(\sin(\hat{\theta}-\overline{\theta})\cos(2\overline{\theta}) + \cos(\hat{\theta}-\overline{\theta})\sin(2\overline{\theta})\right) \\ \Longleftrightarrow\ \hat{\kappa}_{n1} &= \overline{\kappa}_{n1}\cos^2(\hat{\theta}-\overline{\theta}) + \overline{\kappa}_{n2}\sin^2(\hat{\theta}-\overline{\theta}) \\ &\quad +(\overline{\kappa}_{n2}-\overline{\kappa}_{n1})\frac{\sin(2(\hat{\theta}-\overline{\theta}))}{2}\frac{\sin(2\overline{\theta})}{\cos(2\overline{\theta})} \\ \Longleftrightarrow\ \hat{\kappa}_{n1} &= \overline{\kappa}_{n1}\cos^2(\hat{\theta}-\overline{\theta}) + \overline{\kappa}_{n2}\sin^2(\hat{\theta}-\overline{\theta}) + \overline{\tau}_{g1}\sin(2(\hat{\theta}-\overline{\theta}))\ , \qquad (3.56) \\ &\quad \text{(using (3.53)).}\end{aligned}$$

Similarly, from (3.52), (3.54)

$$\begin{aligned}
\hat{\kappa}_{n2}\cos 2\overline{\theta} &= \overline{\kappa}_{n1}\left(\sin^2\hat{\theta}\cos^2\overline{\theta} - \cos^2\hat{\theta}\sin^2\overline{\theta}\right) \\
&\quad +\overline{\kappa}_{n2}\left(\cos^2\hat{\theta}\cos^2\overline{\theta} - \sin^2\hat{\theta}\sin^2\overline{\theta}\right) \\
&= \overline{\kappa}_{n1}\sin(\hat{\theta}-\overline{\theta})\sin(\hat{\theta}+\overline{\theta}) + \overline{\kappa}_{n2}\cos(\hat{\theta}-\overline{\theta})\cos(\hat{\theta}+\overline{\theta}) \\
&= \overline{\kappa}_{n1}\sin(\hat{\theta}-\overline{\theta})\left(\sin(\hat{\theta}-\overline{\theta})\cos(2\overline{\theta}) + \cos(\hat{\theta}-\overline{\theta})\sin(2\overline{\theta})\right) \\
&\quad +\overline{\kappa}_{n2}\cos(\hat{\theta}-\overline{\theta})\left(\cos(\hat{\theta}-\overline{\theta})\cos(2\overline{\theta}) - \sin(\hat{\theta}-\overline{\theta})\sin(2\overline{\theta})\right) \\
\iff \hat{\kappa}_{n2} &= \overline{\kappa}_{n1}\sin^2(\hat{\theta}-\overline{\theta}) + \overline{\kappa}_{n2}\cos^2(\hat{\theta}-\overline{\theta}) \\
&\quad -(\overline{\kappa}_{n2}-\overline{\kappa}_{n1})\frac{\sin(2(\hat{\theta}-\overline{\theta}))}{2}\frac{\sin(2\overline{\theta})}{\cos(2\overline{\theta})} \\
\iff \hat{\kappa}_{n2} &= \overline{\kappa}_{n1}\sin^2(\hat{\theta}-\overline{\theta}) + \overline{\kappa}_{n2}\cos^2(\hat{\theta}-\overline{\theta}) - \overline{\tau}_{g1}\sin(2(\hat{\theta}-\overline{\theta}))\ , \qquad (3.57) \\
&\quad \text{(using (3.53)).}
\end{aligned}$$

Then, using (3.53), (3.55)

$$\begin{aligned}
\hat{\tau}_{g1} &= \frac{(\overline{\kappa}_{n2}-\overline{\kappa}_{n1})\sin 2\hat{\theta}}{2\cos(2\overline{\theta})} \\
&= \frac{(\overline{\kappa}_{n2}-\overline{\kappa}_{n1})}{2\cos(2\overline{\theta})}\left(\sin(2(\hat{\theta}-\overline{\theta}))\cos(2\overline{\theta}) + \cos(2(\hat{\theta}-\overline{\theta}))\sin(2\overline{\theta})\right) \\
&= \frac{1}{2}(\overline{\kappa}_{n2}-\overline{\kappa}_{n1})\sin(2(\hat{\theta}-\overline{\theta})) \\
&\quad +\frac{1}{2}\cos(2(\hat{\theta}-\overline{\theta}))(\overline{\kappa}_{n2}-\overline{\kappa}_{n1})\frac{\sin(2\overline{\theta})}{\cos(2\overline{\theta})} \\
\iff \hat{\tau}_{g1} &= \frac{1}{2}(\overline{\kappa}_{n2}-\overline{\kappa}_{n1})\sin(2(\hat{\theta}-\overline{\theta})) + \overline{\tau}_{g1}\cos(2(\hat{\theta}-\overline{\theta}))\ , \qquad (3.58) \\
&\quad \text{(using (3.53)).}
\end{aligned}$$

The equations (3.56), (3.57), (3.58) give formulae for $\hat{\kappa}_{n1}$, $\hat{\kappa}_{n2}$, $\hat{\tau}_{g1}$ in terms of $\overline{\kappa}_{n1}$, $\overline{\kappa}_{n2}$, $\overline{\tau}_{g1}$, and $(\hat{\theta}-\overline{\theta})$, which is the angle from $\overline{e}_1$ to $\hat{e}_1$. Now consider these quantities on the medial sheet γ_i at $\gamma_i(r_0, 0)$ on the A_1^3 curve and let T, $W_i = N_i \times T$, κ_i^T, κ_i^W, τ_{gi}^T be respectively $\overline{e}_1$, $\overline{e}_2$, $\overline{\kappa}_{n1}$, $\overline{\kappa}_{n2}$, $\overline{\tau}_{g1}$. Also let T_i, U_i be respectively $\hat{e}_1$, $\hat{e}_2$. Then, by definition, κ_i^r, κ_i^t, τ_i^r are respectively $\hat{\kappa}_{n1}$, $\hat{\kappa}_{n2}$, $\hat{\tau}_{g1}$. Then $(\hat{\theta}-\overline{\theta}) = \alpha_i$ by definition of α_i. Compare Figures 3.5, left and 3.8. We can then substitute into (3.56), (3.57), (3.58) to get new formulae for κ_i^r, κ_i^t, $\tau_i^t = -\tau_i^r$, and we get the following.

Lemma 3.4.4.2 *The following formulae hold at $\gamma_i(r_0, 0)$ on the A_1^3 curve:*

$$\begin{aligned}
\kappa_i^r &= \kappa_i^T \cos^2\alpha_i + \kappa_i^W \sin^2\alpha_i + \tau_{gi}^T \sin(2\alpha_i) \ , \\
\kappa_i^t &= \kappa_i^T \sin^2\alpha_i + \kappa_i^W \cos^2\alpha_i - \tau_{gi}^T \sin(2\alpha_i) \ , \\
\tau_i^t &= -\tau_i^r = \frac{1}{2}(\kappa_i^T - \kappa_i^W)\sin(2\alpha_i) - \tau_{gi}^T \cos(2\alpha_i) \ ,
\end{aligned}$$

where κ_i^T, τ_{gi}^T are respectively the normal curvature, geodesic torsion of γ_i in the direction of T at $\gamma_i(r_0, 0)$ and the rest of the notation used is contained in Table 3.1.

Introducing the Geometry of the A_1^3 Curve

Now we shall find expressions for κ_i^T, τ_{gi}^T in terms of κ, τ, respectively the curvature and torsion of the A_1^3 curve (see Table 3.1). We have the expression (3.29) for W_i, valid along the A_1^3 curve. Then we have the following, at $\gamma_i(r_0, 0)$:

$$\begin{pmatrix} T' \\ N' \\ B' \end{pmatrix} = \begin{pmatrix} 0 & \kappa & 0 \\ -\kappa & 0 & \tau \\ 0 & -\tau & 0 \end{pmatrix} \begin{pmatrix} T \\ N \\ B \end{pmatrix},$$

where $'$ ('prime') is differentiation with respect to arclength along the A_1^3 curve. Also, at $\gamma_i(r_0, 0)$ we have

$$\begin{pmatrix} T' \\ W_i' \\ N_i' \end{pmatrix} = \begin{pmatrix} 0 & \kappa_{gi}^T & \kappa_i^T \\ -\kappa_{gi}^T & 0 & \tau_{gi}^T \\ -\kappa_i^T & -\tau_{gi}^T & 0 \end{pmatrix} \begin{pmatrix} T \\ W_i \\ N_i \end{pmatrix},$$

where κ_{gi}^T is the geodesic curvature of the A_1^3 curve on γ_i at $\gamma_i(r_0, 0)$. Using (3.27) and comparing coefficients we can obtain formulae for κ_{gi}^T, κ_i^T, and τ_{gi}^T in terms of κ, τ, ψ_i', and ψ_i:

$$\kappa_{gi}^T = \kappa \sin\psi_i \ , \qquad \kappa_i^T = \kappa\cos\psi_i \ , \qquad \tau_{gi}^T = \tau + \psi_i' \ . \tag{3.59}$$

Substitution of these expressions for κ_i^T, τ_{gi}^T into the expressions for κ_i^r, κ_i^t, τ_i^t from Lemma 3.4.4.2 and using Theorem 3.4.2.1, we get the following.

Lemma 3.4.4.3 *The following formulae hold at $\gamma_i(r_0, 0)$ on the A_1^3 curve:*

$$\kappa_i^r = \frac{\kappa \cos\psi_i \cos^2\phi + \kappa_i^W \sin^2\phi \cos^2\theta_i - (\tau + \psi_i')\sin(2\phi)\cos\theta_i}{\cos^2\phi_i} , \tag{3.60}$$

$$\kappa_i^t = \frac{\kappa \cos\psi_i \sin^2\phi \cos^2\theta_i + \kappa_i^W \cos^2\phi + (\tau + \psi_i')\sin(2\phi)\cos\theta_i}{\cos^2\phi_i} , \tag{3.61}$$

$$\tau_i^t = \frac{\frac{1}{2}(\kappa_i^W - \kappa\cos\psi_i)\sin(2\phi)\cos\theta_i + (\tau + \psi_i')(\sin^2\phi\cos^2\theta_i - \cos^2\phi)}{\cos^2\phi_i}, \tag{3.62}$$

where $\cos^2\phi_i = \cos^2\phi + \sin^2\phi\cos^2\theta_i$, *by* (3.38). *Note that*

$$\left.\begin{aligned} \kappa_i^r\kappa_i^t - (\tau_i^t)^2 &= \kappa\kappa_i^W\cos\psi_i - (\tau + \psi_i')^2 , \\ \kappa_i^r + \kappa_i^t &= \kappa\cos\psi_i + \kappa_i^W . \end{aligned}\right\} \tag{3.63}$$

The notation used is contained in Table 3.1.

New Formulae for a_i, a_i^t, a_i^*

Let the A_1^3 curve be parametrized by $r_1 = r_2 = r_3 = r$, that is let it be $\gamma_i(r, t_i(r))$ (same for each i). Then, for $s =$ arclength along the A_1^3 curve, we have $\gamma_i(r, t_i(r)) = \gamma_i(s(r))$ for any r. Differentiating this with respect to r, we get the following:

$$\begin{aligned} T\frac{ds}{dr} &= \frac{\partial\gamma_i}{\partial r_i} + \frac{\partial\gamma_i}{\partial t_i}\frac{dt_i}{dr} \\ &= v_i(\cos\alpha_i T + \sin\alpha_i\sin\psi_i N - \sin\alpha_i\cos\psi_i B) \\ &\quad + \frac{dt_i}{dr} w_i(r, t_i(r))(-\sin\alpha_i T + \cos\alpha_i\sin\psi_i N - \cos\alpha_i\cos\psi_i B) , \end{aligned}$$

using (3.27) and where s is arclength along the A_1^3 curve. Comparing coefficients gives

$$\begin{aligned} \frac{ds}{dr} &= -\frac{1}{\cos\phi} \text{ for } \textit{any } s \\ \Rightarrow \frac{d^2s}{dr^2} &= -\frac{d\phi}{dr}\frac{\sin\phi}{\cos^2\phi} = \phi'\frac{\sin\phi}{\cos^3\phi} \text{ for } \textit{any } s , \\ \frac{dt_i}{dr} &= \frac{\sin\alpha_i}{\cos\phi} \text{ at } (r_i = r_0, t_i = 0), \text{ since } w_i(r_0, 0) = 1 . \end{aligned} \tag{3.64}$$

Then

$$\frac{d}{dr}\left(T\frac{ds}{dr} = \frac{\partial\gamma_i}{\partial r_i} + \frac{\partial\gamma_i}{\partial t_i}\frac{dt_i}{dr}\right) \text{ at } r_i = r_0,\ t_i = 0 \text{ is the same as}$$

$$\kappa N\left(\frac{ds}{dr}\right)^2 + T\frac{d^2s}{dr^2} = \frac{\partial^2\gamma_i}{\partial r_i^2} + 2\frac{\partial^2\gamma_i}{\partial r_i\partial t_i}\frac{dt_i}{dr} + \frac{\partial^2\gamma_i}{\partial t_i^2}\left(\frac{dt_i}{dr}\right)^2 + \frac{\partial\gamma_i}{\partial t_i}\frac{d^2t_i}{dr^2}$$

$$= \left(a_iT_i - a_i^tv_iU_i + \kappa_i^rv_i^2N_i\right) + 2\frac{\sin\alpha_i}{\cos\phi}\left(a_i^tT_i + a_i^*U_i - \tau_i^tv_iN_i\right)$$

$$+\frac{\sin^2\alpha_i}{\cos^2\phi}\left(-\frac{a_i^*}{v_i}T_i + \kappa_i^tN_i\right) + \frac{d^2t_i}{dr^2}U_i$$

using (3.7) and (3.8). Then by equating components it can be shown that this gives the following and nothing else at $r_i = r_0$, $t_i = 0$:

$$\left.\begin{aligned}\frac{d^2t_i}{dr^2} &= -\frac{a_i^t}{\cos\phi_i} - 2\frac{a_i^*\sin\alpha_i}{\cos\phi} + \frac{\kappa\cos\alpha_i\sin\psi_i}{\cos^2\phi} - \frac{\phi'\sin\phi\sin\alpha_i}{\cos^3\phi}\ ,\\ a_i\cos^3\phi &= -2a_i^t\sin\alpha_i\cos^2\phi - a_i^*\sin^2\alpha_i\cos\phi_i\cos\phi\\ &\qquad +\kappa\sin\alpha_i\sin\psi_i\cos\phi + \phi'\sin\phi\cos\alpha_i\ .\end{aligned}\right\} \tag{3.65}$$

(This can be checked by substituting for κ_i^r, κ_i^t, τ_i^t from Lemma 3.4.4.3.)

From (3.28) we have $T = \cos\alpha_iT_i - \sin\alpha_iU_i$ for any A_1^3 point, and so this can be differentiated with respect to r:

$$\begin{aligned}\frac{dT}{ds}\frac{ds}{dr} &= -\alpha_i'\frac{ds}{dr}\left(\sin\alpha_iT_i + \cos\alpha_iU_i\right) + \cos\alpha_i\left(\frac{\partial T_i}{\partial r_i} + \frac{\partial T_i}{\partial t_i}\frac{dt_i}{dr}\right)\\ &\quad - \sin\alpha_i\left(\frac{\partial U_i}{\partial r_i} + \frac{\partial U_i}{\partial t_i}\frac{dt_i}{dr}\right),\end{aligned}$$

which, at $r_i = r_0$, $t_i = 0$, is the same as

$$\begin{aligned}-\frac{\kappa N}{\cos\phi} &= \frac{\alpha_i'}{\cos\phi}\left(\sin\alpha_iT_i + \cos\alpha_iU_i\right)\\ &\quad + \cos\alpha_i\left(-a_i^tU_i - \frac{\kappa_i^r}{\cos\phi_i}N_i + \frac{\sin\alpha_i}{\cos\phi}\left(-a_i^*\cos\phi_iU_i - \tau_i^tN_i\right)\right)\\ &\quad - \sin\alpha_i\left(a_i^tT_i - \frac{\tau_i^t}{\cos\phi_i}N_i + \frac{\sin\alpha_i}{\cos\phi}\left(a_i^*\cos\phi_iT_i + \kappa_i^tN_i\right)\right).\end{aligned}$$

Equating components of the above gives the following and nothing else:

$$a_i^t\cos\phi + a_i^*\cos\phi_i\sin\alpha_i = \alpha_i' + \kappa\sin\psi_i\ . \tag{3.66}$$

The equations (3.28), (3.27) hold at all points of the A_1^3 curve, and so they can be differentiated with respect to arclength along the A_1^3 curve. It can be shown that the equations this gives are the same as (3.60), (3.61), (3.62), (3.65), and (3.66). Then, using (3.38), (3.39), (3.40), (3.41) from Theorem 3.4.2.1, we get the following.

Lemma 3.4.4.4 *The following formulae hold at $\gamma_i(r_0, 0)$ on the A_1^3 curve:*

$$a_i^* \sin\phi \cos\theta_i = a_i^t \cos\phi - \kappa \sin\psi_i - \frac{\theta_i' \cos\phi \sin\phi \sin\theta_i}{\cos^2\phi_i} + \frac{\phi' \cos\theta_i}{\cos^2\phi_i} , \quad (3.67)$$

$$\frac{a_i \cos^3\phi_i}{\sin^2\phi \sin^2\theta_i} = \frac{a_i^t \cos\theta_i \cos^2\phi_i}{\cos\phi \sin\phi \sin^2\theta_i} + \frac{\phi'}{\sin\phi} + \frac{\theta_i' \cos\theta_i}{\cos\phi \sin\theta_i} , \quad (3.68)$$

where $\cos\phi_i$ is given by (3.38) *and the notation used is contained in Table 3.1.*

3.4.5 Obtaining the Complete Set of Consistency Conditions

From (3.42) we can get an expression for $\text{trace}_i^{\pm}$, the trace of $S_{\mathbf{v}_i}^{\pm}$, which is the matrix representation of the radial shape operator of γ_i corresponding to boundary $\gamma_i^{\pm}$ with respect to the basis $\mathbf{v}_i = \{T_i, U_i\}$ at $\gamma_i(r_0, 0)$:

$$\text{trace}_i^{\pm} = -\frac{a_i}{v_i^3 \sin^2\phi_i} + \frac{a_i^*}{v_i^2} \pm \left(\frac{\kappa_i^r}{\sin\phi_i} + \kappa_i^t \sin\phi_i \right).$$

Then, using Lemmas 3.4.4.3 and 3.4.4.4, we get the following.

Lemma 3.4.5.1 *The trace of $S_{\mathbf{v}_i}^{\pm}$ is as follows:*

$$\begin{aligned} \text{trace}_i^{\pm} = & \frac{a_i^t \cos^4\phi_i}{\cos\phi \sin\phi \cos\theta_i \sin^2\theta_i} - \frac{\kappa \sin\psi_i \cos^2\phi_i}{\sin\phi \cos\theta_i} \\ & + \frac{2\phi'}{\sin\phi} + \frac{\theta_i' A_i}{\cos\phi \cos\theta_i \sin\theta_i} \\ & \pm \frac{\left(\kappa \cos\psi_i B_i + \kappa_i^W \sin^2\phi - (\tau + \psi_i') \sin(2\phi) \cos\theta_i\right)}{\sin\phi \sin\theta_i} , \end{aligned} \quad (3.69)$$

where $A_i = \cos^2\theta_i - \cos^2\phi \sin^2\theta_i$, $B_i = \cos^2\phi + \sin^2\phi \sin^2\theta_i$.

Using this expression we get the following.

Theorem 3.4.5.2 (Consistency Condition at A_1^3 Points) *The normal curvatures κ_i^W at $\gamma_i(r_0,0)$ on the A_1^3 curve, for i =1, 2, 3, are uniquely determined by the following:*

$$\begin{aligned}\frac{\kappa_i^{W_i}\sin\phi}{\sin\theta_i} \;=\; & \frac{(a_{i+1}^t\cos^4\phi_{i+1}+\theta'_{i+1}A_{i+1}\sin\phi\sin\theta_{i+1})}{\cos\phi\sin\phi\cos\theta_{i+1}\sin^2\theta_{i+1}} \\ & -\frac{(a_{i+2}^t\cos^4\phi_{i+2}+\theta'_{i+2}A_{i+2}\sin\phi\sin\theta_{i+2})}{\cos\phi\sin\phi\cos\theta_{i+2}\sin^2\theta_{i+2}} \\ & +\frac{\kappa}{\sin\phi}\left(\frac{\sin\psi_{i+2}\cos^2\phi_{i+2}}{\cos\theta_{i+2}}-\frac{\sin\psi_{i+1}\cos^2\phi_{i+1}}{\cos\theta_{i+1}}-\frac{B_i\cos\psi_i}{\sin\theta_i}\right) \\ & +\frac{2(\tau+\psi_i')\cos\phi\cos\theta_i}{\sin\theta_i}\ .\end{aligned} \tag{3.70}$$

Here $A_i = \cos^2\theta_i - \cos^2\phi\sin^2\theta_i$, $B_i = \cos^2\phi + \sin^2\phi\sin^2\theta_i$. The equation (3.70)*, together with Theorem 3.4.2.1 at $(r_0,0)$, gives the complete set of consistency conditions on the medial axis at the A_1^3 point $\gamma_i(r_0,0)$ up to second order. From* (3.70) *we get*

$$\sum_{i=1}^{3}\left(\frac{\kappa_i^W\sin^2\phi-2(\tau+\psi_i')\cos\phi\sin\phi\cos\theta_i+\kappa\cos^2\phi\cos\psi_i}{\sin\theta_i}\right)=0\ , \tag{3.71}$$

which is the same as (3.43)*, but expressed in terms of the coordinate system based on the A_1^3 curve. (See Table 3.1 for a summary of the notation used.)*

Proof. By Lemma 3.4.3.1 we have $\text{trace}_i^- = \text{trace}_{i+1}^-$ for i = 1, 2, 3. Then it is easy to show

$$(\text{trace}_i^+ = \text{trace}_{i+1}^-) - (\text{trace}_{i+1}^+ = \text{trace}_{i+2}^-) + (\text{trace}_{i+2}^+ = \text{trace}_i^-)$$

is the same as (3.70). Conversely, substitution of κ_i^W, κ_{i+1}^W into trace_i^+, trace_{i+1}^- implies that $\text{trace}_i^+ = \text{trace}_{i+1}^-$ for each i. Hence (3.70) for i =1, 2, 3 is the complete solution of $\text{trace}_i^+ = \text{trace}_{i+1}^-$ for each i. By Lemma 3.4.3.1, in order to equate principal curvatures on γ_i^+, γ_{i+1}^- at $\gamma_i(r_0,0)$ we also need to set $\det_i^+ = \det_{i+1}^-$ for i =1, 2, 3. Using (3.42) and Lemmas 3.4.4.3 and 3.4.4.4 we can obtain an expression for $\det_i^\pm$ (the determinant of $S_{\mathbf{v}_i}^\pm$ at $\gamma_i(r_0,0)$). Then we can substitute for κ_1^W, κ_2^W, κ_3^W and, using Maple, it can be shown that $\det_i^+ = \det_{i+1}^-$

is satisfied for $i = 1, 2, 3$. Finally, in addition to the principal curvatures of γ_i^+, γ_{i+1}^- at $(r_0, 0)$ being equal, the surfaces γ_i^+, γ_{i+1}^- are equal at $(r_0, 0)$ if and only if the principal directions at $(r_0, 0)$ are equal. From Proposition 3.4.3.3 this is the same as (3.50) and (3.51) being true. Then, using Lemmas 3.4.4.3 and 3.4.4.4, we can substitute for κ_1^W, κ_2^W, κ_3^W in (3.50), (3.51) and it can be shown using Maple that (3.50), (3.51) are satisfied for i =1, 2, 3. Hence principal curvatures and principal directions of γ_i^+, γ_{i+1}^- for i =1, 2, 3 are equal at $(r_0, 0)$ if and only if (3.70) is true for i =1, 2, 3. Hence the first part of the result. Finally, it is easy to show using the definition of θ_i from Theorem 3.4.2.1 that taking the sum of (3.70) from i =1 to 3, we get (3.71). □

Alternative Versions of the Constraint

Using (3.67) we can express a_i^t in terms of a_i^* and so we get an alternative form of (3.70) from Theorem 3.4.5.2, as below.

Theorem 3.4.5.3 (Consistency Condition at A_1^3 Points) *The normal curvatures κ_i^W at $\gamma_i(r_0, 0)$ on the A_1^3 curve, for i =1, 2, 3, are uniquely determined by the following:*

$$\begin{aligned}\frac{\kappa_i^W \sin\phi}{\sin\theta_i} = \frac{2}{\cos\phi}&\left(\frac{\theta'_{i+1}\cos\theta_{i+1}}{\sin\theta_{i+1}} - \frac{\theta'_{i+2}\cos\theta_{i+2}}{\sin\theta_{i+2}}\right)\\ &+\frac{2(\tau+\psi_i')\cos\phi\cos\theta_i}{\sin\theta_i}\\ &+\frac{\cos^2\phi_{i+1}\left(a_{i+1}^*\cos^2\phi_{i+1} - \frac{\phi'}{\sin\phi}\right)}{\cos^2\phi\sin^2\theta_{i+1}}\\ &-\frac{\cos^2\phi_{i+2}\left(a_{i+2}^*\cos^2\phi_{i+2} - \frac{\phi'}{\sin\phi}\right)}{\cos^2\phi\sin^2\theta_{i+2}}\\ +\frac{\kappa}{\sin\phi}&\left(\frac{\sin\psi_{i+1}\cos^2\phi_{i+1}\cos\theta_{i+1}}{\cos^2\phi\sin^2\theta_{i+1}} - \frac{\sin\psi_{i+2}\cos^2\phi_{i+2}\cos\theta_{i+2}}{\cos^2\phi\sin^2\theta_{i+2}} - \frac{\cos\psi_i B_i}{\sin\theta_i}\right).\end{aligned} \tag{3.72}$$

Here $B_i = \cos^2\phi + \sin^2\phi\sin^2\theta_i$. The equation (3.72), together with Theorem 3.4.2.1 at $(r_0, 0)$, gives the complete set of consistency conditions on the medial axis at the A_1^3 point $\gamma_i(r_0, 0)$ up to second order. Taking the sum of

(3.72) *from i =1 to 3 also gives* (3.71). *(See Table 3.1 for a summary of the notation used.)*

Another version can be obtained as follows. We have

$$\begin{aligned} a_i^t &= \frac{\partial v_i}{\partial t_i} \text{ by definition from §3.2} \\ &= \frac{\partial}{\partial t_i}\left(\frac{-1}{\cos\phi_i}\right) \text{ from (3.6)} \\ &= -\frac{\sin\phi_i}{\cos^2\phi_i}\frac{\partial\phi_i}{\partial t_i} \ . \end{aligned}$$

Then, by (3.27) and (3.29)

$$\begin{aligned} U_i &= -\sin\alpha_i T + \cos\alpha_i W_i \\ \Rightarrow \quad \frac{\partial(*)}{\partial t_i} &= -\sin\alpha_i (*)' + \cos\alpha_i \dot{(*)} \ , \end{aligned}$$

at $(r_0, 0)$, where $\dot{}$ ('dot') means differentiation with respect to arclength along a curve passing through $\gamma_i(r_0, 0)$, with tangent W_i. (See Table 3.1 for a summary of the notation used in the A_1^3 case.) Hence

$$\begin{aligned} a_i^t &= -\frac{\sin\phi_i}{\cos^2\phi_i}(-\phi_i'\sin\alpha_i + \dot{\phi}_i\cos\alpha_i) \\ &= -\frac{\sin\phi_i}{\cos^2\phi_i}\left(-\frac{\sin\alpha_i}{\cos\phi_i}(\phi'\cos\phi\sin\theta_i + \theta_i'\sin\phi\cos\theta_i) + \dot{\phi}_i\cos\alpha_i\right), \end{aligned}$$

by differentiating (3.39) from Theorem 3.4.2.1 with respect to arclength along the A_1^3 curve. Then we get

$$\begin{aligned} a_i^t\cos^4\phi_i = &-\phi'\cos\phi\sin^2\phi\cos\theta_i\sin^2\theta_i - \theta_i'\sin^3\phi\cos^2\theta_i\sin\theta_i \\ &-\dot{\phi}_i\cos\phi_i\cos\phi\sin\phi\sin\theta_i \ . \end{aligned} \tag{3.73}$$

Then, substitution of this into (3.70) from Theorem 3.4.5.2 gives the following.

Theorem 3.4.5.4 (Consistency Condition at A_1^3 Points) *The normal*

curvatures κ_i^W at $\gamma_i(r_0,0)$ on the A_1^3 curve, for i =1, 2, 3, are uniquely determined by the following:

$$\begin{aligned}\frac{\kappa_i^W \sin\phi}{\sin\theta_i} &= \frac{(\theta'_{i+1}\cos\phi\cos(2\theta_{i+1}) - \dot{\phi}_{i+1}\cos\phi_{i+1})}{\cos\theta_{i+1}\sin\theta_{i+1}} \\ &\quad - \frac{(\theta'_{i+2}\cos\phi\cos(2\theta_{i+2}) - \dot{\phi}_{i+2}\cos\phi_{i+2})}{\cos\theta_{i+2}\sin\theta_{i+2}} \\ &\quad + \frac{\kappa}{\sin\phi}\left(\frac{\sin\psi_{i+2}\cos^2\phi_{i+2}}{\cos\theta_{i+2}} - \frac{\sin\psi_{i+1}\cos^2\phi_{i+1}}{\cos\theta_{i+1}} - \frac{\cos\psi_i B_i}{\sin\theta_i}\right) \\ &\quad + \frac{2(\tau+\psi'_i)\cos\phi\cos\theta_i}{\sin\theta_i}\ .\end{aligned} \tag{3.74}$$

Here $B_i = \cos^2\phi + \sin^2\phi\sin^2\theta_i$. The equation (3.74)*, together with Theorem 3.4.2.1 at $(r_0,0)$, gives the complete set of consistency conditions on the medial axis at the A_1^3 point $\gamma_i(r_0,0)$ up to second order. Taking the sum of* (3.74) *from i =1 to 3 also gives* (3.71)*. (See Table 3.1 for a summary of the notation used.)*

Remark 3.4.5.5 Consider when the denominators are zero in (3.70), (3.72) and (3.74). A point for which $\sin\theta_i = 0$ for some i is an A_1A_3 point and will be covered in §3.9, which deals with the A_1A_3 case. When $\sin\phi = 0$ the three points of contact on the boundary are coincident and so the sphere of contact has A_5 contact with the boundary. This case is not generic for a surface, so we ignore it. When $\cos\phi = \cos\theta_i = 0$ then $\cos\phi_i = 0$ (see (3.38)), which means that $\|\nabla r_i\| = 0$. We assumed $\|\nabla r_i\| \neq 0$ for our coordinate system in §3.2 and so, at $\gamma_i(r_0,0)$, one of $\cos\phi$, $\cos\theta_i$ will be non-zero. Hence we can use either (3.72) or (3.74). Points where $\|\nabla r_i\| = 0$ are isolated and only occur for generic surfaces on A_1^2 sheets, so we do not need to consider them in the A_1^3 case.

Now we consider when the radius r has a local maximum or minimum at an A_1^3 point.

Proposition 3.4.5.6 *When the radius r of the sphere of contact at an A_1^3 point $\gamma_i(r_0,0)$ has a local maximum or minimum, the normal curvatures κ_i^W satisfy*

the following:

$$\sum_{i=1}^{3}\left(\frac{\kappa_i^W}{\sin\theta_i}\right)=0\ . \tag{3.75}$$

Proof. From (3.64), at $\gamma_i(r_0,0)$,

$$\frac{dr}{ds}=0 \quad\Longleftrightarrow\quad \cos\phi=0\ .$$

Then setting $\cos\phi=0$ in (3.71) gives the result. □

Remark 3.4.5.7 The equation (3.75) is reminiscent of the second equation of (3.1) for the medial axis in $\mathbb{R}^2$. Note that $\cos\phi=0$ implies $\cos\phi_i=-\cos\theta_i$, $\sin\phi_i=\sin\theta_i$, $\cos\alpha_i=0$, and $\sin\alpha_i=1$, by Theorem 3.4.2.1. Then, from (3.27), we see that $T_i=\sin\psi_i N-\cos\psi_i B$, and hence that T_i, N_i are in the plane of N, B for each i. Then, from (3.3) and (3.5) this means that when $\cos\phi=0$ at $\gamma_i(r_0,0)$ then $\gamma_i(r_0,0)$ and $\gamma_i^{\pm}(r_0,0)$ are all in the same plane for each i. Hence the situation is similar to that of the medial axis in $\mathbb{R}^2$.

3.5 First Example of the A_1^3 Case

Suppose the three medial surfaces γ_i, for i =1, 2, 3 are *general cylinders* intersecting in a line, that is the A_1^3 set here is a *straight line*, the z-axis (see Figure 3.9). The consistency conditions of §3.4, including those of Theorem 3.4.5.2 (or alternatively one of Theorems 3.4.5.3, 3.4.5.4), were obtained using the assumption that the curvature κ of the A_1^3 curve was never zero, enabling a Frenet frame to be set up. If the A_1^3 curve is a straight line then κ is zero for all points of the A_1^3 curve, which means the Frenet frame is not defined. When $\kappa\equiv 0$ the principal normal N and the binormal B to the A_1^3 curve are arbitrary. Hence, in this section we will make choices for N, B and use the consistency conditions of §3.4 to gain information about the radius functions r_1, r_2, r_3 associated to the three medial sheets γ_1, γ_2, γ_3 at a point of the A_1^3 curve, the z-axis.

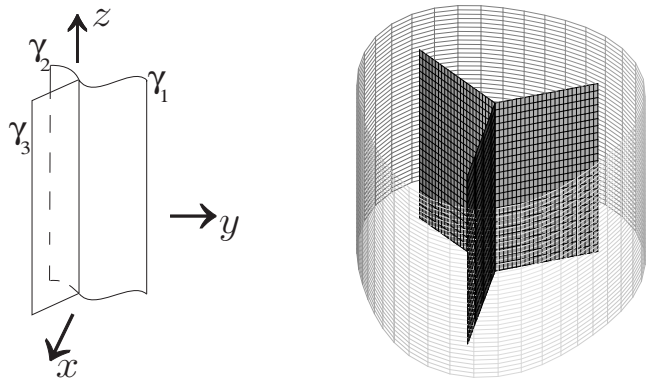

Figure 3.9: Left: an example of the medial axis as three general cylinders with the A_1^3 curve being the z-axis. Right: a further simplification of the medial axis where each medial sheet γ_i, for $i = 1, 2, 3$, is a flat sheet. Also shown is the corresponding boundary surface.

Given that δ_i is a unit speed space curve, we parametrize the cylinders as below:

$$\begin{aligned} \gamma_i(u,z) &= \delta_i(u) + z(0,0,1), \quad \text{where} \quad \delta_i(u) = (X_i(u), Y_i(u), 0) \ , \\ \text{and} \qquad & \left(\frac{dX_i}{du}\right)^2 + \left(\frac{dY_i}{du}\right)^2 = 1 \quad \text{for all } u \ (\delta_i \text{ unit speed}) \ , \\ \text{so} \quad N_i(u,z) &= \eta_i \left(\frac{dY_i}{du}, -\frac{dX_i}{du}, 0\right), \quad \text{where} \quad \eta_i = \pm 1 \ . \end{aligned}$$

Let $\delta_i(u_i) = \mathbf{0}$, for u_i constant, so that $\gamma_1(u_1, z) = \gamma_2(u_2, z) = \gamma_3(u_2, z)$ is a point of the A_1^3 curve. The radii r_1, r_2, r_3 are all equal for points of the A_1^3 curve, so $r(z) = r_1(u_1, z) = r_2(u_2, z) = r_3(u_1, z)$ for all z. Hence all of the derivatives of r_i with respect to z are equal at (u_i, z). We shall consider the point on the A_1^3 curve given by $u = u_i$, $z = 0$, corresponding to $r_i = r_0$, $t_i = 0$.

In this example we illustrate Theorem 3.4.2.1 and one of Theorems 3.4.5.2, 3.4.5.3, 3.4.5.4. Firstly we shall calculate some quantities such as $\cos\phi_i$ that appear in these results and some that will be of use for an example of the A_3 case. Equations (3.9), (3.10), (3.11), (3.12) give such expressions in terms of an arbitrary parametrization. Using these (and replacing (x, y) with (u, z)) we get the following expressions, which hold for all (u, z) near to $u = u_i$, $z = 0$,

where suffices denote differentiation:

$$\frac{\partial \gamma_i}{\partial r_i} = \frac{1}{r_{iu}^2 + r_{iz}^2}\left(r_{iu}\frac{dX_i}{du}, r_{iu}\frac{dY_i}{du}, r_{iz}\right), \tag{3.76}$$

$$v_i = \frac{\epsilon_i}{\sqrt{r_{iu}^2 + r_{iz}^2}}, \quad \text{where} \quad \epsilon_i = \text{sign}(\cos\theta_i)\ , \tag{3.77}$$

$$T_i = \frac{1}{v_i}\frac{\partial \gamma_i}{\partial r_i} = \frac{\epsilon_i}{\sqrt{r_{iu}^2 + r_{iz}^2}}\left(r_{iu}\frac{dX_i}{du}, r_{iu}\frac{dY_i}{du}, r_{iz}\right), \tag{3.78}$$

$$U_i = N_i \times T_i = \frac{\epsilon_i \eta_i}{\sqrt{r_{iu}^2 + r_{iz}^2}}\left(-r_{iz}\frac{dX_i}{du}, -r_{iz}\frac{dY_i}{du}, r_{iu}\right), \tag{3.79}$$

$$N_i^{\pm} = \left(r_{iu}\frac{dX_i}{du}, r_{iu}\frac{dY_i}{du}, r_{iz}\right) \mp \eta_i\sqrt{1 - r_{iu}^2 - r_{iz}^2}\left(\frac{dY_i}{du}, -\frac{dX_i}{du}, 0\right). \tag{3.80}$$

Using

$$\begin{aligned}
\frac{\partial \gamma_i}{\partial r_i}\frac{\partial r_i}{\partial u} + \frac{\partial \gamma_i}{\partial t_i}\frac{\partial t_i}{\partial u} &= \frac{\partial \gamma_i}{\partial u} = \left(\frac{dX_i}{du}, \frac{dY_i}{du}, 0\right), \\
\frac{\partial \gamma_i}{\partial r_i}\frac{\partial r_i}{\partial z} + \frac{\partial \gamma_i}{\partial t_i}\frac{\partial t_i}{\partial z} &= \frac{\partial \gamma_i}{\partial z} = (0, 0, 1)\ ,
\end{aligned}$$

and the facts that $\partial\gamma_i/\partial r_i \cdot \partial\gamma_i/\partial t_i = 0$ for all (r_i, t_i) near $(r_i = r_0, t = 0)$ and that $\partial\gamma_i/\partial t_i = U_i$ at $r_i = r_0$ (see (3.4)), we obtain the following:

$$t_{iu} = -\frac{\epsilon_i \eta_i r_{iz}}{\sqrt{r_{iu}^2 + r_{iz}^2}}\ , \quad t_{iz} = \frac{\epsilon_i \eta_i r_{iu}}{\sqrt{r_{iu}^2 + r_{iz}^2}}\ , \tag{3.81}$$

$$\frac{\partial \gamma_i}{\partial t_i} = \frac{\epsilon_i \eta_i}{\sqrt{r_{iu}^2 + r_{iz}^2}}\left(-r_{iz}\frac{dX_i}{du}, -r_{iz}\frac{dY_i}{du}, r_{iu}\right), \tag{3.82}$$

all evaluated at $r_i = r_0$.

Now for second order terms. By definition a_i, a_i^t are respectively $\partial v_i/\partial r_i$, $\partial v_i/\partial t_i$. So we need to calculate these quantities in terms of the parametrizations of the cylinders γ_i. From the change of variables $(u, z) \mapsto (r_i, t_i)$ we get

$$\begin{pmatrix} u_{r_i} & u_{t_i} \\ z_{r_i} & z_{t_i} \end{pmatrix} = \begin{pmatrix} r_{iu} & r_{iz} \\ t_{iu} & t_{iz} \end{pmatrix}^{-1} = \frac{1}{r_{iu}t_{iz} - r_{iz}t_{iu}}\begin{pmatrix} t_{iz} & -r_{iz} \\ -t_{iu} & r_{iu} \end{pmatrix}. \tag{3.83}$$

Using this and differentiating (3.77) with subscript i (which is allowed since it

holds for all (u, z) close to $u = u_i$, $z = 0$) we get the following:

$$\frac{a_i}{v_i} = -\frac{(r_{iu}^2 r_{iuu} + 2r_{iu}r_{iz}r_{iuz} + r_{iz}^2 r_{izz})}{(r_{iu}^2 + r_{iz}^2)^2} , \tag{3.84}$$

$$a_i^t = \eta_i \frac{(r_{iu}r_{iz}r_{iuu} + (r_{iz}^2 - r_{iu}^2)r_{iuz} - r_{iu}r_{iz}r_{izz})}{(r_{iu}^2 + r_{iz}^2)^2} , \tag{3.85}$$

both evaluated at $r_i = r_0$. Now to calculate a_i^*. From (3.7) and (3.8) we see that

$$a_i^* = \frac{\partial^2 \gamma_i}{\partial r_i \partial t_i} \cdot U_i = -v_i \frac{\partial^2 \gamma_i}{\partial t_i^2} \cdot T_i .$$

Using the chain rule on $\partial\gamma_i/\partial u$, $\partial\gamma_i/\partial z$ and using (3.81), (3.84) and (3.85) at $r_i = r_0$ gives the following:

$$a_i^* = \frac{r_{iz}^2 r_{iuu} - 2r_{iu}r_{iz}r_{iuz} + r_{iu}^2 r_{izz}}{(r_{iu}^2 + r_{iz}^2)^2} . \tag{3.86}$$

We can also calculate the terms of the geometry: κ_i^r, κ_i^t, and τ_i^t. Although these are not required for the constraints, they will be of use in §3.8. From (3.7) we have

$$\begin{aligned}
\kappa_i^r &= \frac{1}{v_i^2}\frac{\partial^2 \gamma_i}{\partial r_i^2} \cdot N_i = -\frac{1}{v_i^2}\frac{\partial \gamma_i}{\partial r_i} \cdot \frac{\partial N_i}{\partial r_i} , \\
-v_i \tau_i^t &= \frac{\partial^2 \gamma_i}{\partial r_i \partial t_i} \cdot N_i = -\frac{\partial \gamma_i}{\partial r_i} \cdot \frac{\partial N_i}{\partial t_i} , \\
\kappa_i^t &= \frac{\partial^2 \gamma_i}{\partial t_i^2} \cdot N_i = -\frac{\partial \gamma_i}{\partial t_i} \cdot \frac{\partial N_i}{\partial t_i} .
\end{aligned}$$

Using (3.83), we can calculate $\partial N_i/\partial r_i$ and $\partial N_i/\partial t_i$, evaluated at $r_i = r_0$ Then, using (3.76) and (3.82) we get

$$\kappa_i^r = \frac{\eta_i r_{iu}^2}{r_{iu}^2 + r_{iz}^2}\left(\frac{d^2X_i}{du^2}\frac{dY_i}{du} - \frac{dX_i}{du}\frac{d^2Y_i}{du^2}\right), \tag{3.87}$$

$$\kappa_i^t = \frac{\eta_i r_{iz}^2}{r_{iu}^2 + r_{iz}^2}\left(\frac{d^2X_i}{du^2}\frac{dY_i}{du} - \frac{dX_i}{du}\frac{d^2Y_i}{du^2}\right), \tag{3.88}$$

$$\tau_i^t = \frac{r_{iu}r_{iz}}{r_{iu}^2 + r_{iz}^2}\left(\frac{d^2X_i}{du^2}\frac{dY_i}{du} - \frac{dX_i}{du}\frac{d^2Y_i}{du^2}\right), \tag{3.89}$$

all evaluated at $r_i = r_0$.

We want to gain information about the radius functions r_i along the A_1^3 curve from Theorem 3.4.2.1 and one of Theorems 3.4.5.2, 3.4.5.3, 3.4.5.4, which must hold at points of the A_1^3 axis. As described above, the Frenet frame is not defined when κ is zero, but since $\kappa \equiv 0$ we choose $T = (0, 0, 1)$, and $N = (0, 1, 0)$ and then $B = T \times N = (-1, 0, 0)$. Then $\kappa \equiv 0$ and $\tau \equiv 0$. The A_1^3 curve is $\gamma_i(u_i, z) = (0, 0, z)$, so by (3.27) we have

$$\begin{aligned} N_i &= \cos\psi_i N + \sin\psi_i B \\ \Rightarrow \quad (-\sin\psi_i, \cos\psi_i, 0) &= \eta_i \left(\frac{dY_i}{du}(u_i), -\frac{dX_i}{du}(u_i), 0 \right) \\ \Rightarrow \quad \frac{dX_i}{du}(u_i) = -\eta_i \cos\psi_i \quad &, \quad \frac{dY_i}{du}(u_i) = -\eta_i \sin\psi_i \ , \end{aligned} \tag{3.90}$$

for any z and where the derivatives of δ_i are evaluated at $u = u_i$. Using these we can get expressions for $\cos\theta_i$, $\sin\theta_i$, since by definition $\theta_i = \psi_{i+2} - \psi_{i+1}$. Note that the ψ_i are constants along the A_1^3 curves, that is at $(u = u_i, z)$. Hence $\psi_i' \equiv 0$ along the A_1^3 curve. By (3.64) we have $dr/ds = -\cos\phi$, where s is arclength along the A_1^3 curve. In our example z is arclength along the A_1^3 curve, so we have

$$\cos\phi = -r_{iz}(u_i, z) = -r_z \quad \Rightarrow \quad \phi' = \frac{r_{zz}}{\sin\phi} \ .$$

We assumed ϕ was obtuse along the A_1^3 curve in the general case, so $\cos\phi < 0$. Hence $r_z > 0$.

3.5.1 First Order

Now we shall consider Theorem 3.4.2.1, which gives

$$\begin{aligned} \cos\phi_i &= \epsilon_i \cos\phi \sqrt{1 + \tan^2\phi \cos^2\theta_i} = -\epsilon_i r_z \sqrt{1 + \frac{(1 - r_z^2)}{r_z^2} \cos^2\theta_i} \\ &= -\epsilon_i \sqrt{r_{iu}^2 + r_z^2}, \quad \text{from (3.77)} \ , \\ \Rightarrow \quad r_{iu}^2 &= (1 - r_z^2)\cos^2\theta_i \text{ and so } (1 - r_z^2) \geq 0 \ , \end{aligned}$$

for any z and where the derivatives of δ_i are evaluated at $u = u_i$. Using (3.80) and the fact that $N_i^+ = N_{i+1}^-$ along the A_1^3 curve we get

$$r_{iu} = -\eta_i \cos\theta_i \sqrt{1 - r_z^2} \ \text{ at } (u = u_i, z) \ . \tag{3.91}$$

Hence we can uniquely determine $r_{iu}(u_i, z)$ in terms of $r_z(z)$ and the first order derivatives of $\delta_{1,2,3}$ at $u = u_{1,2,3}$ and so we have the following.

Remark 3.5.1.1 Knowledge of the first order derivatives of the radius along the A_1^3 curve and of the curves δ_i at a point of the A_1^3 curve uniquely determines the first derivatives of the r_i in every direction.

3.5.2 Second Order

Now we shall consider the second order constraints, that is (3.72) from Theorem 3.4.5.3. For the moment $\cos\phi$ is assumed to be non-zero, that is $r_z \neq 0$. Most of the terms vanish since $\kappa \equiv 0$, $\tau \equiv 0$ and $\psi_i' \equiv 0$ along the A_1^3 curve. Firstly, we can differentiate (3.91) along the A_1^3 curve, that is with respect to z, to get an expression for $r_{iuz}(u_i, z)$:

$$r_{iuz} = \frac{\eta_i \cos\theta_i r_z r_{zz}}{\sqrt{1 - r_z^2}} \ .$$

We have $\phi' = r_{zz}/\sin\phi$ and (3.86) gives us a_i^*, so the last term we need is κ_i^W. By definition

$$W_i = N_i \times T \ , \ \kappa_i^W = -\dot{N}_i \cdot W_i \ ,$$

where by definition $\dot{}$ ('dot') means differentiation with respect to arclength along a curve passing through $\gamma_i(r_0, 0)$ with tangent W_i (see Table 3.1). Now

$$W_i = -\eta_i \left(\frac{dX_i}{du}, \frac{dY_i}{du}, 0 \right) = -\eta_i \frac{\partial \gamma_i}{\partial u}(u, z = 0) \ ,$$

and so for this example let $\dot{}$ ('dot') be the same as $(-\eta_i d/du)$ at $z = 0$ for all u on γ_i. Therefore

$$\kappa_i^W = -\left(-\eta_i \frac{dN_i}{du}(u, 0) \right) \cdot W_i = -\eta_i \left(\frac{dX_i}{du}\frac{d^2Y_i}{du^2} - \frac{d^2X_i}{du^2}\frac{dY_i}{du} \right). \qquad (3.92)$$

Using these expressions, (3.74) from Theorem 3.4.5.3 becomes the following at $(u = u_i, z = 0)$:

$$\begin{aligned} \frac{\kappa_i^W \sqrt{1 - r_z^2}}{\sin\theta_i} = & \frac{(r_{(i+1)u}^2 + r_z^2)}{r_z^2 \sin^2\theta_{i+1}} \left(r_z^2 r_{(i+1)uu} + \frac{r_{zz}}{(1 - r_z^2)} \left((1 - r_z^4)\cos^2\theta_{i+1} - 1 \right) \right) \\ & - \frac{(r_{(i+2)u}^2 + r_z^2)}{r_z^2 \sin^2\theta_{i+2}} \left(r_z^2 r_{(i+2)uu} + \frac{r_{zz}}{(1 - r_z^2)} \left((1 - r_z^4)\cos^2\theta_{i+2} - 1 \right) \right), \end{aligned}$$

for i =1, 2, 3 and where κ_i^W is given by (3.92). Attempting to solve these consistency conditions for $r_{iuu}(u_i, 0)$ for $i = 1, 2, 3$ only gives

$$\begin{aligned}
r_{2uu}\frac{(r_{2u}^2 + r_z^2)}{\sin^2\theta_2} &= -\frac{\kappa_3^W \sin\phi}{\sin\theta_3} + \frac{(r_{1u}^2 + r_z^2)r_{zz}}{r_z^2(1-r_z^2)\sin^2\theta_1}(\cos^2\theta_1(1-r_z^4) - 1) \\
&\quad + \frac{(r_{1u}^2 + r_z^2)r_{1uu}}{\sin^2\theta_1} - \frac{(r_{2u}^2 + r_z^2)r_{zz}}{r_z^2(1-r_z^2)\sin^2\theta_2}(\cos^2\theta_2(1-r_z^4) - 1) \ , \\
r_{3uu}\frac{(r_{3u}^2 + r_z^2)}{\sin^2\theta_3} &= \frac{\kappa_2^W \sin\phi}{\sin\theta_2} + \frac{(r_{1u}^2 + r_z^2)r_{zz}}{r_z^2(1-r_z^2)\sin^2\theta_1}(\cos^2\theta_1(1-r_z^4) - 1) \\
&\quad + \frac{(r_{1u}^2 + r_z^2)r_{1uu}}{\sin^2\theta_1} - \frac{(r_{3u}^2 + r_z^2)r_{zz}}{r_z^2(1-r_z^2)\sin^2\theta_3}(\cos^2\theta_3(1-r_z^4) - 1) \ , \\
\sum_{i=1}^{3}\left(\frac{\kappa_i^W}{\sin\theta_i}\right) &= 0 \ ,
\end{aligned}$$

so we can only solve for two of $r_{1uu}(u_1, 0)$, $r_{2uu}(u_2, 0)$, $r_{3uu}(u_3, 0)$. This last equation is a constraint on the curves δ_i – it must be satisfied if there is to be a smooth reconstruction of the boundary. Compare this with the second equation of (3.1) in $\mathbb{R}^2$, since for three general cylinders the three points of contact of the tritangent sphere with the boundary are in the same plane as the corresponding A_1^3 point.

Now consider the case when $\cos\phi = 0$. Using Theorem 3.4.2.1, substitution of $\cos\phi = 0$ in (3.74), with some simplification, gives the following:

$$\frac{\kappa_i^W}{\sin\theta_i} = \frac{\dot{\phi}_{i+1}}{\sin\theta_{i+1}} - \frac{\dot{\phi}_{i+2}}{\sin\theta_{i+2}} \tag{3.93}$$

In this example $\cos\phi = 0 \iff r_z = 0$. We have that $\dot{}$ ('dot') is the same as $(-\eta_i d/du)$ on γ_i and, using (3.77), we get

$$\dot{\phi}_i \cos\phi_i = \frac{\eta_i(r_{iu}r_{iuu} + r_{iz}r_{iuz})}{\sin\phi_i} \ \text{ at } (u = u_i, z) \ .$$

Then, using Theorem 3.4.2.1 we get $\dot{\phi}_i = r_{iuu}/\sin\theta_i$ when $r_z(0) = 0$ at $(u_i, 0)$. Hence (3.93) becomes

$$\frac{\kappa_i^W \sin\phi}{\sin\theta_i} = \frac{r_{(i+1)uu}}{\sin^2\theta_{i+1}} - \frac{r_{(i+2)uu}}{\sin^2\theta_{i+2}} \ .$$

This then gives

$$r_{2uu} = \frac{r_{1uu}}{\sin^2\theta_1} - \frac{\kappa_3^W \sin\phi}{\sin\theta_3} \ , \ r_{3uu} = \frac{r_{1uu}}{\sin^2\theta_1} + \frac{\kappa_2^W \sin\phi}{\sin\theta_2} \ ,$$

$$\text{and} \qquad \sum_{i=1}^{3} \frac{\kappa_i^W}{\sin\theta_i} = 0 \ ,$$

at a point of the A_1^3 curve for which $\cos\phi = 0$. So again we can only solve for two of $r_{1uu}(u_1, 0)$, $r_{2uu}(u_2, 0)$, $r_{3uu}(u_3, 0)$.

Remark 3.5.2.1 In summary, for a given set of three general cylinders, the derivatives $r_z(0)$, $r_{1uu}(u_1, 0)$ and $r_{zz}(0)$ and the first and second derivatives of δ_i at $u = u_i$ uniquely determine all of the other derivatives (up to second order) of r_i in all directions at $(u = u_i, z = 0)$ for $i = 1, 2, 3$. The curves δ_i must also satisfy the constraint:

$$\sum_{i=1}^{3} \frac{\kappa_i^W}{\sin\theta_i} = 0 \ , \quad \text{that is}$$

$$\sum_{i=1}^{3} \left(\frac{\frac{d^2X_i}{du^2}(u_i)\frac{dY_i}{du}(u_i) - \frac{dX_i}{du}(u_i)\frac{d^2Y_i}{du^2}(u_i)}{\frac{dX_{i+1}}{du}(u_{i+1})\frac{dY_{i+2}}{du}(u_{i+2}) - \frac{dX_{i+2}}{du}(u_{i+2})\frac{dY_{i+1}}{du}(u_{i+1})} \right) = 0 \ .$$

3.5.3 Three Planes

Now consider the curves δ_i as straight lines, so the γ_i are planes, parametrized as below:

$$\begin{aligned} \delta_1(u) &= (X_1(u), Y_1(u), 0) = (u, 0, 0) \ , \\ \delta_2(u) &= (X_2(u), Y_2(u), 0) = \frac{(-u, \lambda u, 0)}{\sqrt{1+\lambda^2}} \ , \\ \delta_3(u) &= (X_3(u), Y_3(u), 0) = \frac{(-u, -\rho u, 0)}{\sqrt{1+\rho^2}} \ , \end{aligned}$$

for $u \geq 0$ and where λ, ρ are both positive constants. Then $u_1 = u_2 = u_3 = 0$ corresponds to the A_1^3 point. Using (3.90) we get

$$\begin{aligned} \cos\psi_1 &= -\eta_1 \ , \ \sin\psi_1 = 0 \ , \\ \cos\psi_2 &= \frac{\eta_2}{\sqrt{1+\lambda^2}} \ , \quad \sin\psi_2 = -\frac{\eta_2\lambda}{\sqrt{1+\lambda^2}} \ , \\ \cos\psi_3 &= \frac{\eta_3}{\sqrt{1+\rho^2}} \ , \quad \sin\psi_3 = \frac{\eta_3\rho}{\sqrt{1+\rho^2}} \ . \end{aligned}$$

Then

$$\begin{aligned}
\sin\theta_1 &= \sin(\psi_3-\psi_2) = \frac{\eta_2\eta_3(\lambda+\rho)}{\sqrt{1+\lambda^2}\sqrt{1+\rho^2}}\ ,\\
\sin\theta_2 &= \sin(\psi_1-\psi_3) = \frac{\eta_1\eta_3\rho}{\sqrt{1+\rho^2}}\ ,\\
\sin\theta_3 &= \sin(\psi_2-\psi_1) = \frac{\eta_1\eta_2\lambda}{\sqrt{1+\lambda^2}}\ .
\end{aligned}$$

Since $\sin\theta_i > 0$ for each i we get $\eta_1 = \eta_2 = \eta_3$. Then

$$\begin{aligned}
\cos\theta_1 &= \cos(\psi_3-\psi_2) = \frac{1-\lambda\rho}{\sqrt{1+\lambda^2}\sqrt{1+\rho^2}}\ ,\\
\cos\theta_2 &= \cos(\psi_1-\psi_3) = \frac{-1}{\sqrt{1+\rho^2}}\ ,\\
\cos\theta_3 &= \cos(\psi_2-\psi_1) = \frac{-1}{\sqrt{1+\lambda^2}}\ .
\end{aligned}$$

By definition (see Theorem 3.4.2.1) we have that

$$\mathrm{sign}(\cos\phi_i) = -\mathrm{sign}(\cos\theta_i) = -\epsilon_i = -\mathrm{sign}(v_i)\ ,$$

by (3.6). Therefore, for this example, we get

$$\mathrm{sign}(v_1) = \mathrm{sign}(1-\rho\lambda)\ ,\ v_2 < 0\ ,\ v_3 < 0\ .$$

So there are two cases: if the angle between the half-lines δ_2, δ_3 is acute, then $v_1 > 0$, $v_2 < 0$, $v_3 < 0$; if the angle between δ_2, δ_3 is obtuse, then $v_i < 0$ for $i = 1, 2, 3$. When $(1-\rho\lambda) = 0$ then $\cos\theta_1 = 0$. By Remark 3.4.2.2 when this happens we must interpret ϵ_1 as the sign of v_1. Hence there are still two cases: v_1 positive or negative.

3.5.4 Three Circular Cylinders

Now consider the curves δ_i as segments of circles, so the γ_i are segments of circular cylinders, parametrized as below:

$$\delta_i(u) = \left(p_i + d_i\cos\left(\frac{u}{d_i}\right), q_i + d_i\sin\left(\frac{u}{d_i}\right), 0\right),$$

where p_i, q_i, and d_i are constants, and $d_i > 0$ for each i. Then (3.30) becomes

$$\sum_{i=1}^{3} \eta_i \sin\phi_i \left(\cos\left(\frac{u_i}{d_i}\right), \sin\left(\frac{u_i}{d_i}\right), 0 \right) = \mathbf{0} \ .$$

From (3.92) we get $\kappa_i^W = -\eta_i/d_i$ for all u. Then

$$\sum_{i=1}^{3} \frac{\kappa_i^W}{\sin\theta_i} = 0 \ \text{ becomes } \ \sum_{i=1}^{3} \frac{\eta_i}{d_i \sin\theta_i} = 0$$

and, since $d_i > 0$, $\sin\theta_i > 0$ for each i, we cannot have all of η_1, η_2, η_3 the same sign. (Recall from the start of this section that η_i is defined by

$$N_i(u,z) \ = \ \eta_i \left(\frac{dY_i}{du}, -\frac{dX_i}{du}, 0 \right), \ \text{ where } \ \eta_i = \pm 1 \ .)$$

3.6 Second Example of the A_1^3 Case

Let the boundary surface be a parabolic gutter given by $z = by^2$ and the plane $x = p$ for $b > 0$, $p > 0$ constants. The boundary is not smooth for points where $x = p$ intersects with $z = by^2$, but we imagine the boundary is 'smoothed off' near to these points. A sphere whose centre lies on the A_1^3 curve has two points of contact with $z = by^2$ and one with $x = p$. See Figure 3.10 where $b = 1$, $p = 0.6$. We shall explicitly calculate the medial axis and all of the terms which appear in the constraints in the A_1^3 case given by one of Theorems 3.4.5.2, 3.4.5.3, 3.4.5.4. These constraints can be verified in this case.

3.6.1 Calculating the Medial Axis

Firstly consider a sphere tangent to the parabolic gutter in two places. A general point of the normal to $z = by^2$ at (x, y, by^2) is

$$(x, y, by^2) + \mu(0, -2by, 1) \ ,$$

where $\mu > 0$ since $(0, -2by, 1)$ is an inward normal (compare with $N^{\pm}$ from (3.5) which points from the boundary towards the centre of the corresponding

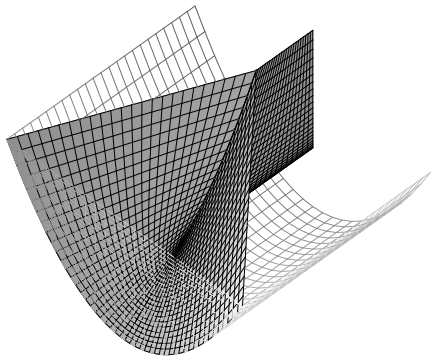

Figure 3.10: An example of a boundary surface consisting of a parabolic gutter $z = by^2$ with a flat end $x = p$ for $b = 1$, $p = 0.6$ and its medial axis near to an A_1^3 curve. The boundary is in wireframe, the medial axis is shaded. The A_1^3 curve is where the three medial sheets intersect. The A_3 curve, or edge, lies on the flat medial sheet and corresponds to centres of bitangent spheres where the two points of contact have come into coincidence at the bottom of the gutter. This edge is a straight line parametrized by $(u, 0, 1/2b)$ and ends at an A_1A_3 point, where the A_1^3 curve also ends.

sphere). By symmetry the centre of the sphere will lie on the plane $Y = 0$ and the points of contact of the sphere with the parabolic gutter will have equal and opposite values for y. Hence $\mu = 1/2b$ and the centre of the sphere is

$$\left(x, 0, by^2 + \frac{1}{2b}\right).$$

From (3.3) we have $r = \|\gamma^{\pm} - \gamma\|$, and so the radius of the sphere tangent to the parabolic gutter at (x, y, by^2) and $(x, -y, by^2)$ is

$$\begin{aligned} & \|(x, y, by^2) + \mu(0, -2by, 1) - (x, y, by^2)\| \\ = \; & \|(x, -y, by^2) + \mu(0, -2by, 1) - (x, -y, by^2)\| \\ = \; & \frac{1}{2b}\sqrt{1 + 4b^2y^2}\ . \end{aligned}$$

Hence, labelling the A_1^2 sheet corresponding to the two points of contact on the parabolic gutter as γ_1, we have

$$\gamma_1(x, y) = \left(x, 0, by^2 + \frac{1}{2b}\right)\ ,\ r_1(x, y) = \frac{1}{2b}\sqrt{1 + 4b^2y^2}\ . \tag{3.94}$$

In a similar way, labelling γ_3 as the A_1^2 sheet corresponding to the points of contact (p,u,v) and (x,y,by^2), we get

$$\begin{aligned} \gamma_3(x,y) &= \big(x, y(1-2b\lambda), by^2+\lambda\big) \ , \ r_3(x,y) = p - x \ , \qquad (3.95) \\ \text{where } \ \lambda &= \frac{p-x}{\sqrt{1+4b^2y^2}} \ . \end{aligned}$$

(This is labelled γ_3 since if it were labelled γ_2, it can be shown that conventions taken in the general case are violated.) Symmetry gives the other medial sheet γ_2 corresponding to the points of contact (p,u,v) and $(x,-y,by^2)$

$$\gamma_2(x,y) = \big(x, -y(1-2b\lambda), by^2+\lambda\big) \ , \ r_2(x,y) = p - x \ . \qquad (3.96)$$

Hence (3.94), (3.95), and (3.96) give us parametrizations of the three medial sheets γ_1, γ_2, γ_3 and their corresponding radius functions r_1, r_2, r_3 in terms of (x,y), where $y>0$ and (x,y,by^2) is a point on the parabolic gutter.

Using the parametrizations, the terms involved in the consistency conditions of Theorem 3.4.5.2, (or Theorem 3.4.5.3, or Theorem 3.4.5.4) can be calculated. From (3.94), (3.95), and (3.96) we get the following:

$$\begin{aligned} N_1(x,y) &= (0,\eta_1,0) \ , \\ N_2(x,y) &= \frac{\eta_2}{\sqrt{2}\sqrt{1+4b^2y^2}} \left(\sqrt{1+4b^2y^2}, 2by, 1\right) , \\ N_3(x,y) &= \frac{\eta_3}{\sqrt{2}\sqrt{1+4b^2y^2}} \left(\sqrt{1+4b^2y^2}, -2by, 1\right) , \end{aligned}$$

where $\eta_1 = \pm 1$, $\eta_2 = \pm 1$, $\eta_3 = \pm 1$. From (3.11) we get

$$\begin{aligned} \cos^2\phi_1 = \frac{1}{1+4b^2y^2} \ &\Rightarrow \ \sin\phi_1 = \frac{2by}{\sqrt{1+4b^2y^2}} \ , \\ \cos^2\phi_2 = \frac{1}{2} \ &\Rightarrow \ \sin\phi_2 = \frac{1}{\sqrt{2}} \ , \\ \cos^2\phi_3 = \frac{1}{2} \ &\Rightarrow \ \sin\phi_3 = \frac{1}{\sqrt{2}} \ , \text{ all evaluated at } (x,y) \ . \end{aligned}$$

Since ϕ_2 and ϕ_3 are constants for all x, y and $\cos\phi_i = -1/v_i$ (see Table 3.1) we have that a_2, a_2^t, a_3, a_3^t are zero for all x, y, since $a_i = \partial v_i/\partial r_i$, $a_i^t = \partial v_i/\partial t_i$ by

definition. (See §3.2 immediately before (3.7).) For a_1, a_1^t consider (3.83), where (u, z) is replaced by (x, y) and where suffices are used to denote differentiation:

$$a_1 = \frac{v_{1x}t_{1y} - v_{1y}t_{1x}}{r_{1x}t_{1y} - r_{1y}t_{1x}} = \frac{v_{1y}}{r_{1y}} \ , \quad a_1^t = \frac{-v_{1x}r_{1y} + v_{1y}r_{1x}}{r_{1x}t_{1y} - r_{1y}t_{1x}} = 0 \ ,$$

since v_{1x}, r_{1x} are zero for all x, y.

3.6.2 Involving the A_1^3 Curve

The centre of the sphere tangent to the parabolic gutter at (x, y, by^2) and $(x, -y, by^2)$, and to the plane $x = p$ is given by setting $\gamma_1(x, y) = \gamma_2(x, y) = \gamma_3(x, y)$ from (3.94), (3.95), and (3.96). If we label this centre as $C(y)$, we get

$$C(y) = \left(p - \frac{1}{2b}\sqrt{1 + 4b^2y^2}, 0, by^2 + \frac{1}{2b} \right) \ , \ r(y) = \frac{1}{2b}\sqrt{1 + 4b^2y^2} \ , \quad (3.97)$$

where $r(y)$ is the radius of the tritangent sphere. The expressions of (3.97) give a parametrization of the A_1^3 curve, which we label C, and so we can obtain expressions for T, N, B, κ, τ (see Table 3.1). We get

$$\begin{aligned}
\frac{ds}{dy} &= 2\sqrt{2}by\frac{\sqrt{1 + 2b^2y^2}}{\sqrt{1 + 4b^2y^2}} \ , \text{ where } s \text{ is arclength on } C \ , \\
T(y) &= \frac{1}{\sqrt{2}\sqrt{1 + 2b^2y^2}} \left(-1, 0, \sqrt{1 + 4b^2y^2} \right) , \\
N(y) &= \frac{1}{\sqrt{2}\sqrt{1 + 2b^2y^2}} \left(\sqrt{1 + 4b^2y^2}, 0, 1 \right) , \\
B(y) &= (0, 1, 0) \ , \\
\kappa(y) &= \frac{b}{\sqrt{2}(1 + 2b^2y^2)^{3/2}} \ , \ \tau(y) = 0 \ .
\end{aligned}$$

We expect B to be a constant vector and τ to be zero at every point of the A_1^3 curve since C lies in a plane. From (3.64) we have $dr/ds = -\cos\phi$, so for this example we get

$$\begin{aligned}
\cos\phi &= -\frac{1}{\sqrt{2}\sqrt{1 + 2b^2y^2}} \quad \Rightarrow \quad \sin\phi = \frac{\sqrt{1 + 4b^2y^2}}{\sqrt{2}\sqrt{1 + 2b^2y^2}} \\
\Rightarrow \quad \phi' &= -\frac{b}{\sqrt{2}(1 + 2b^2y^2)^{3/2}} \ ,
\end{aligned}$$

where $'$ ('prime') means differentiation with respect to arclength s along the A_1^3 curve. Note that $\cos\phi$ is always negative, which agrees with the convention of T being in the direction of r increasing.

We can find expressions for the angles ψ_i as follows (see Table 3.1). From (3.27) we have $\cos\psi_i = N \cdot N_i$ and $\sin\psi_i = B \cdot N_i$, so

$$\cos\psi_1 = 0 \ , \ \sin\psi_1 = \eta_1 = \pm 1 \ \text{ for all } y \ .$$

Using $\theta_i = \psi_{i+2} - \psi_{i+1}$ and the fact that $\sin\theta_i > 0$ for each i, it can be shown that $\eta_3 = -\eta_2 = \sin\psi_1$ and

$$\cos\psi_2 = -\cos\psi_3 = -\sin\psi_1 \frac{\sqrt{1+2b^2y^2}}{\sqrt{1+4b^2y^2}} \ ,$$
$$\sin\psi_2 = \sin\psi_3 = -\frac{\sqrt{2}by\sin\psi_1}{\sqrt{1+4b^2y^2}} \ .$$

Using these expressions we get

$$\psi_1' = 0 \ , \ \psi_2' = -\psi_3' = \frac{1}{2y(1+2b^2y^2)\sqrt{1+4b^2y^2}} \ .$$

Now for the geometrical terms involved in Theorems 3.4.5.2, 3.4.5.3 and 3.4.5.4. Since N_1 is a constant vector for all x, y we have $\kappa_1^W = 0$ for all x, y. By definition $\dot{}$ ('dot') is differentiation with respect to arclength along a curve passing through $\gamma_i(r_0, 0)$ with tangent W_i (see Table 3.1), and so we have

$$W_i = \frac{\partial\gamma_i}{\partial x}\dot{x}_i + \frac{\partial\gamma_i}{\partial y}\dot{y}_i \ \text{ at } C(y) \ , \quad \dot{N}_i = \frac{\partial N_i}{\partial x}\dot{x}_i + \frac{\partial N_i}{\partial y}\dot{y}_i \ .$$

We solve the first equation for $\dot{x}_i$, $\dot{y}_i$ to get $\dot{N}_i$ from the second and then, since $\kappa_i^W = -\dot{N}_i \cdot W_i$ by definition, we get

$$\kappa_2^W = -\kappa_3^W = -\frac{\sin\psi_1}{2\sqrt{2}by^2\sqrt{1+4b^2y^2}(1+2b^2y^2)} \ .$$

3.6.3 The Consistency Conditions in this Example

Having calculated all of the terms involved in (3.70) from Theorem 3.4.5.2, it can be shown that (3.70) is satisfied for $i = 1, 2, 3$ if and only if $\sin\psi_1 = -1$.

As a check we can substitute the following into (3.72), (3.74) respectively from Theorems 3.4.5.3, 3.4.5.4:

$$\begin{aligned} a_1^* &= 0\ ,\ a_2^* = a_3^* = -\frac{1}{2by^2\sqrt{1+4b^2y^2}}\ , \\ \dot{\phi}_1\cos\phi_1 &= -\frac{1}{\sqrt{2}y\sqrt{1+2b^2y^2}(1+4b^2y^2)^{3/2}}\ ,\ \dot{\phi}_2 = \dot{\phi}_3 = 0\ , \end{aligned}$$

using $\sin\psi_1 = -1$. These were obtained from (3.67), (3.73).

3.7 The A_1^4 Case

When there is a sphere tangent to a surface in four distinct points, its centre is said to be an A_1^4 point. In this case the medial axis is locally six sheets γ_i, for $i = 1, \ldots, 6$, which meet at the A_1^4 point (and so the A_1^4 point is also referred to as a '6-junction point'). There are four A_1^3 curves which meet and end at an A_1^4 point and each medial sheet γ_i contains two A_1^3 curves. Let the A_1^3 curves be labelled P, Q, L, M, so that we have the following.

1. The curve P is the transversal intersection of γ_1, γ_2, and γ_3.
2. The curve Q is the transversal intersection of γ_3, γ_4, and γ_5.
3. The curve L is the transversal intersection of γ_2, γ_5, and γ_6.
4. The curve M is the transversal intersection of γ_1, γ_4, and γ_6.

This is as in Figure 3.11. We want to use the constraints from §3.4 which hold along an A_1^3 curve to obtain information about the medial axis at an A_1^4 point. Firstly, we consider the reconstruction of the four boundary points given certain information on the medial axis.

3.7.1 Recovery of the Points of Tangency

Let T_P, T_Q, T_L, T_M be respectively the unit tangents to the curves P, Q, L, M. As in the A_1^3 case, T_P, T_Q, T_L, T_M are assumed to point in the direction

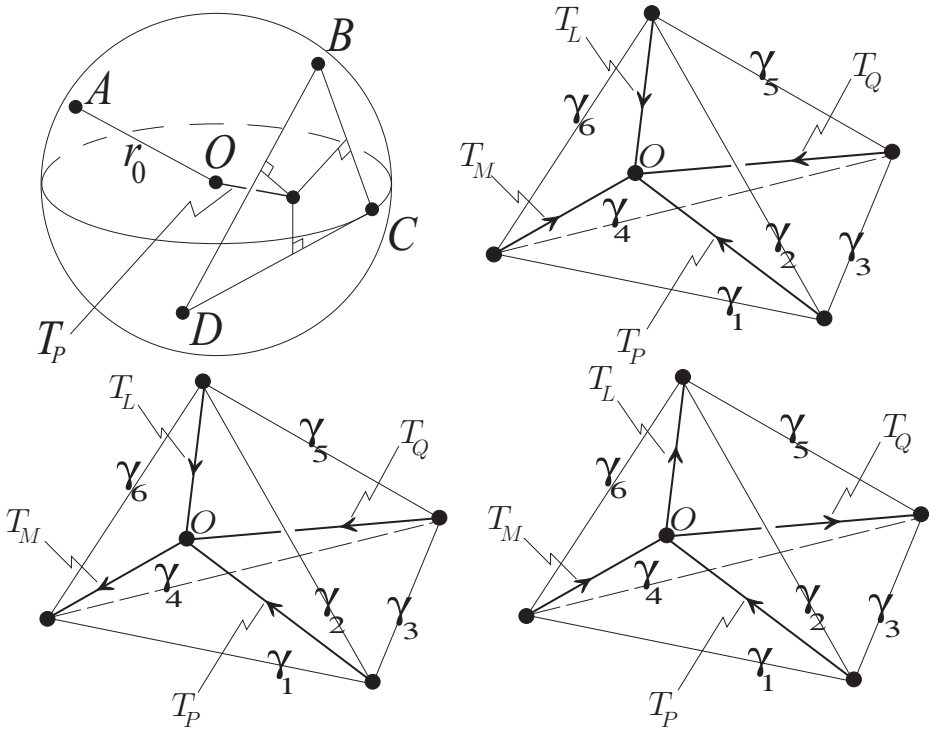

Figure 3.11: The A_1^4 case, corresponding to the centre O of a sphere of radius r_0 tangent to the boundary at four points A, B, C, D. Top left: the points of contact and the line from the A_1^4 point O to the circumcentre of the triangle through B, C and D. The tangent vector T_P to the A_1^3 curve given by spheres with tangency to the boundary surface in three points near to B, C, D is parallel to this line and so is perpendicular to the triangle through B, C and D. The other three diagrams are of the tangent planes to the medial axis near to an A_1^4 point: taken together, these look locally like a tetrahedron. The bold lines are the tangent lines to the four A_1^3 curves which meet at the A_1^4 point. The tangent planes to the six medial sheets γ_i are identified by the edge which connects two vertices of the tetrahedron. The last three pictures show the three possible configurations of r increasing along the four A_1^3 curves. Arrows indicate the direction of increasing radius r.

of increasing radius along P, Q, L, M. Also, it is assumed that no three of T_P, T_Q, T_L, T_M are coplanar. As shown in [GK04], there are three possible combinations for these tangents to point towards or away from the A_1^4 point. See Figure 3.11. We assume we are given T_P, T_Q, T_L, T_M; the tangent planes to the six medial sheets; and the radius r_0 sphere tangent to the boundary at the four contact points at the A_1^4 point. The A_1^4 point is labelled as O and the four contact points as A, B, C, D. Let $\mathbf{a}$, $\mathbf{b}$, $\mathbf{c}$, $\mathbf{d}$ be respectively the vectors from O to A, to B, to C, and to D. Going back to the A_1^3 case, we had that the tangent to the A_1^3 curve was perpendicular to the plane of contact points. (Check this by using $\gamma_i^+ = \gamma_{i+1}^-$, (3.3), (3.5), and (3.27).) Hence we let T_P, T_Q, T_L, T_M be respectively perpendicular to the planes BCD, ACD, ABD, ABC. Using this, we have the following.

- The point A reflects in the plane spanned by T_L, T_M to give B.
- The point B reflects in the plane spanned by T_P, T_M to give C.
- The point A reflects in the plane spanned by T_Q, T_M to give C.
- The point A reflects in the plane spanned by T_Q, T_L to give D.
- The point B reflects in the plane spanned by T_P, T_L to give D.
- The point C reflects in the plane spanned by T_P, T_Q to give D.

These mean that

$$\begin{aligned}
\mathbf{b} &= \mathbf{a} - 2\frac{[\mathbf{a}, T_L, T_M]}{\|T_L \times T_M\|^2}(T_L \times T_M) \ , \\
\mathbf{c} &= \mathbf{a} - 2\frac{[\mathbf{a}, T_Q, T_M]}{\|T_Q \times T_M\|^2}(T_Q \times T_M) \ , \\
\mathbf{d} &= \mathbf{a} - 2\frac{[\mathbf{a}, T_Q, T_L]}{\|T_Q \times T_L\|^2}(T_Q \times T_L) \ , \\
\mathbf{d} &= \mathbf{b} - 2\frac{[\mathbf{b}, T_P, T_L]}{\|T_P \times T_L\|^2}(T_P \times T_L) \ , \\
\mathbf{d} &= \mathbf{c} - 2\frac{[\mathbf{c}, T_P, T_Q]}{\|T_P \times T_Q\|^2}(T_P \times T_Q) \ , \\
\mathbf{b} &= \mathbf{c} - 2\frac{[\mathbf{c}, T_P, T_M]}{\|T_P \times T_M\|^2}(T_P \times T_M) \ ,
\end{aligned}$$

where for example $[\mathbf{a}, T_L, T_M]$ means $\mathbf{a} \cdot (T_L \times T_M)$. Note that these vector equations depend only on the tangent *lines* to the A_1^3 curves, since the equations are unchanged by substituting $-T_P$ for T_P, or $-T_Q$ for T_Q, or $-T_L$ for T_L, or $-T_M$ for T_M. Using the fact that $\|\mathbf{a}\| = \|\mathbf{b}\| = \|\mathbf{c}\| = \|\mathbf{d}\| = r_0$, these six vector equations can be solved for $\mathbf{a}$, $\mathbf{b}$, $\mathbf{c}$ and $\mathbf{d}$ and we get two sets of solutions:

$$\{\mathbf{a} = \delta\mathbf{a}_0, \mathbf{b} = \delta\mathbf{b}_0, \mathbf{c} = \delta\mathbf{c}_0, \mathbf{d} = \delta\mathbf{d}_0\} \ , \tag{3.98}$$

where $\delta = \pm 1$ and $\mathbf{a}_0$, $\mathbf{b}_0$, $\mathbf{c}_0$ and $\mathbf{d}_0$ are uniquely determined by the four tangent lines to P, Q, L, M and r_0.

The ambiguity about whether to take $\delta = +1$ or $\delta = -1$, that is to take one set of points of contact or the set of diametrically opposite ones, can be resolved as follows. The tangent plane to the medial sheet containing L and M (that is, γ_6) is given by $\mathbf{x} \cdot (\mathbf{a} - \mathbf{b}) = 0$. Using [GK04, pp.8, 11] we can determine the part of this tangent plane which corresponds to the medial axis, rather than just the symmetry set. On each of the medial sheets γ_i, $i = 1, \ldots, 6$, there are two separatrices between the medial axis and the non-medial axis – these are two of the A_1^3 curves meeting at the A_1^4 point. On the medial sheet containing L and M, the line

$$\mathbf{x} \cdot (\mathbf{a} - \mathbf{b}) = 0 \ , \ \mathbf{x} \cdot (\mathbf{a} - \mathbf{c}) = 0 \tag{3.99}$$

is tangent to one of the separatrices. Then,

$$\mathbf{c} \cdot (\mathbf{a} - \mathbf{c}) = \mathbf{c} \cdot \mathbf{a} - r_0^2 = r_0^2(\cos\beta - 1) \ ,$$

where β is the angle between $\mathbf{a}$ and $\mathbf{c}$. This right-hand side is always ≤ 0, so the side of the line (3.99) which is remote from $\mathbf{c}$ is given by $\mathbf{x} \cdot (\mathbf{a} - \mathbf{c}) \geq 0$. Similarly, the line

$$\mathbf{x} \cdot (\mathbf{a} - \mathbf{b}) = 0 \ , \ \mathbf{x} \cdot (\mathbf{a} - \mathbf{d}) = 0$$

is tangent to the other separatrix and so the side of this line remote from $\mathbf{d}$ is given by $\mathbf{x} \cdot (\mathbf{a} - \mathbf{d}) \geq 0$. Hence, the part of the tangent plane $\mathbf{x} \cdot (\mathbf{a} - \mathbf{b}) = 0$ which corresponds to the medial axis, rather than just the symmetry set, is

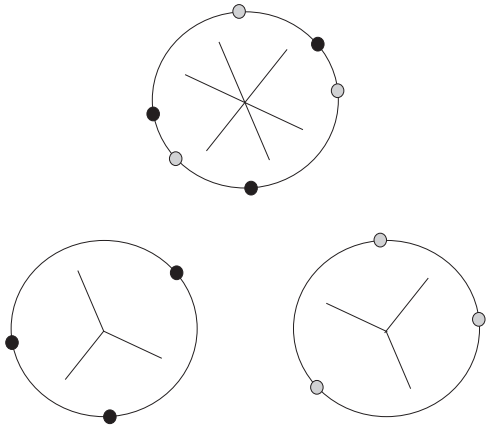

Figure 3.12: The A_1^3 case in $\mathbb{R}^2$ – see Figure 3.1 for another picture of this case. The picture at the top shows the tangent lines to the symmetry set at an A_1^3 point, the two pictures at the bottom show the two possibilities for the tangents corresponding to the medial branches. Hence, given the tangent lines to the three medial branches, there are two possible sets of solutions for the points of tangency between the sphere and the boundary curve: the set of grey points and the set of black points.

given by $\mathbf{x} \cdot (\mathbf{a} - \mathbf{c}) \geq 0$ and $\mathbf{x} \cdot (\mathbf{a} - \mathbf{d}) \geq 0$. If we have the knowledge of what part of this tangent plane corresponds to the medial axis, we can get a point $\mathbf{x} = \mathbf{x}_0$, assumed not to be the A_1^4 point, which lies on the part of this tangent plane corresponding to the medial axis. Then, using (3.98), we have

$$\begin{aligned} \mathbf{x}_0 \cdot (\mathbf{a}_0 - \mathbf{b}_0) &= 0 \quad , \\ \delta\mathbf{x}_0 \cdot (\mathbf{a}_0 - \mathbf{c}_0) \geq 0 \quad &, \quad \delta\mathbf{x}_0 \cdot (\mathbf{a}_0 - \mathbf{d}_0) \geq 0 \ . \end{aligned}$$

These are now relations in known quantities, except δ, since $\mathbf{a}_0$, $\mathbf{b}_0$, $\mathbf{c}_0$ and $\mathbf{d}_0$ are uniquely determined by the four tangent lines to P, Q, L, M and r_0. Given that $\mathbf{x} = \mathbf{x}_0$ is assumed not to be the A_1^4 point, we know that at least one of $\mathbf{x}_0 \cdot (\mathbf{a}_0 - \mathbf{c}_0)$, $\mathbf{x}_0 \cdot (\mathbf{a}_0 - \mathbf{d}_0)$ is > 0. Hence we can determine the sign of δ, and so we can decide which of the two possible solutions (3.98) is the correct one for the points of contact. Hence the following has been proved.

Proposition 3.7.1.1 (Reconstruction in the A_1^4 Case) *The four points of tangency between a sphere and the boundary surface are uniquely determined by*

the lines of tangency to the four A_1^3 curves at an A_1^4 point, the knowledge of what parts of the tangent planes to the A_1^2 sheets of the symmetry set correspond to the medial axis, and the radius r_0 of the sphere centred at the A_1^4 point. Given only the lines of tangency to the four A_1^3 curves at the A_1^4 point and r_0, then the points of tangency are only determined up to a choice of two solutions of the form (3.98)*, where $\delta = \pm 1$, and $\mathbf{a}_0$, $\mathbf{b}_0$, $\mathbf{c}_0$ and $\mathbf{d}_0$ are uniquely determined by the four tangent lines to the A_1^3 curves and r_0.*

Remark 3.7.1.2 The reconstruction of the four points of contact in the A_1^4 case in $\mathbb{R}^3$ is reminiscent of the reconstruction of the three points of contact in the A_1^3 case in $\mathbb{R}^2$. Given the lines of tangency to the three medial branches and the radius of the sphere centred at the A_1^3 point, the three points of tangency on the boundary curve are determined up to two possible choices: each point of one solution is the diametrical opposite of a point of the other solution. This arises because there are two choices for the configuration of tangents to the medial branches at the A_1^3 point, given the tangent lines to the symmetry set (see Figure 3.12). However, given the tangent vectors oriented into the medial branches, in addition to the radius of the sphere centred at the A_1^3 point, the points of tangency on the boundary curve are uniquely determined.

3.7.2 Consistency Conditions in the A_1^4 Case

Now we shall consider the consistency conditions of §3.4. These lead to quite complicated equations in the A_1^4 case, so we will give details of some constraints which can be obtained simply, but these do not constitute a complete set of constraints. For each A_1^3 curve we want the same situation as in Figure 3.7, that is, the circle of contact points is oriented anti-clockwise, looking along the opposite direction of the tangent to the A_1^3 curve. However, this means that there are two formulae for N_i on γ_i at the A_1^4 point in terms of the Frenet frame of the two A_1^3 curves on γ_i, and these formulae might be the same or minus each other, because of the conventions taken for each A_1^3 curve. So, from (3.27) we have the following at an A_1^4 point, where N_P, B_P, ψ_{1P}, etc. are defined

analogous to the A_1^3 case:

$$\begin{aligned}
N_{1P} &= \cos\psi_{1P}N_P + \sin\psi_{1P}B_P \quad , \quad N_{1M} = \cos\psi_{1M}N_M + \sin\psi_{1M}B_M \ , \\
N_{2P} &= \cos\psi_{2P}N_P + \sin\psi_{2P}B_P \quad , \quad N_{2L} = \cos\psi_{1L}N_L + \sin\psi_{2L}B_L \ , \\
N_{3P} &= \cos\psi_{3P}N_P + \sin\psi_{3P}B_P \quad , \quad N_{3L} = \cos\psi_{3Q}N_Q + \sin\psi_{3Q}B_Q \ , \\
N_{4Q} &= \cos\psi_{4Q}N_Q + \sin\psi_{4Q}B_Q \quad , \quad N_{4M} = \cos\psi_{4M}N_M + \sin\psi_{4M}B_M \ , \\
N_{5Q} &= \cos\psi_{5Q}N_Q + \sin\psi_{5Q}B_Q \quad , \quad N_{5L} = \cos\psi_{5L}N_L + \sin\psi_{5L}B_L \ , \\
N_{6L} &= \cos\psi_{6L}N_L + \sin\psi_{6L}B_L \quad , \quad N_{6M} = \cos\psi_{6M}N_M + \sin\psi_{6M}B_M \ , \\
\text{where} \quad N_{1P} &= \eta_1 N_{1M} \quad , \quad N_{2P} = \eta_2 N_{2L} \quad , \quad N_{3P} = \eta_3 N_{3Q} \ , \\
N_{4Q} &= \eta_4 N_{4M} \quad , \quad N_{5Q} = \eta_5 N_{5L} \quad , \quad N_{6L} = \eta_6 N_{6M} \ ,
\end{aligned}$$

for $\eta_i = \pm 1$. By examining the three cases of the direction of r increasing along the A_1^3 curves as in the three pictures of Figure 3.11, it can be shown that there are three cases:

(i). $\eta_1 = \eta_2 = \eta_3 = \eta_4 = \eta_5 = \eta_6 = -1$ (top right of Figure 3.11);

(ii). $\eta_1 = \eta_4 = \eta_6 = +1$, $\eta_2 = \eta_3 = \eta_5 = -1$ (bottom left of Figure 3.11);

(iii). $\eta_2 = \eta_3 = \eta_4 = \eta_6 = +1$, $\eta_1 = \eta_5 = -1$ (bottom right of Figure 3.11).

These orientations for each A_1^3 curve also affect the terms of the geometry involved in the A_1^3 constraints from §3.4 at an A_1^4 point. For example, at the A_1^4 point, we have $\kappa_{1P}^r = \eta_1\kappa_{1M}^r$, $\kappa_{1P}^t = \eta_1\kappa_{1M}^t$, $\tau_{1P}^t = \eta_1\tau_{1M}^t$, and similarly for the other medial sheets. Then we can use (3.63) from Lemma 3.4.4.3 to get relations among the geometry of the four A_1^3 curves at the A_1^4 point. The first equation of (3.63) gives the following:

$$\begin{aligned}
\kappa_P\kappa_{1P}^W\cos\psi_{1P} - (\tau_P + \psi'_{1P})^2 &= \kappa_M\kappa_{1M}^W\cos\psi_{1M} - (\tau_M + \psi'_{1M})^2 \ , \\
\kappa_P\kappa_{2P}^W\cos\psi_{2P} - (\tau_P + \psi'_{2P})^2 &= \kappa_L\kappa_{2L}^W\cos\psi_{2L} - (\tau_L + \psi'_{2L})^2 \ , \\
\kappa_P\kappa_{3P}^W\cos\psi_{3P} - (\tau_P + \psi'_{3P})^2 &= \kappa_Q\kappa_{3Q}^W\cos\psi_{3Q} - (\tau_Q + \psi'_{3Q})^2 \ , \\
\kappa_Q\kappa_{4Q}^W\cos\psi_{4Q} - (\tau_Q + \psi'_{4Q})^2 &= \kappa_M\kappa_{4M}^W\cos\psi_{4M} - (\tau_M + \psi'_{4M})^2 \ , \\
\kappa_Q\kappa_{5Q}^W\cos\psi_{5Q} - (\tau_Q + \psi'_{5Q})^2 &= \kappa_L\kappa_{5L}^W\cos\psi_{5L} - (\tau_L + \psi'_{5L})^2 \ , \\
\kappa_L\kappa_{6L}^W\cos\psi_{6L} - (\tau_L + \psi'_{6L})^2 &= \kappa_M\kappa_{6M}^W\cos\psi_{6M} - (\tau_M + \psi'_{6M})^2 \ .
\end{aligned}$$

Then the second equation of (3.63) gives the following:

$$\begin{aligned}
\kappa^W_{1P} + \kappa_P \cos\psi_{1P} &= \eta_1 \left(\kappa^W_{1M} + \kappa_M \cos\psi_{1M}\right) \ , \\
\kappa^W_{2P} + \kappa_P \cos\psi_{2P} &= \eta_2 \left(\kappa^W_{2L} + \kappa_L \cos\psi_{2L}\right) \ , \\
\kappa^W_{3P} + \kappa_P \cos\psi_{3P} &= \eta_3 \left(\kappa^W_{3Q} + \kappa_Q \cos\psi_{3Q}\right) \ , \\
\kappa^W_{4Q} + \kappa_Q \cos\psi_{4Q} &= \eta_4 \left(\kappa^W_{4M} + \kappa_M \cos\psi_{4M}\right) \ , \\
\kappa^W_{5Q} + \kappa_Q \cos\psi_{5Q} &= \eta_5 \left(\kappa^W_{5L} + \kappa_L \cos\psi_{5L}\right) \ , \\
\kappa^W_{6L} + \kappa_L \cos\psi_{6L} &= \eta_6 \left(\kappa^W_{6M} + \kappa_M \cos\psi_{6M}\right) \ .
\end{aligned}$$

These twelve equations can then be solved for the κ^W_*-type terms. Then these solutions can be substituted into the four constraints given by (3.71) from Theorem 3.4.5.2. Then we get the following.

Proposition 3.7.2.1 (Condition at A_1^4 Points) *At an A_1^4 point, the following equations hold. From* (3.71) *for P we get*

$$\begin{aligned}
&\frac{1}{\sin(\psi_{3P}-\psi_{2P})}\left(\frac{(\tau_P+\psi'_{1P})^2-(\tau_M+\psi'_{1M})^2}{\kappa_P\cos\psi_{1P}-\eta_1\kappa_M\cos\psi_{1M}}+\eta_1\kappa_M\cos\psi_{1M}\right)\\
&+\frac{1}{\sin(\psi_{1P}-\psi_{3P})}\left(\frac{(\tau_P+\psi'_{2P})^2-(\tau_L+\psi'_{2L})^2}{\kappa_P\cos\psi_{2P}-\eta_2\kappa_L\cos\psi_{2L}}+\eta_2\kappa_L\cos\psi_{2L}\right)\\
&+\frac{1}{\sin(\psi_{2P}-\psi_{1P})}\left(\frac{(\tau_P+\psi'_{3P})^2-(\tau_Q+\psi'_{3Q})^2}{\kappa_P\cos\psi_{3P}-\eta_3\kappa_Q\cos\psi_{3Q}}+\eta_3\kappa_Q\cos\psi_{3Q}\right)\\
=\ &2\frac{\cos\phi_P}{\sin\phi_P}\left(\frac{(\tau_P+\psi'_{1P})\cos(\psi_{3P}-\psi_{2P})}{\sin(\psi_{3P}-\psi_{2P})}+\frac{(\tau_P+\psi'_{2P})\cos(\psi_{1P}-\psi_{3P})}{\sin(\psi_{1P}-\psi_{3P})}\right.\\
&\qquad\left.+\frac{(\tau_P+\psi'_{3P})\cos(\psi_{2P}-\psi_{1P})}{\sin(\psi_{2P}-\psi_{1P})}\right)\\
&-\frac{\kappa_P\cos^2\phi_P}{\sin^2\phi_P}\left(\frac{\cos\psi_{1P}}{\sin(\psi_{3P}-\psi_{2P})}+\frac{\cos\psi_{2P}}{\sin(\psi_{1P}-\psi_{3P})}+\frac{\cos\psi_{3P}}{\sin(\psi_{2P}-\psi_{1P})}\right).
\end{aligned}$$

From (3.71) *for* Q *we get*

$$\begin{aligned}
&\frac{1}{\sin(\psi_{4Q}-\psi_{5Q})}\left(\frac{(\tau_Q+\psi'_{3Q})^2-(\tau_P+\psi'_{3P})^2}{\kappa_Q\cos\psi_{3Q}-\eta_3\kappa_P\cos\psi_{3P}}+\eta_3\kappa_P\cos\psi_{3P}\right)\\
&+\frac{1}{\sin(\psi_{5Q}-\psi_{3Q})}\left(\frac{(\tau_Q+\psi'_{4Q})^2-(\tau_M+\psi'_{4M})^2}{\kappa_Q\cos\psi_{4Q}-\eta_4\kappa_M\cos\psi_{4M}}+\eta_4\kappa_M\cos\psi_{4M}\right)\\
&+\frac{1}{\sin(\psi_{3Q}-\psi_{4Q})}\left(\frac{(\tau_Q+\psi'_{5Q})^2-(\tau_L+\psi'_{5L})^2}{\kappa_Q\cos\psi_{5Q}-\eta_5\kappa_L\cos\psi_{5L}}+\eta_5\kappa_L\cos\psi_{5L}\right)\\
=\;& 2\frac{\cos\phi_Q}{\sin\phi_Q}\left(\frac{(\tau_Q+\psi'_{3Q})\cos(\psi_{4Q}-\psi_{5Q})}{\sin(\psi_{4Q}-\psi_{5Q})}+\frac{(\tau_Q+\psi'_{4Q})\cos(\psi_{5Q}-\psi_{3Q})}{\sin(\psi_{5Q}-\psi_{3Q})}\right.\\
&\qquad\left.+\frac{(\tau_Q+\psi'_{5Q})\cos(\psi_{3Q}-\psi_{4Q})}{\sin(\psi_{3Q}-\psi_{4Q})}\right)\\
&-\frac{\kappa_Q\cos^2\phi_Q}{\sin^2\phi_Q}\left(\frac{\cos\psi_{3Q}}{\sin(\psi_{4Q}-\psi_{5Q})}+\frac{\cos\psi_{4Q}}{\sin(\psi_{5Q}-\psi_{3Q})}+\frac{\cos\psi_{5Q}}{\sin(\psi_{3Q}-\psi_{4Q})}\right).
\end{aligned}$$

From (3.71) *for* L *we get*

$$\begin{aligned}
&\frac{1}{\sin(\psi_{5L}-\psi_{6L})}\left(\frac{(\tau_L+\psi'_{2L})^2-(\tau_P+\psi'_{2P})^2}{\kappa_L\cos\psi_{2L}-\eta_2\kappa_P\cos\psi_{2P}}+\eta_2\kappa_P\cos\psi_{2P}\right)\\
&+\frac{1}{\sin(\psi_{6L}-\psi_{2L})}\left(\frac{(\tau_L+\psi'_{5L})^2-(\tau_Q+\psi'_{5Q})^2}{\kappa_L\cos\psi_{5L}-\eta_5\kappa_Q\cos\psi_{5Q}}+\eta_5\kappa_Q\cos\psi_{5Q}\right)\\
&+\frac{1}{\sin(\psi_{2L}-\psi_{5L})}\left(\frac{(\tau_L+\psi'_{6L})^2-(\tau_M+\psi'_{6M})^2}{\kappa_L\cos\psi_{6L}-\eta_6\kappa_M\cos\psi_{6M}}+\eta_6\kappa_M\cos\psi_{6M}\right)\\
=\;& 2\frac{\cos\phi_L}{\sin\phi_L}\left(\frac{(\tau_L+\psi'_{2L})\cos(\psi_{5L}-\psi_{6L})}{\sin(\psi_{5L}-\psi_{6L})}+\frac{(\tau_L+\psi'_{5L})\cos(\psi_{6L}-\psi_{2L})}{\sin(\psi_{6L}-\psi_{2L})}\right.\\
&\qquad\left.+\frac{(\tau_L+\psi'_{6L})\cos(\psi_{2L}-\psi_{5L})}{\sin(\psi_{2L}-\psi_{5L})}\right)\\
&-\frac{\kappa_L\cos^2\phi_L}{\sin^2\phi_L}\left(\frac{\cos\psi_{2L}}{\sin(\psi_{5L}-\psi_{6L})}+\frac{\cos\psi_{5L}}{\sin(\psi_{6L}-\psi_{2L})}+\frac{\cos\psi_{6L}}{\sin(\psi_{2L}-\psi_{5L})}\right).
\end{aligned}$$

And finally, from (3.71) *for* M *we get*

$$\begin{aligned}
&\frac{1}{\sin(\psi_{6M}-\psi_{4M})}\left(\frac{(\tau_M+\psi'_{1M})^2-(\tau_P+\psi'_{1P})^2}{\kappa_M\cos\psi_{1M}-\eta_1\kappa_P\cos\psi_{1P}}+\eta_1\kappa_P\cos\psi_{1P}\right)\\
+&\frac{1}{\sin(\psi_{1M}-\psi_{6M})}\left(\frac{(\tau_M+\psi'_{4M})^2-(\tau_Q+\psi'_{4Q})^2}{\kappa_M\cos\psi_{4M}-\eta_4\kappa_Q\cos\psi_{4Q}}+\eta_4\kappa_Q\cos\psi_{4Q}\right)\\
+&\frac{1}{\sin(\psi_{4M}-\psi_{1M})}\left(\frac{(\tau_M+\psi'_{6M})^2-(\tau_L+\psi'_{6L})^2}{\kappa_M\cos\psi_{6M}-\eta_6\kappa_L\cos\psi_{6L}}+\eta_6\kappa_L\cos\psi_{6L}\right)\\
=\;& 2\frac{\cos\phi_M}{\sin\phi_M}\left(\frac{(\tau_M+\psi'_{1M})\cos(\psi_{6M}-\psi_{4M})}{\sin(\psi_{6M}-\psi_{4M})}+\frac{(\tau_M+\psi'_{4M})\cos(\psi_{1M}-\psi_{6M})}{\sin(\psi_{1M}-\psi_{6M})}\right.\\
&\qquad\left.+\frac{(\tau_M+\psi'_{6M})\cos(\psi_{4M}-\psi_{1M})}{\sin(\psi_{4M}-\psi_{1M})}\right)\\
&-\frac{\kappa_M\cos^2\phi_M}{\sin^2\phi_M}\left(\frac{\cos\psi_{1M}}{\sin(\psi_{6M}-\psi_{4M})}+\frac{\cos\psi_{4M}}{\sin(\psi_{1M}-\psi_{6M})}+\frac{\cos\psi_{6M}}{\sin(\psi_{4M}-\psi_{1M})}\right).
\end{aligned}$$

Remark 3.7.2.2 The equations of Proposition 3.7.2.1 are constraints on the geometry of the four A_1^3 curves and the derivatives of angles between principal normals to the A_1^3 curves and the normals to the medial sheets γ_i for $i=1,\ldots,6$ at the A_1^4 point.

3.8 The A_3 Case

Consider the medial axis γ locally as a single (A_1^2) sheet. When the two points of contact on the boundary surface $\gamma^\pm$ come into coincidence the medial axis is locally a surface with boundary – this boundary is the A_3 curve, referred to as the *edge* of the medial axis. The corresponding curve on the boundary $\gamma^\pm$ is called a *ridge* curve and its points are *ridge points*. From (3.3) we have

$$\gamma^\pm=\gamma-rN^\pm$$

and, using (3.5), we see that $\gamma^+=\gamma^-$ if and only if $\cos^2\phi=1$. Hence, from (3.6), a point of the edge is a point where $v^2=1$. Consider Figure 3.3 – the A_3 case corresponds to $\phi=0$ or π.

In §3.1, the conditions on the medial axis in $\mathbb{R}^2$ at an endpoint (A_3) were discussed. The condition on the radius function was that r'' should be non-zero at the endpoint, where $'$ ('prime') means differentiation with respect to arclength on the boundary curve. Also there was (3.2), an expression for the curvature κ of the medial axis at an endpoint in terms of the curvature k of the boundary curve. This section contains the analogues of these in $\mathbb{R}^3$; there is a condition (3.102) contained in Proposition 3.8.1.2 for the smoothness of the boundary at A_1^2 points (for the condition at A_3 points, substitute $v^2 = 1$ to get (3.103)). Also, (3.107) from Proposition 3.8.2.1 is a formula for the Gauss curvature of the medial axis at an A_3 point in terms of the derivatives of the boundary.

3.8.1 Smoothness Condition on the Boundary

The envelope of spheres centred on γ is

$$\left.\begin{array}{l} \left\{\mathbf{x}: \quad \text{there exist } r,\, t \text{ with } \quad F = \frac{\partial F}{\partial r} = \frac{\partial F}{\partial t} = 0\right\} \\ \text{where} \quad F = (\mathbf{x} - \gamma(r,t)) \cdot (\mathbf{x} - \gamma(r,t)) - r^2. \end{array}\right\} \tag{3.100}$$

Consider the following:

$$\left.\begin{array}{ccc} \mathbb{R}^5 & \xrightarrow{\;g\;} & \mathbb{R}^3 \\ (x,y,z,r,t) & \longmapsto & \left(F, \frac{\partial F}{\partial r}, \frac{\partial F}{\partial t}\right) \\ \pi \big\downarrow & & \\ \mathbb{R}^3 & & \\ (x,y,z) & & \end{array}\right\} \tag{3.101}$$

The medial axis is $\pi(g^{-1}(\mathbf{0}))$. For $g^{-1}(\mathbf{0})$ to be smooth we need $\mathbf{0}$ to be a regular value of g. Then, for $\mathbf{x} = (x,y,z)$ and $\gamma(r,t) = (X(r,t), Y(r,t), Z(r,t))$, the

Jacobian J of g evaluated at (r,t) is given by

$$-\frac{1}{2}J(r,t) = \begin{pmatrix} F_x & F_y & F_z & F_r & F_t \\ F_{xr} & F_{yr} & F_{zr} & F_{rr} & F_{rt} \\ F_{xt} & F_{yt} & F_{zt} & F_{rt} & F_{tt} \end{pmatrix}$$

$$= \begin{pmatrix} X-x & Y-y & Z-z & 0 & 0 \\ X_r & Y_r & Z_r & (\mathbf{x}-\gamma)\cdot\gamma_{rr} - v^2 + 1 & (\mathbf{x}-\gamma)\cdot\gamma_{rt} \\ X_t & Y_t & Z_t & (\mathbf{x}-\gamma)\cdot\gamma_{rt} & (\mathbf{x}-\gamma)\cdot\gamma_{tt} - w^2 \end{pmatrix}.$$

We have $\mathbf{x} = \gamma^{\pm}$. Now consider the three left most columns of the above. From (3.3), (3.4), (3.5), and (3.6) we have

$$\begin{aligned} (X-x, Y-y, Z-z) &= \gamma - \gamma^{\pm} = \frac{r}{v}T \mp r\sqrt{1-\frac{1}{v^2}}N \ , \\ (X_r, Y_r, Z_r) &= \gamma_r = vT \ , \\ (X_t, Y_t, Z_t) &= \gamma_t = wU \ . \end{aligned}$$

These three vectors are linearly independent if and only if $v^2 \neq 1$. Therefore, when $v^2 \neq 1$ at $(r = r_0, t = 0)$ there is a 3×3 minor of $J(r_0, 0)$ which is non-zero, and so in this case $\mathbf{0}$ is a regular value of g.

When $v^2 = 1$ at $(r_0, 0)$ we need to consider the other 3×3 minors of $J(r_0, 0)$. In this case we have

$$(\gamma^{\pm}(r_0,0) - \gamma(r_0,0)) = -\frac{r_0}{v}T$$

and, from (3.7) we have

$$\begin{aligned} (\gamma^{\pm}(r_0,0) - \gamma(r_0,0))\cdot\gamma_{rr}(r_0,0) &= -\frac{r_0 a}{v} \ , \\ (\gamma^{\pm}(r_0,0) - \gamma(r_0,0))\cdot\gamma_{rt}(r_0,0) &= -\frac{r_0 a^t}{v} \ , \\ (\gamma^{\pm}(r_0,0) - \gamma(r_0,0))\cdot\gamma_{tt}(r_0,0) &= \frac{r_0 a^*}{v^2} = r_0 a^* \ . \end{aligned}$$

Let $T(r_0,0) = (T_1, T_2, T_3)$ and $U(r_0,0) = (U_1, U_2, U_3)$. Then, using the fact that $w(r_0,t) = 1$ for all t near $t = 0$, we have

$$J(r_0,0) = -2\begin{pmatrix} \frac{r_0}{v}T_1 & \frac{r_0}{v}T_2 & \frac{r_0}{v}T_3 & 0 & 0 \\ vT_1 & vT_2 & vT_3 & -\frac{r_0 a}{v} & -\frac{r_0 a^t}{v} \\ U_1 & U_2 & U_3 & -\frac{r_0 a^t}{v} & r_0 a^* - 1 \end{pmatrix}.$$

We know that $\mathbf{0}$ is not a regular value of g at $(r_0, 0)$ if and only if all of the 3×3 minors of $J(r_0, 0)$ are zero. Given $r_0 > 0$, this is true if and only if all of the following are true, where a, a^t, and a^* are all evaluated at $(r_0, 0)$:

$$
\begin{aligned}
&a(T_1U_2 - U_1T_2) = 0 \ , \ a(T_1U_3 - U_1T_3) = 0 \ , \ a(T_2U_3 - U_2T_3) = 0 \ , \\
&a^t(T_1U_2 - U_1T_2) = 0 \ , \ a^t(T_1U_3 - U_1T_3) = 0 \ , \ a^t(T_2U_3 - U_2T_3) = 0 \ , \\
&T_1\left(r_0\left(\frac{aa^*}{v} + (a^t)^2\right) - \frac{a}{v}\right) = 0 \ , \\
&T_2\left(r_0\left(\frac{aa^*}{v} + (a^t)^2\right) - \frac{a}{v}\right) = 0 \ , \\
&T_3\left(r_0\left(\frac{aa^*}{v} + (a^t)^2\right) - \frac{a}{v}\right) = 0 \ .
\end{aligned}
$$

We have $N(r_0, 0) = (T_2U_3 - U_2T_3, T_3U_1 - U_3T_1, T_1U_2 - U_1T_2)$ by definition. We assume that T, U and N are not zero vectors, so *all* of the 3×3 minors of $J(r_0, 0)$ are zero from the above if and only if $a = 0$ *and* $a^t = 0$. Hence we have the following.

Lemma 3.8.1.1 *Consider the medial axis as* $\pi(g^{-1}(\mathbf{0}))$ *given by* (3.100) *and* (3.101)*. When* $\gamma(r_0, 0)$ *is an* A_1^2 *point (so* $v^2 \neq 1$*) then* $g^{-1}(\mathbf{0})$ *is smooth at* $\gamma(r_0, 0)$*. When* $\gamma(r_0, 0)$ *is an* A_3 *point (so* $v^2 = 1$*) then* $g^{-1}(\mathbf{0})$ *is smooth at* $\gamma(r_0, 0)$ *if and only if at least one of* a, a^t *is non-zero.*

For $\gamma^{\pm}$ to be smooth near to $(r_0, 0)$, that is for $\pi(g^{-1}(\mathbf{0}))$ to be smooth, we require that $g^{-1}(\mathbf{0})$ is smooth (that is that $\mathbf{0}$ is a regular value of g) and that, if $\underline{\xi} = (\xi_1, \xi_2, \xi_3, \xi_4, \xi_5)$ is a tangent vector to $g^{-1}(\mathbf{0})$ at $(r_0, 0)$ in $\mathbb{R}^5$ and projects to $(0, 0, 0)$ in $\mathbb{R}^3$, then $\underline{\xi} = \mathbf{0}$. In other words, we require that no non-zero tangent vectors to $g^{-1}(\mathbf{0})$ are sent to $(0, 0, 0)$ in $\mathbb{R}^3$ by π. We have the following, which is true when $\gamma(r_0, 0)$ is an A_1^2 point or an A_3 point. (When $\gamma(r_0, 0)$ is an A_3 point, substitute $v^2 = 1$.) From $\pi : (x, y, z, r, t) \to (x, y, z)$ we

see that $\xi_1 = \xi_2 = \xi_3 = 0$. Then $\underline{\xi}$ is sent to $(0,0,0)$ by π if and only if

$$J(r_0,0)\begin{pmatrix} 0 \\ 0 \\ 0 \\ \xi_4 \\ \xi_5 \end{pmatrix} = \begin{pmatrix} 0 \\ 0 \\ 0 \end{pmatrix} \iff$$

$$\begin{aligned} ((\mathbf{x}-\gamma)\cdot\gamma_{rr} - v^2 + 1)\xi_4 + ((\mathbf{x}-\gamma)\cdot\gamma_{rt})\xi_5 &= 0\ , \\ \text{and}\ \ ((\mathbf{x}-\gamma)\cdot\gamma_{rt})\xi_4 + ((\mathbf{x}-\gamma)\cdot\gamma_{tt} - 1)\xi_5 &= 0\ , \end{aligned}$$

where $\mathbf{x} = \gamma^{\pm}$. If

$$((\mathbf{x}-\gamma)\cdot\gamma_{rr} - v^2 + 1)((\mathbf{x}-\gamma)\cdot\gamma_{tt} - 1) - ((\mathbf{x}-\gamma)\cdot\gamma_{rt})^2 \neq 0\ ,$$

where the left-hand side is evaluated at $(r_0,0)$, then $\xi_4 = \xi_5 = 0$, and so the only tangent vector to $g^{-1}(\mathbf{0})$ which projects to $\mathbf{0}$ under π is $\mathbf{0}$. We have

$$\begin{aligned} \mathbf{x}-\gamma &= -\frac{r}{v}T \pm r\sqrt{1-\frac{1}{v^2}}N\ , \\ \text{so}\ \ (\mathbf{x}-\gamma)\cdot\gamma_{rr} &= -\frac{ra}{v} \pm rv^2\kappa^r\sqrt{1-\frac{1}{v^2}}\ , \\ (\mathbf{x}-\gamma)\cdot\gamma_{rt} &= -\frac{ra^t}{v} \mp rv\tau^t\sqrt{1-\frac{1}{v^2}}\ , \\ (\mathbf{x}-\gamma)\cdot\gamma_{tt} &= \frac{ra^*}{v^2} \pm r\kappa^t\sqrt{1-\frac{1}{v^2}}\ . \end{aligned}$$

Using these, we get the following.

Proposition 3.8.1.2 (Smoothness of the Boundary) *When γ is locally a single sheet, the condition for smoothness of the boundary $\gamma^{\pm}$ at $(r_0,0)$ (corresponding either to an A_1^2 point or to an A_3 point) is*

$$\begin{aligned} 0 \neq\ & -\frac{r_0^2}{v^2}\left(\frac{aa^*}{v} + (a^t)^2\right) + \frac{r_0 a}{v} \\ & +(v^2-1)\left(r_0^2(\kappa^r\kappa^t - (\tau^t)^2) - \frac{r_0 a^*}{v^2} + 1\right) \\ & \pm r_0\sqrt{1-\frac{1}{v^2}}\left(r_0\left(a^*\kappa^r - \frac{a\kappa^t}{v} - 2a^t\tau^t\right) - v^2\kappa^r + (1-v^2)\kappa^t\right). \end{aligned} \tag{3.102}$$

(For ridge points substitute $v^2 = 1$.)

Proof. By Lemma 3.8.1.1, when $v^2 \neq 1$ at $\gamma(r_0, 0)$ we have that $g^{-1}(\mathbf{0})$ is smooth. Then $\pi(g^{-1}(\mathbf{0}))$ is smooth if (3.102) holds. When $v^2 = 1$ at $\gamma(r_0, 0)$ we have that $g^{-1}(\mathbf{0})$ is smooth if and only if at least one of a, a^t is non-zero. Hence $\pi(g^{-1}(\mathbf{0}))$ is smooth if, in addition, we have (3.102); in other words if

$$0 \neq -r_0 \left(\frac{aa^*}{v} + (a^t)^2 \right) + \frac{a}{v} \ . \tag{3.103}$$

But if (3.103) holds then at least one of a, a^t being non-zero follows. Hence (3.102) with $v^2 = 1$ is the condition for smoothness of $\gamma^{\pm}$ at a ridge point. □

Remark 3.8.1.3 Consider the medial axis in $\mathbb{R}^2$. As stated at the start of this section, the condition for smoothness of the boundary curve at a point corresponding to an endpoint (A_3) of the medial axis in two dimensions is that $r''(0) \neq 0$. Using a similar method as was employed to obtain the condition (3.102) for smoothness in Proposition 3.8.1.2, the same can be done for the medial axis in $\mathbb{R}^2$. The envelope of circles centred on the medial axis γ is

$$\left\{ \mathbf{x} : \quad \text{there exists } s \text{ with } \ G = \frac{\partial G}{\partial s} = 0 \right\}$$

where $G = (\mathbf{x} - \gamma(s)) \cdot (\mathbf{x} - \gamma(s)) - r(s)^2$. Then, the corresponding boundary curve is smooth at $\gamma(s)$ (corresponding to an A_1^2 point or an A_3 point) if

$$\frac{\partial^2 G}{\partial s^2} = 1 - r'^2 - rr'' \mp r\kappa\sqrt{1 - r'^2} \neq 0 \ .$$

(For an endpoint, substitute $r' = \pm 1$.)

Smoothness Condition for a General Cylinder

From the first example of the A_1^3 case (§3.5) we had expressions (3.84), (3.85), (3.86), (3.87), (3.88), (3.89) respectively for a_i, a_i^t, a_i^*, κ_i^r, κ_i^t, τ_i^t for a medial sheet γ_i in terms of the radius function $r_i(u, z)$. These expressions are also valid away from the A_1^3 curve. Hence we can consider the expressions for a single

medial sheet γ which is a general cylinder given by

$$\begin{aligned} \gamma(u,z) &= \delta(u) + z(0,0,1), \quad \text{where} \quad \delta(u) = (X_i(u), Y_i(u), 0) \ , \\ \text{and} \qquad & \left(\frac{dX}{du}\right)^2 + \left(\frac{dY}{du}\right)^2 = 1 \quad \text{for all } u \ (\delta \text{ unit speed}) \ , \\ \text{so} \quad N(u,z) &= \eta\left(\frac{dY}{du}, -\frac{dX}{du}, 0\right), \quad \text{where} \quad \eta = \pm 1 \ . \end{aligned}$$

Consider the smoothness condition (3.102) from Proposition 3.8.1.2 for the boundary surface $\gamma^{\pm}$ corresponding to γ as a general cylinder parametrized as above. Then (3.102) becomes

$$\begin{aligned} 0 \neq & -r_0\left(r_0(r_{uz} - r_{uu}r_{zz}) + \frac{r_u^2 r_{uu} + 2r_u r_z r_{uz} + r_z^2 r_{zz})}{r_u^2 + r_z^2}\right) \\ & +(1 - r_u^2 - r_z^2)\left(1 - r_0\frac{(r_z^2 r_{uu} - 2r_u r_z r_{uz} + r_u^2 r_{zz})}{r_u^2 + r_z^2}\right) \\ & \pm\eta\sqrt{1 - r_u^2 - r_z^2}(r_0 r_{zz} + r_z^2 - 1)\left(\frac{d^2X_i}{du^2}\frac{dY_i}{du} - \frac{dX_i}{du}\frac{d^2Y_i}{du^2}\right). \end{aligned}$$

Hence this is the condition for the boundary $\gamma^{\pm}$ to be smooth at an A_1^2 or an A_3 point (for A_3, set $r_u^2 + r_z^2 = 1$).

3.8.2 Gauss Curvature on the Medial Axis at an A_3 Point

We want to obtain the analogue of (3.2) in $\mathbb{R}^3$, that is to acquire a result connecting the geometry of the boundary and the geometry of the medial axis at the edge. A parametrization of the medial axis near to an edge point can be obtained in Maple by taking the associated boundary in Monge form near to a ridge point. Let the boundary be $(x, y, f(x,y))$, where

$$\left.\begin{aligned} f(x,y) = & \tfrac{1}{2}(\kappa_1 x^2 + \kappa_2 y^2) + ((0)x^3 + b_1 x^2 y + b_2 x y^2 + b_3 y^3) \\ & +(c_0 x^4 + c_1 x^3 y + c_2 x^2 y^2 + c_3 x y^3 + c_4 y^4) \\ & +(d_0 x^5 + d_1 x^4 y + d_2 x^3 y^2 + d_3 x^2 y^3 + d_4 x y^4 + d_5 y^5) + \cdots \ . \end{aligned}\right\} (3.104)$$

Since the coefficient of x^3 is zero, the ridge corresponds to the x-direction and a ridge point corresponds to $x = y = 0$. We proceed by taking two points

$(u,v,f(u,v))$, $(s,t,f(s,t))$ near to $\mathbf{0}$. From (3.3), the condition for there to be a sphere tangent to the boundary at these two points is that

$$(u,v,f(u,v)) + rN_1(u,v) = (s,t,f(s,t)) + rN_2(s,t)\ , \tag{3.105}$$

where r is the radius of the bitangent sphere and N_1, N_2 are the unit normals to the boundary at (u,v) and at (s,t), respectively. Then we solve for u, v and r as functions of s and t such that (3.105) is satisfied. Using Maple a parametrization of the medial axis near to an edge point can be calculated explicitly. We get

$$\begin{aligned} r(s,t) &= \frac{1}{\kappa_1} - \frac{2b_1}{\kappa_1^2}t + \frac{\kappa_1^3 - 8c_0}{2\kappa_1^2}s^2 - \frac{2c_1}{\kappa_1^2}st + (*)t^2 \\ &\quad -\frac{4d_0}{\kappa_1^2}s^3 + (*)s^2t + (*)st^2 + (*)t^3 + \text{h.o.t.}\ , \end{aligned} \tag{3.106}$$

where the more complicated coefficients are denoted $(*)$. The parametrization of the medial axis near to an edge point is then $(G_1(s,t), G_2(s,t), G_3(s,t)) = (s,t,f(s,t)) - r(s,t)N_2(s,t)$ where

$$\begin{aligned} G_1(s,t) &= -\frac{b_2}{\kappa_1}t^2 - \frac{c_1}{\kappa_1}s^2t + 4\left(\frac{(\kappa_1^3 - 8c_0)b_2^2 + (\kappa_1 - \kappa_2)c_1^2 + 4b_1b_2c_1}{\kappa_1((\kappa_1-\kappa_2)(\kappa_1^3-8c_0) - 4b_1^2)}\right)st^2 \\ &\quad + \frac{2b_1b_2 - \kappa_1c_3}{\kappa_1^2}t^3 - \frac{d_0}{\kappa_1}s^4 + (*)s^3t + (*)s^2t^2 \\ &\quad + (*)st^3 + (*)t^4 + \text{h.o.t.}\ , \\ G_2(s,t) &= \left(\frac{\kappa_1 - \kappa_2}{\kappa_1}\right)t - \frac{b_1}{\kappa_1}s^2 - \frac{2b_2}{\kappa_1}st + \left(\frac{2\kappa_2b_1 - 3\kappa_1b_3}{\kappa_1^2}\right)t^2 - \frac{c_1}{\kappa_1}s^3 \\ &\quad + 2\left(\frac{b_1^2 - \kappa_1c_2 + 2\kappa_2c_0}{\kappa_1^2}\right)s^2t + \left(\frac{4b_1b_2 - 3\kappa_1c_3 + 2\kappa_2c_1}{\kappa_1^2}\right)st^2 \\ &\quad + (*)t^3 + \left(\frac{4b_1c_0 - \kappa_1d_1}{\kappa_1^2}\right)s^4 \\ &\quad + 2\left(\frac{2b_1c_1 + 4b_2c_0 + 2\kappa_2d_0 - \kappa_1d_2}{\kappa_1^2}\right)s^3t + (*)s^2t^2 \\ &\quad + (*)st^3 + (*)t^4 + \text{h.o.t.}\ , \\ G_3(s,t) &= \frac{1}{\kappa_1} - \frac{2b_1}{\kappa_1^2}t + \left(\frac{\kappa_1^3 - 8c_0}{2\kappa_1^2}\right)s^2 - \frac{2c_1}{\kappa_1^2}st + (*)t^2 \\ &\quad -\frac{4d_0}{\kappa_1^2}s^3 + (*)s^2t + (*)st^2 + (*)t^3 + \text{h.o.t.} \end{aligned}$$

A standard formula for the Gauss curvature K at a point $\mathbf{p}$ of a surface is as follows, where suffices denote differentiation:

$$\begin{aligned} K &= \frac{eg - f^2}{EG - F^2} \text{ , where} \\ E &= X_u \cdot X_u \ , \ F = X_u \cdot X_v \ , \ G = X_v \cdot X_v \ , \\ \tilde{e} &= X_{uu} \cdot N \ , \ \tilde{f} = X_{uv} \cdot N \ , \ \tilde{g} = X_{vv} \cdot N \ , \end{aligned}$$

where N is a unit normal to S at $\mathbf{p}$. Using this formula for K and the parametrization $G(s,t)$ of the medial axis near to an A_3 point we can calculate the Gauss curvature on the medial axis at (s,t).

Proposition 3.8.2.1 *The limiting value (if it exists) of the Gauss curvature K (which is the product of the principal curvatures on the medial axis) as x, y tend to zero, that is as we tend towards the edge point, is as follows:*

$$K = \frac{4(4b_2d_0 - c_1^2)\kappa_1^4}{((\kappa_1 - \kappa_2)(\kappa_1^3 - 8c_0) - 4b_1^2)^2} \ . \tag{3.107}$$

(The reason for the qualifying 'if it exists' is that not all of the limiting directions tending towards the edge point $(0,0,1/\kappa_1)$ have been considered in the calculation of (3.107)*.)*

The denominator of the right-hand side of (3.107) is zero only if $\mathbf{0}$ corresponds to an A_4 point, which we assume is not true. Compare this value with the expression for the limiting value of the curvature of the medial axis in $\mathbb{R}^2$ at the endpoint given by (3.2). This depends on the third derivative of the curvature of the boundary, that is it depends on the 5-jet of the boundary at the corresponding point. The limiting value of K as in (3.107) also depends on the 5-jet of the boundary in three dimensions.

Equation (3.107) gives a criterion for $K = 0$ on the medial axis. We can also express K in terms of derivatives of the principal curvatures κ_1 and κ_2 at $(x,y) = (0,0)$ on the boundary by using Maple to expand the principal curvatures κ_1, κ_2 as functions of x and y near to $x = y = 0$. (See [HGYGM99,

pp.128-142].) Then we get

$$\begin{aligned}
\kappa_1(0,0) &= \kappa_1 \ \text{(const.)} \ , \quad \kappa_2(0,0) = \kappa_2 \ \text{(const.)} \ , \\
\kappa_{1x}(0,0) &= 2b_1, \quad \kappa_{2x}(0,0) = 2b_2 \ , \\
\kappa_{1xx}(0,0) &= \frac{8b_1^2 - 3\kappa_1^3(\kappa_1 - \kappa_2)}{\kappa_1 - \kappa_2} + 24c_0 \ , \\
\kappa_{1xy}(0,0) &= \frac{8b_1 b_2}{\kappa_1 - \kappa_2} + 6c_1 \ , \\
\kappa_{1xxx}(0,0) &= 24b_1 \left(\frac{3c_1(\kappa_1 - \kappa_2) + 2b_1 b_2}{(\kappa_1 - \kappa_2)^2} \right) + 120d_0 \ .
\end{aligned}$$

Using (3.107) we can express the limiting value of K at an edge point in terms of the derivatives of κ_1 and κ_2 as follows:

$$K = \frac{\kappa_1^4((\kappa_1 - \kappa_2)^2(3\kappa_{2x}\kappa_{1xxx} - 5\kappa_{1xy}^2) + 2(\kappa_1 - \kappa_2)\kappa_{1x}\kappa_{2x}\kappa_{1xy} - 2\kappa_{1x}^2\kappa_{2x}^2)}{5(\kappa_1 - \kappa_2)^2(\kappa_{1x}^2 + (\kappa_1 - \kappa_2)\kappa_{1xx})^2} \ .$$

The above shows that the Gauss curvature of the medial axis at an edge point depends on up to the third derivatives of the principal curvatures, and so on the fifth derivatives of the boundary at ridge points. This is analogous to the situation in $\mathbb{R}^2$; from (3.2) the curvature of the medial axis in two dimensions at an endpoint depends on up to the third derivative of curvature, so up to fifth derivatives of the boundary curve.

3.8.3 Local Maximum or Minimum of r Along the Ridge

Here is a result about the ridge, which is the space curve lying on $\gamma^{\pm}$ whose points are obtained from the points of the edge by (3.3).

Proposition 3.8.3.1 *At a point of the ridge corresponding to the principal curvature κ_1 on the boundary surface given by* (3.104)*, the radius of the sphere of contact with the boundary surface has a local maximum or minimum if and only if κ_1 has a critical point on the boundary.*

Proof. From [HGYGM99, pp.144, 162], the tangent to the ridge curve on the boundary surface given by (3.104) is

$$\left((\kappa_1 - \kappa_2)(8c_0 - \kappa_1^3) + 4b_1^2\right) x + (2c_1(\kappa_1 - \kappa_2) + 4b_1 b_2)\, y = 0 \ .$$

Then the derivative of r along the ridge at $x = y = 0$ is

$$\left((\kappa_1 - \kappa_2)(8c_0 - \kappa_1^3) + 4b_1^2\right) \frac{\partial r}{\partial y}(0,0) - (2c_1(\kappa_1 - \kappa_2) + 4b_1 b_2) \frac{\partial r}{\partial x}(0,0) \ .$$

Using (3.106), this is zero if and only if

$$b_1 \left((\kappa_1 - \kappa_2)(8c_0 - \kappa_1^3) + 4b_1^2\right) = 0 \ .$$

From (3.107) we know that $((\kappa_1 - \kappa_2)(8c_0 - \kappa_1^3) + 4b_1^2) \neq 0$. Hence

$$r \ \text{ has a local maximum or minimum} \quad \Longleftrightarrow \quad b_1 = 0 \ ,$$

which is the same as κ_1 having a critical point on the boundary. □

3.8.4 Principal Curvatures, Principal Directions of the Boundary

Now we shall consider the information sufficient to determine the boundary at ridge points up to second order. Assume we have the edge of the medial axis as a space curve with curvature κ and torsion τ, the tangent planes to the medial sheet, the radius function r on the edge, and the angle α between the tangent to the edge and ∇r ('grad(r)') at a point of the edge.

We can express $N^{\pm}$ in terms of ∇r by using the facts that $\nabla r = T\|\nabla r\|$ and $\cos\phi = -\|\nabla r\|$, so the formula for $N^{\pm}$ from (3.5) becomes

$$N^{\pm} = \nabla r \mp \sqrt{1 - \|\nabla r\|^2} N \ .$$

Hence, as $\sin\phi \to 0$ (corresponding to $\|\nabla r\| \to 1$) we see that $N^{\pm} \to \nabla r$. Since we are given the tangent to the ridge curve and α, we can determine ∇r and hence $N^{\pm}$ at each point of the edge. Then, using (3.3), we have each ridge point and so we have the ridge curve. Since we have the normal $N^{\pm}$ along the ridge, we also have the tangent planes to $\gamma^{\pm}$ along the ridge. Hence we have determined the first order geometry of $\gamma^{\pm}$ along a ridge curve.

Now for the second order geometry of the boundary. Given the ridge curve we have its geodesic curvature, normal curvature, $\hat{\kappa}_{n1}$ say, and geodesic torsion, $\hat{\tau}_{g1}$ say. We also know that one of the principal curvatures of the boundary at a ridge point is $1/r$. We label this $k_1 = 1/r$. Let k_2 be the other principal curvature on $\gamma^{\pm}$ at a ridge point, let $\hat{\theta}$ be the angle from the principal direction corresponding to k_1 to the tangent to the ridge curve, and $\hat{\kappa}_{n2}$ be the normal curvature of $\gamma^{\pm}$ in the tangent direction to $\gamma^{\pm}$ perpendicular to the ridge curve. Equations (3.54), (3.55) give formulae for $\hat{\kappa}_{n1}$, $\hat{\kappa}_{n2}$, $\hat{\tau}_{g1}$. (These were used in the A_1^3 case, but are valid here too.) We can solve these to obtain formulae for $\hat{\theta}$, k_2, and $\hat{\kappa}_{n2}$, and we get

$$\begin{aligned} k_2 &= \hat{\kappa}_{n1} + \frac{\hat{\tau}_{g1}^2}{\hat{\kappa}_{n1} - k_1} \ , \ \hat{\kappa}_{n2} = k_1 + \frac{\hat{\tau}_{g1}^2}{\hat{\kappa}_{n1} - k_1} \ , \\ \cos\hat{\theta} &= \pm \frac{\hat{\tau}_{g1}}{\sqrt{\hat{\tau}_{g1}^2 + (\hat{\kappa}_{n1} - k_1)^2}} \ , \ \sin\hat{\theta} = \frac{|\hat{\kappa}_{n1} - k_1|}{\sqrt{\hat{\tau}_{g1}^2 + (\hat{\kappa}_{n1} - k_1)^2}} \ , \end{aligned}$$

where $\mathrm{sign}(\cos\hat{\theta}) = \mathrm{sign}(\hat{\kappa}_{n1} - k_1)$. Hence we can determine the principal curvatures of the boundary at ridge points. However, these formulae are not enough to determine the normal curvature of $\gamma^{\pm}$ in an arbitrary direction V at a point of the ridge; we need the angle from the first principal direction to V in addition to k_1, k_2 (see Lemma 3.4.4.1).

Now for the principal directions on the boundary. Let $(r = r_0, t = 0)$ correspond to an edge point, so $\sin\phi = 0$ at $(r_0, 0)$. Let s, $s^{\pm}$ be respectively arclengths on $\gamma(r,0)$, $\gamma^{\pm}(r,0)$. Then from (3.3), (3.5), and (3.18) we get

$$\begin{aligned} \frac{d\gamma^{\pm}}{ds}(r,0) &= \mp \sin\phi T^{\pm} - r\frac{dN^{\pm}}{ds} \ , \text{ where} \\ \frac{dN^{\pm}}{ds}(r,0) &= \left(\mp \frac{a\cos^3\phi}{\sin\phi} - \kappa^r \right) T^{\pm} + \left(-a^t \cos^2\phi \mp \tau^t \sin\phi \right) U \ . \end{aligned}$$

Using these we get

$$\frac{ds^{\pm}}{ds} = \frac{\sqrt{\left(\mp \sin^2\phi \pm ra\cos^3\phi + r\kappa^r \sin\phi \right)^2 + r^2 \sin^2\phi \left(a^t \cos^2\phi \pm \tau^t \sin\phi \right)^2}}{\sin\phi}$$

at $(r,0)$. Hence

$$\frac{d\gamma^{\pm}}{ds^{\pm}} = \frac{\left(\mp\sin^2\phi \pm ra\cos^3\phi + r\kappa^r\sin\phi\right)T^{\pm} + r\sin\phi\left(a^t\cos^2\phi \pm \tau^t\sin\phi\right)U}{\sqrt{\left(\mp\sin^2\phi \pm ra\cos^3\phi + r\kappa^r\sin\phi\right)^2 + r^2\sin^2\phi\left(a^t\cos^2\phi \pm \tau^t\sin\phi\right)^2}} ,$$
$$\frac{dN^{\pm}}{ds^{\pm}} = \frac{\left(\mp a\cos^3\phi - \kappa^r\sin\phi\right)T^{\pm} + \left(-a^t\cos^2\phi \mp \tau^t\sin\phi\right)\sin\phi U}{\sqrt{\left(\mp\sin^2\phi \pm ra\cos^3\phi + r\kappa^r\sin\phi\right)^2 + r^2\sin^2\phi\left(a^t\cos^2\phi \pm \tau^t\sin\phi\right)^2}} ,$$

both at $(r,0)$. Then as we let $r \to r_0$, so that $\sin\phi \to 0$ and $\cos^2\phi \to 1$, we get

$$\lim_{r\to r_0}\left(\frac{dN^{\pm}}{ds^{\pm}}(r,0)\right) = \frac{\mp a}{r_0|a|}N \ , \quad \lim_{r\to r_0}\left(\frac{d\gamma^{\pm}}{ds^{\pm}}(r,0)\right) = \frac{\pm a}{|a|}N \ . \tag{3.108}$$

Now let $t^{\pm}$ be arclength on $\gamma^{\pm}(r_0,t)$. Then from (3.3), (3.5), and (3.19) we get

$$\begin{aligned}\frac{d\gamma^{\pm}}{dt}(r_0,t) &= U - r_0\frac{dN^{\pm}}{dt} \ , \text{ where}\\ \frac{dN^{\pm}}{dt}(r_0,t) &= \left(\pm\frac{a^t\cos^2\phi}{\sin\phi} + \tau^t\right)T^{\pm} + \left(a^*\cos^2\phi \pm \kappa^t\sin\phi\right)U \ .\end{aligned}$$

From these we get

$$\frac{dt^{\pm}}{dt} = \frac{\sqrt{r_0^2\left(\pm a^t\cos^2\phi + \tau^t\sin\phi\right)^2 + \sin^2\phi\left(1 - r_0a^*\cos^2\phi \mp r_0\kappa^t\sin\phi\right)^2}}{\sin\phi}$$

at (r_0,t). Hence

$$\frac{d\gamma^{\pm}}{dt^{\pm}} = \frac{r_0\left(\mp a^t\cos^2\phi - \tau^t\sin\phi\right)T^{\pm} + \sin\phi\left(1 - r_0a^*\cos^2\phi \mp r_0\kappa^t\sin\phi\right)U}{\sqrt{r_0^2\left(\pm a^t\cos^2\phi + \tau^t\sin\phi\right)^2 + \sin^2\phi\left(1 - r_0a^*\cos^2\phi \mp r_0\kappa^t\sin\phi\right)^2}} ,$$
$$\frac{dN^{\pm}}{dt} = \frac{\left(\pm a^t\cos^2\phi + \tau^t\sin\phi\right)T^{\pm} + \sin\phi\left(a^*\cos^2\phi \pm \kappa^t\sin\phi\right)U}{\sqrt{r_0^2\left(\pm a^t\cos^2\phi + \tau^t\sin\phi\right)^2 + \sin^2\phi\left(1 - r_0a^*\cos^2\phi \mp r_0\kappa^t\sin\phi\right)^2}} ,$$

both at (r_0,t). Similar to before, as we let $t \to 0$, so that $\sin\phi \to 0$ and $\cos^2\phi \to 1$, we get

$$\lim_{t\to 0}\left(\frac{dN^{\pm}}{dt^{\pm}}(r_0,t)\right) = \frac{\pm a^t\cos\phi}{r_0|a^t|}N \ , \ \lim_{t\to 0}\left(\frac{d\gamma^{\pm}}{dt^{\pm}}(r_0,t)\right) = \frac{\mp a^t\cos\phi}{|a^t|}N. \tag{3.109}$$

Now we shall interpret (3.108), (3.109). We assume that the boundary $\gamma^{\pm}$ is smooth at all points near to $(r_0,0)$ and so, by (3.102) from Proposition 3.8.1.2,

we know that at least one of a, a^t is non-zero at $(r_0, 0)$. Then (3.108), (3.109) imply that the derivative of $N^{\pm}$ in the N direction is parallel to N itself, and so N is a principal direction of $\gamma^{\pm}$ at ridge points. The vector $N^{\pm}$ becomes parallel to T at edge points, and so the other principal direction on $\gamma^{\pm}$ at ridge points is U.

Hence, the following has been proved.

Proposition 3.8.4.1 *Given the edge of the medial axis as a space curve with curvature κ and torsion τ, the tangent planes to the medial sheet, the radius function r on the edge, and the angle α between the tangent to the edge and ∇r ('grad(r)') at a point of the edge; then the principal curvatures and principal directions of the boundary at a ridge point are determined.*

This shows that not much information about the medial axis at an edge point is needed to give second order information of the boundary at ridge points.

3.9 The A_1A_3 Case

An A_1A_3 point on the medial axis is where an A_1^3 curve and an A_3 curve meet and end, that is the A_1A_3 point is the centre of a sphere which is tangent to a surface in three places, but two of the points of contact coincide. The medial axis near to an A_1A_3 point looks like part of a swallowtail surface with a 'fin' (another medial sheet) intersecting with the swallowtail in a curve (see the self-intersection curve of Figure 3.13). The A_1A_3 point is then the point where the edge curve of the fin meets the other two sheets.

3.9.1 Taking the Limit at Points Tending Towards the A_1A_3 Point

The equations (3.70), (3.72), (3.74), which are respectively from Theorems 3.4.5.2, 3.4.5.3 and 3.4.5.4, all hold at $\gamma_i(r_0, 0)$ on the A_1^3 curve, so they hold

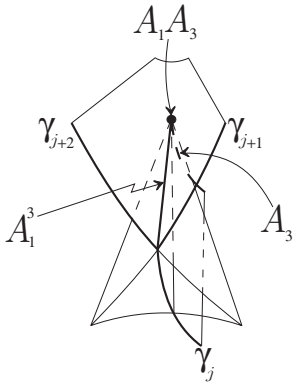

Figure 3.13: The A_1A_3 (or fin point) case. The medial axis is locally part of a swallowtail surface with another sheet meeting along the curve of self-intersection. Part of the swallowtail surface above is only on the symmetry set, not on the medial axis (compare with Figure 3.2). The two sheets of the swallowtail surface that are on the medial axis are labelled γ_{j+1}, γ_{j+2} and the other sheet of the medial axis is labelled γ_j for some j. An A_1^3 curve and an A_3 curve meet and end at an A_1A_3 point.

in the limit as we tend towards an A_1A_3 point. Hence, in order to obtain the forms of (3.70), (3.72), (3.74) at an A_1A_3 point, we need to calculate the limits of the terms involved as two of the points of contact with the boundary surface coincide. Let these points be γ_j^+ and γ_j^- for some j, which means that $\sin\phi_j = 0$ at the A_1A_3 point, from (3.3) and (3.5). From (3.39) this corresponds to $\sin\theta_j = 0$ (we dismissed the possibility of $\sin\phi = 0$ for a generic surface in Remark 3.4.5.5). Therefore the other two sheets γ_{j+1} and γ_{j+2} are part of the swallowtail surface. Let $\sin\phi_j = 0$ in (3.30). This gives

$$\begin{aligned} & \sin\phi_{j+1}N_{j+1} + \sin\phi_{j+2}N_{j+2} = \mathbf{0} \\ \Rightarrow\quad & N_{j+1} = -N_{j+2}\ ,\ \sin\phi_{j+1} = \sin\phi_{j+2} \\ \Rightarrow\quad & \cos\theta_j = N_{j+1}\cdot N_{j+2} = -1\ \Rightarrow\ \theta_j = \psi_{j+2} - \psi_{j+1} = \pi\ . \end{aligned}$$

From this and Theorem 3.4.2.1 we can deduce the following at the A_1A_3 point:

$$\begin{aligned}
&\sin\psi_{j+1} = -\sin\psi_{j+2}\ ,\ \cos\psi_{j+1} = -\cos\psi_{j+2}\ ,\\
&\cos\theta_{j+1} = -\cos\theta_{j+2}\ ,\ \sin\theta_{j+1} = \sin\theta_{j+2}\ ,\\
&\cos\phi_{j+1} = -\cos\phi_{j+2}\ ,\ \text{so}\ v_{j+1} = -v_{j+2}\ .
\end{aligned}$$

From Remark 3.4.2.2 we have $\text{sign}(v_i) = \epsilon_i = \text{sign}(\cos\theta_i)$. Hence at the A_1A_3 point we have $v_j = -1$, $v_{j+1} = -v_{j+2}$, which means that we have two of the velocities negative and one positive at the A_1A_3 point.

Consider the standard swallowtail surface, which is given by

$$\left\{(u_1,u_2,u_3):\quad \exists t\ \text{ with }\ F = \frac{\partial F}{\partial t} = 0\right\},\ \text{where } F = t^4 + u_1t^2 + u_2t + u_3\ .$$

A parametrization of this is

$$X(u,v) = (u, -4v^3 - 2uv, 3v^4 + uv^2)\ .$$

The double curve where two sheets intersect transversally is

$$X(u(t) = -2t^2, v(t) = \pm t) = (-2t^2, 0, t^4)$$

and so the swallowtail point is at $t = 0$.

A general swallowtail surface, $\overline{S}$ say, is a local diffeomorphism of the standard swallowtail surface. Then the medial axis near to an A_1A_3 point is part of $\overline{S}$ and another sheet γ_j which intersects with $\overline{S}$ in the double curve on $\overline{S}$. We let the local diffeomorphism of the standard swallowtail be H:

$$\begin{aligned}
\mathbb{R}^2 \ &\xrightarrow{X}\ \mathbb{R}^3 \ \xrightarrow{H}\ \mathbb{R}^3,\\
(u,v) \ &\longmapsto\ (x,y,z) \ \longmapsto\ (H_1,H_2,H_3),\\
H(x,y,z) = (x + \overline{a}_1y + \overline{a}_2z \ &+\ (b_{11}x^2 + b_{12}xy + b_{13}y^2) + \cdots\ ,\\
\overline{a}_3y + \overline{a}_4z \ &+\ (b_{21}x^2 + b_{22}xy + b_{23}y^2) + \cdots\ ,\\
\overline{a}_5z \ &+\ (b_{31}x^2 + b_{32}xy + b_{33}y^2) + \cdots\ )\ .
\end{aligned}$$

(The linear terms have been labelled so as not to be confused with the accelerations a_1, a_2, a_3 – see §3.2, just above (3.7).) We assume the Jacobian

of H is non-singular, which means that $\overline{a}_3\overline{a}_5 \neq 0$. Then a parametrization of $\overline{S}$ is $H(x(u,v), y(u,v), z(u,v))$, where $x(u,v) = u$, $y(u,v) = -4v^3 - 2uv$, and $z(u,v) = 3v^4 + uv^2$. Then the A_1^3 curve is given by substituting $u = -2t^2$, $v = \pm t$ into $H(x(u,v), y(u,v), z(u,v))$, and so the A_1A_3 point corresponds to $t = 0$. Hence we can calculate all of the terms which appear in the A_1^3 curvature constraints and take their limits tending along the A_1^3 curve towards the A_1A_3 point.

Firstly, N_{j+1}, N_{j+2} are obtained along the double curve on $\overline{S}$ as follows:

$$\begin{aligned} N_{j+1}(t) &= -\frac{H_u \times H_v}{\|H_u \times H_v\|}(u = -2t^2, v = t) \ , \\ N_{j+2}(t) &= \frac{H_u \times H_v}{\|H_u \times H_v\|}(u = -2t^2, v = -t) \ . \end{aligned}$$

Then we get

$$\begin{aligned} \cos\theta_j &= \cos(\psi_{j+2} - \psi_{j+1}) = N_{j+1} \cdot N_{j+2} = -1 + 2\frac{\overline{a}_5^2}{\overline{a}_3^2}t^2 + O(t^4) \ , \\ \sin\theta_j &= \sqrt{1 - \cos^2\theta_j} = 2\left|\frac{\overline{a}_5}{\overline{a}_3}\right| t + O(t^3) \end{aligned} \tag{3.110}$$

along the A_1^3 curve, and so $\sin\theta_j \to 0$, $\cos\theta_j \to -1$, as $t \to 0$, as expected. Let the A_1^3 curve on $\overline{S}$ be $C(t)$. Then we can calculate T, N, B as functions of t, and so obtain κ, τ. We get

$$\begin{aligned} \frac{ds}{dt} &= t(4 - 4(\overline{a}_2 + 4b_{11})t^2 + O(t^4)) \ , \\ \kappa &= \frac{\sqrt{(\overline{a}_4 + 4b_{21})^2 + (\overline{a}_5 + 4b_{31})^2}}{2} + O(t^2) \ , \\ \tau &= \frac{12\left(c_{31}(\overline{a}_4 + 4b_{21}) - c_{21}(\overline{a}_5 + 4b_{31})\right)}{(\overline{a}_4 + 4b_{21})^2 + (\overline{a}_5 + 4b_{31})^2} + O(t^2) \ , \end{aligned}$$

where s is arclength on C. Since we assumed κ was never zero when setting up the $[T, N, B]$ frame, we have that $(\overline{a}_4 + 4b_{21})^2 + (\overline{a}_5 + 4b_{31})^2 \neq 0$, and so at least one of $(\overline{a}_4 + 4b_{21})$, $(\overline{a}_5 + 4b_{31})$ is non-zero. Then we get

$$\begin{aligned} \cos\psi_{j+1} &= N_{j+1}(t) \cdot N(t) = \frac{(\overline{a}_3(\overline{a}_5 + 4b_{31}) - \overline{a}_5(\overline{a}_4 + 4b_{21})t + O(t^2))}{|\overline{a}_3|\sqrt{(\overline{a}_4 + 4b_{21})^2 + (\overline{a}_5 + 4b_{31})^2}} \ , \\ \cos\psi_{j+2} &= N_{j+2}(t) \cdot N(t) = \frac{(-\overline{a}_3(\overline{a}_5 + 4b_{31}) - \overline{a}_5(\overline{a}_4 + 4b_{21})t + O(t^2))}{|\overline{a}_3|\sqrt{(\overline{a}_4 + 4b_{21})^2 + (\overline{a}_5 + 4b_{31})^2}} \ . \end{aligned}$$

Since $\sin\psi_{j+2} = -\sin\psi_{j+1}$ at the A_1A_3 point, we get the following.

$$\begin{aligned}
\sin\psi_{j+1} &= \eta\frac{(|\overline{a}_4+4b_{21}|+O(t))}{\sqrt{(\overline{a}_4+4b_{21})^2+(\overline{a}_5+4b_{31})^2}}\ , \\
\sin\psi_{j+2} &= -\eta\frac{(|\overline{a}_4+4b_{21}|+O(t))}{\sqrt{(\overline{a}_4+4b_{21})^2+(\overline{a}_5+4b_{31})^2}}\ ,
\end{aligned}$$

where $\eta = \pm 1$. Since $\sin\psi_{j+2} = -\sin\psi_{j+1}$ at $t=0$, then by the power series for $\sin\psi_{j+1}$, $\sin\psi_{j+2}$ above and the fact that $\psi_{j+2} \neq \psi_{j+1}$, this means that $(a_4+4b_{21}) \neq 0$. Using these formulae, we can obtain ψ'_{j+1}, ψ'_{j+2} at t:

$$\begin{aligned}
\psi'_{j+1} &= -\frac{d(\cos\psi_{j+1})}{dt}\frac{1}{\sin\psi_{j+1}\frac{ds}{dt}} \\
&= \frac{1}{t}\left(\frac{\overline{a}_5(\overline{a}_4+4b_{21})+O(t)}{\eta|\overline{a}_3|(|\overline{a}_4+4b_{21}|+O(t))(4-4(\overline{a}_2+4b_{11})t^2+O(t^4))}\right), \\
\psi'_{j+2} &= -\frac{d(\cos\psi_{j+2})}{dt}\frac{1}{\sin\psi_{j+2}\frac{ds}{dt}} \\
&= -\frac{1}{t}\left(\frac{\overline{a}_5(\overline{a}_4+4b_{21})+O(t)}{\eta|\overline{a}_3|(|\overline{a}_4+4b_{21}|+O(t))(4-4(\overline{a}_2+4b_{11})t^2+O(t^4))}\right).
\end{aligned}$$

Therefore we have the following.

Lemma 3.9.1.1 *The derivatives ψ'_{j+1}, ψ'_{j+2} tend to infinity like $1/t$ as t tends to zero. Then*

$$\lim_{\sin\theta_j\to 0}(\psi'_{j+1}\sin\theta_j) = -\lim_{\sin\theta_j\to 0}(\psi'_{j+2}\sin\theta_j) = \frac{\eta\overline{a}_5|\overline{a}_5|}{2\overline{a}_3^2}\mathrm{sign}(\overline{a}_4+4b_{21})\ ,$$

which is finite.

Now to calculate expressions for κ^W_{j+1}, κ^W_{j+2} at t. Lemma 3.4.4.1 gives an expression for the normal curvature in a given direction, but its disadvantage is that it is in terms of the principal directions on the given surface. Another expression for the normal curvature k_n in the direction $\lambda X_u + \mu X_v$ for a surface S parametrized by $X(u,v)$ is

$$\frac{e\lambda^2+2f\lambda\mu+g\mu^2}{E\lambda^2+2F\lambda\mu+G\mu^2}\ ,$$

where E, F, G, e, f, g are the coefficients of the first and second fundamental forms on S. Now consider $\overline{S}$. A tangent to the double curve C is

$$\left(H_u \frac{du}{dt} + H_v \frac{dv}{dt} \right) \text{ at } u = -2t^2, v = \pm t \ .$$

Then a tangent vector perpendicular to this is

$$\begin{aligned} & (H_u \times H_v) \times \left(H_u \frac{du}{dt} + H_v \frac{dv}{dt} \right) \\ = \ & \left(-\frac{du}{dt}\overline{F} - \frac{dv}{dt}\overline{G} \right) H_u + \left(\frac{du}{dt}\overline{E} + \frac{dv}{dt}\overline{F} \right) H_v \ , \end{aligned}$$

evaluated at $u = -2t^2$, $v = \pm t$, where $\overline{E}$, $\overline{F}$, $\overline{G}$ are the coefficients of the first fundamental form on $\overline{S}$ with respect to the parametrization $H(u, v)$. Therefore

$$\begin{aligned} \kappa^W_{j+1} &= \frac{\overline{e}_{j+1}\lambda^2_{j+1} + 2\overline{f}_{j+1}\lambda_{j+1}\mu_{j+1} + \overline{g}_{j+1}\mu^2_{j+1}}{\overline{E}_{j+1}\lambda^2_{j+1} + 2\overline{F}_{j+1}\lambda_{j+1}\mu_{j+1} + \overline{G}_{j+1}\mu^2_{j+1}} \ , \text{ where} \\ & \lambda_{j+1} = 4t\overline{F}_{j+1} - \overline{G}_{j+1} \ , \ \mu_{j+1} = -4t\overline{E}_{j+1} + \overline{F}_{j+1} \ , \\ & \overline{e}_{j+1} = H_{uu} \cdot N_{j+1} \ , \ \overline{f}_{j+1} = H_{uv} \cdot N_{j+1} \ , \ \overline{g}_{j+1} = H_{vv} \cdot N_{j+1} \ , \\ & \overline{E}_{j+1} = H_u \cdot H_u \ , \ \overline{F}_{j+1} = H_u \cdot H_v \ , \ \overline{G}_{j+1} = H_v \cdot H_v \ , \\ & \text{all evaluated at } u = -2t^2 \ , \ v = t \ , \\ \text{and } \kappa^W_{j+2} &= \frac{\overline{e}_{j+2}\lambda^2_{j+2} + 2\overline{f}_{j+2}\lambda_{j+2}\mu_{j+2} + \overline{g}_{j+2}\mu^2_{j+2}}{\overline{E}_{j+2}\lambda^2_{j+2} + 2\overline{F}_{j+2}\lambda_{j+2}\mu_{j+2} + \overline{G}_{j+2}\mu^2_{j+2}} \ , \text{where} \\ & \lambda_3 = 4t\overline{F}_3 + \overline{G}_3 \ , \ \mu_3 = -4t\overline{E}_3 - \overline{F}_3 \ , \\ & \overline{e}_{j+2} = H_{uu} \cdot N_{j+2} \ , \ \overline{f}_{j+2} = H_{uv} \cdot N_{j+2} \ , \ \overline{g}_{j+2} = H_{vv} \cdot N_{j+2} \ , \\ & \overline{E}_{j+2} = H_u \cdot H_u \ , \ \overline{F}_{j+2} = H_u \cdot H_v \ , \ \overline{G}_{j+2} = H_v \cdot H_v \ , \\ & \text{all evaluated at } u = -2t^2 \ , \ v = -t \ . \end{aligned}$$

Using these formulae, we get

$$\begin{aligned} \kappa^W_{j+1} &= \frac{1}{t^2} \left(\frac{128\overline{a}_3\overline{a}_5 + 128\overline{a}_5(4\overline{a}_1\overline{a}_3 - \overline{a}_4)t + O(t^2)}{|\overline{a}_3|(1024\overline{a}_3^2 + O(t))} \right) , \\ \kappa^W_{j+2} &= \frac{1}{t^2} \left(\frac{-128\overline{a}_3\overline{a}_5 + 128\overline{a}_5(4\overline{a}_1\overline{a}_3 - \overline{a}_4)t + O(t^2)}{|\overline{a}_3|(1024\overline{a}_3^2 + O(t))} \right) . \end{aligned}$$

Hence we have the following.

Lemma 3.9.1.2 *The normal curvatures κ^W_{j+1}, κ^W_{j+2} tend to infinity like $1/t^2$ as t tends to zero. Then*

$$\lim_{\sin\theta_j\to 0}(\kappa^W_{j+1}\sin^2\theta_j) \;=\; -\lim_{\sin\theta_j\to 0}(\kappa^W_{j+2}\sin^2\theta_j) = \frac{\overline{a}^3_5}{2\overline{a}^3_3|\overline{a}_3|}\ ,$$

which is finite.

3.9.2 The A^3_1 Consistency Conditions at an A_1A_3 point

Using Lemmas 3.9.1.1 and 3.9.1.2 we can obtain the forms of (3.72), (3.74) when $\sin\theta_j = 0$. Since γ_j is not part of the swallowtail surface it is a smooth sheet, and so a_j, a^t_j, a^*_j, κ^r_j, κ^t_j, and τ^t_j are all finite as $\sin\theta_j \to 0$. Then, when we let $\sin\theta_j \to 0$ in (3.67) for $i = j$ from Lemma 3.4.4.4 and use Lemma 3.9.1.1, we get that ϕ' is finite at the A_1A_3 point. Similarly, letting $\sin\theta_j \to 0$ in (3.60) and (3.73) for $i = j$ gives that both $\dot{\phi}_j\sin\theta_j$ and ψ'_j tend to finite numbers. From Remark 3.4.5.5 we can use either (3.72) or (3.74), since $\cos\phi = \cos\theta_i = 0$ is impossible for any i where $\nabla r_i \neq \mathbf{0}$.

Firstly we shall consider the limiting form of (3.72) from Theorem 3.4.5.3. For this, we assume $\cos\phi \neq 0$. For $i = j+1$, multiplying (3.72) by $\sin^2\theta_j$ and then setting $\sin\theta_j = 0$ we get

$$\begin{aligned}\frac{\kappa^W_{j+1}\sin^2\theta_j\sin\phi}{\sin\theta_{j+1}} \;=\; & -\frac{2\theta'_j\sin\theta_j(-1)}{\cos\phi} + \frac{a^*_{j+2}\sin^2\theta_j\cos^4\phi_{j+2}}{\cos^2\phi\sin^2\theta_{j+2}} - \frac{a^*_j}{\cos^2\phi}\\ & + \frac{\phi'}{\cos^2\phi\sin\phi} + \frac{\kappa}{\sin\phi}\left(-\frac{\sin\psi_j(-1)}{\cos^2\phi}\right),\end{aligned}$$

which implies $a^*_{j+2}\sin^2\theta_j$ is finite at the A_1A_3 point, since all of the other terms are finite. Then for $i = j+2$, multiplying (3.72) by $\sin^2\theta_j$ and then setting $\sin\theta_j = 0$ we get

$$\begin{aligned}\frac{\kappa^W_{j+2}\sin^2\theta_j\sin\phi}{\sin\theta_{j+2}} \;=\; & \frac{2\theta'_j\sin\theta_j(-1)}{\cos\phi} - \frac{a^*_{j+1}\sin^2\theta_j\cos^4\phi_{j+1}}{\cos^2\phi\sin^2\theta_{j+1}} + \frac{a^*_j}{\cos^2\phi}\\ & - \frac{\phi'}{\cos^2\phi\sin\phi} + \frac{\kappa}{\sin\phi}\left(\frac{\sin\psi_j(-1)}{\cos^2\phi}\right),\end{aligned}$$

which implies $a^*_{j+1}\sin^2\theta_j$ is finite at the A_1A_3 point, again since all of the other terms are finite. Note that $a^*_{j+1}\sin^2\theta_j = a^*_{j+2}\sin^2\theta_j$ when $\sin\theta_j = 0$, since

$\kappa^W_{j+1}\sin^2\theta_j = -\kappa^W_{j+2}\sin^2\theta_j$ at $\sin\theta_j = 0$. Finally, for $i = j$, multiplying (3.72) by $\sin\theta_j$ and then setting $\sin\theta_j = 0$ gives

$$\begin{aligned}\kappa^W_j \sin\phi &= \frac{2\cos\theta_{j+1}}{\cos\phi\sin\theta_{j+1}}(\theta'_{j+1}\sin\theta_j + \theta'_{j+2}\sin\theta_j) + 2(\tau+\psi'_j)\cos\phi(-1)\\ &\quad + \frac{\cos^4\phi_{j+1}}{\cos^2\phi\sin^2\theta_{j+1}}(a^*_{j+1} - a^*_{j+2})\sin\theta_j + \frac{\kappa}{\sin\phi}(-\cos\psi_j\cos^2\phi)\ .\end{aligned}$$

Hence $(a^*_{j+1} - a^*_{j+2})\sin\theta_j$ is finite when $\sin\theta_j = 0$. Hence we get the following.

Proposition 3.9.2.1 *As an A^3_1 point tends towards an A_1A_3 point along an A^3_1 curve, the medial sheets must satisfy the following:*

$$\begin{aligned}\lim_{\sin\theta_j\to 0}\left(a^*_{j+1}\sin^2\theta_j\right) &= \lim_{\sin\theta_j\to 0}\left(a^*_{j+2}\sin^2\theta_j\right)\ ,\\ \lim_{\sin\theta_j\to 0}\left((a^*_{j+1} - a^*_{j+2})\sin\theta_j\right) &\ \textit{exists}\ ,\\ \lim_{\sin\theta_j\to 0}\left(\frac{(\kappa^W_{j+1}\sin^2\theta_j)\cos\phi\sin\phi}{\sin\theta_{j+1}}\right) &= -\lim_{\sin\theta_j\to 0}\left(\frac{(\kappa^W_{j+2}\sin^2\theta_j)\cos\phi\sin\phi}{\sin\theta_{j+1}}\right)\\ = \lim_{\sin\theta_j\to 0}\left(\frac{a^*_{j+1}\sin^2\theta_j\cos^4\phi_{j+1}}{\cos\phi\sin^2\theta_{j+1}} - 4\psi'_{j+1}\sin\theta_j + \frac{\phi' + \kappa\sin\psi_j - a^*_j\sin\phi}{\cos\phi\sin\phi}\right),&\end{aligned}$$

$$\begin{aligned}\lim_{\sin\theta_j\to 0}\left(\kappa^W_j\sin\phi\right) = \lim_{\sin\theta_j\to 0}\Bigg(&\frac{(a^*_{j+1} - a^*_{j+2})\sin\theta_j\cos^4\phi_{j+1}}{\cos^2\phi\sin^2\theta_{j+1}} - 2\left(\tau+\psi'_j\right)\cos\phi\\ &+ \frac{4\psi'_{j+1}\sin\theta_j\cos\theta_{j+1}}{\cos\phi\sin\theta_{j+1}} - \frac{\kappa\cos\psi_j\cos^2\phi}{\sin\phi}\Bigg).\end{aligned}$$

Here $\cos\phi \neq 0$ and the notation used is contained in Table 3.1.

Now we shall consider the limiting form of (3.74) from Theorem 3.4.5.4. For this, we assume $\cos\theta_i \neq 0$ for any i. When $\cos\theta_i = 0$ then Proposition 3.9.2.1 holds, since $\cos\phi \neq 0$ when $\cos\theta_i = 0$. A similar argument to that which resulted in Proposition 3.9.2.1 gives the following.

Proposition 3.9.2.2 *As an A^3_1 point tends towards an A_1A_3 point along an A^3_1 curve, the medial sheets must satisfy the following:*

$$\lim_{\sin\theta_j\to 0}\left(\dot\phi_{j+1}\sin^2\theta_j\right)=\lim_{\sin\theta_j\to 0}\left(\dot\phi_{j+2}\sin^2\theta_j\right),$$

$$\lim_{\sin\theta_j\to 0}\left((\dot\phi_{j+1}-\dot\phi_{j+2})\sin\theta_j\right)\ \textit{exists}\ ,$$

$$\lim_{\sin\theta_j\to 0}\left(\frac{\left(\kappa^W_{j+1}\sin^2\theta_j\right)\sin\phi}{\sin\theta_{j+1}}\right)=-\lim_{\sin\theta_j\to 0}\left(\frac{\left(\kappa^W_{j+2}\sin^2\theta_j\right)\sin\phi}{\sin\theta_{j+1}}\right)$$

$$=\lim_{\sin\theta_j\to 0}\left(-\frac{\dot\phi_{j+1}\sin^2\theta_j\cos\phi_{j+1}}{\cos\theta_{j+1}\sin\theta_{j+1}}-2\psi'_{j+1}\sin\theta_j\cos\phi-\dot\phi_j\sin\theta_j\right),$$

$$\lim_{\sin\theta_j\to 0}\left(\kappa^W_j\sin\phi\right)=\lim_{\sin\theta_j\to 0}\left(\frac{(\dot\phi_{j+2}-\dot\phi_{j+1})\sin\theta_j\cos\phi_{j+1}}{\cos\theta_{j+1}\sin\theta_{j+1}}-2\left(\tau+\psi'_j\right)\cos\phi\right.$$

$$\left.+\frac{2\psi'_{j+1}\sin\theta_j\cos\phi\cos(2\theta_{j+1})}{\cos\theta_{j+1}\sin\theta_{j+1}}-\frac{\kappa\cos\psi_j\cos^2\phi}{\sin\phi}\right).$$

Here $\cos\theta_i\neq 0$ *for any* i *and the notation used is contained in Table 3.1.*

3.9.3 Second Example of A_1^3 Case (Continued)

As stated in the first part (in §3.6) of this example we can calculate explicitly the terms which appear in Theorems 3.4.5.2, 3.4.5.3, and 3.4.5.4. Similarly we can illustrate Propositions 3.9.2.1, 3.9.2.2 by taking the limit as $\sin\theta_j\to 0$. Two of the points of contact on the parabolic gutter (given by $z=by^2$) were (x,y,by^2) and $(x,-y,by^2)$. These coincide when $y=0$. Hence the A_1^3 point $C(y)$ from (3.97) is an A_1A_3 point when $y=0$. Then we can say that γ_1 is the sheet which is not part of the swallowtail surface, since $\sin\theta_1=0$, $\sin\theta_2\neq 0$ and $\sin\theta_3\neq 0$ at $y=0$. Hence $j=1$ in this example. From §3.6 we had

$$a_1^*=0\ ,\ a_2^*=a_3^*=-\frac{1}{2by^2\sqrt{1+4b^2y^2}}\ ,$$

so a_2^* and a_3^* tend to infinity like $1/y^2$ as $y\to 0$. Then, since

$$\sin\theta_1=\frac{2\sqrt{2}by\sqrt{1+2b^2y^2}}{1+4b^2y^2}\ ,$$

we get $a_2^*\sin^2\theta_1\to a_3^*\sin^2\theta_1$ and $(a_2^*-a_3^*)\sin\theta_1\to$ a finite number as $y\to 0$, as in Proposition 3.9.2.1. The latter happens since $a_2^*=a_3^*$ for all (x,y). Also

from §3.6 we had

$$\dot{\phi}_1 \cos\phi_1 = -\frac{1}{\sqrt{2}y\sqrt{1+2b^2y^2}(1+4b^2y^2)^{3/2}} \ , \ \dot{\phi}_2 = \dot{\phi}_3 = 0 \ ,$$

so $\dot{\phi}_3 \sin^2\theta_1 \to \dot{\phi}_3 \sin^2\theta_1$ and $(\dot{\phi}_2 - \dot{\phi}_3)\sin\theta_1 \to$ a finite number as $y \to 0$, as in Proposition 3.9.2.2. Finally, from §3.6 we had

$$\kappa_2^W = -\kappa_3^W = \frac{1}{2\sqrt{2}by^2\sqrt{1+4b^2y^2}(1+2b^2y^2)} \ ,$$

so κ_2^W and κ_3^W tend to infinity like $1/y^2$ as $y \to 0$. It can be shown that the results of Proposition 3.9.2.1 are satisfied as $y \to 0$.

Chapter 4

Transitions on the Euclidean Symmetry Set and Medial Axis in Three Dimensions

4.1 Introduction

The complete list of possible transitions on the full bifurcation set of a generic family of functions of one variable was obtained in [BG86]. Also, the method of realizing the transitions on a family of distance-squared functions in two dimensions was described. This involved obtaining conditions on the family such that the considered singularity was versally unfolded and that the sections of the bifurcation set of the family were generic. Even though functions of one variable were considered in [BG86], the methods used were general and so can be employed in the case of functions of two variables, except when considering the so-called *bad planes*. In this case some additional work needs to be done – see the important Remark 4.2.1.1. Hence, the aim of this chapter is to carry out a similar study of one-parameter families of symmetry sets and of medial axes in three dimensions, using the same methods, for certain generic transitions. Connected to the evolution of the symmetry set in a generic family of surfaces is work by Bogaevsky [Bog90, Bog02a], which provides a complete

list of transitions (perestroikas) of generic 'minimum functions'.

The singularities that we expect to occur on a one-parameter family of medial axes in three dimensions are A_1^4, A_1^5, A_5, A_1A_3 (two types) and $A_1^2A_3$ (two types) (see [GK02, p.724]). We study these singularities in this chapter (except for A_1^5) and one of the singularities which are expected to happen only on the symmetry set, and not on the medial axis, namely A_1A_4. For each considered transition we want to obtain a family of surfaces in three dimensions for which the distance-squared function has a certain singularity at a value of the parameter of the family of surfaces. Then we require the singularity to be versally unfolded and we will obtain conditions for the sections of the 'big bifurcation set' (to be explained below) of the distance-squared function to be generic. Such conditions below will be interpreted geometrically and involve naturally occurring objects – most intriguingly the osculating plane of a line of curvature on a surface in $\mathbb{R}^3$.

The local structure of the medial axis as it undergoes such transitions is described in [GKP05], where some of the conditions obtained in this chapter are verified. However, [GKP05] does not concentrate on the conditions for realizing the transitions and so a paper which does focus on this would be desirable (see §4.7).

Definition 4.1.1 *A function h where*

$$\begin{aligned} h : \mathbb{R}^2, (0,0) &\to \mathbb{R} \\ (x_1, x_2) &\mapsto h(x_1, x_2) \end{aligned}$$

is said to have type A_k at $(0,0)$ when h is right-equivalent (take a diffeomorphism of $\mathbb{R}^2$ and add a constant) to $\pm x_2^2 \pm x_1^{k+1}$.

Bogaevsky [Bog02b] produced the following list of possible one-dimensional strata which can pass through the singularities of symmetry sets in $\mathbb{R}^3$. The stratum $D_4^{\pm}$ does not occur for the singularities considered in this chapter.

Possible 1-D strata passing through the considered singularities	
One-level strata	Two-level strata
A_1^4	A_1^2/A_1^3
$A_1^2A_2$	A_1^3/A_2
A_2^2	A_1^2/A_1A_2
A_1A_3	A_2/A_1A_2
A_4	A_1^2/A_3
$D_4^{\pm}$	A_2/A_3

As mentioned above we will require unfoldings to be versal, so here is a brief summary of what this means, using the appendix from [BGG85]. Consider an *n-parameter unfolding* $g : (\mathbb{R}^m \times \mathbb{R}^n, (q, u_0)) \to \mathbb{R}$ of a multi-germ $g_0 : (\mathbb{R}^m, q) \to \mathbb{R}$, where $g(q_i, u_0) = g_0(q_i)$ for all i and $q = (q_1, \ldots, q_n)$. Let k be 'sufficient', that is not less than the maximal degree of determinacy of the singularities $g_{0,i} : (\mathbb{R}^m, q_i) \to \mathbb{R}$. Then, from [BGG85], g is *versal* if

$$\begin{aligned} &\text{the } k\text{-multi-jets of } \frac{\partial g}{\partial u_1}(-, u_0) \ , \ldots , \frac{\partial g}{\partial u_n}(-, u_0) \text{ at } q \ , \text{ and } (1, \ldots, 1) \\ &\text{span } \ \frac{\mathcal{E}(m)}{J_{g_{0,1}}} \oplus \cdots \oplus \frac{\mathcal{E}(m)}{J_{g_{0,n}}} \ , \end{aligned}$$

where $\mathcal{E}(m)$ is the algebra of germs at 0 of smooth functions on $\mathbb{R}^m$ and $J_{g_{0,i}}$ is the Jacobian ideal of $g_{0,i}$. The vector $(1, \ldots, 1)$ corresponds to the fact that we are allowed to add the same constant to each $g_{0,i}$.

4.2 The A_5 Transition

In this section we aim to find a family of surfaces in three dimensions which exhibits an A_5 transition and to give an example with pictures of such a family. As in [BG86] we firstly consider the standard versal unfolding of an A_5 singularity:

$$\left.\begin{aligned} G : \mathbb{R}^2 \times \mathbb{R}^4 \to \mathbb{R} \ , \\ (X, Y, u_1, u_2, u_3, u_4) \mapsto Y^2 + X^6 + u_1X^4 + u_2X^3 + u_3X^2 + u_4X \ . \end{aligned}\right\} \quad (4.1)$$

Here $\mathbb{R}^2$ corresponds to (X, Y) and $\mathbb{R}^4$ corresponds to the *unfolding parameters* (u_1, u_2, u_3, u_4). Now we require the *big bifurcation set* of G, which is

$$\begin{aligned}\mathrm{Bif}_G = \{(u_1, u_2, u_3, u_4) \ : \ & G \text{ has a degenerate singularity for some } (X, Y) \\ & \text{or } G \text{ has two singularities at the same level } \} \ .\end{aligned}$$

The sets of Bif_G for which G has two singularities at the same level are called A_1^2 sets, and the ones for which G has a degenerate singularity are called A_2 sets. This big bifurcation set is a three-dimensional object in $\mathbb{R}^4_{\mathbf{u}}$ (that is (u_1, u_2, u_3, u_4)-space) and the A_5 point is at the origin. Taking sections of the big bifurcation set with non-singular surfaces near to $(0, 0, 0, 0)$ gives one of the possible full bifurcation sets near to the A_5 singularity. Then taking a family of such non-singular surfaces gives a family of full bifurcation sets which pass through the A_5 point. There is only one A_1^2 set in Bif_G:

$$\left.\begin{aligned}\{(u_1, u_2, u_3, u_4) : u_2 &= -2(X_1 + X_2)(2X_1^2 + X_1X_2 + 2X_2^2 + u_1) \ , \\ u_3 &= u_1(X_1^2 + 4X_1X_2 + X_2^2) \\ &\quad +3(X_1^2 + 3X_1X_2 + X_2^2)(X_1^2 + X_1X_2 + X_2^2) \ , \\ u_4 &= -2X_1X_2(X_1 + X_2)(u_1 + 3(X_1^2 + X_1X_2 + X_2^2)) \ , \\ &\quad \text{for } X_1 \neq X_2,\ X_1 \neq 0,\ X_2 \neq 0\} \ .\end{aligned}\right\} \quad (4.2)$$

The A_2 set of Bif_G is given by

$$\left.\begin{aligned}\{(u_1, u_2, u_3, u_4) : u_3 &= -3X(5X^3 + 2u_1X + u_2) \ , \\ u_4 &= X^2(24X^3 + 8u_1X + 3u_2) \ , \ \text{for } X \neq 0\} \ .\end{aligned}\right\} \quad (4.3)$$

4.2.1 Bad 3-spaces

Following [BG86], a three-dimensional subspace through the origin in $\mathbb{R}^4_{\mathbf{u}}$ given by

$$\lambda_1u_1 + \lambda_2u_2 + \lambda_3u_3 + \lambda_4u_4 = 0 \quad (4.4)$$

is called a *bad 3-space* if it contains the limit of tangent spaces to a stratum of Bif_G at points tending to the origin. An as yet unresolved problem connected to this is described in the remark below.

Remark 4.2.1.1 In this chapter we have assumed that all limits of tangent spaces to strata of dimension greater than one contain a limit of tangent spaces to a one-dimensional stratum. This was the case in [BG86] and in correspondence with Bogaevsky [Bog02b] he has confirmed that this is true in all the cases he has checked, but there is as yet no general proof. Clearly this is an interesting topic for further investigation; for the purposes of the present chapter we note that our list of cases agrees with that of Bogaevsky, but in principle there might be additional normal forms for generic functions on these bifurcation sets.

Calculations show that of the possible one-dimensional strata only the following occur for an A_5 transition:

$$\begin{aligned}
A_2^2 :\ \{(u_1,u_2,u_3,u_4) &= (-3X^2, 0, 3X^4, 0)\}\ ,\\
A_1A_3 :\ \{(u_1,u_2,u_3,u_4) &= (-6X^2, 4X^3, 9X^4, -12X^5)\}\ ,\\
A_4 :\ \{(u_1,u_2,u_3,u_4) &= (-15X^2, 40X^3, -45X^4, 24X^5)\}\ ,\\
A_1^2/A_1^3 :\ \{(u_1,u_2,u_3,u_4) &= (-6X^2, 0, 9X^4, 0)\}\ ,\\
A_1^2/A_1A_2 :\ \{(u_1,u_2,u_3,u_4) &= \left(-\left(3+2^{1/3}+2^{2/3}\right)X^2, \left(-\frac{(2+2^{1/3})}{3}\right)X^3,\right.\\
&\quad \left(\frac{23(2^{2/3})+44+28(2^{1/3})}{12}\right)X^4,\\
&\quad \left.\left(\frac{4+2(2^{1/3})+2^{2/3}}{6}\right)X^5\right)\Big\}\ ,\\
A_1^2/A_3 :\ \{(u_1,u_2,u_3,u_4) &= (-X^2, 0, 0, 0)\}\ ,\\
A_2/A_3 :\ \{(u_1,u_2,u_3,u_4) &= (-135X^2, -40X^3, 120X^4, 96X^5)\}\ ,
\end{aligned}$$

where $X \neq 0$. It is easy to see that this limit of tangent vectors is $(1,0,0,0)$. Hence, when considering the limits of tangent spaces to the one-dimensional strata, the bad 3-spaces in $\mathbb{R}^4_{\mathbf{u}}$ are (4.4) for which $\lambda_1 = 0$. There might be other bad 3-spaces (see Remark 4.2.1.1).

In $\mathbb{R}P^3$ the 3-space $\lambda_1u_1 + \lambda_2u_2 + \lambda_3u_3 + \lambda_4u_4 = 0$ is represented by a point $(\lambda_1 : \lambda_2 : \lambda_3 : \lambda_4)$. If Δ is the set of bad 3-spaces, we are interested the number of regions in $\mathbb{R}P^3 - \Delta$, and also the amount of types of transition given

by taking 3-spaces which have representations from within these regions. By doing this we aim to identify the various types of transition and obtain criteria for realizing them. For the A_5 transition $\mathbb{R}P^3 - \Delta$ is in

$$\{(\lambda_1 : \lambda_2 : \lambda_3 : \lambda_4) : \lambda_1 u_1 + \lambda_2 u_2 + \lambda_3 u_3 + \lambda_4 u_4 = 0, \lambda_1 \neq 0\} \ . \tag{4.5}$$

If there are no other bad 3-spaces then $\mathbb{R}P^3 - \Delta$ has one region and hence there is only one type of A_5 transition.

4.2.2 Representations of the A_5 Transition

To obtain pictures of the symmetry set as it goes through an A_5 transition, we choose a particular 3-space which is not a bad space. From (4.5) the choice of

$$\{(u_1, u_2, u_3, u_4) : u_1 = k \text{ const.}\}$$

is not a bad 3-space, provided there are no bad 3-spaces given by considering limits of tangent spaces to two- and three-dimensional strata. In this case taking the sections of this with the A_1^2 sets of Bif_G for various k gives the A_5 transition on the family of symmetry sets. In Figures 4.1, 4.2 are pictures of these sections, in (u_2, u_3, u_4)-space.

Bogaevsky [Bog02b] suggested the following alternative to Figures 4.1, 4.2. Let $\pi(u_1, u_2, u_3, u_4) = (\xi, \eta)$ be a projection such that its fibre lies on an isochrone $\tau(u_1, u_2, u_3, u_4) = u_1 = k$. That is, $\tau(\cdot) = \sigma(\pi(\cdot))$ where $\sigma(\xi, \eta)$ is a smooth function. Consider in the plane with coordinates (ξ, η) the projection of all one-dimensional strata of the A_1^2 and A_2 sets of Bif_G, given by (4.2), (4.3). For some point (ξ_0, η_0) of the complement to this projection we can draw the curve $\pi^{-1}(\xi_0, \eta_0) \cap \mathrm{Bif}_G$. This 'clock face' with the curve $\sigma(\xi_0, \eta_0) = 0$ helps to imagine the transition. It can be shown that the choice of

$$\pi(u_1, u_2, u_3, u_4) = \left(u_2 + \frac{1}{10}(u_3 + u_4), u_1\right)$$

has the fact that π restricted to each of the two- and three-dimensional strata of Bif_G is a submersion at smooth points close to the origin. Also, the choice of $\sigma(\xi, \eta) = \eta$ means that $\sigma(\pi(u_1, u_2, u_3, u_4)) = u_1$.

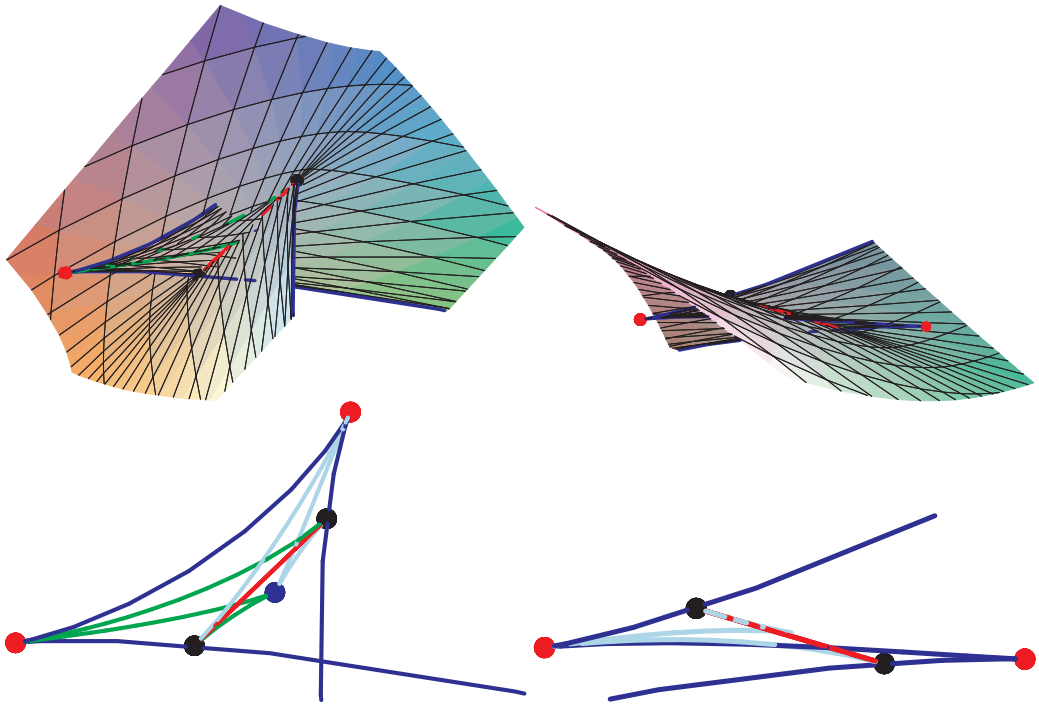

Figure 4.1: The sections of the A_1^2 sets of Bif_G, the big bifurcation set of the standard unfolding G given by (4.1), with the planes $u_1 = k$ (const.). In these pictures, $k = -0.5$. Top: Two different views of the A_1^2 sets and the special curves on them. Bottom: only the special curves and special points are shown. The blue, red curves correspond respectively to A_3, A_1^3 curves. The green, turquoise curves are A_1A_2 curves. The black, red and blue points correspond respectively to A_1A_3, A_4, A_2^2 points. Not all of the surfaces and curves in these pictures lie on the medial axis; the A_3 (blue) curve would end on the medial axis where it meets the A_1^3 (red) curve, and the A_1A_2 curves and A_4, A_2^2 points would not lie on the medial axis.

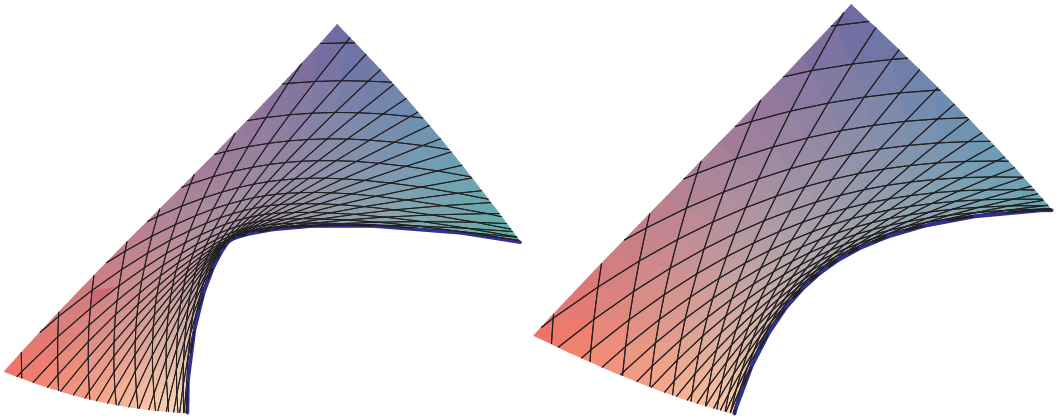

Figure 4.2: Left: $k = 0$, the moment of transition. All of the structure of the previous picture has collapsed, except for the A_3 (blue) curve, on which is an A_5 point. Right: $k = 0.5$. There is a smooth A_3 curve on the medial axis.

Figure 4.3 shows the projections under π of the one-dimensional strata of Bif_G in the plane with coordinates (ξ, η). These are labelled; for example the one-dimensional stratum corresponding to an A_4 singularity of the standard unfolding (4.1) is labelled A_4. Also drawn is the curve $\sigma = -0.5$, which intersects the projections of the one-dimensional strata in the points labelled p_i. The points on $\sigma = -0.5$ which lie between the projections of the one-dimensional strata are labelled q_i. Finally, the point m_2 corresponds to the A_5 point. Figures 4.4 to 4.12 show $\pi^{-1}(p_i) \cap \mathrm{Bif_G}$, $\pi^{-1}(q_i) \cap \mathrm{Bif_G}$ and $\pi^{-1}(m_2) \cap \mathrm{Bif_G}$. In order to obtain $\pi^{-1}(\xi_0, \eta_0) \cap \{A_1^2 \text{ set given by (4.2)}\}$ for ξ_0, η_0 constants, it is necessary to solve equal to zero a polynomial in X_1 and X_2. Hence the boxes in each of Figures 4.4 to 4.12 are the set of X_1, X_2 near to zero for which this equation is satisfied for (ξ_0, η_0) corresponding to one of the points p_i, q_i or m_2. Some of the transitions that occur in these pictures can be observed in these 'pre-sets' – see the captions to Figures 4.4 to 4.12.

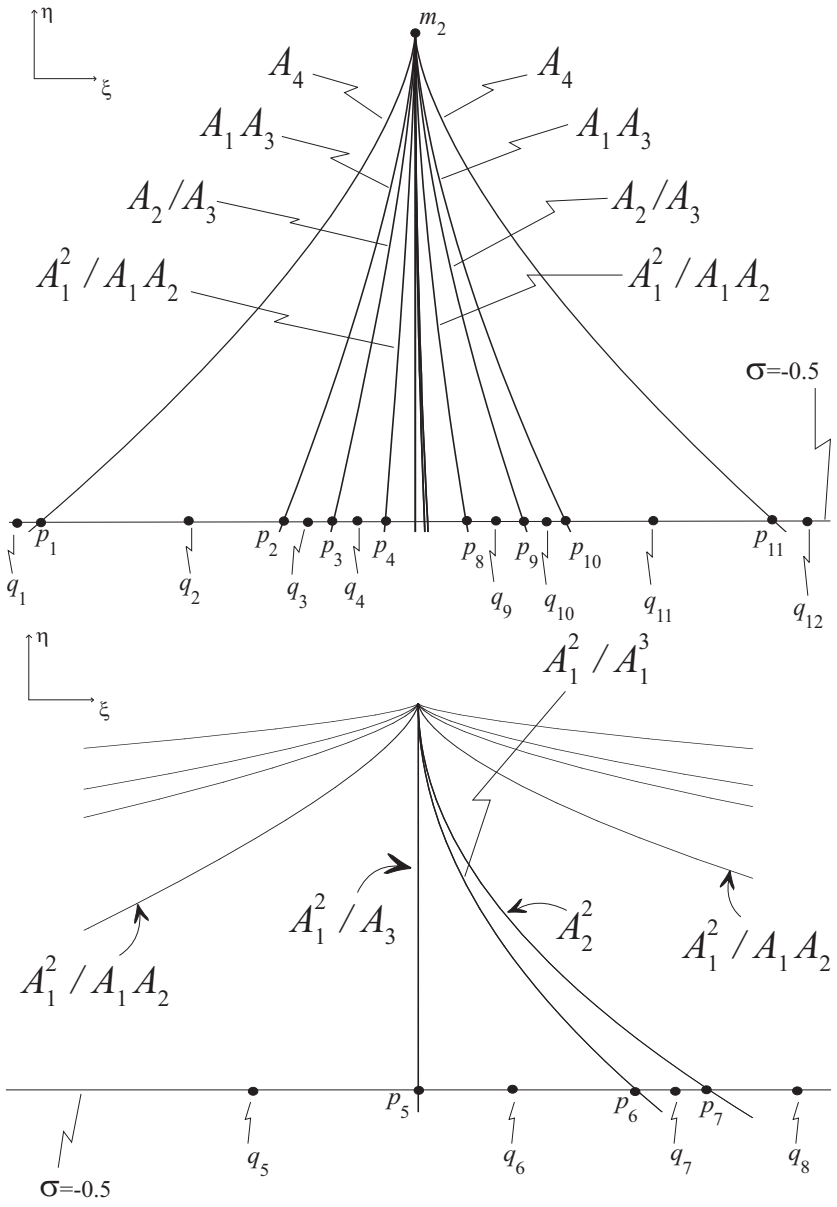

Figure 4.3: Representing the A_5 transition. The picture at the bottom is of the picture at the top, but with the ξ-axis stretched. The curves labelled A_4, etc. are the projections under π of the one-dimensional strata of Bif_G for the A_5 transition. A curve $\sigma = -0.5$ intersects these in points p_i. In Figures 4.4 to 4.12, the intersections $\pi^{-1}(p_i) \cap \mathrm{Bif_G}$, $\pi^{-1}(q_i) \cap \mathrm{Bif_G}$ and $\pi^{-1}(m_2) \cap \mathrm{Bif_G}$ are drawn.

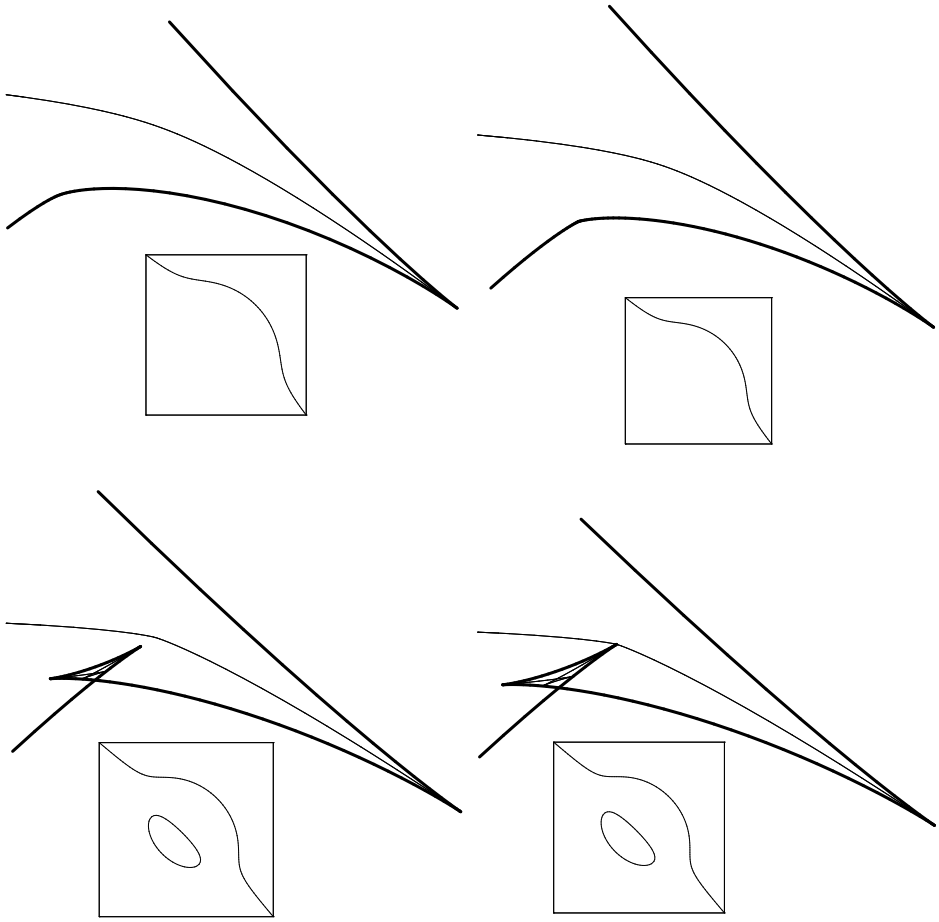

Figure 4.4: In Figures 4.4 to 4.12, the intersections $\pi^{-1}(p_i) \cap \mathrm{Bif}_{\mathrm{G}}$, $\pi^{-1}(q_i) \cap \mathrm{Bif}_{\mathrm{G}}$ and $\pi^{-1}(m_2) \cap \mathrm{Bif}_{\mathrm{G}}$ are drawn (see Figure 4.3 for an explanation of what p_i, q_i, m_2 are). The intersection with the A_2 part of Bif_G is drawn in bold, the intersection with the A_1^2 part is the thinner curve. The boxes underneath the curves are the set of X_1, X_2 such that $\pi^{-1}(\xi_0, \eta_0)$, for ξ_0, η_0 constants, intersects with the A_1^2 set given by (4.2). Some of the transitions that occur in these pictures can be observed in these 'pre-sets'. Top, from left: q_1, p_1; bottom, from left: q_2, p_2. Top right: a new piece of A_1^2 set is about to form. Bottom left: this new piece of A_1^2 set is a swallowtail with endpoints coinciding with newly created cusps on the A_2 set. This new piece is visible on the pre-set. Bottom right: a cusp of the A_2 curve meets a part of the A_1^2 set.

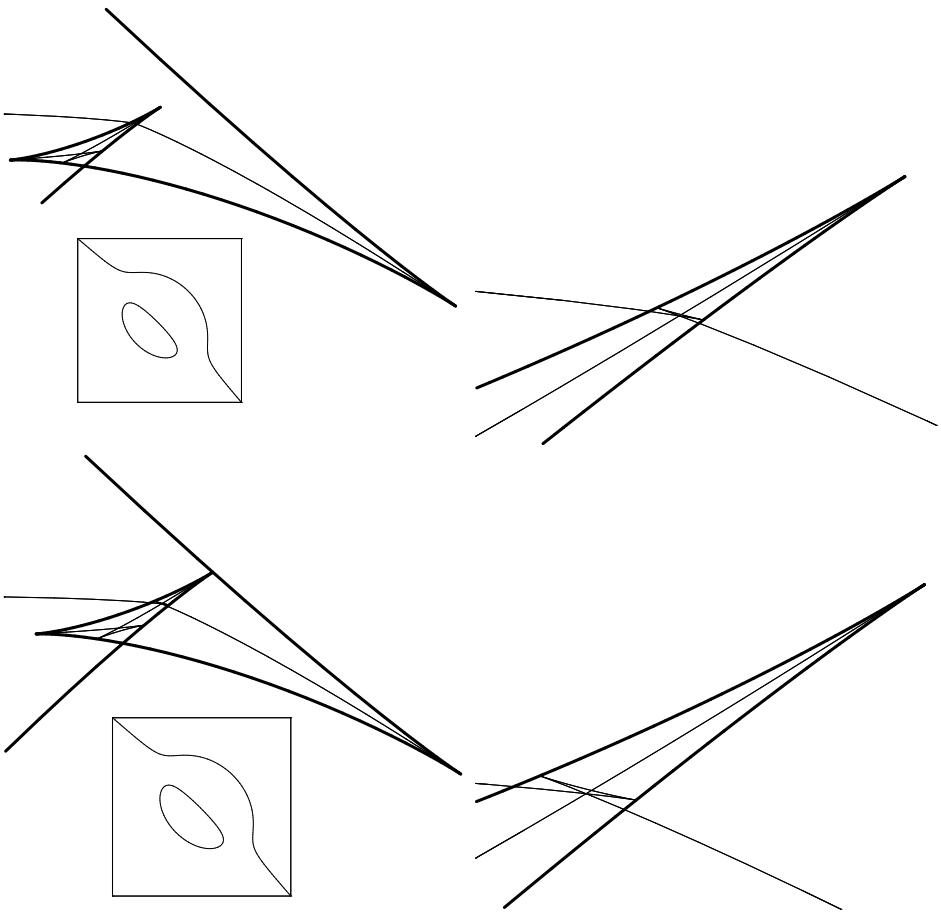

Figure 4.5: Top: q_3 (right: a closer look at the picture on the left); bottom: p_3 (right: closer look). Top: there are two newly created cusps on the A_1^2 set. Bottom: a cusp of the A_2 set now meets another part of the A_2 set.

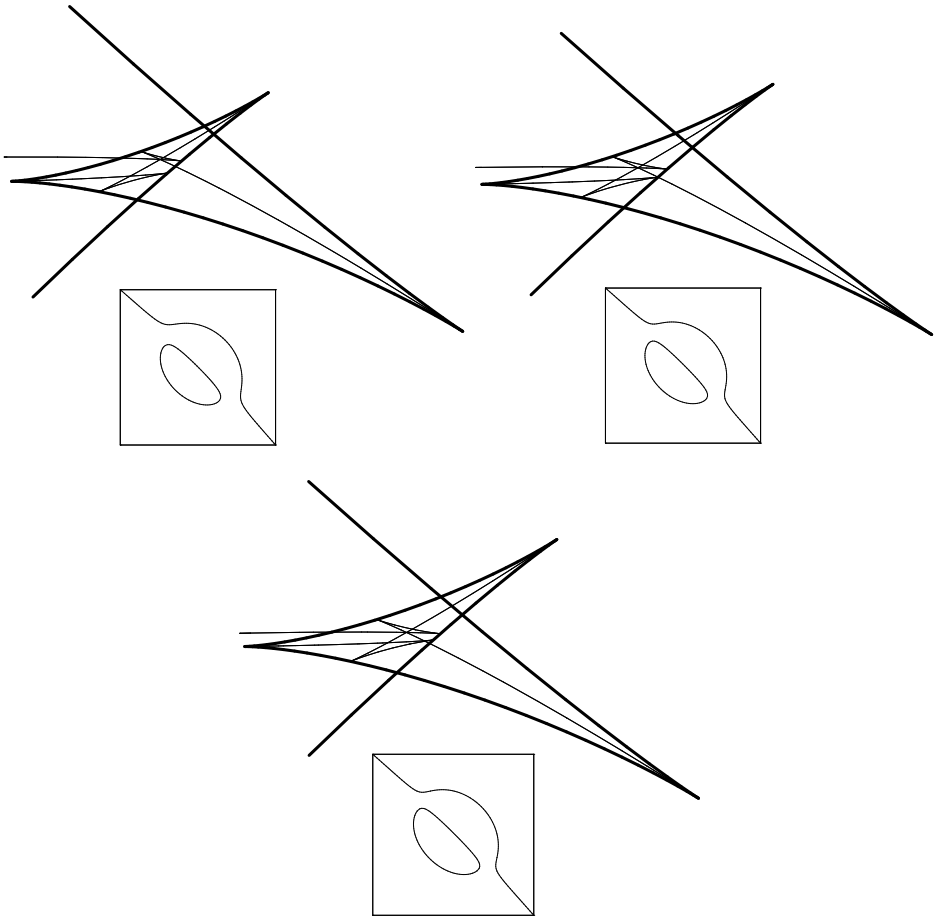

Figure 4.6: Top, from left: q_4, p_4; bottom: q_5. Top left: the A_2 piece now intersects the other A_2 piece with a cusp in two points. Top right: a cusp of the A_1^2 set now meets another part of the A_1^2 set. Bottom right: an A_1^2 piece with a cusp meets another part of the A_1^2 set in two points.

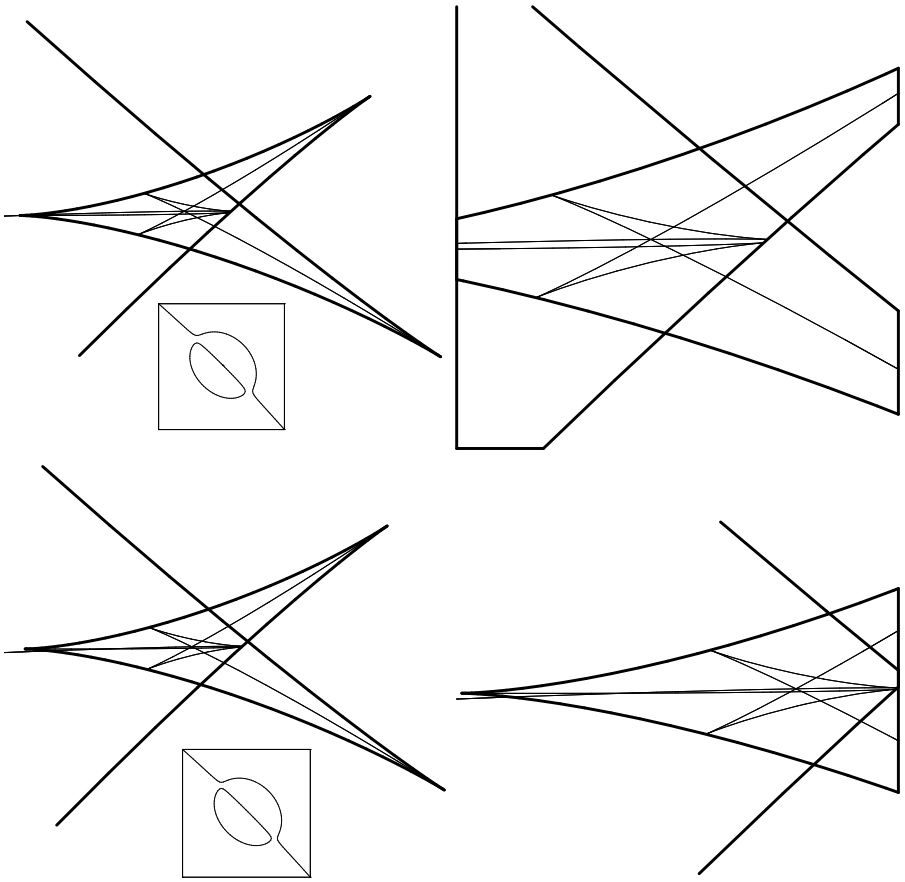

Figure 4.7: Top: p_5 (right: closer look); bottom: q_6 (right: closer look). Top: a part of the A_1^2 set passes through the leftmost cusp of the A_2 set. Bottom: the branch of the A_1^2 no longer passes through the leftmost cusp of the A_2 set.

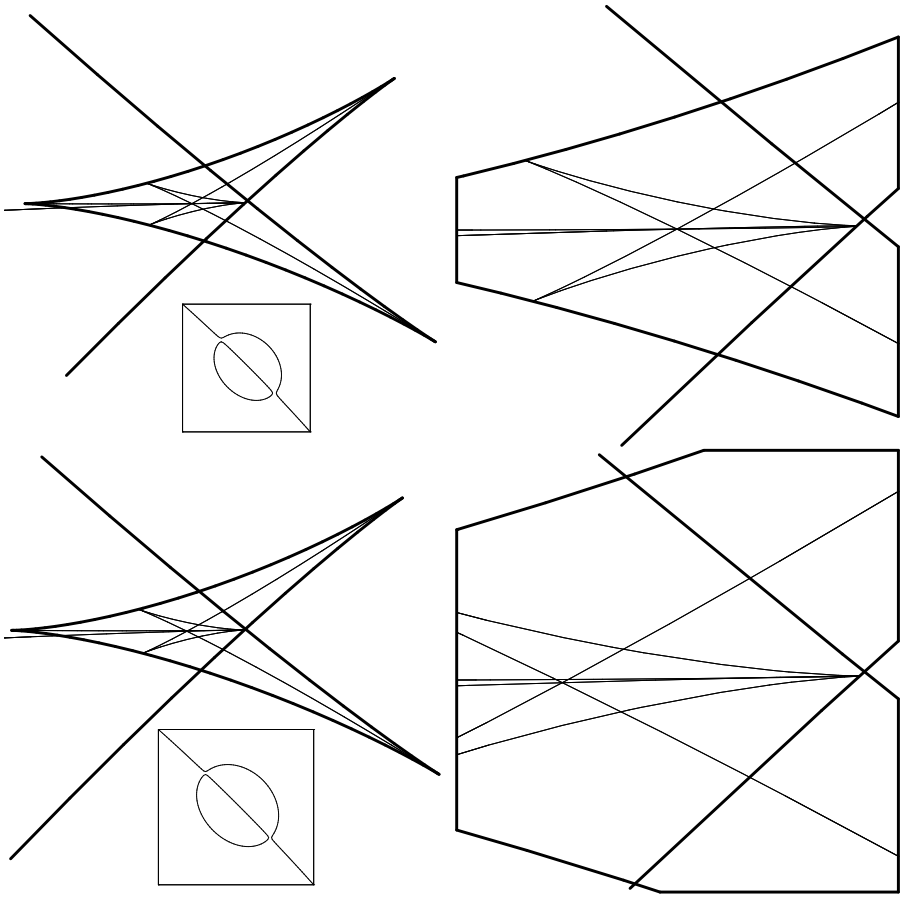

Figure 4.8: Top: p_6 (right: closer look); bottom: q_7 (right: closer look). Top: there is now a point where four branches of the A_1^2 set meet. Bottom: now there is only a triple intersection and two double intersections nearby.

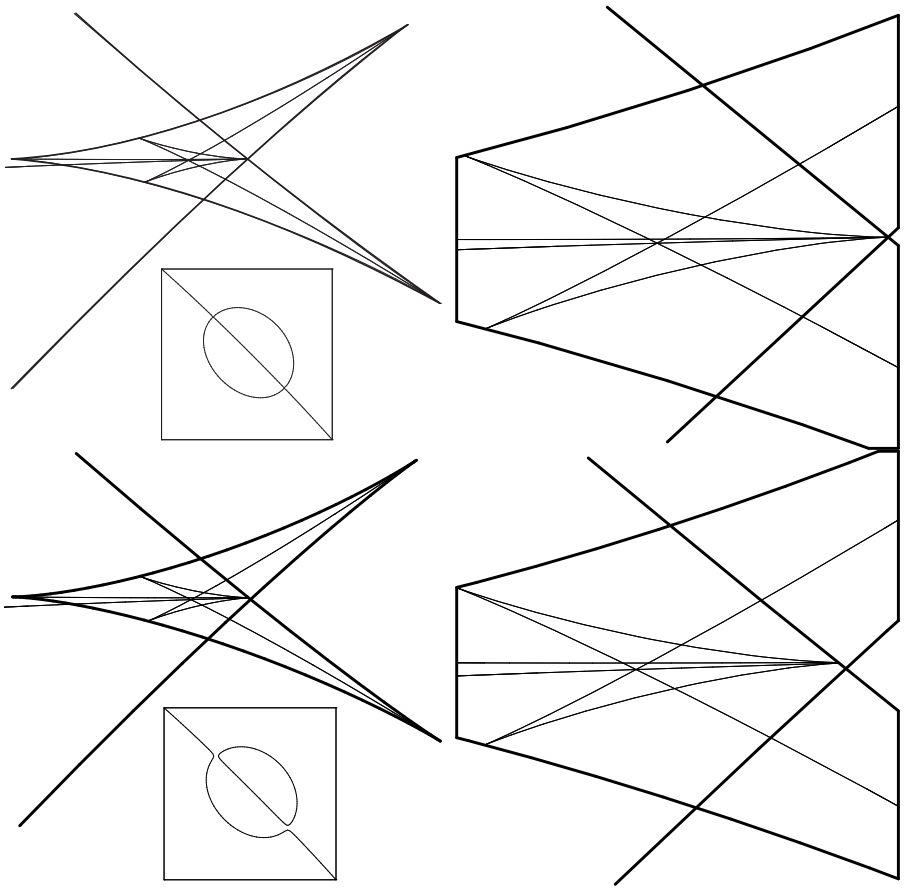

Figure 4.9: Top: p_7 (right: closer look); bottom: q_8 (right: closer look). Top: the moment of a nib transition on the A_1^2 set – two cusps of the A_1^2 set coincide at an intersection of two pieces of the A_2 set. After this transition the branches will pair off differently from before. The moment of transition is visible on the pre-set, since there are two self crossings here. Bottom: the two cusps of the A_1^2 set now lie only on one piece of the A_2 set and they do not coincide. The branches on the pre-set and on the A_1^2 set are now paired differently.

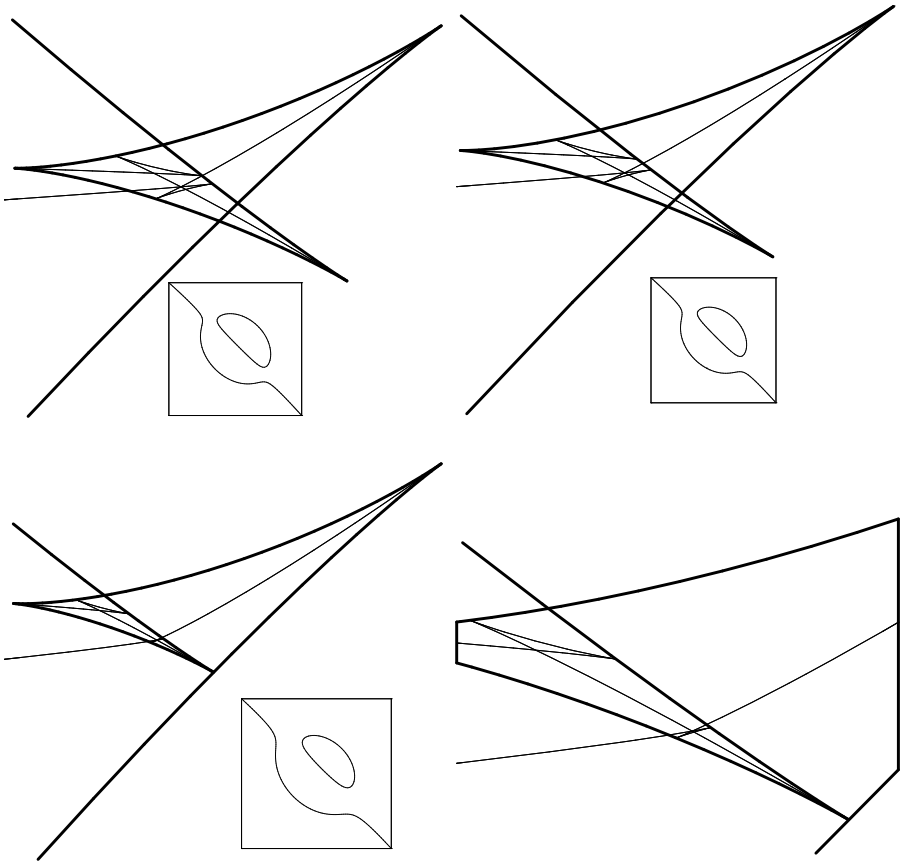

Figure 4.10: Top, from left: p_8, q_9; bottom: p_9. Top left: one of the cusps of the A_1^2 set meets another piece of the A_1^2 set and a piece of the A_2 set. Top right: the same cusp meets only the A_2 set, not the A_1^2 set. Bottom: a cusp of the A_2 set now meets another piece of the A_2 set.

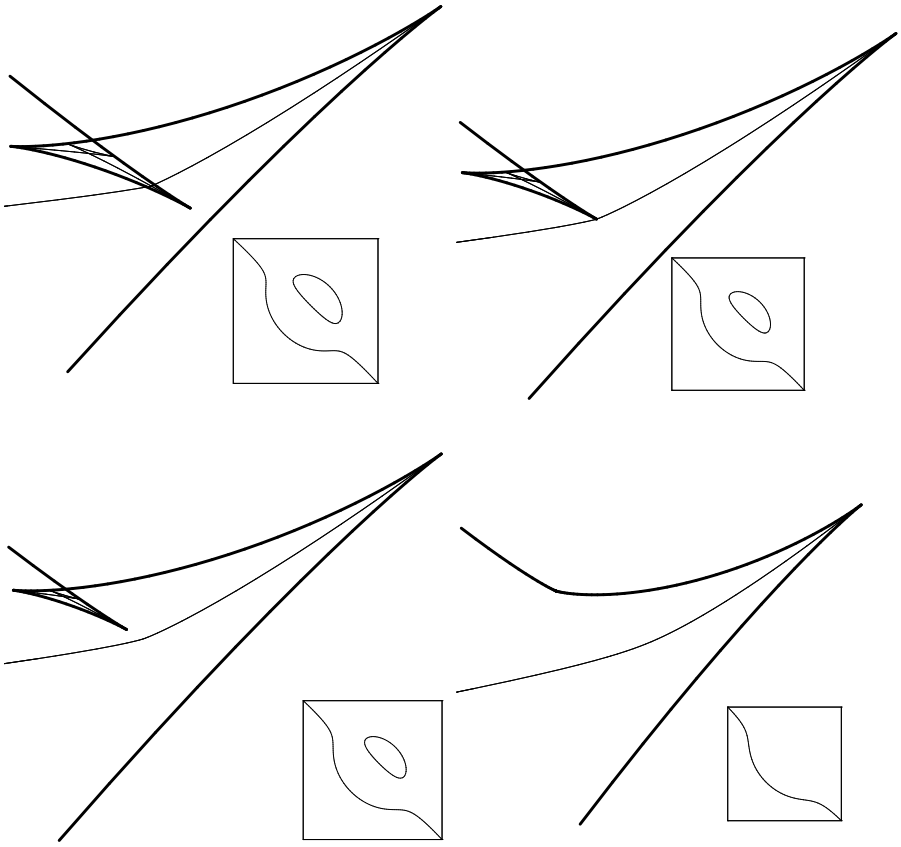

Figure 4.11: Top, from left: q_{10}, p_{10}; bottom, from left: q_{11}, p_{11}. Top left: the part of the A_2 set near to the cusp at the bottom of the picture no longer intersects another part of the A_2 set nearby. Top right: a cusp of the A_2 set meets a part of the A_1^2 set and two cusps of the A_1^2 set collapse. Bottom left: the cusp of the A_2 set no longer meets a part of the A_1^2 set, which is smooth nearby. Bottom right: the moment of a piece of the A_1^2 set vanishing and two cusps collapsing on the A_2 set.

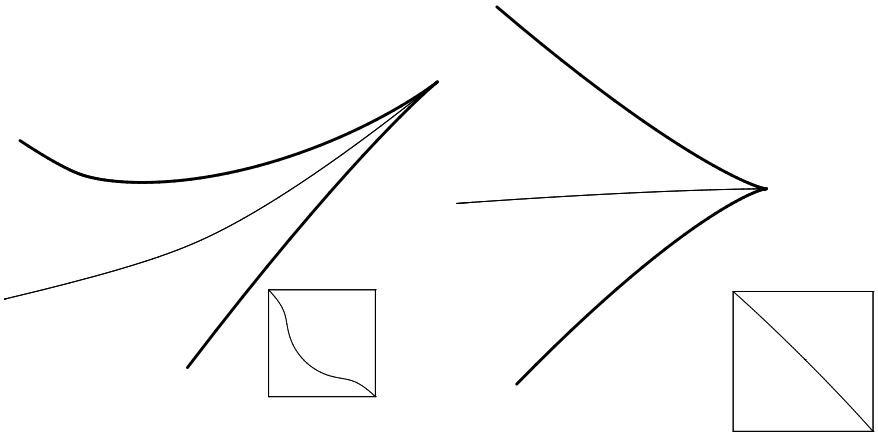

Figure 4.12: From left: q_{12}, m_2. Left: a piece of the A_1^2 set has now vanished and two cusps of the A_2 set have disappeared, leaving the A_2 set smooth nearby. This picture is the same as that for q_1. Right: this corresponds to the A_5 point. There is a cusp worse than (t^2, t^3) on the A_2 set.

4.2.3 A Family of Surfaces

Now we shall connect these calculations for the standard unfolding of an A_5 singularity with a family F of distance-squared functions from a one-parameter family of surfaces in $\mathbb{R}^3$ to a point in $\mathbb{R}^3$. Consider a family of surfaces in Monge form given by $z = f(x, y, t)$ where

$$\left.\begin{aligned} f_0(x,y) &= f(x,y,0) \\ &= \tfrac{1}{2}(\kappa_1 x^2 + \kappa_2 y^2) + (b_0 x^3 + b_1 x^2 y + b_2 x y^2 + b_3 y^3) \\ &\quad +(c_0 x^4 + c_1 x^3 y + c_2 x^2 y^2 + c_3 x y^3 + c_4 y^4) \\ &\quad +(d_0 x^5 + d_1 x^4 y + d_2 x^3 y^2 + d_3 x^2 y^3 + d_4 x y^4 + d_5 y^5) \\ &\quad +(e_0 x^6 + e_1 x^5 y + e_2 x^4 y^2 + e_3 x^3 y^3 + e_4 x^2 y^4 + e_5 x y^5 + e_6 y^6) \\ &\quad +\cdots \end{aligned}\right\} \quad (4.6)$$

where we assume $\kappa_1 \neq \kappa_2$, so that $(0, 0, f_0(0, 0))$ is not an umbilic, and that $\kappa_1 \neq 0$. Then the family F is given by

$$\left.\begin{aligned} &F : \mathbb{R}^2 \times \mathbb{R}^4, (0,0,0,\mathbf{p}_0) \to \mathbb{R} \ , \\ &(x,y,t,a,b,c) \mapsto \|(x,y,f(x,y,t)) - (a,b,c)\|^2 \ . \end{aligned}\right\} \quad (4.7)$$

Hence $F(x,y,t,a,b,c)$ is the square of the distance from a point $(a,b,c) \in \mathbb{R}^3$ to a point $(x,y,f(x,y,t))$.

We want to realize an A_5 transition on this family and so firstly we use Definition 4.1.1. Let F_0 be such that $F_0(x,y) = F(x,y,0,\mathbf{p}_0)$. Then we require F_0 to be right-equivalent to $\pm y^2 \pm x^6$.

Right-equivalence to $\pm y^2 \pm x^3$. We have

$$\begin{aligned} F(x,y,0,a,b,c) &= (x-a)^2 + (y-b)^2 + (f_0(x,y)-c)^2 \\ &= a^2+b^2+c^2 - 2ax - 2by + (1-c\kappa_1)x^2 + (1-c\kappa_2)y^2 \\ &\quad -2c(b_0x^3 + b_1x^2y + b_2xy^2 + b_3y^3) + \text{h.o.t. in } x,y. \end{aligned}$$

Hence for F_0 to be right-equivalent to $\pm y^2 \pm x^3$ we need $a=b=0$ and $c=1/\kappa_1$, so $\mathbf{p}_0 = (0,0,1/\kappa_1)$. (This is where we require $\kappa_1 \neq 0$.) We need the y^2 term to remain, which means that we assume $1-\kappa_2/\kappa_1 \neq 0$. Let

$$\lambda = 1 - \frac{\kappa_2}{\kappa_1} \ , \ \epsilon = \text{sign}(\lambda) \ .$$

Then take the change of variables

$$x \mapsto x \ , \ y \mapsto y - \left(\frac{b_1x^2 + b_2xy + b_3y^2}{\kappa_1 - \kappa_2} \right) = y_1 \ ,$$

which makes $F(x,y(y_1),0,0,0,1/\kappa_1) = \dfrac{1}{\kappa_1^2} + \left(1 - \dfrac{\kappa_2}{\kappa_1}\right) y_1^2 - \dfrac{2b_0}{\kappa_1}x^3 + \text{h.o.t.}$

Then if we take a further change of variables

$$x \mapsto \left(\sqrt[3]{-\frac{2b_0}{\kappa_1}} \right) x \ , \ y_1 \mapsto \left(\sqrt{|\lambda|} \right) y_1$$

we get that F_0 is right-equivalent to $\epsilon y^2 + x^3$ when $b_0 \neq 0$ (since, by [A74], this is 3-determined). Hence F_0 *has type* A_2 *if* $\mathbf{p}_0 = (0,0,1/\kappa_1)$, $\kappa_1 \neq 0$, $\lambda \neq 0$ *and* $b_0 \neq 0$.

The following uses the same methods to obtain conditions for F_0 to have A_3, A_4, and A_5 at $x=y=0$. We assume that $\mathbf{p}_0 = (0,0,1/\kappa_1)$, $\kappa_1 \neq 0$, $\lambda \neq 0$ and $b_0 = 0$.

Right-equivalence to $\pm y^2 \pm x^4$. If $\alpha_0 \neq 0$ where

$$\alpha_0 = \frac{\kappa_1^2}{4} - \frac{b_1^2}{\kappa_1(\kappa_1 - \kappa_2)} - \frac{2c_0}{\kappa_1}$$

then F_0 is right-equivalent to $\epsilon y^2 + \eta x^4$, where $\eta = \text{sign}(\alpha_0)$, and so F_0 has type A_3 at $x = y = 0$.

Right-equivalence to $\pm y^2 \pm x^5$. Given $\alpha_0 = 0$ and $\beta_0 \neq 0$, where

$$\beta_0 = -\frac{2b_1(c_1(\kappa_1 - \kappa_2) + b_1 b_2)}{\kappa_1(\kappa_1 - \kappa_2)^2} - \frac{2d_0}{\kappa_1} \ ,$$

then F_0 is right-equivalent to $\epsilon y^2 + x^5$ and so has A_4 at $x = y = 0$.

Right-equivalence to $\pm y^2 \pm x^6$. If $\alpha_0 = \beta_0 = 0$ and $\gamma_0 \neq 0$, where

$$\begin{aligned} \gamma_0 \ = \ & \frac{\kappa_1^4}{8} - \frac{(2b_1 d_1 + c_1^2)}{\kappa_1(\kappa_1 - \kappa_2)} + \frac{b_1(b_1\kappa_1^3 - 4b_1 c_2 - 8b_2 c_1)}{2\kappa_1(\kappa_1 - \kappa_2)^2} \\ & - \frac{2b_1^2(b_1 b_3 + 2b_2^2)}{\kappa_1(\kappa_1 - \kappa_2)^3} - \frac{2e_0}{\kappa_1} \ , \end{aligned}$$

then F_0 is right-equivalent to $\epsilon y^2 + \nu x^6$, where $\nu = \text{sign}(\gamma_0)$ and so has A_5 at $x = y = 0$.

Summary. If $\mathbf{p}_0 = (0, 0, 1/\kappa_1)$, $\kappa_1 \neq 0$, $\lambda \neq 0$, $b_0 = 0$, $\alpha_0 = 0$, $\beta_0 = 0$ and $\gamma_0 \neq 0$ then F_0 has type A_5. Moreover, if $\text{sign}(\lambda) = \text{sign}(\gamma_0)$ then F_0 is right-equivalent to $\pm(y^2 + x^6)$, which corresponds to an isolated intersection between the sphere centred at $(0, 0, 1/\kappa_1)$ of radius $1/\kappa_1$ and the surface $z = f_0(x, y)$ at the origin. This is what we want, since we are interested in the A_5 transition on the medial axis rather than on the part of the symmetry set which is not on the medial axis.

4.2.4 Condition for Versal Unfolding

Given that F_0 has type A_5 we then require the A_5 singularity to be versally unfolded by F. The condition for an unfolding to be versal was described in

§4.1. For the A_5 transition we require that the 6-multi-jets of

$$\frac{\partial F}{\partial t}\ ,\frac{\partial F}{\partial a}\ ,\frac{\partial F}{\partial b}\ ,\frac{\partial F}{\partial c}\ \text{ (all evaluated at } t=a=b=0,\ c=1/\kappa_1)$$
$$\text{should span } \frac{\mathcal{E}(2)}{J_{F_0}} \text{ (ignoring constant terms),}$$

where J_{F_0} is the Jacobian ideal of F_0, and so is spanned by $\partial F_0/\partial x$, $\partial F_0/\partial y$. We need only consider the 6-multi-jets since the A_5 singularity is 6-determined. Strictly speaking we should have $\partial F/\partial(c-1/\kappa_1)$, since we allow small changes in $(c-1/\kappa_1)$ in order to obtain all singularities near to A_5. However, this does not make any difference to the formulae. We obtain $\mathcal{E}(2)/J_{F_0}$ by taking polynomial multiples of $\partial F_0/\partial x$, $\partial F_0/\partial y$ to remove monomials in x, y contained in $\mathcal{E}(2)$. If we take $f(x,y,t)=f_0(x,y)+tx^4$ in (4.6) it can be shown that F versally unfolds the A_5 singularity if

$$\begin{pmatrix} \kappa_1 & 0 & 0 \\ 0 & 2b_1(\kappa_1-\kappa_2) & -2b_1^2 \\ b_1 & 2b_2 & c_1 \\ 0 & \kappa_1-\kappa_2 & -b_1 \end{pmatrix} \text{ has maximal rank.}$$

Hence the condition for F to be a versal unfolding of an A_5 singularity is that

$$c_1(\kappa_1-\kappa_2)+2b_1b_2\neq 0\ . \tag{4.8}$$

4.2.5 Conditions for Generic Sections

We will now connect the unfolding F given by (4.6), (4.7) and $f(x,y,t)=f_0(x,y)+tx^4$ with the standard unfolding G, from (4.1), of the A_5 singularity. Given that F has the property that F_0 has type A_5 at $x=y=0$ and that it versally unfolds the A_5 singularity (which happens when (4.8) is satisfied), we can say that F and G are *isomorphic as unfoldings* (from [BGG85]) and so G can be induced from F by

$$G(X,Y,\mathbf{u})=F(A(X,Y,\mathbf{u}),B(\mathbf{u}))+C(\mathbf{u}) \tag{4.9}$$

where $A : (\mathbb{R}^2 \times \mathbb{R}^4, (\mathbf{0}, \mathbf{0})) \to \mathbb{R}^2$ is a germ with $A(-, \mathbf{0})$ invertible, $B : (\mathbb{R}^4, \mathbf{0}) \to (\mathbb{R}^4, (0, \mathbf{p}_0))$ is an invertible germ and $C : (\mathbb{R}^4, \mathbf{0}) \to (\mathbb{R}, -1/\kappa_1^2)$ is a germ.

Now the big bifurcation set (Bif_F) of F is a three-dimensional object in $\mathbb{R}^4$, corresponding to (t, a, b, c)-space. Sections of this give the symmetry set and focal set of the surface $z = f(x, y, t)$ at values of t. We require these sections to be generic, which imposes restrictions on the family F, obtained from the following:

$$\begin{array}{ccccccc} \mathbb{R}^2 \times \mathbb{R}^4 & \stackrel{F\times\mathrm{id}}{\longrightarrow} & \mathbb{R} \times \mathbb{R}^4 & \longrightarrow & \mathbb{R}^4 & \stackrel{\pi}{\longrightarrow} & \mathbb{R} \\ (A \times B)\uparrow & & (-C \times B)\uparrow & & B\uparrow & \nearrow h & \\ \mathbb{R}^2 \times \mathbb{R}^4 & \stackrel{G\times\mathrm{id}}{\longrightarrow} & \mathbb{R} \times \mathbb{R}^4 & \longrightarrow & \mathbb{R}^4 & & \end{array}$$

Using this commutative diagram we can get the condition for avoiding bad sections of Bif_F by using the condition for a bad 3-space in the standard case. The tangent space to Bif_G is given by the kernel of h:

$$\ker dh : \mathbb{R}^4 \to \mathbb{R}, \text{ which has matrix } \left(\frac{\partial h}{\partial u_1}, \frac{\partial h}{\partial u_2}, \frac{\partial h}{\partial u_3}, \frac{\partial h}{\partial u_4}\right)\Big|_{\mathbf{u}=\mathbf{0}} .$$

Hence, from (4.5), we see that the generic functions h are those for which $\partial h/\partial u_1 \neq 0$ at $\mathbf{u} = \mathbf{0}$, with possibly other functions given by considering tangent spaces to the two- and three-dimensional strata (see Remark 4.2.1.1). From the commutative diagram we see that $h = \pi \circ B$, where $\pi : (t, a, b, c) \mapsto t$ and so some generic sections of Bif_F are given by

$$\frac{\partial B_1}{\partial u_1}\Big|_{\mathbf{u}=\mathbf{0}} u_1 + \frac{\partial B_1}{\partial u_2}\Big|_{\mathbf{u}=\mathbf{0}} u_2 + \frac{\partial B_1}{\partial u_3}\Big|_{\mathbf{u}=\mathbf{0}} u_3 + \frac{\partial B_1}{\partial u_4}\Big|_{\mathbf{u}=\mathbf{0}} u_4 = 0 \ ,$$
$$\text{for which } \frac{\partial B_1}{\partial u_1}\Big|_{\mathbf{u}=\mathbf{0}} \neq 0, \text{ where } B_1 \text{ is the first component of } B \ .$$

The remaining task is to link this condition with the unfolding F, which is

done by using the relationship (4.9) between F and G. We get

$$\left(\begin{array}{cccc} \frac{\partial G}{\partial u_1} & \frac{\partial G}{\partial u_2} & \frac{\partial G}{\partial u_3} & \frac{\partial G}{\partial u_4} \end{array} \right)\Big|_{(X,Y,\mathbf{0})} = \left(\begin{array}{cccc} X^4 & X^3 & X^2 & X \end{array} \right)$$

$$= \left(\begin{array}{cc} \frac{\partial F}{\partial x} & \frac{\partial F}{\partial y} \end{array} \right)\Big|_{(A(X,Y,\mathbf{0}),B(\mathbf{0}))} \times \left(\begin{array}{cccc} \frac{\partial A_x}{\partial u_1} & \frac{\partial A_x}{\partial u_2} & \frac{\partial A_x}{\partial u_3} & \frac{\partial A_x}{\partial u_4} \\ \frac{\partial A_y}{\partial u_1} & \frac{\partial A_y}{\partial u_2} & \frac{\partial A_y}{\partial u_3} & \frac{\partial A_y}{\partial u_4} \end{array} \right)\Big|_{(X,Y,\mathbf{0})}$$

$$+ \left(\begin{array}{cccc} \frac{\partial F}{\partial t} & \frac{\partial F}{\partial a} & \frac{\partial F}{\partial b} & \frac{\partial F}{\partial c} \end{array} \right)\Big|_{(A(X,Y,\mathbf{0}),B(\mathbf{0}))} \times \left(\begin{array}{cccc} \frac{\partial B_1}{\partial u_1} & \frac{\partial B_1}{\partial u_2} & \frac{\partial B_1}{\partial u_3} & \frac{\partial B_1}{\partial u_4} \\ \frac{\partial B_2}{\partial u_1} & \frac{\partial B_2}{\partial u_2} & \frac{\partial B_2}{\partial u_3} & \frac{\partial B_2}{\partial u_4} \\ \frac{\partial B_3}{\partial u_1} & \frac{\partial B_3}{\partial u_2} & \frac{\partial B_3}{\partial u_3} & \frac{\partial B_3}{\partial u_4} \\ \frac{\partial B_4}{\partial u_1} & \frac{\partial B_4}{\partial u_2} & \frac{\partial B_4}{\partial u_3} & \frac{\partial B_4}{\partial u_4} \end{array} \right)\Big|_{\mathbf{u}=\mathbf{0}}$$

$$+ \left(\begin{array}{cccc} \frac{\partial C}{\partial u_1} & \frac{\partial C}{\partial u_2} & \frac{\partial C}{\partial u_3} & \frac{\partial C}{\partial u_4} \end{array} \right)\Big|_{\mathbf{u}=\mathbf{0}} .$$

Consider the Taylor expansions at $X = Y = 0$ of the components of both sides of the above; the left-hand side evaluated at $(X, Y, \mathbf{0})$, the right-hand side evaluated at $(A(X, Y, \mathbf{0}), B(\mathbf{0}))$. In particular we want the coefficients of X, X^2, X^3, X^4 of these Taylor expansions. Using the relation (4.9) at $\mathbf{u} = \mathbf{0}$:

$$Y^2 + X^6 = F\left(A(X, Y, \mathbf{0}), \left(0, 0, 0, \frac{1}{\kappa_1}\right)\right) + C(\mathbf{0}) \text{ for all } X,\ Y,$$

it can be shown that the coefficients of X, X^2, X^3, X^4 in the Taylor expansions at $X = Y = 0$ of $\partial F/\partial x$, and of $\partial F/\partial y$, evaluated at $(A(X, Y, \mathbf{0}), B(\mathbf{0}))$ are all

zero. Hence we get the following:

$$
\begin{aligned}
I_4 &= M \times JB \ , \quad \text{where} \\
JB &= \left(\begin{array}{cccc}
\frac{\partial B_1}{\partial u_1} & \frac{\partial B_1}{\partial u_2} & \frac{\partial B_1}{\partial u_3} & \frac{\partial B_1}{\partial u_4} \\
\frac{\partial B_2}{\partial u_1} & \frac{\partial B_2}{\partial u_2} & \frac{\partial B_2}{\partial u_3} & \frac{\partial B_2}{\partial u_4} \\
\frac{\partial B_3}{\partial u_1} & \frac{\partial B_3}{\partial u_2} & \frac{\partial B_3}{\partial u_3} & \frac{\partial B_3}{\partial u_4} \\
\frac{\partial B_4}{\partial u_1} & \frac{\partial B_4}{\partial u_2} & \frac{\partial B_4}{\partial u_3} & \frac{\partial B_4}{\partial u_4}
\end{array} \right) \Bigg|_{\mathbf{u}=\mathbf{0}} , \\
M &= \left(\begin{array}{l}
\text{coeff. of } X^4 \text{ in Taylor exp. of } \frac{\partial F}{\partial t}, \frac{\partial F}{\partial a}, \frac{\partial F}{\partial b}, \frac{\partial F}{\partial c} \\
\text{coeff. of } X^3 \text{ in } \ldots \\
\text{coeff. of } X^2 \text{ in } \ldots \\
\text{coeff. of } X \text{ in } \ldots
\end{array} \right) \Bigg|_{A(X,Y,\mathbf{0}),B(\mathbf{0})}
\end{aligned}
$$

and I_4 is the (4×4) identity matrix. Since we have assumed the condition (4.8) for F to be a versal unfolding is satisfied, we can say that the determinant of JB is non-zero and so $JB = M^{-1}$. We can calculate the matrix M^{-1} in the terms that appear in the of the family F using the relation (4.9). Then we find that

$$\frac{\partial B_1}{\partial u_1}(\mathbf{0}) \neq 0 \iff c_1(\kappa_1 - \kappa_2) + 2b_1 b_2 \neq 0 \ ,$$

which we know is true, since we assumed (4.8) holds. Hence, *provided there are no additional normal forms for generic functions other than the h with $\partial h/\partial u_1 \neq 0$ at $\mathbf{u} = \mathbf{0}$, if F is a versal unfolding of the A_5 singularity, the sections of* Bif_F *are generic.*

So we have the following.

Proposition 4.2.5.1 *The necessary conditions for the one-parameter family of symmetry sets of the family of surfaces $z = f_0(x, y) + tx^4$, where $f_0(x, y)$ is*

given by (4.6)*, to exhibit an* A_5 *transition are that*

$$\begin{aligned}
0 &= b_0 \ , \\
0 &= \frac{\kappa_1^2}{4} - \frac{b_1^2}{\kappa_1(\kappa_1-\kappa_2)} - \frac{2c_0}{\kappa_1} \ , \\
0 &= -\frac{2b_1(c_1(\kappa_1-\kappa_2)+b_1b_2)}{\kappa_1(\kappa_1-\kappa_2)^2} - \frac{2d_0}{\kappa_1} \ , \\
0 &\neq \frac{\kappa_1^4}{8} - \frac{(2b_1d_1+c_1^2)}{\kappa_1(\kappa_1-\kappa_2)} + \frac{b_1(b_1\kappa_1^3-4b_1c_2-8b_2c_1)}{2\kappa_1(\kappa_1-\kappa_2)^2} \\
&\quad -\frac{2b_1^2(b_1b_3+2b_2^2)}{\kappa_1(\kappa_1-\kappa_2)^3} - \frac{2e_0}{\kappa_1} \ , \\
0 &\neq c_1(\kappa_1-\kappa_2)+2b_1b_2 \ .
\end{aligned}$$

Moreover if the sign of the right-hand side of the fourth condition is the same as the sign of $(\kappa_1-\kappa_2)/\kappa_1$ *then the transition occurs on the medial axis. The first four conditions ensure that the origin is an* A_5 *point at the moment of transition and the last condition means the* A_5 *singularity is versally unfolded by* F *(given by* (4.6)*,* (4.7)*) and that the plane sections of the big bifurcation set are generic, provided there are no additional normal forms for generic functions given by considering the limits of tangent spaces to two- and three-dimensional strata (see Remark 4.2.1.1).*

4.2.6 Interpretation of the A_5 Condition

There are several interpretations of the last condition of Proposition 4.2.5.1. From [HGYGM99, pp.144, 162], the local equation of the ridge corresponding to κ_1 at the origin is

$$\begin{aligned}
3\left((\kappa_1-\kappa_2)(8c_0-\kappa_1^3)+4b_1^2\right)x + 6\left(c_1(\kappa_1-\kappa_2)+2b_1b_2\right)y+\cdots &= 0 \\
\iff (0)x + 6\left(c_1(\kappa_1-\kappa_2)+2b_1b_2\right)y+\cdots &= 0 \ ,
\end{aligned}$$

since the origin is an A_5 point and so the first four conditions of Proposition 4.2.5.1 hold. Then the last condition of Proposition 4.2.5.1 is that $0 \neq c_1(\kappa_1-\kappa_2)+2b_1b_2$, which is the same as the ridge curve corresponding to κ_1 being non-singular at the origin.

Another interpretation is given by considering the line of curvature corresponding to κ_1. When the first four conditions of Proposition 4.2.5.1 are satisfied, this line of curvature is given by $z = f_0(x, y(x))$ where

$$\begin{aligned} y(x) &= \left(\frac{b_1}{\kappa_1 - \kappa_2}\right) x^2 + \left(\frac{c_1(\kappa_1 - \kappa_2) + 2b_1 b_2}{(\kappa_1 - \kappa_2)^2}\right) x^3 + \cdots, \\ \text{giving } \quad f_0(x, y(x)) &= \frac{\kappa_1}{2} x^2 + \frac{\kappa_1(\kappa_1^2(\kappa_1 - \kappa_2)^2 + 4b_1^2)}{8(\kappa_1 - \kappa_2)^2} x^4 \\ &\quad + \frac{\kappa_1 b_1(c_1(\kappa_1 - \kappa_2) + 2b_1 b_2)}{(\kappa_1 - \kappa_2)^2} x^5 + \cdots . \end{aligned}$$

Then the torsion τ of this curve is zero at $x = 0$ if and only if $c_1(\kappa_1 - \kappa_2) + 2b_1 b_2 = 0$. Hence the condition $c_1(\kappa_1 - \kappa_2) + 2b_1 b_2 \neq 0$ means that the torsion of the line of curvature corresponding to κ_1 is non-zero. Alternatively, the condition $c_1(\kappa_1 - \kappa_2) + 2b_1 b_2 \neq 0$ means that the projection of the line of curvature corresponding to κ_1 to the (x, y)-plane does not have an inflexion when $b_1 \neq 0$.

Secondly, choose $\kappa_1 > \kappa_2$ without loss of generality, since $(\kappa_1 - \kappa_2) \neq 0$. Then we want $\text{sign}(\kappa_1) =$ the sign of the right-hand side of the fourth condition of Proposition 4.2.5.1 for the transition to be on the medial axis. Given this, it can be shown that the expansion of κ_1 along the line of curvature corresponding to κ_1 is

$$\kappa_1(x) = \kappa_1(0) - (\text{positive const.})x^4 + \cdots$$

and so κ_1 has a maximum at $x = 0$.

4.2.7 Example

Take numerical values for the coefficients of $f_0(x, y)$ so that the conditions of Proposition 4.2.5.1 are satisfied. Let

$$\begin{aligned} f_0(x,y) &= \frac{1}{2}\left(x^2 + \frac{1}{4}y^2\right) + \left(\frac{1}{2}x^2y + \frac{3}{10}xy^2 - \frac{1}{5}y^3\right) \\ &\quad + \left(-\frac{1}{24}x^4\right) + \left(-\frac{2}{15}x^5\right) + \left(\frac{1363}{10800} - \frac{1}{10}\right)x^6, \\ \text{that is} \qquad & \kappa_1 = 1,\ \kappa_2 = \frac{1}{4}, \\ & b_0 = 0,\ b_1 = \frac{1}{2},\ b_2 = \frac{3}{10},\ b_3 = -\frac{1}{5}, \\ & c_0 = -\frac{1}{24},\ d_0 = -\frac{2}{15},\ e_0 = \frac{1363}{10800} - \frac{1}{10} \end{aligned}$$

and all the other coefficients are zero in the formula (4.6) for $f_0(x, y)$. All of the conditions of Proposition 4.2.5.1 are satisfied for these values. Hence the necessary conditions are satisfied for a generic A_5 transition to occur on the family of distance-squared functions F given by (4.7) for $f_0(x, y)$ with the numerical values for the coefficients taken as above. It can be shown that the right-hand side of the fourth condition of Proposition 4.2.5.1 is positive. Then, since $(\kappa_1 - \kappa_2) > 0$ and $\kappa_1 > 0$, the transition takes place on the medial axis of the surface $z = f(x, y, t)$ at values of t moving from positive to negative.

As an A_5 transition occurs on the medial axis, certain events happen on the surface $z = f(x, y, t)$ at various values of t. See Figures 4.13, 4.14 for an example of what happens to ridge curves during an A_5 transition.

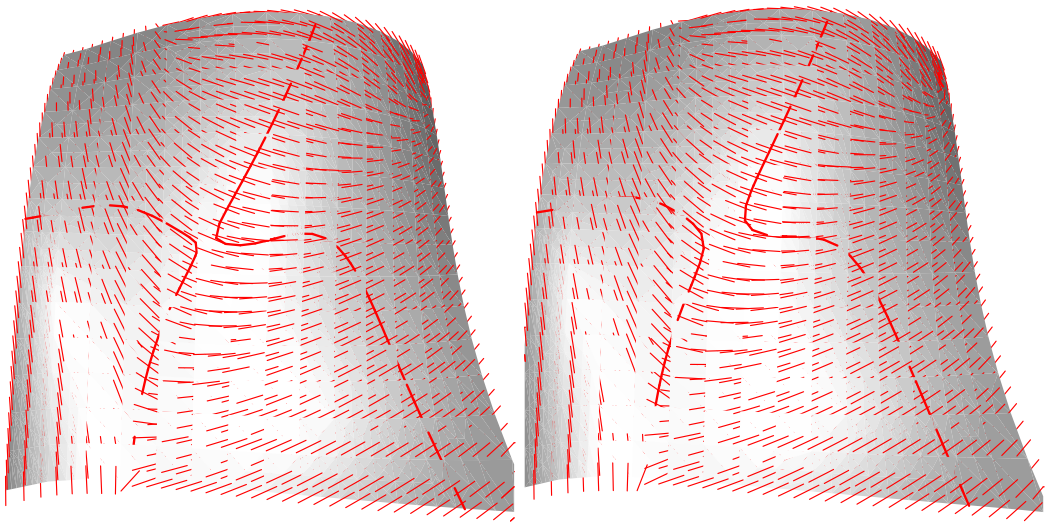

Figure 4.13: An example of the surface $z = f(x, y, t)$ at values of t; on the left $t = 0.03$, on the right $t = 0$. Drawn on each surface are the principal direction field and the ridge curves corresponding to the larger principal curvature. (The ridge should be a continuous curve, but owing to numerical errors it sometimes 'dives' underneath the surface and so cannot be seen.) The ridge curves on the right of the surfaces are of interest: as the medial axis goes through the A_5 transition, the ridge curve loses two A_4 points, that is points at which the ridge has a turning point and is tangent to the corresponding principal direction. Left: the A_4 points are still on the ridge curve on the right of the surface. Right: at $t = 0$ the ridge has degenerate tangency with the principal direction at $x = y = 0$ – this corresponds to the A_5 point.

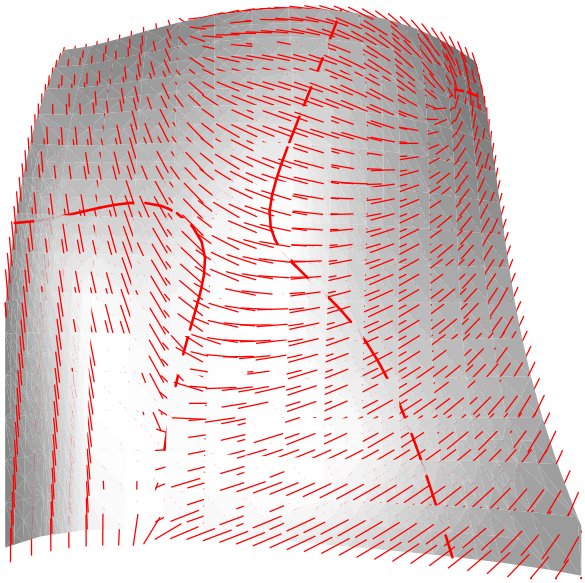

Figure 4.14: The continued example of the surface $z = f(x, y, t)$; this picture is at $t = -0.1$. This is after the A_5 transition and the ridge curve has lost two A_4 points, since there are no points on the ridge at which the ridge has a turning point and is tangent to the corresponding principal direction.

4.3 The $A_1^2A_3$ Transitions

Now we shall use the same methods for the $A_1^2A_3$ cases as employed for the A_5 transition. The standard multi-versal unfolding of an $A_1^2A_3$ singularity is

$$\left.\begin{array}{l} G : \mathbb{R}^2 \times \mathbb{R}^4 \to \mathbb{R} \ , \ \text{ given by the three unfoldings} \\ G_1 : (X_1, Y_1, u_1, u_2, u_3, u_4) \mapsto Y_1^2 + X_1^4 + u_1X_1^2 + u_2X_1 \ , \\ G_2 : (X_2, Y_2, u_1, u_2, u_3, u_4) \mapsto Y_2^2 + X_2^2 + u_3 \ , \\ G_3 : (X_3, Y_3, u_1, u_2, u_3, u_4) \mapsto Y_3^2 + X_3^2 + u_4 \ . \end{array}\right\} \tag{4.10}$$

4.3.1 The Bad 3-spaces

We need to calculate the bad 3-spaces, in other words those spaces in $\mathbb{R}^4_{\mathbf{u}}$ given by (4.4) which contain any of the limiting tangent vectors to the strata of the big bifurcation set of G given by (4.10). For (4.10), the one-dimensional strata are

$$\begin{aligned} A_1^4 : \ \{(u_1, u_2, u_3, u_4) &= (-2X^2, 0, -X^4, -X^4)\} \ , \\ A_1^2A_2 : \ \{(u_1, u_2, u_3, u_4) &= (-6X^2, 8X^3, 3X^4, 3X^4)\} \ , \\ A_1A_3 : \ \{(u_1, u_2, u_3, u_4) &= (0, 0, u_3, 0)\} \\ \cup\{(u_1, u_2, u_3, u_4) &= (0, 0, 0, u_4)\} \ , \\ A_1^2/A_1^3 : \ \{(u_1, u_2, u_3, u_4) &= (-2X^2, 0, 0, 0)\} \ , \\ A_2/A_1^3 : \ \{(u_1, u_2, u_3, u_4) &= (-6X^2, 8X^3, -24X^4, -24X^4)\} \ , \\ A_1^2/A_1A_2 : \ \{(u_1, u_2, u_3, u_4) &= (-6X^2, 8X^3, 3X^4, -24X^4)\} \\ \cup\{(u_1, u_2, u_3, u_4) &= (-6X^2, 8X^3, -24X^4, 3X^4)\} \ , \\ A_1^2/A_3 : \ \{(u_1, u_2, u_3, u_4) &= (0, 0, u_3, u_3)\} \ . \end{aligned}$$

We can see that the limits of tangent vectors to these one-dimensional strata are $(1, 0, 0, 0)$, $(0, 0, 1, 0)$, $(0, 0, 0, 1)$ and $(0, 0, 1, 1)$. *Hence the bad 3-spaces are* (4.4) *where* $\lambda_1 = 0$ *or* $\lambda_3 = 0$ *or* $\lambda_4 = 0$ *or* $\lambda_3 + \lambda_4 = 0$, with other possible bad 3-spaces given by considering limits of tangent spaces to two- and three-dimensional strata (see Remark 4.2.1.1).

As we did for the A_5 transition, we need to determine the number of regions in $\mathbb{R}P^3 - \Delta$, where Δ is the set of bad 3-spaces. From this we can decide the number of types of transition and obtain criteria for realizing each one. Since λ_2 is not mentioned in Δ, we need only consider $(\lambda_1 : \lambda_3 : \lambda_4)$ as a point in $\mathbb{R}P^2$.

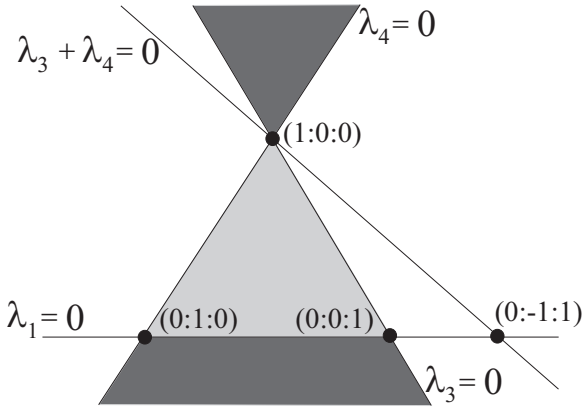

Figure 4.15: The $A_1^2A_3$ case: the non-shaded region gives one type of transition, the lightly shaded region gives another type, and the darkly shaded region gives the last type of transition.

Given that there are no additional bad 3-spaces, it can be shown that there are three possible types of $A_1^2A_3$ transition, according to the region in which $(\lambda_1 : \lambda_3 : \lambda_4)$ lies in Figure 4.15; the non-shaded region gives one type, the lightly shaded region gives another type, and the darkly shaded region gives the last type of transition. From Proposition 4.3.5.1 below, we get that one of these types of transition cannot be realized by a family of distance-squared functions. We get the following.

Proposition 4.3.1.1 *Provided the bad 3-spaces are* (4.4) *where* $\lambda_1 = 0$ *or* $\lambda_3 = 0$ *or* $\lambda_4 = 0$ *or* $\lambda_3 + \lambda_4 = 0$*, then the sections* $\lambda_1 u_1 + \lambda_2 u_2 + \lambda_3 u_3 + \lambda_4 u_4 = \text{const.}$ *of the big bifurcation set of the standard unfolding* G *from* (4.10) *give one of three possible transitions, distinguished by the following:*

- $\lambda_3\lambda_4 < 0$ *corresponds to* $A_1^2A_3$-I*;*

- $\text{sign}(\lambda_1) = -\text{sign}(\lambda_3) = -\text{sign}(\lambda_4)$ *corresponds to* $A_1^2A_3$-II*;*
- $\text{sign}(\lambda_1) = \text{sign}(\lambda_3) = \text{sign}(\lambda_4)$ *corresponds to the other possible type of* $A_1^2A_3$ *transition.*

4.3.2 Representations of the $A_1^2A_3$ Transition

The pictures of the sections of the big bifurcation set of the standard unfolding G from (4.10) can be obtained in the same way as for the A_5 singularity (see §4.2.2). Hence, when considering the list of bad 3-spaces in Proposition 4.3.1.1, the three possible cases are illustrated in Figures 4.16 to 4.18. In this case a one-parameter family of symmetry sets must look like one of the three transitions in these figures (in fact it will be shown in Proposition 4.3.5.1 below that one of the cases cannot occur for a one-parameter family of symmetry sets). Pictures of the medial axis in the two occurring cases can be deduced from Figures 4.16 to 4.18 and are drawn in Figure 4.19.

4.3.3 A Family of Surfaces

Now we shall connect these calculations for the standard unfolding of an $A_1^2A_3$ singularity with a family of distance-squared functions on a one-parameter family of surfaces in three dimensions. We consider the unfolding

$$\left.\begin{array}{l} F : \mathbb{R}^2 \times \mathbb{R}^4, (0,0,0,0,0,1/\kappa_1) \to \mathbb{R} \text{ , given by the three unfoldings} \\ F_1(x_1, y_1, t, a, b, c) = (x_1 - a)^2 + (y_1 - b)^2 \\ \qquad\qquad +(f_0(x,y) + tg_1(x_1, y_1) - c)^2 \text{ ,} \\ F_2(x_2, y_2, t, a, b, c) = \|\gamma_2(x_2, y_2, t) - (a, b, c)\|^2 \text{ ,} \\ F_3(x_3, y_3, t, a, b, c) = \|\gamma_3(x_3, y_3, t) - (a, b, c)\|^2 \text{ ,} \end{array}\right\} \quad (4.11)$$

where $f_0(x_1, y_1)$ is given by (4.6) and $F_{0,1}$ has type A_3 at $x_1 = y_1 = 0$, where $F_{0,i}(x_i, y_i) = F_i(x_i, y_i, 0, 0, 0, 1/\kappa_1)$. This means that $b_0 = 0$ and

$$\frac{\kappa_1^2}{4} - \frac{b_1^2}{\kappa_1(\kappa_1 - \kappa_2)} - \frac{2c_0}{\kappa_1} \neq 0 \text{ .}$$

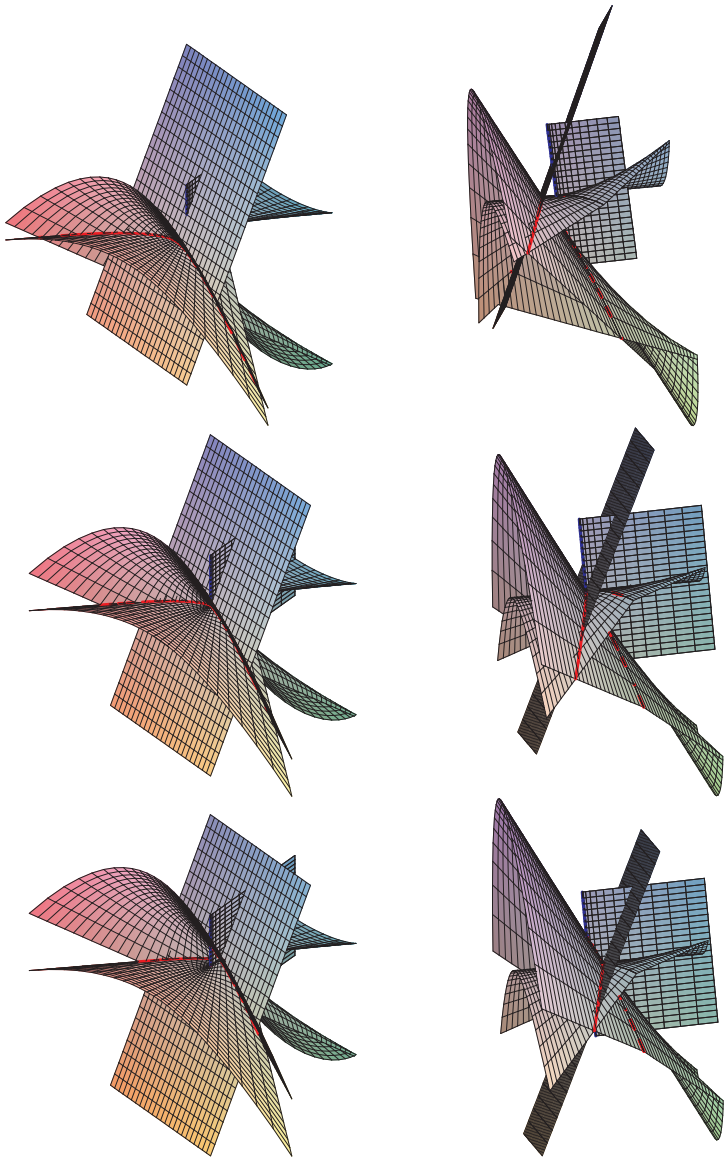

Figure 4.16: Sections of the big bifurcation set of the standard unfolding G from (4.10) in the case $A_1^2A_3$-I of Proposition 4.3.1.1. Top: two views before the transition, middle: two views at the moment of transition, bottom: two views after the transition. The blue, red curves correspond respectively to A_3, A_1^3 curves. This is one of the possibilities for a one-parameter family of symmetry sets (See Figure 4.19 for pictures of the medial axis in this case).

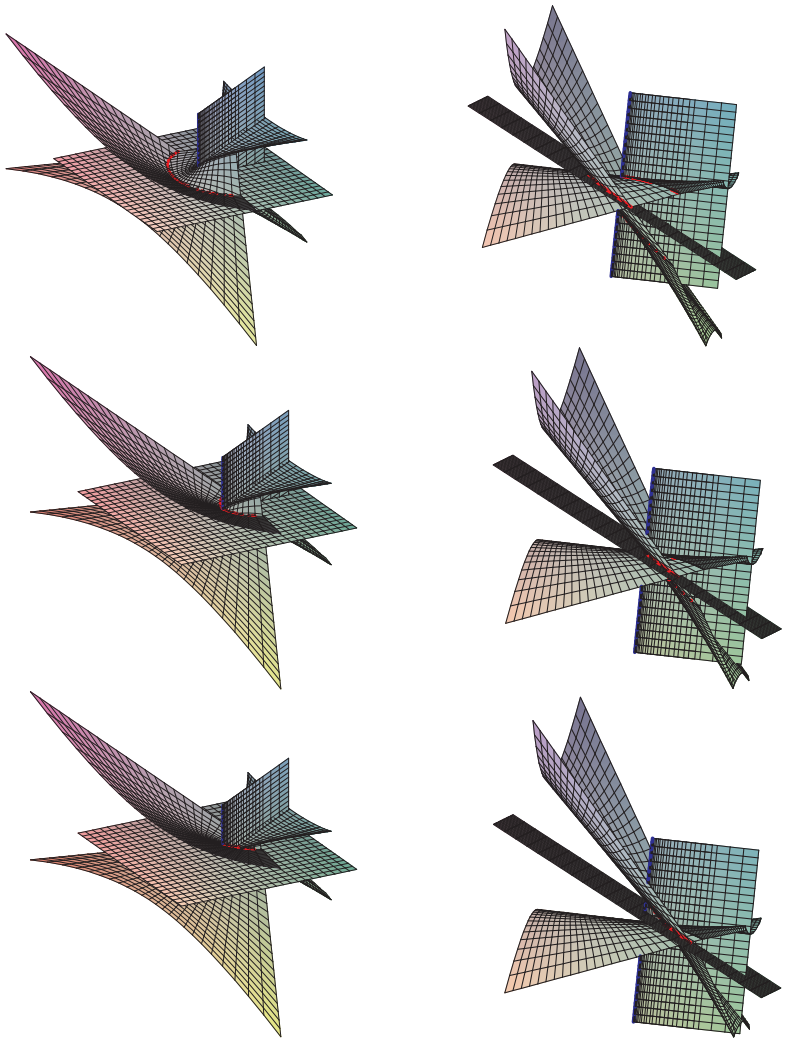

Figure 4.17: Sections of the big bifurcation set of the standard unfolding G from (4.10) in the case $A_1^2A_3$-II of Proposition 4.3.1.1. Top: two views before the transition, middle: two views at the moment of transition, bottom: two views after the transition. The blue, red curves correspond respectively to A_3, A_1^3 curves. This is the second possibility for a one-parameter family of symmetry sets (See Figure 4.19 for pictures of the medial axis in this case).

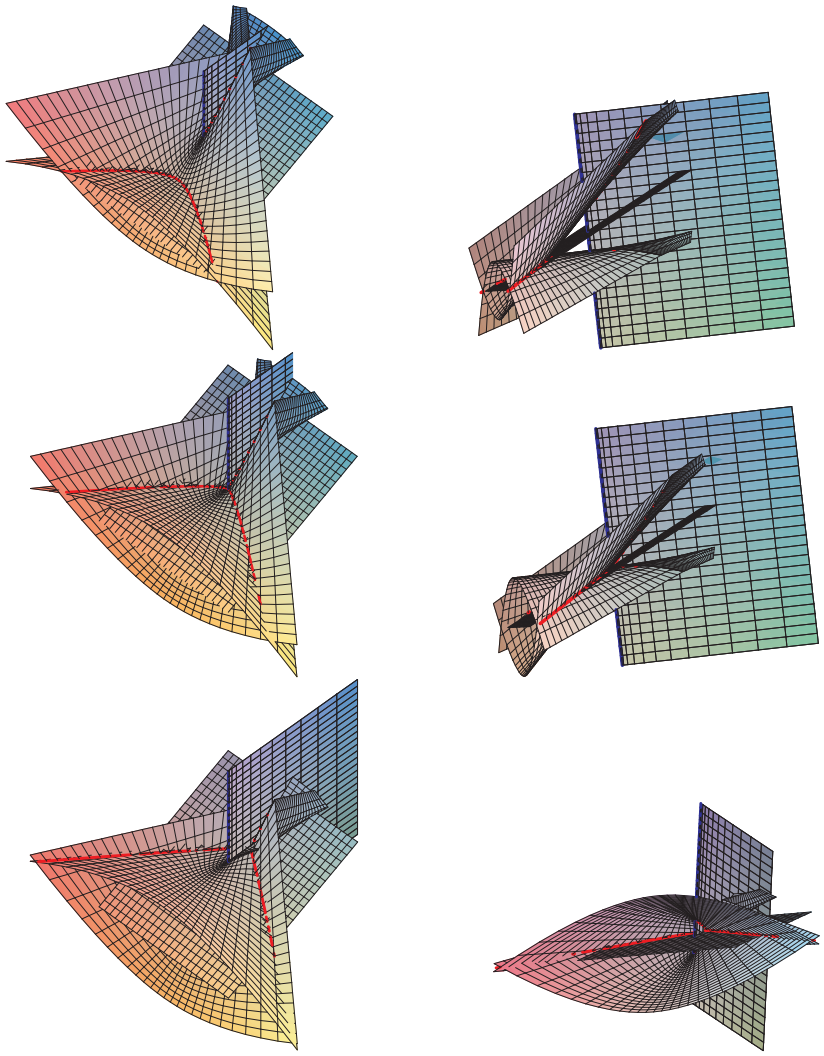

Figure 4.18: The third type of transition as listed in Proposition 4.3.1.1 of sections of the big bifurcation set of the standard unfolding G from (4.10). This does not occur for a one-parameter family of symmetry sets. Top: two views before the transition, middle: two views at the moment of transition, bottom: two views after the transition. The blue, red curves correspond respectively to A_3, A_1^3 curves.

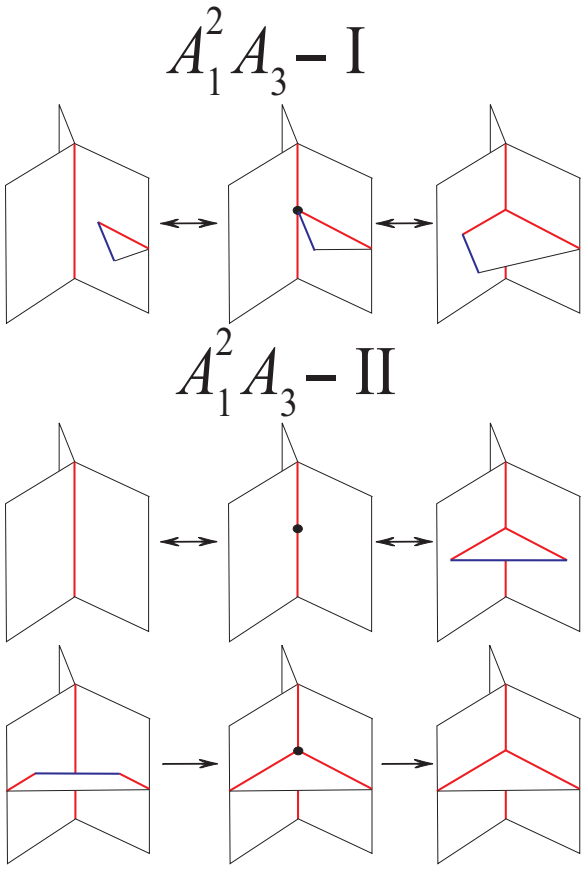

Figure 4.19: The medial axis corresponding to two possible types of $A_1^2A_3$ transition on a one-parameter family of symmetry sets from Figures 4.16, 4.17 and 4.18. The third case does not occur. The blue, red curves correspond respectively to A_3, A_1^3 curves.

We also want $F_{0,2}$ and $F_{0,3}$ to have type A_1 at $x_2 = y_2 = 0$ and at $x_3 = y_3 = 0$ respectively. This corresponds to the sphere of centre $(0, 0, 1/\kappa_1)$, radius $1/\kappa_1$ having A_1 contact at two points on the two families γ_2, γ_3 of surfaces at $t = 0$.

Consider F_2. Let the point of contact with the sphere and the surface given by $\gamma_2(x_2, y_2, 0)$ at $x_2 = y_2 = 0$ be

$$\mathbf{x}_{0,2} = (p_{0,2}, q_{0,2}, w_{0,2}) = \frac{1}{\kappa_1}(\cos\phi_2 \cos\lambda_2, \cos\phi_2 \sin\lambda_2, \sin\phi_2 + 1) \ , \qquad (4.12)$$

where ϕ_2, λ_2 are constants. Then the tangent plane to this surface is given by

$$((x, y, z) - (p_{0,2}, q_{0,2}, w_{0,2})) \cdot (\kappa_1(p_{0,2}, q_{0,2}, w_{0,2}) - (0, 0, 1)) = 0 \ .$$

Depending on the parametrization of the surface, we consider three forms of $F_2(x_2, y_2, t, a, b, c)$ as follows:

$$\begin{aligned}
F_2 &\equiv (f_{2,1}(x_2, y_2) + t g_{2,1}(x_2, y_2) - a)^2 \\
&\quad + (y_2 + q_{0,2} - b)^2 + (x_2 + w_{0,2} - c)^2 \qquad (4.13) \\
\text{where } f_{2,1}(x_2, y_2) &= p_{0,2} + y_2\left(-\frac{q_{0,2}}{p_{0,2}}\right) + x_2\left(\frac{1 - \kappa_1 w_{0,2}}{\kappa_1 p_{0,2}}\right) + \cdots \\
\text{or } F_2 &\equiv (x_2 + p_{0,2} - a)^2 + (f_{2,2}(x_2, y_2) + t g_{2,2}(x_2, y_2) - b)^2 \\
&\quad + (y_2 + w_{0,2} - c)^2 \qquad (4.14) \\
\text{where } f_{2,2}(x_2, y_2) &= q_{0,2} + x_2\left(-\frac{p_{0,2}}{q_{0,2}}\right) + y_2\left(\frac{1 - \kappa_1 w_{0,2}}{\kappa_1 q_{0,2}}\right) + \cdots \\
\text{or } F_2 &\equiv (x_2 + p_{0,2} - a)^2 + (y_2 + q_{0,2} - b)^2 \\
&\quad + (f_{2,3}(x_2, y_2) + t g_{2,3}(x_2, y_2) - c)^2 \qquad (4.15) \\
\text{where } f_{2,3}(x_2, y_2) &= w_{0,2} + x_2\left(\frac{\kappa_1 p_{0,2}}{1 - \kappa_1 w_{0,2}}\right) + y_2\left(\frac{\kappa_1 q_{0,2}}{1 - \kappa_1 w_{0,2}}\right) + \cdots \ .
\end{aligned}$$

We can choose at least one of these since not all of $p_{0,2}$, $q_{0,2}$, $(1 - \kappa_1 w_{0,2})$ are zero. We assume $F_{0,2}$ has type A_1 at $x_2 = y_2 = 0$, which means the second order terms of $f_{2,1}$, $f_{2,2}$, $f_{2,3}$ satisfy certain conditions. We have similar expressions in the case of F_3, given by one of (4.13), (4.14), (4.15), with x_2, y_2, $(-)_{*,2}$ replaced respectively by x_3, y_3, $(-)_{*,3}$.

4.3.4 Condition for Versal Unfolding

Using the end of §4.1 we get that F is versal if

$$\left(\frac{\partial F_1}{\partial t}, \frac{\partial F_2}{\partial t}, \frac{\partial F_3}{\partial t}\right), \left(\frac{\partial F_1}{\partial a}, \frac{\partial F_2}{\partial a}, \frac{\partial F_3}{\partial a}\right), \left(\frac{\partial F_1}{\partial b}, \frac{\partial F_2}{\partial b}, \frac{\partial F_3}{\partial b}\right),$$
$$\left(\frac{\partial F_1}{\partial c}, \frac{\partial F_2}{\partial c}, \frac{\partial F_3}{\partial c}\right) \text{ (all evaluated at } t = a = b = 0,\ c = 1/\kappa_1)$$
$$\text{and (1,1,1) span } \frac{\mathcal{E}(2)}{J_{F_{0,1}}} \oplus \mathrm{sp}\{1\} \oplus \mathrm{sp}\{1\} \ ,$$

where we only consider terms of degree ≤ 4 for F_1, terms of degree ≤ 2 for F_2 and terms of degree ≤ 2 for F_3. If we let $g_1(x_1, y_1) = \eta_0 + \eta_1 x_1 + \eta_2 y_1 + \eta_3 x_1^2 + \cdots$ then F is versal if

$$\begin{vmatrix} \eta_0 & \eta_1 & \eta_2 & \left(\eta_3 - \frac{\eta_0 \kappa_1^2}{2}\right) & -\frac{\kappa_1}{2}\delta_2 & -\frac{\kappa_1}{2}\delta_3 \\ 0 & 1 & 0 & 0 & \frac{\cos\phi_2 \cos\lambda_2}{\kappa_1} & \frac{\cos\phi_3 \cos\lambda_3}{\kappa_1} \\ 0 & 0 & 1 & 0 & \frac{\cos\phi_2 \sin\lambda_2}{\kappa_1} & \frac{\cos\phi_3 \sin\lambda_3}{\kappa_1} \\ 1 & 0 & 0 & -\frac{\kappa_1^2}{2} & -\sin\phi_2 & -\sin\phi_3 \\ 1 & 0 & 0 & 0 & 1 & 1 \\ 0 & 0 & \kappa_1 - \kappa_2 & -b_1 & 0 & 0 \end{vmatrix} \neq 0 \ , \qquad (4.16)$$

where

$$\delta_2 \ = \ \begin{cases} 2g_{2,1}(0,0)\frac{\cos\phi_2 \cos\lambda_2}{\kappa_1} & \text{if } F_2 \text{ is of form (4.13)} \\ 2g_{2,2}(0,0)\frac{\cos\phi_2 \sin\lambda_2}{\kappa_1} & \text{if } F_2 \text{ is of form (4.14)} \\ 2g_{2,3}(0,0)\frac{\sin\phi_2}{\kappa_1} & \text{if } F_2 \text{ is of form (4.15)} \end{cases}$$

and δ_3 is similarly defined (replace $g_{2,*}$ by $g_{3,*}$, etc.).

4.3.5 Conditions for Generic Sections

We found that the list of bad 3-spaces included (4.4) where $\lambda_1 = 0$ or $\lambda_3 = 0$ or $\lambda_4 = 0$ or $\lambda_3 + \lambda_4 = 0$. Then, given that these hold, Proposition 4.3.1.1 gave criteria for the type of $A_1^2 A_3$ transition. As in the case of an A_5 transition we have the relation

$$G_i(X_i, Y_i, \mathbf{u}) = F(A_i(X_i, Y_i, \mathbf{u}), B(\mathbf{u})) + C(\mathbf{u})$$

where each $A_i : (\mathbb{R}^2 \times \mathbb{R}^4, (\mathbf{0}, \mathbf{0})) \to \mathbb{R}^2$ is a germ with $A_i(-, \mathbf{0})$ invertible, $B : (\mathbb{R}^4, \mathbf{0}) \to (\mathbb{R}^4, (0, \mathbf{p}_0))$ is an invertible germ and $C : (\mathbb{R}^4, \mathbf{0}) \to (\mathbb{R}, -1/\kappa_1^2)$ is a germ. Using this relation in the same way as for the A_5 transition we obtain the geometrical interpretation of the conditions for generic sections and for the criterion for the type of $A_1^2A_3$ transition, as follows.

Proposition 4.3.5.1 *The necessary conditions for the one-parameter family of symmetry sets of the families of surfaces $z = f_0(x_1, y_1) + tg_1(x_1, y_1)$, where $f_0(x_1, y_1)$ is given by* (4.6)*, and those given by $\gamma_2(x_2, y_2, t)$, $\gamma_3(x_3, y_3, t)$ (see* (4.11)*) to exhibit an $A_1^2A_3$ transition are that*

$$\begin{aligned} b_0 &= 0 \ , \\ \frac{\kappa_1^2}{4} - \frac{b_1^2}{\kappa_1(\kappa_1 - \kappa_2)} - \frac{2c_0}{\kappa_1} &\neq 0 \ , \end{aligned}$$

that $F_{0,2}$, $F_{0,3}$ have type A_1 respectively at $x_2 = y_2 = 0$, $x_3 = y_3 = 0$, that the versality condition (4.16) *holds, and that the following necessary conditions for generic sections hold*

$$\left.\begin{aligned} \cos\phi_2 \sin\lambda_2(1 + \sin\phi_3) - \cos\phi_3 \sin\lambda_3(1 + \sin\phi_2) \neq 0 \ , \\ 2b_1(1 + \sin\phi_2) - \kappa_1(\kappa_1 - \kappa_2)\cos\phi_2 \sin\lambda_2 \neq 0 \ , \\ 2b_1(1 + \sin\phi_3) - \kappa_1(\kappa_1 - \kappa_2)\cos\phi_3 \sin\lambda_3 \neq 0 \ , \\ 2b_1(\sin\phi_3 - \sin\phi_2) + \kappa_1(\kappa_1 - \kappa_2)(\cos\phi_2 \sin\lambda_2 - \cos\phi_3 \sin\lambda_3) \neq 0 \ . \end{aligned}\right\} \quad (4.17)$$

Moreover, the transition is of type $A_1^2A_3$-I, $A_1^2A_3$-II when

$$\begin{aligned} &(2b_1(1 + \sin\phi_3) - \kappa_1(\kappa_1 - \kappa_2)\cos\phi_3 \sin\lambda_3) \\ &\times (-2b_1(1 + \sin\phi_2) + \kappa_1(\kappa_1 - \kappa_2)\cos\phi_2 \sin\lambda_2) \end{aligned} \quad (4.18)$$

is respectively negative, positive, provided there are no additional normal forms for generic functions given by considering the limits of tangent spaces to two- and three-dimensional strata (see Remark 4.2.1.1). The third type of transition as described in Proposition 4.3.1.1 cannot be realized by a one-parameter family of distance-squared functions.

4.3.6 Interpretation of the $A_1^2A_3$ Conditions

The condition (4.16) for versality of the geometric family F is difficult to understand, so we consider firstly the necessary conditions (4.17) for generic sections and the sign of (4.18), which determines the type of transition, provided there are no further conditions for generic sections. Using [HGYGM99, p.142] we get the following. Let $\mathbf{t}$, $\mathbf{n}$, be respectively the unit tangent, principal normal to the line of curvature corresponding to κ_1 on the surface $z = f_0(x, y)$, given by (4.6). Note that the tangent to the line of curvature corresponding to κ_1 at a point is the same as the principal direction corresponding to κ_1 at the point. Then, for $\mathbf{x}_{0,2}$ as a vector as in (4.12) (and similarly for $\mathbf{x}_{0,3}$), we have

$$\begin{aligned}
\mathbf{t}(0) = (1,0,0) \quad &, \quad \mathbf{n}(0) \parallel \left(0, \frac{2b_1}{\kappa_1 - \kappa_2}, \kappa_1\right), \\
\text{the first condition of (4.17)} \quad &\Longleftrightarrow \quad \mathbf{t}(0) \cdot (\mathbf{x}_{0,2} \times \mathbf{x}_{0,3}) \neq 0 \ , \\
\text{the second condition of (4.17)} \quad &\Longleftrightarrow \quad \mathbf{x}_{0,2} \cdot (\mathbf{t}(0) \times \mathbf{n}(0)) \neq 0 \ , \\
\text{the third condition of (4.17)} \quad &\Longleftrightarrow \quad \mathbf{x}_{0,3} \cdot (\mathbf{t}(0) \times \mathbf{n}(0)) \neq 0 \ , \\
\text{the fourth condition of (4.17)} \quad &\Longleftrightarrow \quad (\mathbf{x}_{0,2} - \mathbf{x}_{0,3}) \cdot (\mathbf{t}(0) \times \mathbf{n}(0)) \neq 0 \ .
\end{aligned}$$

Hence, *the first condition of* (4.17) *is the same as stating that the tangent to the line of curvature corresponding to* κ_1 *must not lie in the plane containing the origin and the points* $\mathbf{x}_{0,2}$, $\mathbf{x}_{0,3}$. In other words, *the first condition of* (4.17) *is the same as stating that the principal direction corresponding to* κ_1 *must not lie in the plane containing the origin and the points* $\mathbf{x}_{0,2}$, $\mathbf{x}_{0,3}$. Let Ω be the osculating plane of the line of curvature corresponding to κ_1 at the origin. Then *the second condition of* (4.17) *is the same as stating that the line through the origin and the point* $\mathbf{x}_{0,2}$ *must not lie in* Ω. Similarly for the third condition of (4.17) and the point $\mathbf{x}_{0,3}$. Finally, *the fourth condition of* (4.17) *is the same as stating that the line through* $\mathbf{x}_{0,2}$ *and* $\mathbf{x}_{0,3}$ *must not be parallel to* Ω.

In a similar way we can get an interpretation of the sign of (4.18):

$$\text{sign of (4.18)} = \text{sign of } \left(\mathbf{x}_{0,3} \cdot (\mathbf{t}(0) \times \mathbf{n}(0))\right) \left(-\mathbf{x}_{0,2} \cdot (\mathbf{t}(0) \times \mathbf{n}(0))\right) \ .$$

Hence *the symmetry set of the families of surfaces as in Proposition 4.3.5.1 exhibits respectively an* $A_1^2A_3$-I, $A_1^2A_3$-II *transition if* $\mathbf{x}_{0,2}$, $\mathbf{x}_{0,3}$ *are on the same*

side, opposite sides of Ω*, provided there are no conditions for generic sections other than* (4.17).

Consider the condition (4.16) in a simplified situation. Assume the families γ_1, γ_3 given by (4.11) do not change with t, which means that η_0, η_1, η_2, η_3 and δ_3 are all zero in (4.16). Then, (4.16) becomes

$$\delta_2 \left(2b_1(1+\sin\phi_3) - \kappa_1(\kappa_1-\kappa_2)\cos\phi_3\sin\lambda_3\right) \neq 0 \ ,$$

where δ_2 is defined immediately after (4.16). Hence the simplified version of (4.16) becomes

$$\begin{aligned}
&g_{2,1}(0,0)\cos\phi_2\cos\lambda_2 \left(2b_1(1+\sin\phi_3) - \kappa_1(\kappa_1-\kappa_2)\cos\phi_3\sin\lambda_3\right) \neq 0 \\
&\qquad \text{when } F_2 \text{ is of form (4.13)} \ , \\
&g_{2,2}(0,0)\cos\phi_2\sin\lambda_2 \left(2b_1(1+\sin\phi_3) - \kappa_1(\kappa_1-\kappa_2)\cos\phi_3\sin\lambda_3\right) \neq 0 \\
&\qquad \text{when } F_2 \text{ is of form (4.14)} \ , \\
&g_{2,3}(0,0)\sin\phi_2 \left(2b_1(1+\sin\phi_3) - \kappa_1(\kappa_1-\kappa_2)\cos\phi_3\sin\lambda_3\right) \neq 0 \\
&\qquad \text{when } F_2 \text{ is of form (4.15)} \ .
\end{aligned}$$

Take each of $g_{2,1}(0,0)$, $g_{2,2}(0,0)$, $g_{2,3}(0,0)$ to be non-zero. Using the fact that the unit surface normal $\mathbf{n}_{0,2}$ to γ_2 at $t=0$ is

$$\mathbf{n}_{0,2} = \mathbf{x}_{0,2} - \left(0,0,\frac{1}{\kappa_1}\right) = (\cos\phi_2\cos\lambda_2, \cos\phi_2\sin\lambda_2, \sin\phi_2) \ ,$$

we can obtain an interpretation of the simplified version of (4.16), which is that *the line from the origin to the point* $\mathbf{x}_{0,3}$ *must not lie in* Ω *and* either $\mathbf{n}_{0,2}$ *must not lie in the (y,z) plane (when* F_2 *is of form* (4.13)*)*, or $\mathbf{n}_{0,2}$ *must not lie in the (x,z) plane (when* F_2 *is of form* (4.14)*)*, or $\mathbf{n}_{0,2}$ *must not lie in the (x,y) plane (when* F_2 *is of form* (4.15)*)*. These last three interpretations can be summarized by stating that $\mathbf{n}_{0,2}$ *must not lie in the plane perpendicular to the coordinate direction corresponding to change with the family parameter* t. For example, if the family of surfaces $\gamma_2(x_2, y_2, t)$ corresponds to translating the surface $\gamma_2(x_2, y_2, 0)$ in any direction, then for versality we require the direction of translation not to lie in the tangent plane to $\gamma_2(x_2, y_2, 0)$ at the point of contact $\mathbf{x}_{0,2}$.

4.3.7 Example

Consider the example from §3.6 of the parabolic gutter with a flat end, but with slightly changed notation to agree with this chapter. Take the three unfoldings from (4.11) to be

$$\begin{aligned} F_1(x_1, y_1, t, a, b, c) &= \left|\left|\left(x_1, y_1, \frac{\kappa_1 x_1^2}{2}\right) - (a, b, c)\right|\right|^2, \\ F_2(x_2, y_2, t, a, b, c) &= \left|\left|\left(x_2, \frac{1}{\kappa_1} + t, y_2\right) - (a, b, c)\right|\right|^2, \\ F_3(x_3, y_3, t, a, b, c) &= \left|\left|\left(x_3, y_3, dy_2 + \frac{1 + \sqrt{1 + d^2}}{\kappa_1}\right) - (a, b, c)\right|\right|^2, \end{aligned}$$

for d a positive constant. So F_2 is of form (4.14) and F_3 is of form (4.15) (with x_2, y_2 replaced by x_3, y_3 and so on). Hence we take the parabolic gutter $z = \kappa_1 x^2/2$ with a roof $z = dy + (1 + \sqrt{1 + d^2})/\kappa_1$ and the flat end $y = 1/\kappa_1 + t$ as the three local pieces of boundary and consider the medial axis of these surfaces at values of t close to zero. The effect of changing t is that the end $y = 1/\kappa_1 + t$ moves away from the origin along the y-axis and the other two surfaces remain unaltered. Hence $g_1 \equiv 0$ (and so $\eta_i = 0$ for each i), $g_{2,2} \equiv 1$, $g_{3,3} \equiv 0$.

The medial axis corresponding to the local boundary surfaces $z = \kappa_1 x^2/2$, $z = dy + (1 + \sqrt{1 + d^2})/\kappa_1$ and $y = 1/\kappa_1 + t$ at values of t can be calculated explicitly. However, these calculations are very similar to those done for the example in §3.6 of the constraints on the medial axis in three dimensions, where local boundary was a parabolic gutter $z = by^2$ with a flat end $x = p$, and so the calculations are omitted. The points of contact on the flat end and on the roof given by (4.12) are

$$\mathbf{x}_{0,2} = \frac{(0, 1, 1)}{\kappa_1}, \quad \mathbf{x}_{0,3} = \frac{\left(0, -d, 1 + \sqrt{1 + d^2}\right)}{\kappa_1 \sqrt{1 + d^2}},$$

so we can obtain ϕ_2, λ_2, ϕ_3, λ_3. Using these we can check that (4.16) and each of the conditions given by (4.17) hold. For this example

$$(4.18) = \left(-\kappa_1^2 \left(-\frac{d}{\sqrt{1 + d^2}}\right)\right)\left(\kappa_1^2\right) > 0$$

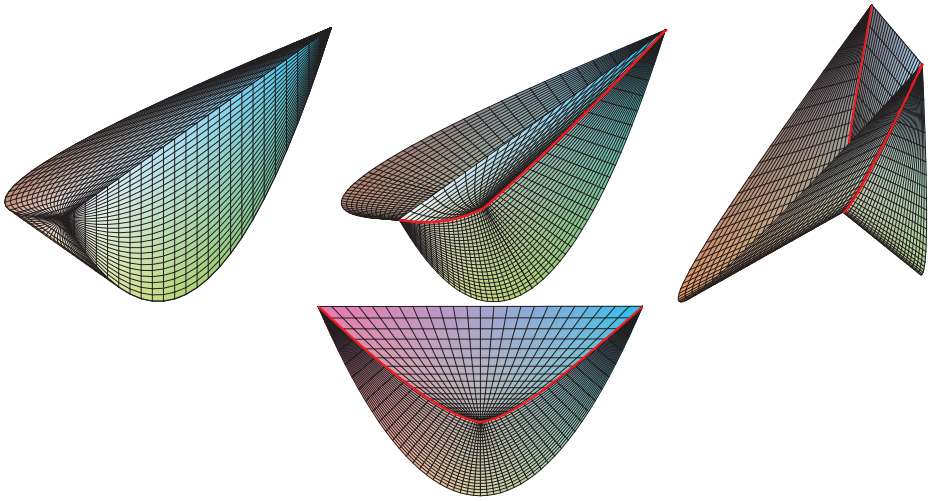

Figure 4.20: Figures 4.20 to 4.22 are of an example of the $A_1^2A_3$-II transition. This figure is for $t = -0.2$, that is before the transition. Top left: the boundary surface; top centre, top right: the corresponding medial axis from two points of view; bottom: the medial axis from another point of view. The red curve is an A_1^3 curve.

and so the symmetry set exhibits an $A_1^2A_3$-II transition, provided there are no conditions for generic sections other than (4.17).

The interpretations of the $A_1^2A_3$ conditions given immediately before this example can be easily verified in this example, as follows. In this example, the plane containing $\mathbf{0}$, $\mathbf{x}_{0,2}$ and $\mathbf{x}_{0,3}$ is $x = 0$; and Ω, the osculating plane of the line of curvature corresponding to κ_1 at the origin, is $y = 0$. It is easy to show that the tangent $(1, 0, 0)$ to the line of curvature corresponding to κ_1 does not lie in the plane $x = 0$, that $\mathbf{x}_{0,2}$ and $\mathbf{x}_{0,3}$ do not lie in the plane $y = 0$ and that the line through $\mathbf{x}_{0,2}$, $\mathbf{x}_{0,3}$ does not lie in the plane $y = 0$. Hence all of the interpretations of the conditions (4.16) hold for this example. Finally, we see that the y-coordinates of $\mathbf{x}_{0,2}$ and $\mathbf{x}_{0,3}$ have opposite signs and so $\mathbf{0}$, $\mathbf{x}_{0,2}$ and $\mathbf{x}_{0,3}$ lie on opposite sides of $y = 0$ and so we have an $A_1^2A_3$-II transition on the medial axis.

Figures 4.20, 4.21 and 4.22 show the transition on the medial axis where $d = 1$, $\kappa_1 = 2$.

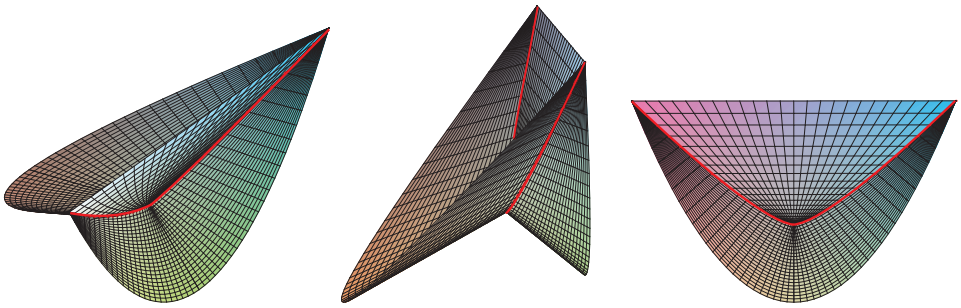

Figure 4.21: The moment of transition ($t = 0$): these pictures are different views of the medial axis, which has acquired an $A_1^2A_3$ point.

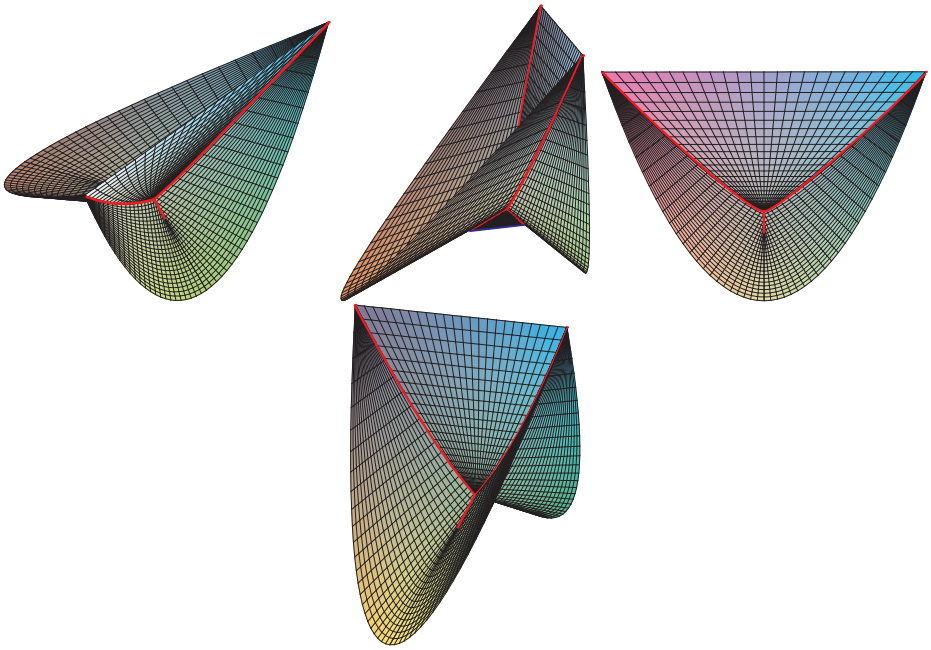

Figure 4.22: These are all different views of the medial axis for $t = 0.5$, so the $A_1^2A_3$-II transition has taken place. An extra medial sheet with an edge curve (the blue curve) has been created. This curve has two endpoints (A_1A_3 points) which lie on two created A_1^3 curves lying on the new medial sheet. So we now have four (red) A_1^3 curves which meet at an A_1^4 point created by the transition.

4.4 The A_1A_4 Transition

For this transition, we follow the method as used in §4.2, but omit the details. This transition is different from the others considered in this chapter in that it does not occur on a one-parameter family of medial axes, but only on a one-parameter family of symmetry sets. The family of symmetry sets looks locally like the pictures in Figures 4.23, 4.24 as it goes through an A_1A_4 transition. As in the transitions considered previously there might be other cases of A_1A_4 transitions – see Remark 4.2.1.1.

Take a family of distance-squared functions on a one-parameter family of surfaces in three dimensions. Consider the unfolding

$$\left.\begin{array}{l} F : \mathbb{R}^2 \times \mathbb{R}^4, (0,0,0,0,0,1/\kappa_1) \to \mathbb{R} \ , \text{ given by the two unfoldings} \\ F_1(x_1, y_1, t, a, b, c) = (x_1 - a)^2 + (y_1 - b)^2 \\ \qquad\qquad +(f_0(x, y) + tg_1(x_1, y_1) - c)^2 \ , \\ F_2(x_2, y_2, t, a, b, c) = \|\gamma_2(x_2, y_2, t) - (a, b, c)\|^2 \ , \end{array}\right\} \quad (4.19)$$

where $f_0(x_1, y_1)$ is given by (4.6) and $F_{0,1}$ has type A_4 at $x_1 = y_1 = 0$, where $F_{0,i}(x_i, y_i) = F_i(x_i, y_i, 0, 0, 0, 1/\kappa_1)$. This means that

$$\begin{array}{rcl} b_0 = \dfrac{\kappa_1^2}{4} - \dfrac{b_1^2}{\kappa_1(\kappa_1 - \kappa_2)} - \dfrac{2c_0}{\kappa_1} & = & 0 \ , \\ -\dfrac{2b_1(c_1(\kappa_1 - \kappa_2) + b_1b_2)}{\kappa_1(\kappa_1 - \kappa_2)^2} - \dfrac{2d_0}{\kappa_1} & \neq & 0 \ . \end{array}$$

We assume $F_{0,2}$ has type A_1 at $x_2 = y_2 = 0$ and that F_2 has one of the forms (4.13), (4.14) or (4.15). Then we get the following.

Proposition 4.4.1 *The necessary conditions for the one-parameter family of symmetry sets of the families of surfaces $z = f_0(x_1, y_1) + tg_1(x_1, y_1)$, where $f_0(x_1, y_1)$ is given by (4.6), $g_1(x_1, y_1) = \eta_0 + \eta_1x_1 + \eta_2y_1 + \eta_3x_1^2 + \eta_4x_1y_1 + (*)y_1^2 + \eta_5x_1^3 + \cdots$ and the one given by $\gamma_2(x_2, y_2, t)$ to exhibit an A_1A_4 transition are that*

$$\begin{array}{rcl} b_0 = \dfrac{\kappa_1^2}{4} - \dfrac{b_1^2}{\kappa_1(\kappa_1 - \kappa_2)} - \dfrac{2c_0}{\kappa_1} & = & 0 \ , \\ -\dfrac{2b_1(c_1(\kappa_1 - \kappa_2) + b_1b_2)}{\kappa_1(\kappa_1 - \kappa_2)^2} - \dfrac{2d_0}{\kappa_1} & \neq & 0 \ , \end{array}$$

that $F_{0,2}$ has type A_1 at $x_2 = y_2 = 0$, that the versality condition holds:

$$\left|\begin{array}{ccccccc} \eta_0 & \eta_1 & \eta_2 & \left(\eta_3 - \frac{\eta_0\kappa_1^2}{2}\right) & \eta_4 & \left(\eta_5 - \frac{\eta_1\kappa_1^2}{2}\right) & -\frac{\kappa_1}{2}\delta_2 \\ 0 & 1 & 0 & 0 & 0 & 0 & \frac{\cos\phi_2\cos\lambda_2}{\kappa_1} \\ 0 & 0 & 1 & 0 & 0 & 0 & \frac{\cos\phi_2\sin\lambda_2}{\kappa_1} \\ 1 & 0 & 0 & -\frac{\kappa_1^2}{2} & 0 & 0 & -\sin\phi_2 \\ 0 & 0 & \kappa_1-\kappa_2 & -b_1 & -2b_2 & -c_1 & 0 \\ 0 & 0 & & 0 & \kappa_1-\kappa_2 & -b_1 & 0 \\ 1 & 0 & 0 & 0 & 0 & 0 & 1 \end{array}\right| \neq 0, \quad (4.20)$$

where

$$\delta_2 \;=\; \begin{cases} 2g_{2,1}(0,0)\frac{\cos\phi_2\cos\lambda_2}{\kappa_1} & \text{if } F_2 \text{ is of form (4.13)}\ , \\ 2g_{2,2}(0,0)\frac{\cos\phi_2\sin\lambda_2}{\kappa_1} & \text{if } F_2 \text{ is of form (4.14)}\ , \\ 2g_{2,3}(0,0)\frac{\sin\phi_2}{\kappa_1} & \text{if } F_2 \text{ is of form (4.15)}\ , \end{cases}$$

and that the following necessary conditions for generic sections hold.

$$\left.\begin{aligned} 2b_1b_2 + c_1(\kappa_1-\kappa_2) &\neq 0 \\ 2b_1(1+\sin\phi_2) - \kappa_1(\kappa_1-\kappa_2)\cos\phi_2\sin\lambda_2 &\neq 0 \end{aligned}\right\} \quad (4.21)$$

There is only one type of A_1A_4 transition, provided no others arise when considering the limits of tangent spaces to two- and three-dimensional strata (see Remark 4.2.1.1).

Interpretation of the A_1A_4 Conditions

The condition (4.20) for the unfolding F to be versal is complicated, as in the $A_1^2A_3$ case. Hence, we consider again a simpler situation, where the family γ_1 given by (4.19) does not change with t, which means that $g_1(x_1, y_1) \equiv 0$, and so η_0, η_1, η_2, η_3, η_4, η_5 are all zero in (4.20), which becomes

$$\delta_2\left(2b_1b_2 + c_1(\kappa_1-\kappa_2)\right) \neq 0\ ,$$

where δ_2 is defined immediately after (4.20). Using the interpretations in §4.2.6, §4.3.6 and assuming $g_{2,1}(0,0)$, $g_{2,2}(0,0)$, $g_{2,3}(0,0)$ are all non-zero, we get that

this simplified version of the versality condition (4.20) is the same as stating that *the ridge curve corresponding to* κ_1 *must be non-singular and that the unit normal to* γ_2 *at* $t = 0$ *must not lie in the plane perpendicular to the coordinate direction corresponding to change with the family parameter* t. For example, if the family of surfaces $\gamma_2(x_2, y_2, t)$ corresponds to translating the surface $\gamma_2(x_2, y_2, 0)$ in any direction, then for versality we require the direction of translation not to lie in the tangent plane to $\gamma_2(x_2, y_2, 0)$ at the point of contact $\mathbf{x}_{0,2}$.

Now consider the necessary conditions for generic sections. The first condition of (4.21) is that of the non-singularity of the ridge curve corresponding to κ_1. Using §4.3.6, *the second condition of* (4.21) *is the same as stating that the line from the origin to the point* $\mathbf{x}_{0,2}$ *must not lie in the osculating plane of the line of curvature corresponding to* κ_1 *at the origin.*

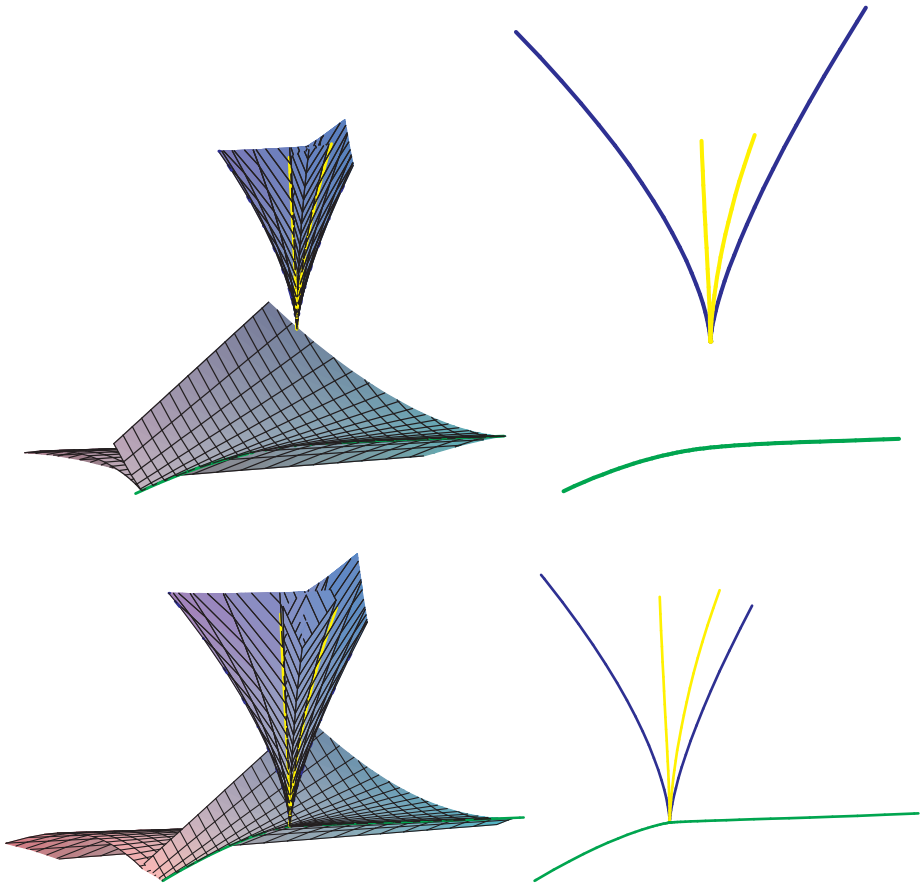

Figure 4.23: A one-parameter family of symmetry sets looks locally like the pictures in this figure and Figure 4.24 as it goes through an A_1A_4 transition. It is possible that there are other cases of A_1A_4 transitions (see Remark 4.2.1.1). None of these surfaces is part of the medial axis. In Figures 4.23, 4.24 the green and yellow curves are A_1A_2 curves, the red curves are A_1^3 curves and the blue curves are A_3 curves. Top: before the transition. Here there is a swallowtail surface and a surface with a cusp edge. Top right: just the curves are drawn, not the surfaces. Bottom: the moment of transition. The swallowtail surface intersects with the other surface in a point, the A_1A_4 point. Bottom right: the curves all meet at the A_1A_4 point.

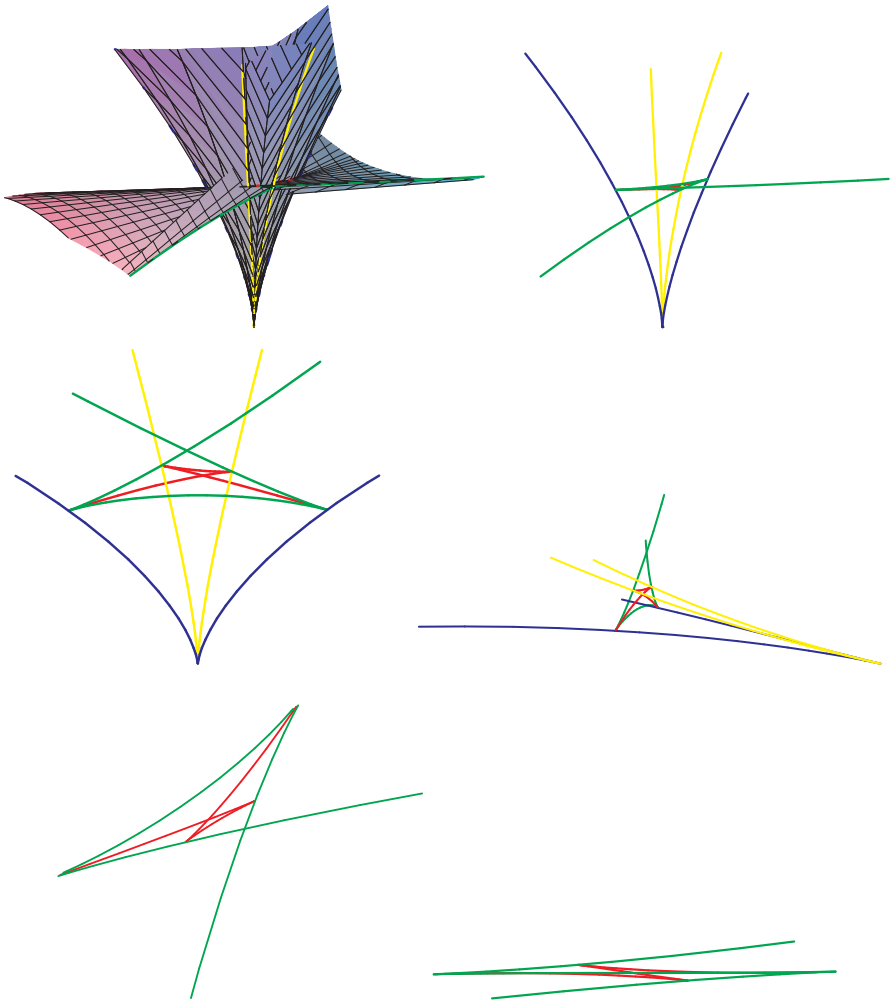

Figure 4.24: After the transition. The swallowtail surface now intersects with the other surface in a curve. There is now an A_1^3 curve (red) which meets the (blue) A_3 at A_1A_3 points, where the A_1^3 curve ends – these endpoints coincide with the cusps of the (green) A_1A_2 curve. The red curve has two cusps which coincide with the intersections of the two A_1A_2 curves (yellow, green). The yellow curve only meets another curve at the cusps of the A_3 (blue) curve. The pictures at the bottom show just the green and red curves, but these do not self-intersect, which is shown by the picture on the right.

4.5 The A_1A_3 Transitions

The A_1A_3 transitions are different from the previous transitions – the big bifurcation sets of the standard multi-versal unfolding are products. There are at least four possible types of transitions for the standard multi-versal unfolding of an A_1A_3 singularity, but it is stated below in Proposition 4.5.1 that two of the four identified are not possible for a one-parameter family of symmetry sets in $\mathbb{R}^3$. Hence a family of symmetry sets looks locally like the pictures in one of Figures 4.25, 4.26 as it goes through the an A_1A_3 transition, allowing for other possible cases of A_1A_4 transitions (see Remark 4.2.1.1). We take a family of distance-squared functions on a one-parameter family of surfaces in three dimensions. Then we consider the unfolding given by (4.19) where $f_0(x_1, y_1)$ is given by (4.6) and $F_{0,1}$, where $F_{0,i}(x_i, y_i) = F_i(x_i, y_i, 0, 0, 0, 1/\kappa_1)$, has type A_3 at $x_1 = y_1 = 0$. We assume $F_{0,2}$ has type A_1 at $x_2 = y_2 = 0$ and that F_2 has one of the forms (4.13), (4.14) or (4.15).

The method is as follows. We require that when the family parameter t is fixed, then a, b, c do not versally unfold the A_1A_3 singularity, but that t, a, b, c do. To realize the various types of transition we consider the three-dimensional space with coordinates (u_1, u_2, u_3) of the standard bifurcation set of the standard multi-versal unfolding of an A_1A_3 singularity (so we ignore the u_4 component in the four-dimensional space with coordinates (u_1, u_2, u_3u_4)). Then we obtain generic linear functions h on this set and use projections $h(u_1, u_2, u_3)\pm u_4^2$ to realize the various types of transition. We get the following.

Proposition 4.5.1 *The necessary conditions for the one-parameter family of symmetry sets of the families of surfaces $z = f_0(x_1, y_1) + tg_1(x_1, y_1)$, where $f_0(x_1, y_1)$ is given by (4.6), $g_1(x_1, y_1) = \eta_0 + \eta_1x_1 + \eta_2y_1 + \eta_3x_1^2 + \cdots$ and the one given by $\gamma_2(x_2, y_2, t)$ to exhibit an A_1A_3 transition are that*

$$b_0 = 0,\ \frac{\kappa_1^2}{4} - \frac{b_1^2}{\kappa_1(\kappa_1 - \kappa_2)} - \frac{2c_0}{\kappa_1} \neq 0\ ,$$

that $F_{0,2}$ has type A_1 at $x_2 = y_2 = 0$, that the versality conditions hold:

$$b_1 = \frac{\kappa_1(\kappa_1 - \kappa_2)\cos\phi_2 \sin\lambda_2}{2(1+\sin\phi_2)} \ , \tag{4.22}$$

$$\left.\begin{array}{c} 0 \neq \delta_2\kappa_1^3 - 2\eta_0\kappa_1^2\sin\phi_2 + 2\eta_1\kappa_1\cos\phi_2\cos\lambda_2 \\ +2\eta_2\kappa_1\cos\phi_2\sin\lambda_2 + 4\eta_3(1+\sin\phi_2) \end{array}\right\} \tag{4.23}$$

where

$$\delta_2 \ = \ \left\{\begin{array}{ll} 2g_{2,1}(0,0)\frac{\cos\phi_2\cos\lambda_2}{\kappa_1} & \textit{if } F_2 \textit{ is of form } (4.13) \ , \\ 2g_{2,2}(0,0)\frac{\cos\phi_2\sin\lambda_2}{\kappa_1} & \textit{if } F_2 \textit{ is of form } (4.14) \ , \\ 2g_{2,3}(0,0)\frac{\sin\phi_2}{\kappa_1} & \textit{if } F_2 \textit{ is of form } (4.15) \ . \end{array}\right.$$

Generic sections are automatic, provided no other conditions for generic sections arise arise when considering the limits of tangent spaces to two- and three-dimensional strata (see Remark 4.2.1.1). Moreover, the transitions of Figures 4.27, 4.28 do not occur on a one-parameter family of symmetry sets. The additional criterion for realizing either A_1A_3-I or A_1A_3-II is not yet known.

Remark 4.5.2 We require an expression for $\partial^2 B_1/\partial u_4^2(\mathbf{0})$ in order to decide the type of A_1A_3, since

$$h(u_1,u_2,u_3) \pm u_4^4 = \pi(B(\mathbf{u})) = B_1(\mathbf{u}) \ .$$

This has proved very difficult owing to the very complicated expressions. Hence we consider a geometric reason to distinguish the two cases. From Figures 4.25, 4.26 we see that in the A_1A_3-II case there is an A_1^3 curve through the A_1A_3 point at the moment of transition, but in the A_1A_3-I case there is no A_1^3 curve through the A_1A_3 point at the moment of transition. Hence we can examine the condition for there to be an A_1^3 curve on the symmetry set at points near to those corresponding to A_1, A_3 points of contact.

Consider the case where the A_1 surface $\gamma_2(x_2,y_2,0)$ is a plane. It can be shown that the parameters x_1, y_1 on the A_3 surface $z = f_0(x_1,y_1)$ can be used as parameters for the pre-symmetry set, given certain open conditions on the A_1 point. Hence we have a parametrization of the pre-symmetry set given by

$$(x_1,y_1) \xrightarrow{\psi} (x_2,y_2) \ .$$

Then it can be shown that the critical set Σ of ψ is singular if and only if (4.22) holds. Furthermore, the condition for Σ to be an isolated point or not can be calculated, but even in this case it is very complicated and involves the degree 4 terms on the surface $\gamma_1(x_1, y_1, 0)$. Hence the condition for an A_1^3 curve to exist can be calculated, but it is too complicated to be understood.

Interpretation of the A_1A_3 Conditions

Using §4.3.6, the condition (4.22) is the same as stating that *the line through the origin and the point of contact* $\mathbf{x}_{0,2}$ *on the* A_1 *surface must lie in the osculating plane of the line of curvature corresponding to* κ_1 *at the origin.* The condition (4.23) for the unfolding F to be versal is complicated, as in the $A_1^2A_3$ and A_1A_4 cases. Hence, we consider again a simpler situation, where the family γ_1 given by (4.19) does not change with t, which means that $g_1(x_1, y_1) \equiv 0$, and so η_0, η_1, η_2, η_3 are all zero in (4.23), which becomes $\delta_2 \neq 0$. Using the interpretations in §4.3.6 and assuming $g_{2,1}(0,0)$, $g_{2,2}(0,0)$, $g_{2,3}(0,0)$ are all non-zero, we get that in the case of the family of surfaces $\gamma_2(x_2, y_2, t)$ corresponding to translating the surface $\gamma_2(x_2, y_2, 0)$ in any direction, then for versality we require the direction of translation not to lie in the tangent plane to $\gamma_2(x_2, y_2, 0)$ at the point of contact $\mathbf{x}_{0,2}$.

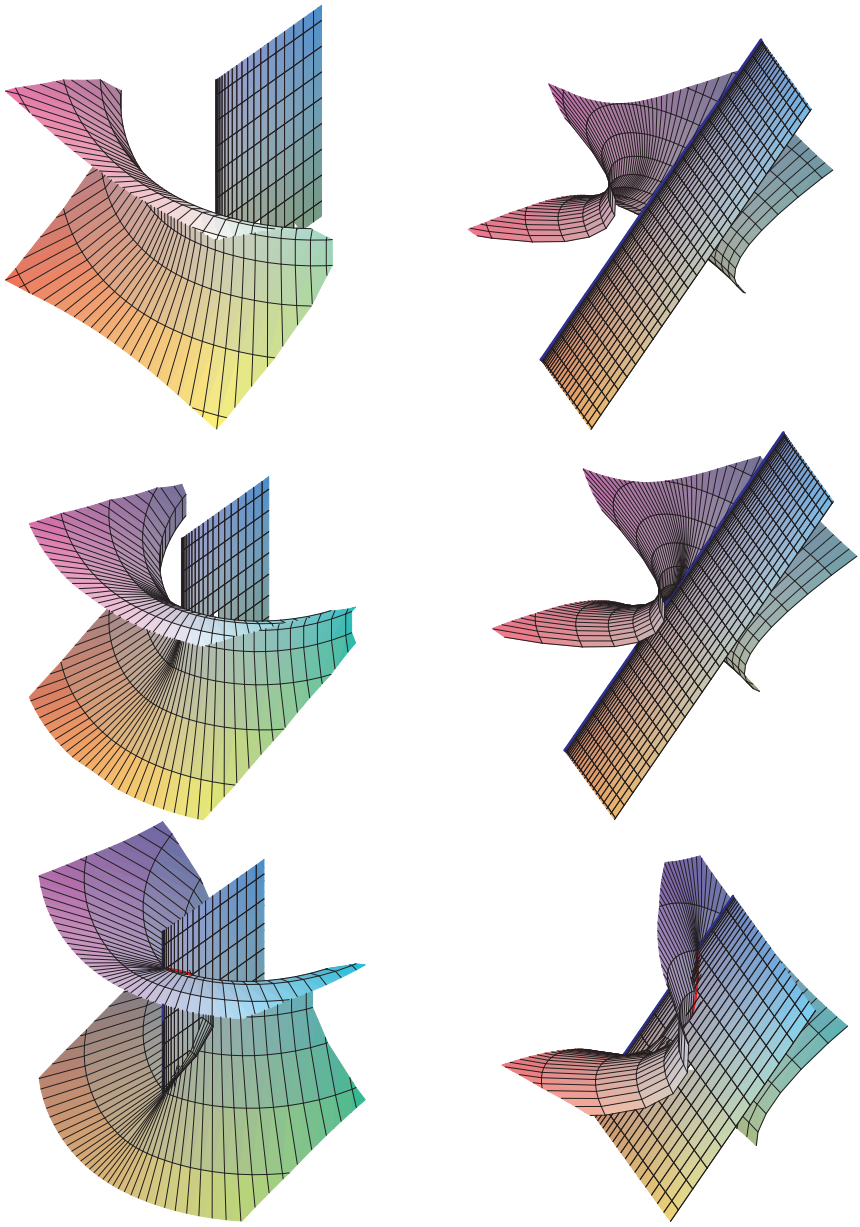

Figure 4.25: A one-parameter family of symmetry sets looks locally like these pictures, as it goes through an A_1A_3-I transition. Top: two views before the transition, middle: two views at the moment of transition, bottom: two views after the transition. In Figures 4.25 to 4.28, the blue, red curves correspond respectively to A_3, A_1^3 curves. After the transition an A_1^3 curve has been created.

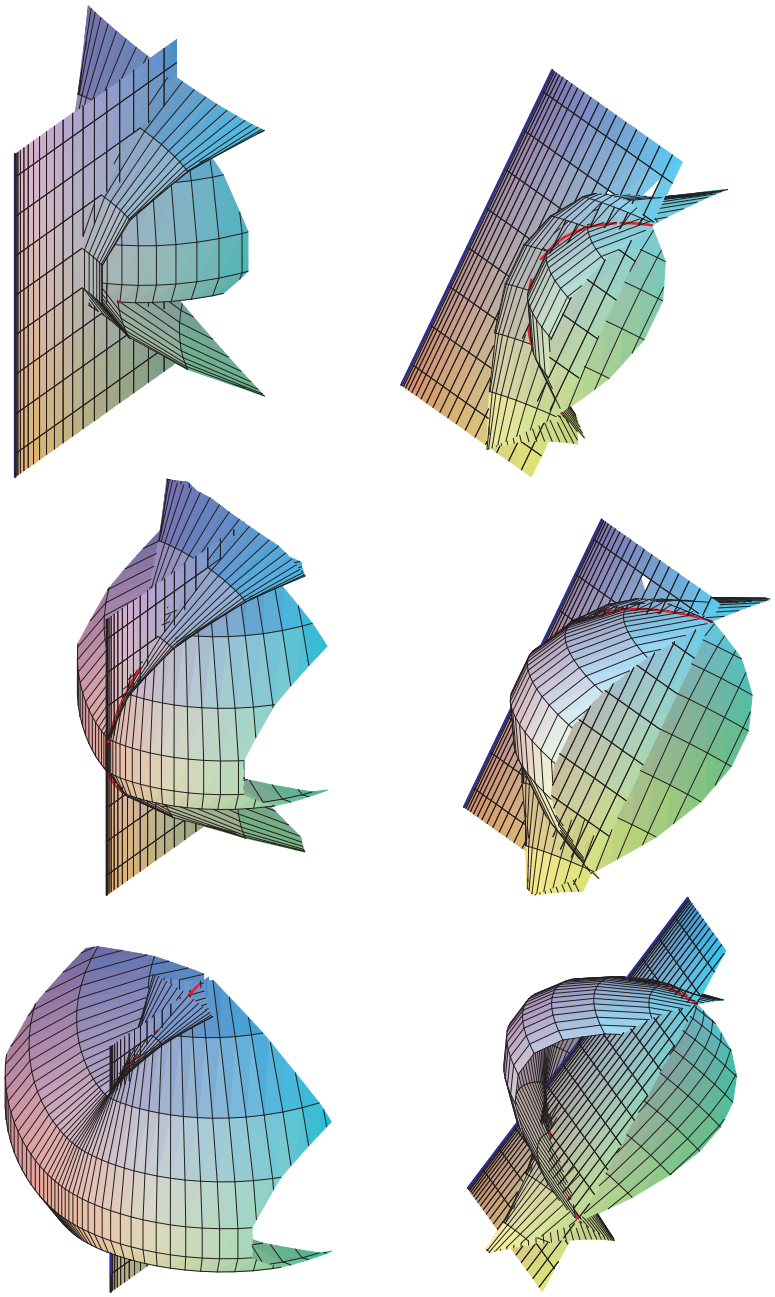

Figure 4.26: The A_1A_3-II transition on a one-parameter family of symmetry sets. Top: two views before the transition, middle: two views at the moment of transition, bottom: two views after the transition. At the moment of transition the A_1^3 and A_3 curves are tangent.

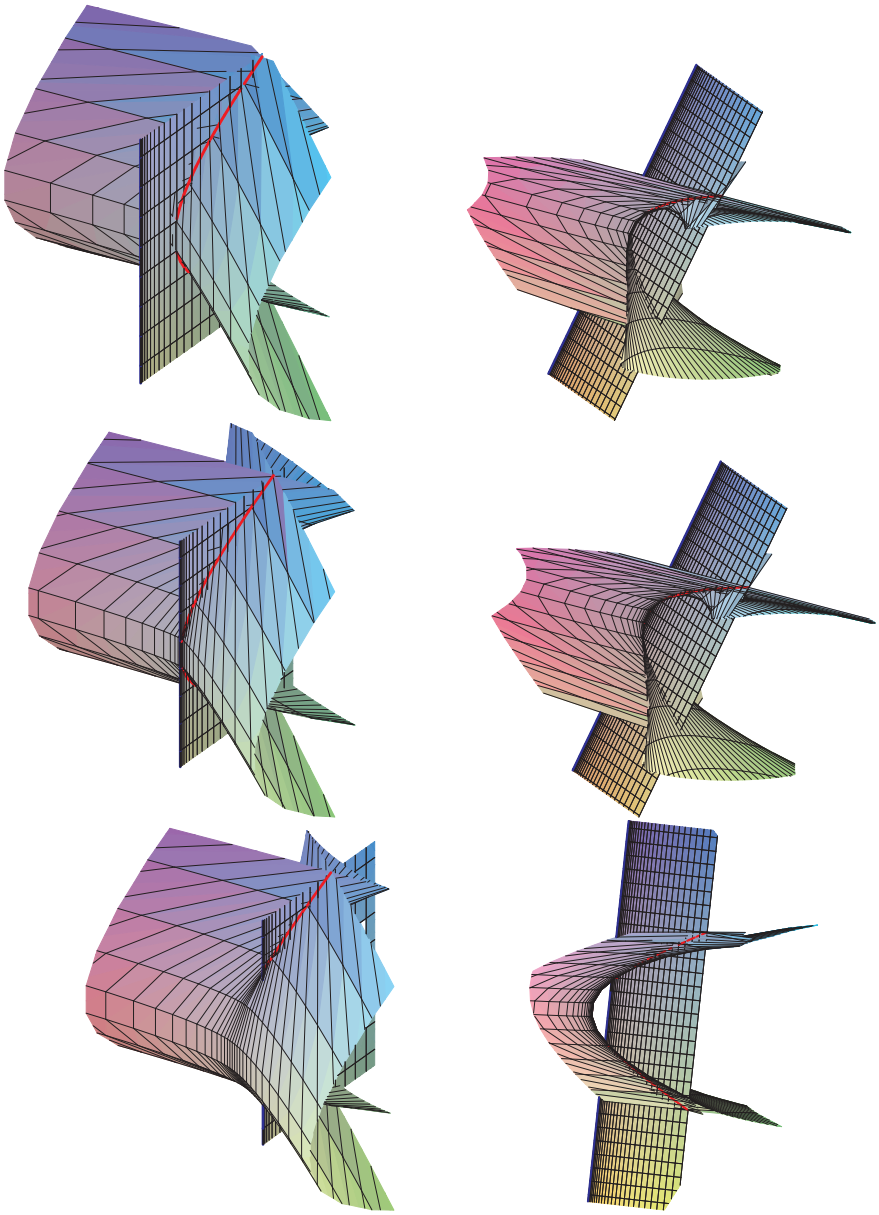

Figure 4.27: The third type of A_1A_3 transition – this cannot occur for a one-parameter family of symmetry sets. This type is possible for the standard multi-versal unfolding. Top: two views before the transition, middle: two views at the moment of transition, bottom: two views after the transition. At the moment of transition the A_1^3, A_3 curves are tangent and after the transition there are two A_1^3 curves which end at the (A_1A_3) points of intersection with the A_3 curve.

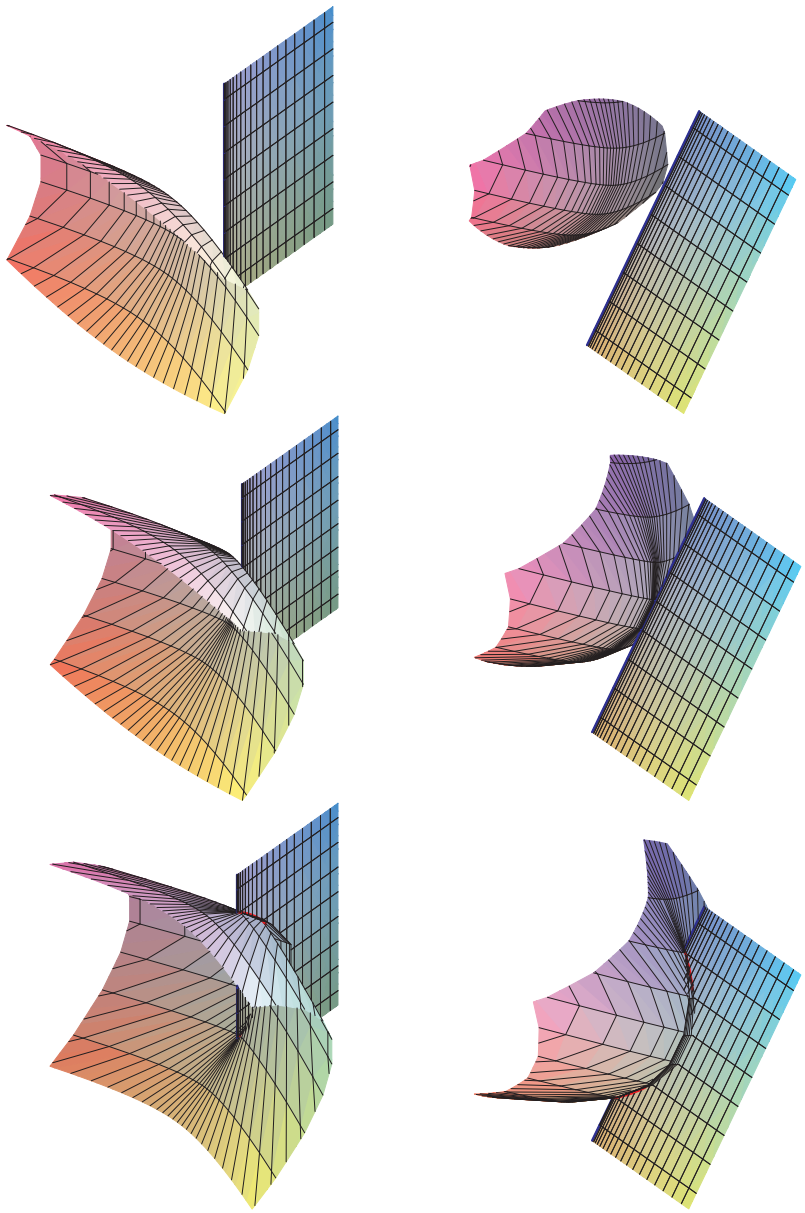

Figure 4.28: The fourth type of A_1A_3 transition – this also cannot occur for a one-parameter family of symmetry sets. This type is possible for the standard multi-versal unfolding. Top: two views before the transition, middle: two views at the moment of transition, bottom: two views after the transition. At the moment of transition the A_1^3, A_3 curves are tangent and after the transition there are two A_1^3 curves which end at the (A_1A_3) points of intersection with the A_3 curve.

4.6 The A_1^4 Transitions

The A_1^4 transitions are similar to the A_1A_3 transitions in that the big bifurcation sets of the standard multi-versal unfolding are products. Hence the method for the following is omitted. In [GK02] there are three types of transitions listed which are possible for the standard multi-versal unfolding of an A_1^4 singularity, but [GK02] states that only one of these types is possible for a one-parameter family of medial axes in $\mathbb{R}^3$.

We consider four families of surface $\gamma_i(x_i, y_i, t)$ for $i = 1, \ldots, 4$ and four corresponding distance-squared functions F_i when $\gamma_i(x_i, y_i, t)$ is one of three forms:

$$\begin{aligned} F_i &\equiv (f_{i,1}(x_i, y_i) + tg_{i,1}(x_i, y_i) - a)^2 \\ &\quad + (y_i + q_{0,i} - b)^2 + (x_i + w_{0,i} - c)^2 \qquad (4.24) \\ \text{where } f_{i,1}(x_i, y_i) &= p_{0,i} + y_i\left(-\frac{q_{0,i}}{p_{0,i}}\right) + x_i\left(\frac{r_0 - w_{0,i}}{p_{0,i}}\right) + \cdots \\ \text{or } F_i &\equiv (x_i + p_{0,i} - a)^2 + (f_{i,2}(x_i, y_i) + tg_{i,2}(x_i, y_i) - b)^2 \\ &\quad + (y_i + w_{0,i} - c)^2 \qquad (4.25) \\ \text{where } f_{i,2}(x_i, y_i) &= q_{0,i} + x_i\left(-\frac{p_{0,i}}{q_{0,i}}\right) + y_i\left(\frac{r_0 - w_{0,i}}{q_{0,i}}\right) + \cdots \\ \text{or } F_i &\equiv (x_i + p_{0,i} - a)^2 + (y_i + q_{0,i} - b)^2 \\ &\quad + (f_{i,3}(x_i, y_i) + tg_{i,3}(x_i, y_i) - c)^2 \qquad (4.26) \\ \text{where } f_{i,3}(x_i, y_i) &= w_{0,i} + x_i\left(\frac{p_{0,i}}{r_0 - w_{0,i}}\right) + y_i\left(\frac{q_{0,i}}{r_0 - w_{0,i}}\right) + \cdots \end{aligned}$$

where the point of contact on the surface $\gamma_i(x_i, y_i, 0)$ at $x_i = y_i = 0$ is

$$\mathbf{x}_{0,i} = (p_{0,i}, q_{0,i}, w_{0,i}) = r_0(\cos\phi_i \cos\lambda_i, \cos\phi_i \sin\lambda_i, \sin\phi_i + 1)$$

where ϕ_i, λ_i are constants. Also, r_0 (const.) is the radius of the sphere of contact with the surfaces $\gamma_i(x_i, y_i, 0)$ at $x_i = y_i = 0$. We get the following.

Proposition 4.6.1 *Consider the one-parameter family of symmetry sets of the families of surfaces $\gamma_i(x_i, y_i, t)$ given by one of the forms* (4.24), (4.25), (4.26). *Let the point of contact $\mathbf{x}_{0,1}$ be the origin, so $\phi_1 = 3\pi/2$ and then we have F_1 is*

of form (4.26) *for* $i = 1$. *The family of symmetry sets exhibits an* A_1^4 *transition if each* $F_{0,i}$ *has type* A_1 *at* $x_i = y_i = 0$, *for* $i = 2, 3, 4$; *if the versality conditions hold:*

$$\left.\begin{aligned} 0 = {} & p_{0,2}(q_{0,3}w_{0,4} - q_{0,4}w_{0,3}) + p_{0,3}(q_{0,4}w_{0,2} - q_{0,2}w_{0,4}) \\ & + p_{0,4}(q_{0,2}w_{0,3} - q_{0,3}w_{0,2}) \end{aligned}\right\} \tag{4.27}$$

$$\left.\begin{aligned} 0 \neq {} & \delta_1\left(p_{0,2}(w_{0,4} - w_{0,3}) + p_{0,3}(w_{0,2} - w_{0,3}) + p_{0,4}(w_{0,3} - w_{0,2})\right) \\ & + \delta_2(p_{0,3}w_{0,4} - p_{0,4}w_{0,3}) + \delta_3(p_{0,4}w_{0,2} - p_{0,2}w_{0,4}) \\ & + \delta_4(p_{0,2}w_{0,3} - p_{0,3}w_{0,2}) \end{aligned}\right\} \tag{4.28}$$

where

$$\delta_i \;=\; \begin{cases} 2g_{i,1}(0,0)r_0\cos\phi_i\cos\lambda_i & \text{if } F_i \text{ is of form (4.24)}, \\ 2g_{i,2}(0,0)r_0\cos\phi_i\sin\lambda_i & \text{if } F_i \text{ is of form (4.25)}, \\ 2g_{i,3}(0,0)r_0\sin\phi_i & \text{if } F_i \text{ is of form (4.26)}, \end{cases}$$

and that the sections of the big bifurcation set of the unfoldings F_i *are generic. Since* $\mathbf{x}_{0,1}$ *is chosen to be the origin we have that* F_1 *is of the form* (4.26) *for* $i = 1$ *and so* $\delta_1 = -2g_{i,3}(0,0)r_0$.

The above only contains the conditions for versality; the conditions for generic sections have yet to be calculated. See §4.7 and [GK02] for more detail on the A_1^4 transition.

Interpretation of the A_1^4 Conditions

The first condition for versality (4.27) is the same as requiring the four points of tangency $\mathbf{x}_{0,i} = (p_{0,i}, q_{0,i}, w_{0,i})$ on $\gamma_i(x_i, y_i, 0)$ for $i = 1, \ldots, 4$ are coplanar. Again consider a simplified version of the second condition for versality (4.28), where families γ_1, γ_3, γ_4 do not change with t, so that $\delta_1 = \delta_3 = \delta_4 = 0$. Then (4.28) becomes $\delta_2(p_{0,3}w_{0,4} - p_{0,4}w_{0,3}) \neq 0$. Using the interpretations in §4.3.6 and assuming $g_{2,1}(0,0)$, $g_{2,2}(0,0)$, $g_{2,3}(0,0)$ are all non-zero, we get that the simplified version of (4.28) is the same as stating that *the unit normal to* γ_2 *at* $t = 0$ *must not lie in the plane perpendicular to the coordinate direction corresponding to change with the family parameter* t and that $\mathbf{x}_{0,3} \times \mathbf{x}_{0,4}$ must not lie in the (x, z)-plane.

4.7 Further Research

The above contains the necessary conditions for realizing the A_5, A_1A_3-I, A_1A_3-II, $A_1^2A_3$-I, $A_1^2A_3$-II and A_1A_4 transitions on a one-parameter family of symmetry sets in $\mathbb{R}^3$. Also, there is some work done towards the conditions for realizing the A_1^4 transition. This remains to be completed, along with the remaining transition on a one-parameter family of symmetry sets which also occurs on a one-parameter family of medial axes, the A_1^5 transition. There are other transitions besides A_1A_4 that are expected on a generic one-parameter family of symmetry sets, which do not occur on the medial axis. The same methods as used in this chapter can be used to obtain the conditions for realizing these.

For each of the transitions considered in this chapter we did not consider the limits of tangent spaces to strata of dimension greater than one, since we assumed all of these contain a limit of tangent spaces to a one-dimensional stratum (see Remark 4.2.1.1). Since this does not necessarily follow from [BG86] a general proof of this is required. Failing that it will be necessary to check for each transition that the limits of tangent spaces to strata of dimension greater than one do not produce additional normal forms for generic functions.

As mentioned at the start of this chapter, a paper summarizing the methods used in this chapter and the conditions obtained, together with any further research, would be a natural completion of this area of research.

Bibliography

[A74] V. I. Arnol'd, 'Normal forms of functions in neighbourhoods of degenerate critical points', *Russian Mathematical Surveys*, **29** (1974), 10-50.

[Blu02] H. Blum, 'Biological shape and visual science I', *Journal of Theoretical Biology*, **38** (1978), 1-28.

[Bog90] I. A. Bogaevsky, 'Metamorphoses of singularities of minimum functions and bifurcations of shock waves of the Burgers equation with vanishing viscosity', *St. Petersburg (Leningrad) Math. J.*, **1** (1990), 807-823.

[Bog02a] I. A. Bogaevsky, 'Perestroikas of shocks and singularities of minimum functions', *Physica D: Nonlinear Phenomena*, **173** (2002), 1-28.

[Bog02b] I. A. Bogaevsky, 'Perestroikas of symmetry sets in 3D space', private communication with I. A. Bogaevsky.

[BG86] J. W. Bruce & P. J. Giblin, 'Growth, motion and one-parameter families of symmetry sets', *Proceedings of the Royal Society of Edinburgh*, **104A** (1986), 179-204.

[BG92] J. W. Bruce & P. J. Giblin, *Curves and Singularities*, Cambridge University Press (1992).

[BGG85] J. W. Bruce, P. J. Giblin & C. G. Gibson 'Symmetry sets', *Proceedings of the Royal Society of Edinburgh*, **101A** (1985), 163-186.

[CP89] S. Chen & R. E. Parent, 'Shape averaging and its applications to industrial design', *CGA*, **9(1)** (1989), 47-54.

[D03] J. Damon, 'On the smoothness and geometry of boundaries associated to skeletal structures I: sufficient conditions for smoothness', *Annales Inst. Fourier*, **53** (2003), 1941-1985.

[D04] J. Damon, 'On the smoothness and geometry of boundaries associated to skeletal structures II: geometry in the Blum case', *Compositio Mathematica*, **140** (2004), 1657-1674.

[D05] J. Damon, 'Determining the geometry of boundaries of objects from medial data', *International Journal of Computer Vision*, **63** (2005), 45-64.

[GB85] P. J. Giblin & S. A. Brassett, 'Local symmetry of plane curves', *American Mathematical Monthly*, **92** (1985), 689-707.

[GK99] P. J. Giblin & B. Kimia, 'On the local form and transitions of symmetry sets, medial axes, and shocks', *Proceedings of the IEEE International Conference on Computer Vision*, (1999), 385-391.

[GK02] P. J. Giblin & B. B. Kimia, 'Transitions of the 3D medial axis under a one-parameter family of deformations', *Proceedings of the European Conference on Computer Vision 2002*, Lecture Notes in Computer Science, **2351** (2002), 718-734.

[GK03] P. J. Giblin & B. B. Kimia, 'On the intrinsic reconstruction of shape from its symmetries', *IEEE Transactions on Pattern Analysis and Machine Intelligence*, **25** (2003), 895-911.

[GK04] P. J. Giblin & B. Kimia, 'A formal classification of 3D medial axis points and their local geometry' *IEEE Transactions on Pattern Analysis and Machine Intelligence*, **26** (2004), 238-251.

[GKP05] P. J. Giblin, B. Kimia & A. J. Pollitt, 'Transitions of the 3D medial axis under a one-parameter family of deformations, preprint (27 pages).

[GS98] P. J. Giblin & G. Sapiro, 'Affine-invariant distances, envelopes and symmetry sets', *Geometriae Dedicata*, **71** (1998), 237-261.

[GS00] P. J. Giblin & G. Sapiro, 'Affine versions of the symmetry set', *Research Notes in Mathematics* **412**, *Real and complex singularities*, eds: J. W. Bruce, F. Tari, Chapman and Hall/CRC (2000), 173-187.

[Gibs98] C. G. Gibson, *Elementary Geometry of Algebraic Curves*, Cambridge University Press (1998), 137-138.

[GreMil98] U. Grenander & M. Miller, 'Computational anatomy: an emerging discipline', *Quarterly of Applied Mathematics*, **LVI(4)** (1998), 617-694.

[HGYGM99] P. L. Hallinan, G. G. Gordon, A. L. Yuille, P. J. Giblin & D. Mumford, *Two- and Three-Dimensional Patterns of the Face*, A K Peters, Ltd. (1999).

[IS98] S. Izumiya & T. Sano, 'Generic affine differential geometry of plane curves', *Proceedings of the Royal Society of Edinburgh*, **41** (1998), 315-324.

[LSMP] *Liverpool Surface Modelling Package* (LSMP), written by Richard Morris for Silicon Graphics and X Windows. See R.J.Morris, 'The use of computer graphics for solving problems in singularity theory', in *Visualization in Mathematics*, H.-C.Hege & K.Polthier, Heidelburg: Springer-Verlag (1997), 173-187.

[MAPLE] *Maple*, Computer algebra & graphics package, distributed by Waterloo Maple Software, Waterloo, Ontario, Canada.

[M03] D. Mumford, 'The shape of objects in two and three dimensions', *Gibbs Lecture 2003*, to appear in *Notices of the American Mathematical Society.*

[PGK04] A. J. Pollitt, P. J. Giblin, & B. Kimia 'Consistency conditions on the medial axis', *Proceedings of the European Conference on Computer Vision*

2004, ed. T. Pajdla & J. Matas, Lecture Notes in Computer Science, **3022** (2004), 530-541.

[PGK05] A. J. Pollitt, P. J. Giblin, & B. Kimia 'Consistency conditions on the medial axis', preprint (31 pages).

[S99] D. Siersma, 'Properties of conflict sets in the plane', *Geometry and Topology of Caustics*, ed. S. Janeczko and V. M. Zakalyukin, Banach Center Publications, **50**, Warsaw (1999), 267-276.

[SSG99] J. Sotomayor, D. Siersma & R. Garcia, 'Curvatures of conflict surfaces in Euclidean 3-space', *Geometry and Topology of Caustics*, ed. S. Janeczko & V. M. Zakalyukin, Banach Center Publications, **50**, Warsaw (1999), 277-285.

[Su83] Su B., *Affine Differential Geometry*, Science Press, Beijing/ Gordon and Breach, New York (1983).